UNIVERSIDAD COMPLUTENSE DE MADRID

FACULTAD DE MEDICINA

TESIS DOCTORAL

Desarrollo de células CAR NK derivadas de sangre de cordón umbilical multieditadas mediante CRISPR/Cas9 para mejorar su persistencia y eficacia frente a Mieloma Múltiple

Development of CRISPR/Cas9 multi-edited cord blood-derived CAR NK cells to improve their persistence and antitumor potential against Multiple Myeloma

MEMORIA PARA OPTAR AL GRADO DE DOCTORA

PRESENTADA POR

Eva Castellano Esparza

DIRIGIDA POR

Joaquín Martínez López

Antonio Valeri Lozano

UNIVERSIDAD COMPLUTENSE DE MADRID

FACULTAD DE MEDICINA

DOCTORADO EN BIOQUÍMICA, BIOLOGÍA MOLECULAR Y BIOMEDICINA

TESIS DOCTORAL

Desarrollo de células CAR NK derivadas de sangre de cordón umbilical multieditadas mediante CRISPR/Cas9 para mejorar su persistencia y eficacia frente a Mieloma Múltiple

Development of CRISPR/Cas9 multi-edited cord blood-derived CAR NK cells to improve their persistence and antitumor potential against Multiple Myeloma

MEMORIA PARA OPTAR AL GRADO DE DOCTOR

PRESENTADA POR

Eva Castellano Esparza

DIRECTORES

Joaquín Martínez López

Antonio Valeri Lozano

Madrid, 2025

A mis padres, Fernando y Lourdes.

A mi hermana, Paula.

A mi compañero de vida, Javi.

AGRADECIMIENTOS

En primer lugar, me gustaría agradecer a todas aquellas madres que han donado y donan sus cordones umbilicales a bancos públicos y a investigación, ayudando a miles de pacientes que realmente necesitan esas muestras y contribuyendo inmensamente al desarrollo de nuevas terapias. Pero, sobre todo, quiero hacer reconocimiento a todos aquellos pacientes de MM que, aun estando pasando por momentos complicados y por múltiples procedimientos médicos, donan de forma altruista sus muestras para que la investigación pueda avanzar. En gran medida, esta tesis es por y para vosotros y ojalá algún día pueda realmente mejorar vuestra calidad de vida.

En segundo lugar, me gustaría agradecer la dedicación de los directores de esta tesis. Joaquín, muchas gracias por haberme permitido realizar esta tesis doctoral en el departamento de Hematología Traslacional, por confiar en que algún día esto podrá ser trasladado a la clínica y por haberme brindado grandes oportunidades aprovechando al máximo esta etapa de formación. Gracias por tu gran optimismo y motivación con los resultados más simples. Antonio, gracias por haber llevado las riendas de este proyecto con tus novedosas ideas y propuestas. A pesar de ser tu *predoc* con más proyectos "back-up" fallidos, al final lo hemos conseguido. Gracias por tus consejos de supervivencia ante situaciones catastróficas o tus guías de viaje para cualquier lugar del mundo. Por último, aunque no figurará nunca en la portada de esta tesis, quiero reconocer mi agradecimiento a Paula, que indiscutiblemente será siempre también co-directora de este proyecto. Gracias por acogerme en el CIEMAT desde el principio como una chica más del FAEDITeam. No hay un "papá científico" sin su "mamá científica" y desde luego tú has demostrado ser la mejor. Gracias por tu optimismo y ambición, por tu paciencia y por tu mediación en situaciones complicadas. Por ayudarnos a desarrollar esta tesis y por siempre sacar un mínimo hueco en tu agenda siempre llena. Y que no vengan ahora comentarios envidiosos, que ambos sabéis que esta tesis no se habría llevado a cabo sin ninguno de los dos…

También quiero agradecer a todo mi equipo del departamento de Hematología Traslacional y de la Unidad de Tumores Hematológicos H12O-CNIO. Todos vosotros, en alguna medida, habéis hecho posible esta tesis. Gracias a las técnicos de laboratorio, en especial a Paqui, toda una experta en amenizar situaciones difíciles y sacar sonrisas, y a las chicas de Biobanco, siempre dispuestas a ayudar en todo y siempre animando la poyata. Gracias los jóvenes pre-doc (o ya no tan pre-docs algunos, pero siempre jóvenes). Roberto, Noemí, Raquel A., Natalia, Alba, MLuz, gracias por compartir penurias, pero también risas y entusiasmo. También al CNIO team, Pedro, Michel, Álvaro y compañía, que siempre saben cómo animar el ambiente y contagian su buen rollo. Gracias a todos, equipo, por toda vuestra ayuda cuando la he necesitado. Gracias también a todos aquellos que me han acompañado estos años en el Hospital 12 de Octubre desde los de

“mito” y los “únicos” que siempre animan cultivos y me ceden pacientemente su tiempo de campana, hasta a Manuel, que estaba ahí tarde tras tarde amenizándome los experimentos y haciendo que las interminables tardes de pre-doc fuesen menos largas. Desde luego, sin todos vosotros estos cinco años no hubiesen sido igual.

Mas concretamente quiero agradecer al team “inmunoterapia”. A Almu, la post-doc polivalente para todo, siempre dispuesta a ayudar y comiéndose los “marrones” de todos los demás. Nunca he conocido a nadie tan persistente como tú con tanto amor por la ciencia y con tan buen corazón. Gracias por toda tu ayuda y por tu paciencia siempre. A mis “ya PhD” compañeras de tesis: Elena y Jessi. Durante tres-cuatro años fuimos una piña inquebrantable para sobrevivir a la tesis. Gracias por estar ahí día tras día, por vuestro apoyo personal, por vuestra ayuda siempre. Gracias por convertiros en amigas y confidentes. En el fondo echo de menos nuestros ratos en la campana de cultivo juntas, calceína tras calceína. Me llena de orgullo ver que estáis allí, en Boston, demostrando en lo buenas científicas que os habéis convertido. Ojalá en algún momento, el tiempo nos vuelva a juntar, porque desde luego, no hay compañeras mejores. Y aunque llegó más tarde, mi Raquel, entró de forma revolucionaria en el laboratorio. Tú también te has convertido en un pilar fundamental que me ha ayudado a sobrellevar esta dura etapa. Mil gracias por tu ayuda y apoyo tanto como “mi” técnico como en la vida personal. Tú también has pasado de ser una compañera, a una verdadera amiga con siempre un cotilleo que “ha llegado a a ti inesperadamente” para contarme, un don para sacarme conversación en mis “antipáticas” mañanas y con siempre un abrazo cuando todo salía mal. Me alegro mucho de que el destino nos haya juntado y de poder cerrar esta etapa predoctoral a tu lado. Gracias a mi Lauri C. por su alegría derrochadora y su optimismo científico, por abrir siempre la puerta de su despacho para echar “una lloradita y a seguir” y por animar cualquier fiesta siempre. A mi Lauri S. también siempre dispuesta a ayudar en todo lo que pueda y ahogar las penas con un buen vinito. A nuestras TFM transitorias Martita y Elena Jr. que llenaron de alegría e ilusión la pecera y estaban siempre ahí para echar un cable. Marta, el unicornio ya es doctor. Por último, también gracias a las recientes incorporaciones, Sandra y Rosa, las niñas que alegran nuestros días con su espíritu joven y sus “chismes” y que siempre tienen tiempo para un desayuno o sobremesa para escuchar pacientemente. La verdad que este último año no hubiese sido tan divertido sin vosotras.

Pero no solo tengo un equipo en el Hospital 12 de Octubre sino también en el CIEMAT, mis chicas del FAEDITeam. Laura U., Bea, Marta, Lucía y Lara, siempre recibiéndome con una sonrisa cuando llegaba al CIEMAT y ayudándome siempre que lo he necesitado, resolviendo todas mis dudas. En especial, quiero agradecer Laura G. por tu gran ayuda técnica en estos últimos años y a Irene, que siempre ha sacado tiempo para nuestro café y ha escuchado pacientemente todos mis

dramas y podcasts. Sois un equipo estupendo y genial y, sin duda, las mejores científicas en edición génica. Gracias por acogerme como una más de "las del Río". Gracias a vosotras y al resto de los jóvenes *ciemateros* por hacerme sentir que el CIEMAT también era mi sitio.

Pero también todos debéis saber que esta tesis no se ha hecho solo en el laboratorio sino también ha sido posible gracias a otras personas que han estado ahí día tras día durante estos años.

Gracias a mis niñas, Paula y Ana, por siempre alardear de vuestra amiga científica, que es muy lista y que algún día ganará un Nobel. Sin duda, sois las mejores compañeras de risas, vinos y vida que podía tener. Gracias a Diego, quién siempre ha aplicado su gran psicología para animarme en momentos duros de estos años y quién por fin podrá llamarme *doctora*. Gracias por esos largos paseos y conversaciones, a veces sin sentido. Gracias a Darío, mi primer compañero de poyata. Aunque juntos formemos un equipo catastrófico, creo que puedo afirmar que eres lo mejor que la Bioquímica me ha dado. Gracias por tu entusiasmo científico siempre, por querer comprender el más mínimo detalle de mi proyecto y animarme a terminarlo. No pierdas nunca esa ilusión investigadora, creo que eres de los pocos que tienen verdadera vocación científica. Y como no, no puedo dejar de agradecer a mi Sandra, que ha estado y estará en todas las etapas de mi vida. Gracias, amiga, por estar ahí siempre en las buenas, en las malas, en las fiestas, en los llantos, en la ciencia y en toda la vida personal.

Gracias a mi familia, por apoyarme incondicionalmente aún sin saber en qué consiste mi trabajo. Gracias a mis tíos Estrella y José por siempre confiar en que lo que hacía valía para algo y animarme a no tirar la toalla. Vuestra "pitagorina" es ahora una "pitagorina doctora". Gracias a mis abuelas, por vuestros "tú vales mucho, que no se te olvide" y tener siempre algo bonito que decirme. Gracias a mi hermana que, aunque no fue elegida, sin duda ha sido la mejor. Gracias por demostrarme que es posible ser la mejor en todo si una se lo propone y gracias por darme a las dos personas que más adoro en este mundo y que me han hacen sonreír y olvidar mis días malos de laboratorio. Y aunque no le adoro tanto (o eso intento hacerle creer), también gracias por darme a "mi hermano postizo" que, al fin y al cabo, ha demostrado ser un cuñado "soportable". En el fondo sabes que te quiero Juan y que nuestros cafés y sándwiches del *Rodilla* me han dado la vida todos estos años. Gracias a Esther, que ya es de mi familia también, por tener siempre un tupper para darme para sobrellevar estos últimos meses duros de escritura, preocupada por si tu hijo no sabía alimentarme en condiciones. Gracias por preguntar día tras día cómo lo llevaba y mandarme un beso por el altavoz. Y, sobre todo, gracias a mis padres, las personas que realmente han hecho esto posible. Gracias por apoyarme y animarme a dedicarme a lo que me gusta, aunque a veces no lo entendáis. Gracias por aguantar mis gritos y malas

maneras, mis agobios o mis tardes aisladas en la habitación con el ordenador. Gracias por alardear siempre de vuestra niña con cualquier persona, pero también por presionarme para que diera el máximo de mí misma en todos los aspectos. En general, mil gracias, por vuestra confianza y paciencia, vuestro apoyo y cariño. Os quiero hasta el infinito.

Y por último, quiero agradecer el apoyo incondicional de aquella persona que llegó para quedarse y ser el mejor compañero de vida. Gracias amor, gracias por tu paciencia infinita todos los días en los que llegaba tarde a casa o tenía que irme un festivo a trabajar. Gracias por amoldar nuestras vacaciones a mis experimentos y por no rechistar cuando tenía que contestar emails. Sé que no lo entiendes ni nunca lo entenderás, pero me has mostrado tu apoyo siempre, sin dudarlo, y eso es lo que te hace especial. Agradezco infinitamente cada una de tus sonrisas, tus abrazos y tus besos en los días buenos, pero también en los malos. Gracias Javi, por hacer mi vida más bonita, por animarme a cumplir todos mis sueños y objetivos y por soñar a mi lado. Esta tesis siempre será de los dos.

En definitiva, gracias a todos por ayudarme a cumplir este objetivo profesional, pero también personal. Os estoy eternamente agradecida.

INDEX

INDEX

LIST OF FIGURES

LIST OF TABLES

RESUMEN

Introducción

El mieloma múltiple (MM) es una neoplasia de células B caracterizada por la proliferación clonal de células plasmáticas anormales (CP) que se acumulan principalmente en la médula ósea (MO). El MM representa el 10-15% de los tumores hematológicos y el 1.8% de todos los tipos de cáncer. A pesar de los avances significativos en el desarrollo de terapias para MM en las últimas décadas, sigue siendo una enfermedad incurable. Por tanto, persiste la necesidad urgente de desarrollar nuevos fármacos y terapias con mecanismos de acción innovadores que puedan superar la profunda inmunosupresión asociada al tumor, especialmente en pacientes con MM en recaída o refractario (MMRR).

A pesar de su impacto revolucionario en el tratamiento de pacientes hemato-oncológicos, la terapia con células CAR T está asociada a toxicidades significativas, procesos de fabricación complejos, largos y costosos, con un control subóptimo de la enfermedad a largo plazo en un número importante de pacientes. Las células CAR NK representan una alternativa prometedora a las CAR T, ofreciendo mayor seguridad, una producción más sencilla y eficiente, a menor coste. Además, la posibilidad de ser aplicadas en un contexto alogénico mejora el acceso a una mayor cantidad de pacientes. No obstante, los estudios preclínicos y los primeros ensayos clínicos han puesto de manifiesto algunos obstáculos de la inmunoterapia CAR NK, como son una limitada persistencia y eficacia, lo que podría afectar a las respuestas clínicas en los pacientes. La presencia de puntos de control inhibitorios inmunes y señales solubles en el microambiente tumoral (TME) inmunosupresor, que es especialmente relevante en fases de progresión del MM, pueden ser responsables de esta reducción en la respuesta terapéutica. Más específicamente, el eje HLA-E/NKG2A, así como la señalización del factor supresor TGF-β, representan dos de estos mecanismos dominantes de resistencia a la terapia CAR NK en este tumor, que podrían ser abordados para mejorar potencialmente la eficacia de esta terapia en MMRR. Asimismo, el desarrollo de estrategias para aumentar la persistencia de las células CAR NK, como la modulación del controlador de la proliferación celular BLIMP1, puede representar una herramienta prometedora para prolongar su persistencia *in vivo* y, por lo tanto, mejorar aumentar su eficacia frente a MM.

Para superar estas limitaciones, la edición genómica utilizando el sistema CRISPR/Cas9 ha surgido como una tecnología versátil para eliminar la expresión de genes involucrados en la resistencia a la terapia CAR NK, y constituye una herramienta potencialmente segura y eficaz que permite abordar de manera directa y simultánea los diferentes obstáculos a los que se enfrenta la terapia CAR NK y generar productos inmunoterapéuticos más eficientes para MMRR.

Objetivos

El objetivo principal de esta tesis es la aplicación de la herramienta de edición genómica CRISPR/Cas9 para mejorar la eficacia terapéutica de células CAR NK derivadas de sangre de cordón umbilical (CB) contra el MM. Específicamente, nuestro objetivo es generar nuevos productos CAR NK editados mediante la interrupción combinada de *KLRC1* (que codifica para la proteína NKG2A) y *TGFBR2*, o la eliminación de *PRDM1* (que codifica para BLIMP1) para aumentar la eficacia y la persistencia de estos efectores, respectivamente. Además, proponemos una estrategia de edición génica múltiple que combine estas dianas simultáneamente para generar un producto CAR NK de nueva generación, con una actividad antitumoral optimizada contra MM.

Resultados

Nuestros resultados demuestran que la interrupción combinada de *KLRC1* y *TGFBR2* en células CAR CB-NK expandidas *in vitro* es factible y reduce eficazmente la expresión de los receptores NKG2A y TGF-βRII sin afectar ni la expresión de la molécula CAR ni la proporción de células CAR NK citotóxicas $CD16^{+}$. El doble knock-out (KO) disminuye transitoriamente la viabilidad, aunque se restaura con el tiempo en cultivo. La interrupción de *KLRC1* y *TGFBR2* mejora el potencial citotóxico de las células CAR NK contra MM y les confiere resistencia a la inhibición mediada por TGF-β *in vitro*. Además, los estudios *in vivo* demuestran que las células CAR NK doble KO tienen mayor capacidad para controlar el crecimiento tumoral que las células no editadas. A pesar de no inducir cambios importantes en el inmunofenotipo o en el perfil de expresión génica, resultados preliminares sugieren que la interrupción de *KLRC1* y *TGFBR2* aumenta la señalización intracelular integrada y la expresión de granzima B, lo que podría justificar, en parte, el mayor potencial antitumoral de estos efectores. Sin embargo, la interrupción génica combinada reduce la capacidad de expansión *in vitro* de las células CAR NK, que podría estar relacionada con una mayor cantidad de daño por dobles roturas en el ADN. Esta respuesta celular puede comprometer la obtención de dosis clínicas del producto y limitar la persistencia a largo plazo y la eficacia antitumoral, como demostramos en nuestro modelo *in vivo* de MM.

La eliminación de *PRDM1* en los efectores CAR NK incrementa su potencial de expansión *in vitro,* confiriéndoles una mayor capacidad proliferativa y retrasando la inducción de senescencia en estas células, sin afectar la viabilidad de los cultivos. Es importante señalar que la ventaja proliferativa es limitada en el tiempo, lo que podría reducir el riesgo de oncogénesis. La interrupción de *PRDM1* induce múltiples cambios inmunofenotípicos y transcriptómicos en las células, lo que confirma el papel de BLIMP1 como un importante regulador no solo del ciclo celular, sino también de múltiples vías adicionales. En general, las células *PRDM1* KO CAR NK

presentan un perfil más inmaduro y proliferativo, con una mayor expresión de receptor α de IL-2 (IL-2Rα) y un aumento de receptores y ligandos que podrían favorecer su migración a los órganos linfáticos secundarios. Estos efectores editados también presentan cambios en la expresión de receptores NK activadores e inhibidores, mayor expresión del CAR y sobreexpresión de algunos genes asociados con la señalización de IFN-γ y TNF-α. Sin embargo, a pesar de estos cambios, mantienen su actividad citolítica y su capacidad de secreción de citoquinas y proteínas citotóxicas contra líneas celulares de MM. Por lo tanto, la interrupción de *PRDM1* mediante CRIPSR/Cas9 parece ser un enfoque eficiente y seguro para aumentar la persistencia de las células CAR NK sin comprometer su capacidad antitumoral.

Finalmente, generamos un producto CAR NK triple KO para combinar las ventajas de la interrupción de *KLRC1*, *TGFBR2* y *PRDM1* en un abordaje simultáneo. La nucleofección en un solo paso (o "*one-shot*") de las tres sgRNAs en las células CAR NK mostró una interrupción génica eficiente y una reducción de la expresión de estas proteínas, pero no logró mejorar su expansión *in vitro,* que se podría asociar a una reducción importante de la viabilidad celular y una alta acumulación de daño en el ADN. El diseño de una estrategia de nucleofección secuencial en dos pasos superó esta limitación, permitiendo la generación de efectores triple KO con altas eficiencias de edición y un mayor potencial de expansión. La edición génica múltiple utilizando estas sgRNAs específicas en combinación con la nucleasa HiFi, no mostró eventos de edición fuera de la diana en los *loci* predichos, ni indujo la generación de reordenamientos cromosómicos detectables o aneuploidías. Las células CAR NK triple KO muestran el mismo potencial proliferativo que las células *PRDM1* KO y tienen una menor inducción de senescencia comparado con las células sin editar. Su inmunofenotipo y perfil de expresión génica son muy similares a los de las células *PRDM1* KO, pero estos cambios no comprometen su actividad antitumoral. Los efectores triple KO son tan citotóxicos como los doble KO contra líneas celulares de MM e incluso contra CP primarias de pacientes de MM *in vitro*. Sin embargo, cuando se ensayaron *in vivo*, las células CAR NK triple KO superaron a los efectores doble KO tanto en términos de persistencia como de eficacia, ya que fueron capaces de eliminar completamente las células de MM y curar al 40% de los animales.

Conclusiones

La interferencia combinada de los ejes NKG2A/HLA-E y TGF-β mediante la edición génica CRISPR/Cas9 mejora la eficacia de las células CAR NK contra MM *in vitro* e *in vivo* y supera la inhibición mediada por TGF-β, sin alterar la expresión de CAR o la proporción de células citotóxicas, activando señales intracelulares que desencadenan las respuestas citolíticas. Sin

embargo, la interrupción simultánea de estos dos genes limita la capacidad de expansión de las células CAR NK.

La eliminación de *PRDM1* representa un enfoque potencialmente seguro y eficiente para aumentar la capacidad de expansión de las células CAR NK sin comprometer su eficacia antitumoral contra MM.

Una estrategia integradora que combina las aproximaciones anteriores permite generar un producto CAR NK multi-editado de nueva generación, que presenta un mayor potencial de expansión, persistencia y capacidad antitumoral contra MM, con mínimo riesgo de generar eventos de edición fuera de la diana, grandes alteraciones estructurales cromosómicas o inducir oncogénesis en los animales tratados.

ABSTRACT

Introduction

Multiple myeloma (MM) is a B-cell malignancy characterized by the clonal proliferation of abnormal plasma cells (PC) that accumulate predominantly in the bone marrow (BM). It accounts for 10-15% of hematologic tumors and 1.8% of all cancers. Despite significant advancements in MM therapies over recent decades, it remains an incurable disease. This underscores the critical need to develop novel drugs and therapies with distinct mechanisms of action that can overcome the severe tumor-associated immunosuppression, especially for relapsed or refractory MM (RRMM) patients.

Despite its groundbreaking impact in the treatment of hemato-oncologic patients, CAR T cell therapy is associated with significant toxicities, complex and long manufacturing processes, high costs, and a suboptimal long-term disease control in a significant number of patients. In contrast, CAR NK cells have emerged as a promising alternative, offering improved safety, easier production and better cost-effectiveness. In addition, the possibility of being applied in an allogeneic setting enhances accessibility for a broader range of patients. Nevertheless, preclinical studies and early clinical trials have highlighted challenges with CAR NK immunotherapy, including limited persistence and efficacy, which could impact clinical outcomes in the patients. The presence of inhibitory immune checkpoints and soluble factors in the immunosuppressive tumor microenvironment (TME), especially remarkable at progression in MM, may be responsible of the reduced therapy responses. More precisely, HLA-E/NKG2A axis as well as TGF-β signaling represent two of these dominant mechanisms of CAR NK resistance in this tumor, which could be targeted to potentially improve the efficacy of CAR NK immunotherapy in RRMM. Furthermore, strategies to augment the short lifespan of these effectors, such as targeting BLIMP1 cell proliferation controller, depict a promising tool to prolong their *in vivo* persistence and, hence, enhance their antitumor potential.

To overcome these limitations, CRISPR/Cas9 genome editing has emerged as a flexible technology to disrupt the expression of genes involved in CAR therapy resistances, offering a potentially safe and effective tool to directly and simultaneously address different CAR NK challenges and generate more efficient immunotherapeutic products for RRMM.

Objectives

The main objective of this thesis is the application of CRISPR/Cas9 genome editing tool to improve the therapeutic efficacy of cord blood (CB)-derived α-BCMA CAR NK cells against MM. Specifically, we aim to generate new gene-edited CAR NK products by the combined disruption of *KLRC1* (encoding for NKG2A) and *TGFBR2* or the knock-out of *PRDM1* (encoding for BLIMP1)

to increase CAR NK cytolytic capacity and persistence, respectively. In addition, we propose a multiplex gene editing strategy combining these targets simultaneously to generate a next-generation triple-edited CAR NK product with optimized antitumor activity against MM.

Results

Our results demonstrate that combined disruption of *KLRC1* and *TGFBR2* in *in vitro* expanded CAR CB-NK cells is feasible and efficiently reduces the surface expression of NKG2A and TGF-βRII receptors without affecting CAR expression, or the proportion of cytotoxic $CD16^{+}$ CAR NK cells. Double knock-out (KO) transiently decreases viability but it is later restored. *KLRC1* and *TGFBR2* disruption improves CAR NK cytotoxic potential against MM and renders CAR NK cells resistant to TGF-β-mediated inhibition *in vitro*. Additionally, *in vivo* studies demonstrate that double KO CAR NK cells have increased ability to control tumor growth than non-edited counterparts. Despite not inducing important changes in NK cell immunophenotype or gene expression profile, preliminary results demonstrate that *KLRC1* and *TGFBR2* disruption augment intracellular kinase integrated signaling and granzyme B production, which could partially explain the higher antitumor potential of these double KO effectors. However, combined gene disruption lessens CAR NK expansion capacity *in vitro*, which could be related to a higher double-strand break (DSB) DNA damage. This cellular response may compromise clinical dose achievement and limit long-term persistence and antitumor efficacy, as was demonstrated in our *in vivo* MM model.

PRDM1 ablation in CAR NK effectors resulted in an enhanced *in vitro* expansion potential of these cells, conferring them with a higher proliferation capacity and delaying NK senescence induction without affecting viability of cell cultures. Importantly, proliferative advantage is limited over time, which reduce potential oncogenic risks. Disruption of *PRDM1* induced multiple immunophenotypic and transcriptomic changes, confirming the role of BLIMP1 as a master regulator not only of cell cycle but also of other multiple pathways. In general, *PRDM1* KO CAR NK cells showed a more immature and proliferative profile with increased IL-2 receptor α (IL-2Rα) expression and upregulation of receptors and ligands that may favor their migration to secondary lymph organs. These cells also showed changes in the expression of activating and inhibitory NK cell receptors, higher CAR expression and overexpression of some genes associated with IFN-γ and TNF-α. However, besides these changes, they maintain their antitumoractivity and their cytokine and cytolytic protein secretion against MM cell lines. Therefore, *PRDM1* disruption seems to be an efficient and safe approach to boost CAR NK cell persistence without compromising antitumor capacity.

Finally, we generated a triple KO CAR NK product to combine the benefits of disrupting *KLRC1*, *TGFBR2* and *PRDM1* in a simultaneous approach. *One-shot* nucleofection of the three sgRNAs in CAR NK cells showed efficient gene disruption and reduced protein expression but failed to potentiate CAR NK *in vitro* expansion, which could be attributed to a prominent reduction of cell viability and high DNA damage accumulation in the cells. A two-step sequential nucleofection approach overpassed this shortcoming allowing the generation of triple KO effectors with high editing efficiencies and improved expansion potential. Multiplex gene editing using specific sgRNAs in combination with HiFi nuclease did not show off-target editing events in predicted loci or induced the generation of detectable chromosomal rearrangements or aneuploidies. Triple KO CAR NK cells show the same proliferative potential as *PRDM1* KO counterparts and both populations exhibit decreased senescence induction compared to non-edited cells. Immunophenotype and gene expression profile of triple KO CAR NK cells is highly similar to *PRDM1* KO cells but, importantly, additional gene ablation does not compromise CAR NK cell antitumor potential. Triple KO effectors are as cytotoxic as double KO against MM cell lines and even primary PC from MM patients *in vitro*. However, when analyzed *in vivo*, triple KO CAR NK cells outperform double KO effectors in terms of both persistence and efficacy, being able to even completely eliminate MM cells and cure 40% of the animals.

Conclusions

Combined targeting of NKG2A/HLA-E and TGF-β axes using CRISPR/Cas9 genome editing improves CAR NK efficacy against MM *in vitro* and *in vivo* and overcomes TGF-β mediated inhibition without altering CAR expression or the percentage of $CD16^+$ CAR NK cells but activating intracellular signaling mediating killing responses. However, double gene disruption impairs cell expansion capacity.

PRDM1 ablation represents a potentially safe and efficient approach to increase CAR NK expansion ability without compromising their antitumor capacity against MM.

An integrative approach combining these two strategies results in a next-generation multi-edited CAR NK product with increased expansion potential, persistence and high antitumor efficacy against MM, with low risk of producing potential off-target editing events, large chromosomal structural alterations or inducing oncogenesis in mice.

INTRODUCTION

1. Multiple Myeloma

1.1. Definition and general aspects

Multiple myeloma (MM) is a clonal B cell malignancy characterized by the aberrant proliferation and accumulation of malignant plasma cells (PC) mainly in the bone marrow (BM). These tumor plasma cells produce high amounts of a monoclonal immunoglobulin (Ig), usually IgG (50-60% of patients) or IgA type (30%), which is also known as M protein or monoclonal component[1,2] (**Figure 1**). In most MM subjects, a complete Ig is secreted. However, around 15-20% of patients have light-chain MM, which is characterized by secretion of κ or λ light chains (LC) instead of a complete Ig. Free light chains (FLC) are smaller in size and can be released in urine, which is known as Bence-Jones proteinuria[3,4]. Around 2-3% of the cases course a non-secretory MM, in which any monoclonal component can be detected in blood or in urine[5]. Although in most of the patients a specific monoclonal Ig or FLC is secreted, it has been also reported the existence of biclonal MM (3-6% of the cases) in which two different monoclonal components can be detected[6].

Clinical manifestations of MM are hypercalcemia, renal failure, bone lesions, anemia, and recurrent infections derived from a severe immunosuppression in the BM[1,2]. Therefore, this tumor was termed “multiple myeloma” referring to a malignancy that has bone marrow origin (“myeloma”) and affects different parts of the axial skeleton (“multiple”) such as the vertebral column, ribs, pelvis, and skull, among others[7].

Usually, MM develops from a premalignant status known as monoclonal gammopathy of undetermined significance (MGUS) or from an asymptomatic or smoldering MM (sMM)[1,8]. In late stages of the disease, MM plasma cells can become independent from bone marrow niches and exert to the bloodstream progressing to plasma cell leukemia (PCL) which is characterized by the presence of ≥ 5% of circulating plasma cells[1,9].

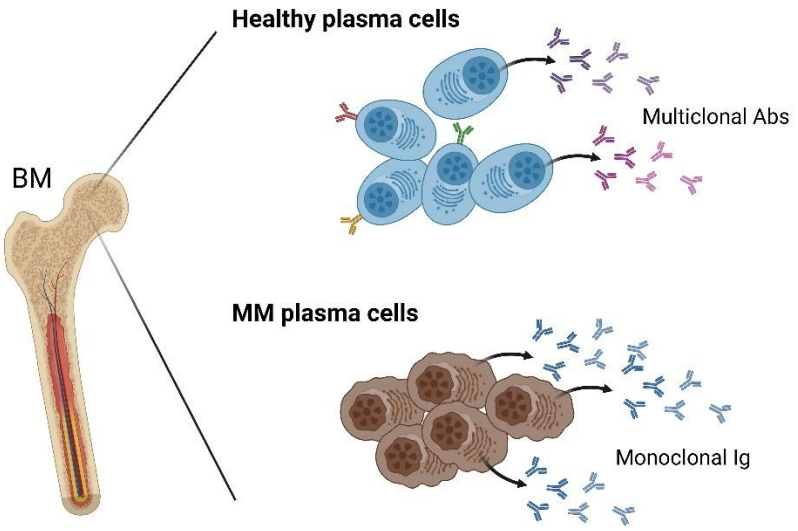

Figure 1. Malignant MM plasma cells secrete monoclonal immunoglobulins. BM: bone marrow; Abs: antibodies; MM: multiple myeloma; Ig: immunoglobulin. Adapted from © 2024 Terese Winslow LLC. Created with BioRender.com.

1.2. Epidemiology

MM is the second most common hematological malignancy after non-Hodgkin lymphoma and represents 10-15% of hematological cancer cases[10,11]. According to the Global American Cancer Society and the National Cancer Institute, MM age standardized incidence rate is 1.8 per 100,000. About 35,780 new MM cases will be diagnosed in 2024, representing 1.8% of all new cancer cases in US[11-13]. In Spain, the *Asociación Española Contra el Cancer* registered around 3500 newly diagnosed patients in 2023[14].

Median age at diagnosis for MM is 69 years. Most of the patients are diagnosed over the age of 65 years (32.2% are diagnosed at 65-74 years, 24.1% at 75-84 years and 8.5% at >85 years). Around 32% of patients are between 45-64 years old and only 3.1% of patients are diagnosed before 44.

The 5-year relative survival for MM patients, calculated between 2014-2020, is 61.6%. Age-standardized mortality is 1.1 per 100,000. Approximately 12,540 deaths, which correspond to 2% of all cancer deaths in the US, are expected to occur because of this disease. In Spain, 1,970 deaths were recorded in 2023. Median Age at death is 76 years old[10-12].

MM is slightly more common in men than women (8.7 vs 5.9 age-adjusted incidence rates for males and females, respectively)[11,12]. Regarding ethnicities, it has been reported a higher incidence in African-American people compared to Caucasians[1,15,16].

1.3. Etiology

No direct causal etiology has been defined for MM. However, environmental factors, autoimmune and inflammatory conditions, and hereditary factors have been associated with the development of this disease[10].

Direct exposure to chemicals such as pesticides used in farming[15,17], engine exhausts[18], hair dyes[19], and organic solvents like benzene and toluene[20] have been reported as risk factors for MGUS and MM development. However, these evidences are still controversial. Other studies have associated exposure to radiation doses higher than 4Gy with MM appearance[21-24].

Obesity has also been correlated with an increased MM incidence[25-29] although other studies have discarded that it negatively impacts on patient outcomes[30,31].

Other risk factors such as autoimmune diseases[32,33] and chronic antigen stimulation produced by viruses such as Hepatitis B (HBV)[34], Hepatitis C (HCV), and Human Immunodeficiency Virus (HIV)[35], have been described for MGUS and MM development. In fact, recent studies in our group demonstrated that by eradicating HCV infection, some MM patients can be controlled or even cured[36]. In line with this, 33% of sporadic MGUS patients produce monoclonal Igs that specifically bind to lysolipids from Gaucher's disease, suggesting that chronic stimulation by this kind of lipids also plays a significant role in MM appearance[37,38].

Finally, although MM is considered a sporadic disease, some studies have observed familial aggregation of MM and MGUS, with increased MM risk among individuals with a family history of plasma cell disorders. Some genome-wide association studies (GWAS) have identified germline variations and polymorphisms in more than 20 risk loci for MM[39-43].

1.4. Physiopathogenesis

Normal PCs originate from hematopoietic progenitor stem cells (HSPCs), which undergo several rounds of differentiation in the bone marrow and secondary lymphoid organs to immature B cells and eventually to PC. When exposed to an antigen, VDJ rearrangements take place in immature B cells generating a diverse primary Ig repertoire. B cells with an IgH-IgL complex (B cell receptor; BCR) on the surface migrate to secondary lymphoid organs where they undergo processes such as affinity maturation, somatic hypermutation, and class-switch recombination to produce highly specific and avid antibodies. In the germinal center, B cells eventually can differentiate into mature antibody-producer cells[44].

Clonal MM PCs derive from post-germinal center (GC) B cells. Double-strand DNA breaks in the Ig loci are required during class-switch recombination and somatic hypermutation, and if they

are not properly repaired, they can induce off-target mutations and rearrangements that provide cells with a growth advantage, leading to the oncogenic transformation of B cells into clonal and malignant PC (**Figure 2**)[2,10,44].

As it was aforementioned, MM usually progresses from an MGUS state. During the early stages of the disease and MGUS onset, primary cytogenetic events occur in post-GC B cells. These primary events comprise either hyperdiploidy of the odd-numbered chromosomes 3, 5, 7, 9, 11, 15, 19 and 21 or translocations involving the IgH locus on chromosome 14 such as t(4;14), t(11;14), t(6;14), t(8;14), t(14;16) and t(14;20) which lead to overexpression of *NSD2/FGFR3*, *CCDN1*, *CCDN3*, *MYC*, *MAF* and *MAFB*, respectively[2,10,16,44,45]. Translocations involving the IgL locus leading *MYC* dysregulation have also been reported in 10% of MM patients and are associated with poor prognosis[46].

Secondary genetic events such as copy number abnormalities, DNA hypomethylation, and acquired mutations appear in later stages of the disease and are associated with MGUS progression to symptomatic MM and even PCL. They confer a competitive advantage on malignant PC in the bone marrow niche and at final stages, they can provide tumor PC the ability to migrate out of the BM niche thus developing a PCL. Principal secondary events include losses of chromosomes 13q, 1p32 or 17p, gains of 1q21, MYC-associated translocations and somatic mutations that generally affect driver genes such as *MYC*, *TP53*, *BRAF*, *KRAS*, *NRAS* and *DIS3* and, consequently alter key MM signaling pathways like RAS-MAPK, nuclear factor-κB (NF-κB) and PI3K-AKT[2,10,16,44,46]. Point mutations in DNA repair genes like *ATR*, *ATM,* and *ZFHX4* have also been reported in 15% of MM patients[47]. Epigenetic changes such as DNA hypomethylation (i.e. *P16*, *MGMT*, *DAPK*, *E-cadherin*, *CDKN,* and *INK* family genes), post-translational modifications (histone methylation or acetylation) or altered mi-RNA expression are also frequent during MM evolution[16,44,48,49].

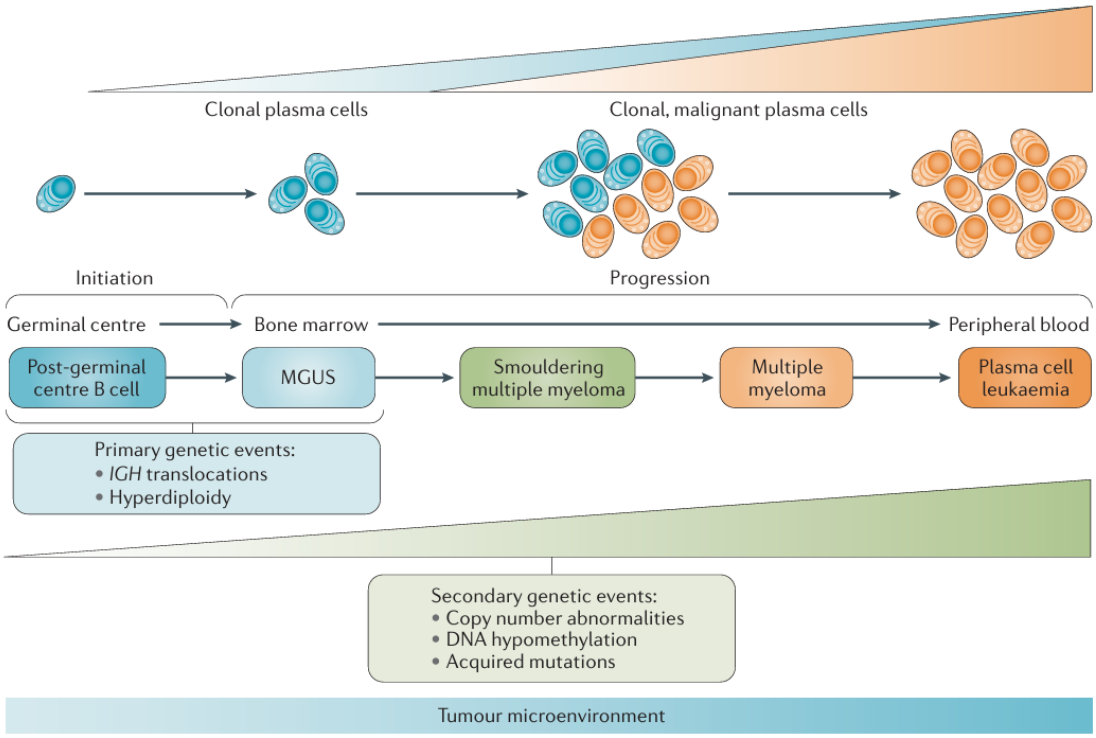

Figure 2. Clonal evolution of MM plasma cells. During initial stages of the disease and MGUS onset, primary cytogenetic events occur in post-germinal center B cells that provide them with a clonal advantage. As disease progresses, secondary genetic events appear and accumulate in MM plasma cells, leading to a competition selection for bone marrow niche. MGUS: monoclonal gammopathy of unknown significance; IGH: immunoglobulin heavy chain locus. Obtained from Kumar et al. Nat Rev Dis Primers, 2017[2].

Although genetic modifications are necessary for MM pathogenesis and influence in MM disease progression and therapy response, other factors such as the BM microenvironment play an important role in MM development, aggressiveness and drug resistance (**Figure 3**).

MM PCs interact with BM mesenchymal stromal cells (MSCs) within the BM niche through adhesion molecules such as VCAM/VLA-4, MUC-1/ICAM and CD40/CD40L, among others. These interactions promote secretion of interleukin (IL)-6, IL-10, IL-8, TNFα (tumor necrosis factor α) and IGF-1 (insulin like growth factor 1) that support the continuous adhesion, growth and proliferation of MM PCs. In response to IL-6, MM PCs secrete VEGF (vascular endothelial growth factor) and bFGF (basic fibroblast growth factor) which bind to their receptors in MSCs and restimulate IL-6 production. These growth factors also interact with their receptors in BM endothelial cells, promoting tumor angiogenesis and autocrine and paracrine loops that enhance MM PC survival. Moreover, MSCs secrete other factors such as SDF-1 (stromal cell-derived factor 1, also known as CXCL12) that binds to CXCR4 receptor in MM promoting their migration to the BM niche and exosomes containing proteins and miRNAs that promote MM cell proliferation and possibly mediate drug resistance[16,48,50].

MM PCs also interfere with osteoclastic activity. Under physiological conditions, bone formation is regulated by RANK (receptor activator for NFκB)-RANKL (RANK ligand)-OPG (osteoprotegerin) pathway that controls osteogenic activity of MSC-derived osteoblasts and osteolytic activity of osteoclasts. However, this balance is altered during MM progression. Interactions between MM PCs and MSCs via VLA-4/VCAM impair OPG/RANK binding and induce secretion of several ILs and activating factors such as MIP1α (macrophage inflammatory protein 1 α or CCL3) and MIP1β (or CCL4) by PCs. These chemokines are responsible for increased RANKL release in the BM niche leading to osteoclast activation and inhibition of osteoblast differentiation. Higher osteoclast activity promotes the secretion of IL-6, IGF-1 and TGF-β (transforming growth factor β) which sustains this aberrant loop. Because of interaction with MM PCs, MSCs acquire epigenetic alterations (mainly affecting *RUNX2*) that stimulate their proliferation and impair osteoblast differentiation. Malignant PCs also secret DKK1 (Dickkopf-related protein 1) and FRP2 (Frizzled-related protein 2) which are inhibitors of WNT signaling pathway that suppress osteoblast activity. Sclerostin produced by both osteocytes and MM PCs inhibits bone formation by altering interactions between bone morphogenetic proteins to their ligands. In summary, these disbalanced interactions within the BM microenvironment lead to an excessive activation of bone-resorbing osteoclasts and inhibition of bone-repairing osteoblasts resulting in hypercalcemia, bone pain, and even bone fractures which are hallmark symptoms of MM pathogenesis[10,16,50-52].

Within the BM niche, there is also a disbalance in the immune environment, especially associated with progression stages. High levels of IL-6, VEGF, and TGF-β promote expansion of immunosuppressive $CD4^+$ Tregs, tumor-associated macrophages (TAMs), and myeloid-derived suppressor cells (MDSCs). Inhibitory signals from MM PCs (increased HLA-I and HLA-E expression[53,54], impaired antigen processing[55], increased expression of PD-L1 and CD80/86[56,57]) together with these immune-repressor cells inhibit cytotoxic activity of $CD8^+$ T and NK cells. As a result, they create a pro-tumoral environment for the MM cells and a hostile context for immune effectors, reducing the efficacy of immunotherapy treatments as it will be described in more detail later[10,16,51]. Remarkably, as disease progresses malignant PCs become more proliferative, being less dependent on inflammation factors such as IL-6 and TGF-β and downregulate critical pathways of IFN-γ (interferon γ) and TNF-α (tumor necrosis factor α) signaling, to avoid immunosurveillance[58].

In late stages of the disease, tumor microenvironment (TME) becomes hypoxic and, as a response, MM PCs reduce expression of CXCR4 receptor and lose interactions with MSCs. This favors the egression of MM cells to the bloodstream causing extramedullary disease (EMD)[59].

In conclusion, combined cytogenetic and genetic alterations together with cell-cell interactions in the BM niche, determine MM onset, pathogenesis, progression, and even therapy resistances.

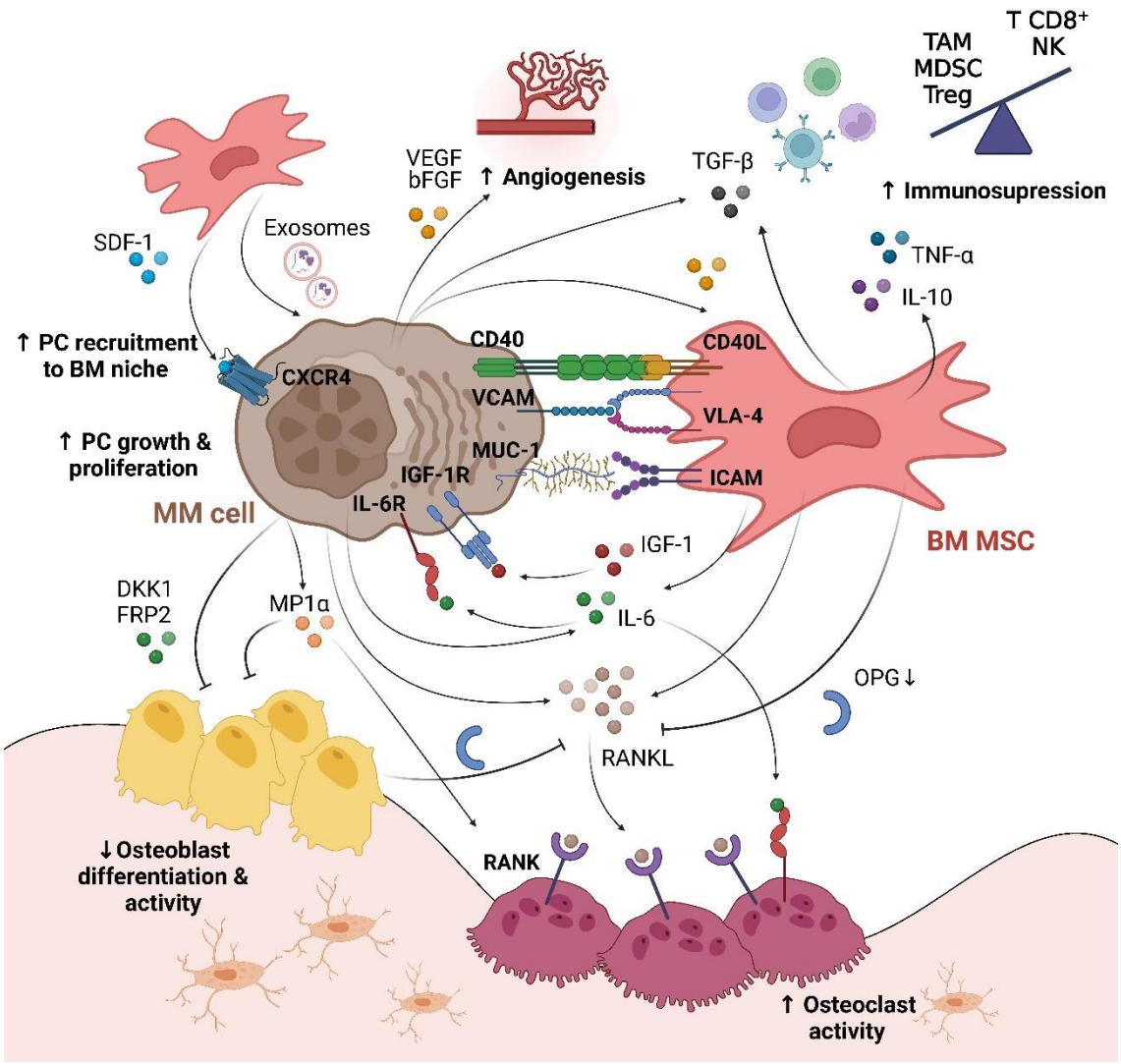

Figure 3. Interactions in the BM niche during MM development. PC: plasma cell; BM: bone marrow; MM: multiple myeloma; BM MSC: bone marrow mesenchymal stromal cell; VEGF: vascular endothelial growth factor; bFGF: basic fibroblast growth factor; SDF-1: stromal cell-derived factor 1; TGF-β: transforming growth factor β; TAM: tumor-associated macrophage; MDSC: myeloid-derived suppressor cell; Treg: regulatory T cells; NK: natural killer; TNF-α: tumor necrosis factor α; IL: interleukin; CXCR4: CXC chemokine receptor 4; VCAM: vascular cell adhesion protein; MUC-1: mucin 1; IL-6R: IL-6 receptor; IGF-1: insulin-like growth factor 1; IGF-1R: insulin-like growth factor 1 receptor; CD40L: CD40 ligand; VLA-4: very late antigen-4; ICAM: intercellular adhesion molecule 1; DKK1: Dickkopf-related protein 1; FRP2: Frizzled-related protein 2; MP1-α: macrophage inflammatory protein 1 α RANK: receptor activator for nuclear factor κ B; RANKL: RANK ligand; OPG: osteoprotegerin. Adapted from Palumbo and Anderson, N Engl J Med, 2011[52]. Created with BioRender.com.

1.5. Clinical manifestations

The main MM clinical symptoms are known as CRAB which stands for hypercalcemia, renal failure, anemia, and bone lesions, and are considered MM-defining events (MDE) during diagnosis[1]. These clinical manifestations are mainly due to the accumulation of MM PCs in BM and other tissues and the high release of the monoclonal Igs.

Hypercalcemia (>11 mg/dL) and bone disease (bone pain and pathological fractures) are a consequence of the enhanced osteoclast activity and bone resorption enhanced by MM PCs and MSCs[60]. Lytic lesions can be detected by imaging and are present in >80% of MM patients at diagnosis being more prevalent during stages of relapse[61].

Renal failure (creatinine clearance <40 mL/min or serum creatinine >2 mg/dL) appears in up to 40% of MM patients due to hypercalcemia and the accumulation of Ig LC secreted by MM cells. Accumulation of calcium precipitates decreases glomerular filtration rates and aggregation of LCs forms urinary casts in the glomeruli and renal tubes causing LC cast nephropathy (LCCN). Additionally, the use of nephrotoxic medications usually complicates MM renal failure[10,62,63].

Normocytic and normochromic anemia characterized by low levels of hemoglobin (>2 g/dL lower than limit of normal levels) is another hallmark MM symptom affecting 70-85% of MM patients. It results from a BM replacement by MM PCs and an increase in MIP1α (CCL3) secretion that suppress HSPCs. Decreased erythropoietin (EPO) production due to renal impairment also contributes to anemia development[10,64,65].

Although not considered as a MDE, most of MM patients (75%) at diagnosis have impaired immune responses to viral and bacterial infections caused by T cell dysfunction and changes in B cell compartment and lack of one or more Igs (immunoparesia)[10,66]. Of note, infection risk is increased due to secondary neutropenia induced by typical MM treatments such as bortezomib (BTZ), melphalan, and stem cell transplant[67,68]. Moreover, recurrent infections are the main cause of MM deaths[69].

Finally, EMD is a very aggressive form of MM in which tumoral PCs become independent from the BM and invade other organs. Plasmacytomas can appear in virtually any area of any tissue in the body. At diagnosis, EMD incidence is low (0.5-5%) and MM PCs are usually localized in skin. However, EMD is reported in 3-15% of MM patients who relapse and usually involves the liver, kidneys, lymph nodes, central nervous system (CNS), breast, pleura, or pericardium[70,71].

1.6. Diagnosis, patient classification and prognosis

As MM clinical symptoms are similar to other illnesses, this disease and its premalignant stages are usually discovered by chance in routine blood and urine tests, including hemogram, biochemistry and protein studies. When the results of these tests suggest a possible MM case, imaging studies (whole-body positron emission and computed tomography (PET-CT) or magnetic resonance imaging (MRI)) are performed to identify possible bone lesions and BM aspirates are extracted for their study. BM analysis includes cytogenetics for the detection of translocations, trisomies and deletions and flow cytometry analysis for determination of malignant PC[1,16,72-75]. MM PCs are commonly immunophenotypically defined as $CD138^+$ $CD38^+$ $CD19^-$, similar to normal PCs, but with aberrant expression of CD56, CD117 (favorable prognosis) and/or CD81 (poor prognosis) and loss of CD45 expression[76-79].

In most cases MM is preceded by a MGUS premalignant state that is clinically diagnosed by serum M protein concentration <3 g/dL, abnormal free LC ratio (<0.26 or >1.65), and the presence of <10% clonal PCs in the BM. MGUS occurs in 5% of the individuals over the age of 50 and incidence increases with age. Approximately 1% of the patients per year with MGUS will progress to MM.

As MGUS progresses along the pathway to MM it usually passes through a sMM state which is defined as higher serum M protein concentration (>3 g/dL) and BM clonal plasmacytosis (10-60% PCs) but in the absence of MDE. During the first 5 years following diagnosis, the risk of progression to active MM is about 10% per year, although the Ig subtype, the percentage of BM PCs, or the presence of certain cytogenetic abnormalities can accelerate progression to MM[8,10,16,80,81].

Since 2014, active MM diagnosis requires the presence of at least one MDE in addition to evidence of ≥10% clonal PC infiltration in BM or a biopsy-proven plasmacytoma. MDE consist of any of the CRAB symptoms or the presence of any of these three biomarkers: ≥60% of clonal PC in BM, serum free LC ratio ≥100, or more than one focal lesion (>5mm) on MRI (commonly known as SLiM criteria)[1,74].

Disorder	Disease definition and criteria
MGUS	Requires all the following: • Serum monoclonal protein (non-IgM type) <3 g/dL • Clonal bone marrow PC <10% • Absence of MDE such as CRAB and SLiM
sMM	Requires all the following: • Serum monoclonal protein ≥3 g/dL or urinary monoclonal protein ≥500 mg/24h and/or clonal bone marrow PC 10-60%. • Absence of MDE such as CRAB and SLiM
MM	Requires both of the following: • Clonal bone marrow PC ≥10% or biopsy-proven plasmacytoma. • Any or more of the following MDE: ○ Evidence of any of CRAB symptoms ○ Evidence of any of the SLiM biomarkers
PCL	Requires both of the following: • Meets diagnostic criteria for MM • Presence of ≥5% circulating PC

Table 1. International myeloma working group diagnostic criteria for multiple myeloma and related plasma cell disorders. MGUS: monoclonal gammopathy of undetermined significance; sMM: smoldering MM; MM: multiple myeloma; PCL: plasma cell leukemia; PC: plasma cell; MDE: myeloma defining events; CRAB: hypercalcemia, renal insufficiency, anemia and bone lesions; SLiM: ≥60% of clonal PC in bone marrow, serum free light chain ratio ≥100 and more than one focal lesion (>5mm) on magnetic resonance imaging. Table adapted from Rajkumar, Am J Hematol. 2024[1].

In 2005, the International Staging System (ISS) was proposed to stratify MM patients at diagnosis and estimate their prognosis considering serum albumin and serum β2-microglobulin (B2M) levels. However, ten years later, a revision of the ISS (R-ISS) was proposed including LDH values and high-risk cytogenetics to the prior classification. Following this system, patients are stratified into 3 different groups (**Table 2**)[1,10,82].

R-ISS stage	Characteristics
I	Requires all the following: • Serum albumin ≥3.5 g/dL • Serum β2-microglobulin <3.5 mg/L • No high-risk cytogenetics • Normal serum LDH levels
II	No fitting stage I or III criteria
III	Requires both of the following: • Serum β2-microglobulin >5.5 mg/L • High-risk cytogenetics [t(4;14), t(14;16) or del(17p)] or elevated LDH levels

Table 2. R-ISS staging system for MM patients. ISS: international staging system; LDH: lactate dehydrogenase. Data from Palumbo et al. J Clin Oncol. 2015[82].

In 2022, a new revision of this R-ISS staging was proposed, the R2-ISS, including two other cytogenetic risk features and better classifying intermediate-risk patients. This system

punctuates patients based on the presence of certain risk factors and, depending on the score, they are classified into 4 groups. Median overall survival (OS) and progression-free survival (PFS) are estimated for each group (**Table 3**)[1,10,83,84].

Risk Factor	Score
ISS-III	1.5
ISS-II	1
Del(17p)	1
t(4;14)	1
High LDH	1
1q+	0.5

R2-ISS Stage (risk)	Score	OS (months)	PFS (months)
I (low)	0	Not reached	68
II (intermediate-low)	0.5-1	109.2	45.5
III (intermediate-high)	1.5-2.5	68.5	30.2
IV (high)	3-5	37.9	19.9

Table 3. R2-ISS staging system for MM patients. ISS: international staging system; LDH: lactate dehydrogenase; OS: overall survival; PFS: progression-free survival. Data from D'Agostino et al. J Clin Oncol. 2022[84].

1.7. Treatments for newly diagnosed MM patients

Currently, front-line treatments for newly diagnosed MM (NDMM) patients are based on autologous stem cell transplant (ASCT) eligibility.

Patients are considered for ASCT based on their physical conditions, age, and comorbidities. Eligible patients receive 3-4 cycles of induction therapy prior to stem cell collection. Commonly used induction therapies are: VRd (BTZ + lenalidomide + dexamethasone), Dara-VRd (daratumumab + VRd), Dara-VTd (daratumumab + BTZ + thalidomide + dexamethasone) or Isa-VRd (isatuximab + VRd). Following ASCT, a lenalidomide maintenance therapy is administered. Eventually, tandem ASCT and BTZ as maintenance regimen can be considered in high-risk patients[1,2].

Non-eligible patients are treated with different combinations of 3 or 4 drugs including immunomodulatory drugs (IMiDs), proteasome inhibitors, monoclonal antibodies (mAbs; i.e. daratumumab and isatuximab), alkylating agents, and/or corticoids[1,2].

1.7.1. Immunomodulatory drugs (IMiDs)

The first IMiD used for MM treatment was thalidomide although new analogues with less neurotoxic adverse effects have been developed such as lenalidomide and pomalidomide, and more recently CELMoDs (Cereblon modulators) like avadomide, iberdomide, and mezigdomide, which are being tested in clinical trials. IMiDs mainly target cereblon, a member of the E3 ubiquitin ligase complexes, mediating proteasome degradation of IKZF1 (Ikaros) and IKZF3 (Aiolos) transcription factors, which are essential for PC differentiation and development. Moreover, IMiDs induce anti-inflammatory and anti-angiogenic effects which compromise tumor

development and boost T cell proliferation and NK cell antitumor activity[85-93]. However, some adverse effects such as thromboembolism, teratogenicity, neutropenia, and infections have been described for IMiDs[94].

1.7.2. Proteasome inhibitors

Correct proteasome activity is crucial in MM cells as the high production of Igs requires an efficient protein turnover in these cells to maintain their homeostasis. Proteasome inhibitors target proteasome β5 subunit and induce accumulation of poly-ubiquitinated or misfolded proteins which cause endoplasmic reticulum (ER) stress and induce apoptosis, preferentially on MM cells. The main proteasome inhibitor used for MM treatment is BTZ together with carfilzomib and ixazomib as second-generation drugs. New drugs such as oprozomib, delanzomib and marizomib are under study[95-97]. Additionally, BTZ has immunomodulatory effects that promote immune cell activation. This drug downregulates HLA-I and HLA-E expression[96,98] whereas increases natural killer group 2 (NKG2) member D ligands (NKG2D-L)[99] and other ligands that sensitize MM cells to NK-mediated killing[96,100] and upregulate expression of activating receptors in NK cells that boost their cytotoxic activity[99,101]. However, high doses of BTZ promote T cell apoptosis and diminish proinflammatory cytokine secretion and costimulatory molecule expression on T cells[102,103]. The use of proteasome inhibitors is associated with toxicities such as neuropathy, neutropenia and thrombocytopenia, cardiovascular events, Herpes virus reactivation and infections[94,95,104,105].

1.7.3. Alkylating agents

Melphalan, cyclophosphamide and bendamustin are alkylating agents that interfere in base repair during transcription and replication and therefore impair tumor cell survival. Although cyclophosphamide and bendamustin are less toxic than melphalan, they still have severe adverse effects. Therefore, they are usually used in a low-dose and short-term regimen as bridging between different treatment lines or as first-line treatment in combination with other drugs for ASCT non-eligible patients. High doses of alkylating agents can be used also as pre-ASCT conditioning regimen. More recently, melflufen (melphalan flufenamide), a peptide-drug conjugate that targets aminopeptidases and rapidly releases alkylating agents into tumor cells, has been recently approved by the FDA for the treatment of relapsed/refractory MM patients (RRMM), resulting more efficient and safer than melphalan treatment[106-108].

1.7.4. Glucocorticoids

Prednisone and dexamethasone are steroid hormones that have been used to treat MM for over 50 years. They bind to glucocorticoid receptors and modulate gene expression repressing

important factors for MM pathogenesis. The final effect is the promotion of a broad anti-inflammatory and immunosuppressive activity. However, due to the multiple signaling pathways modulated by these hormones in whole body tissues, high doses of glucocorticoids can generate severe toxicities thus they should be applied in a low dose in combination with other therapies[109-111].

1.8. Treatments for relapsed/refractory MM patients

RRMM include patients who have not achieved at least a minimal response to first-line treatment within treatment (primary refractory), those that achieve a minimal but non-durable response within 60 days after last treatment administration (refractory), and those that having shown objective responses (at least achieving a partial response) to treatments, again show signals of MM progression after 60 days from last treatment (relapsed)[112].

Depending on whether they are resistant or sensitive to first-line treatments such as lenalidomide, BTZ and/or daratumumab, patients are treated with new triplet or quadruplet drug combinations. These combinations comprise some of the first-line treatments (BTZ, lenalidomide, thalidomide and dexamethasone) and other IMiDs (pomalidomide), proteasome inhibitors (carfilzomib or ixazomib), glucocorticoids and alkylating agents (cyclophosphamide or melflufen) with or without α-CD38 mAbs (isatuximab or daratumumab). Other drugs such as Selinexor and novel immunotherapies targeting BCMA and GPRC5D (BCMA-targeting chimeric antigen receptor (CAR) T therapies and GPRC5D- or BCMA- bispecific Abs (BiAb)), which will be later described, have been approved by the FDA (U.S. Food and Drug Admistration) for the treatment of RRMM[10,112-114] (**Figure 4**).

1.8.1. Selinexor

This drug is an inhibitor of exportin 1 (XPO1) that blocks nuclear exports and thus retains tumor suppressor proteins which control cell cycle and avoids translation of mRNA oncogenes. Furthermore, Selinexor also downregulates expression of HLA-E on malignant B cells and upregulates NK-activating ligands in MM cell surface thus enhancing NK cell antitumor activity. Importantly, Selinexor has shown better performance when used in combination with dexamethasone and/or BTZ. However, major drawbacks of this therapy are their side effects ranging from gastrointestinal and neurological effects, neutropenia, and infections[113,115-117].

1.8.2. Non FDA-approved drug treatments for RRMM

Although they are not yet approved by the FDA for treatment of MM, other drugs such as B-cell lymphoma 2 (BCL-2) and histone deacetylase (HDAC) inhibitors have been used in clinical trials for RRMM treatments.

Venetoclax is a BCL-2 inhibitor used in patients that express high levels of BCL-2 or that harbor t(11;14). CANOVA trial (NCT03539744) and BELLINI trial showed enhanced PFS in RRMM patients treated with Venetoclax in combination with dexamethasone and dexamethasone + BTZ, respectively, but reported diverse cytopenias and gastrointestinal side effects[118-120].

Panobinostat is an HDAC inhibitor that has been used in combination with other drugs like proteasome inhibitors, IMiDs or steroids, showing good efficacy results (PANORAMA1 trial; NCT01023308) but was withdrawn by FDA in 2022 due to lack of complete post-approval clinical studies[121,122].

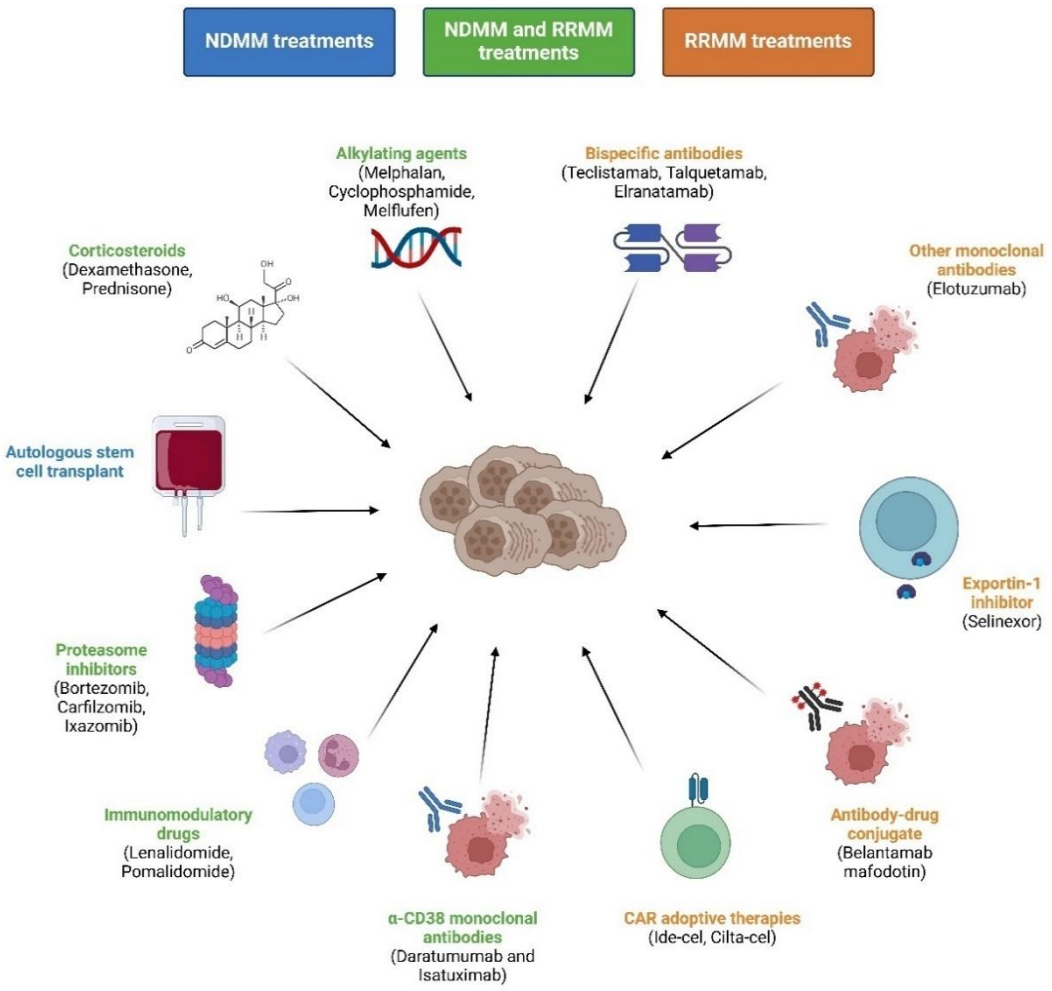

Figure 4. Current FDA-approved medications for treatment of newly diagnosed MM (NDMM) and relapsed/refractory MM (RRMM) patients. Ide-cel: Idecabtagene vicleucel; Cilta-cel: ciltacabtagene autoleucel. Data obtained from the International Myeloma Foundation, 2024[114]. Created with BioRender.com.

1.9. Treatment response

Some studies have demonstrated good clinical responses to first-line MM patients. CASSIOPEIA study showed 73% of complete response (CR) in patients treated with Dara-VTd and ASCT without reaching PFS after 35.4-month follow-up[123]. Moreover, ASCT non-eligible patients treated with Dara-VMP (daratumumab + BTZ + melphalan + prednisone) in the ALCYONE study showed a median PFS of 32.9 months[124]. However, it has been reported that OS in triple- or quad-refractory patients is 9.2 months and in penta-refractory (refractory to α-CD38 Abs, 2 proteasome inhibitors, and 2 IMiDs) is 5.6 months, without taking into account last updates from CAR T and BiAbs responses[125].

Despite the broad therapy armamentarium that is available for treatment of MM patients, the typical course of MM is characterized by periods of remission and relapses with increasingly shorter response periods and an increased number of rescue treatments (**Figure 5**). Therefore, there is an urgent medical need to find new therapeutic strategies against MM.

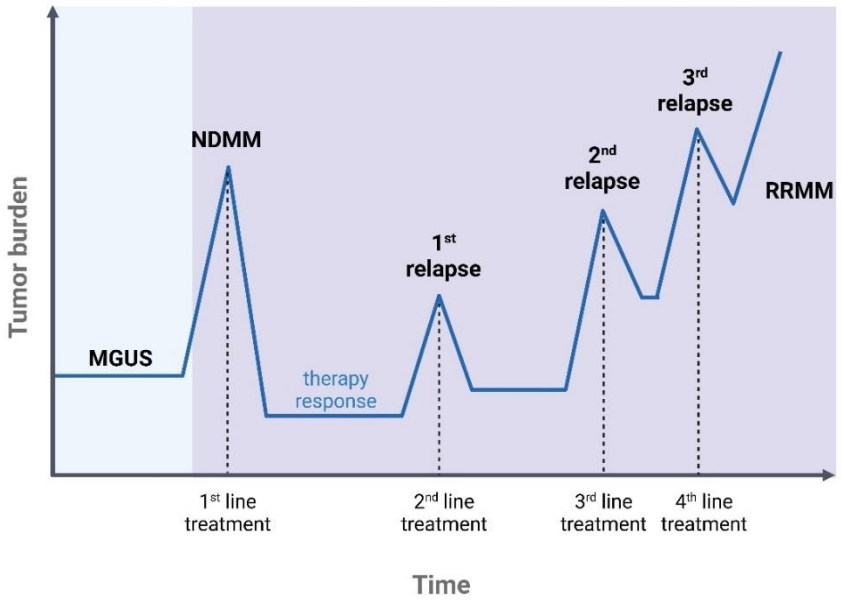

Figure 5. Clinical evolution of MM. After each treatment regimen, remission and response times are shorter. MGUS: monoclonal gammopathy of uncertain significance; NDMM: newly diagnosed MM; RRMM: relapsed/refractory MM.

2. Immunotherapy in MM

Over the last decades, the use of monoclonal antibodies and adoptive cell immunotherapies has revolutionized the treatment of both hematologic and solid tumors. In the context of MM, different immunotherapy products such as mAbs, CAR T, and BiAbs have been already approved by FDA[114], as previously mentioned. Additionally, numerous other approaches and targets against MM cells are currently under study.

2.1. Key immunotherapy targets in MM

One of the main challenges in immunotherapy is selecting targets that are specifically expressed in tumor cells but not in other healthy cells or tissues, to minimize on-target off-tumor toxicities (**Figure 6**).

2.1.1. BCMA (B-cell maturation antigen)

BCMA, also known as CD269 or TNFRSF17, is one of the most exploited targets in MM. This protein is a type III transmembrane glycoprotein that belongs to the TNF-receptor superfamily. BCMA limited expression profile makes it an interesting target as it is mainly present in mature B cells, plasmablasts, and PCs, with increased expression in malignant plasma cells along tumor progression[126].

BCMA binds to B-cell activation factor (BAFF), which is mainly expressed by dendritic cells (DCs), neutrophils, and monocytes and, with higher affinity, to A proliferation-inducing ligand (APRIL), present in monocytes and tumor cells. When BCMA binds to its ligands, it triggers the activation of PI3K/AKT and MAPK/ERK signaling pathways which promote MM cell adhesion to stromal cells, proliferation, and survival of MM cells. Besides, it also induces expression of anti-apoptotic and immunosuppressive proteins such as PD-L1 and TGF-β which contribute to the maintenance of an immunosuppressive TME in MM[127-132]. Remarkably, it has been demonstrated that APRIL and BAFF levels are increased in serum from MM patients compared to healthy donors (HD)[129].

Despite showing an almost specific expression distribution, BCMA is also expressed in neurons and astrocytes in basal ganglia which may lead to neurological side effects can appear when targeting this antigen[133].

It is important to note that BCMA is susceptible to γ-secretase-mediated shedding, thus increasing levels of soluble BCMA (sBCMA), which has been observed in BM from MM patients[134]. The presence of sBCMA can block the interaction of BCMA-targeted therapies with malignant PC, thus constituting a therapy-resistance mechanism. To solve this problem and restore therapeutic efficacy, γ-secretase inhibitors have been developed[135].

2.1.2. GPRC5D (G-protein-coupled receptor class C group 5 member D)

GPRC5D is one of the 7-transmembrane proteins of the G protein-coupled receptor family. This protein is highly expressed on MM cells and correlates with high-risk myeloma markers. Although GPRC5D is suggested to play an important role in tumor proliferation, its function remains unknown. Contrary to BCMA, this protein is unlikely to undergo shedding[136,137].

Besides on MM cells, this antigen is expressed in keratinized tissues and hair follicles[138]. Consequently, GPRC5D BiAbs have shown on-target off-tumor toxicities in nails and skin in more than 60% of MM patients[138,139]. Nonetheless, it is worth noting that preclinical trials using GPRC5D-CAR T cells in mice and monkeys have not reported alopecia[140].

2.1.3. CD38

CD38 is a type II transmembrane protein within the ADP-ribosyl cyclase family. It is widely expressed on most hematopoietic cells including myeloid cells and B, T, and NK cells. The catalytic products of this ectoenzyme promote calcium release and adenosine (ADO) secretion thus enhancing MM immunosuppressive TME[141,142]. CD38 interaction with CD31 or hyaluronic acid also mediates cell migration and adhesion[143].

As expected, due to the broad expression in the immune system, on-target off-tumor toxicities such as reduction in B and T cell numbers or NK cell fratricide, have been described for the use of mAbs against CD38[144,145].

Although daratumumab and isatuximab are first-line treatments for MM patients and have demonstrated great efficacy, the expression of CD38 can be downregulated due to selective pressure after CD38-targeting treatments, therefore limiting the subsequent use of these immunotherapeutic products[141,146].

2.1.4. SLAMF7 (Signaling lymphocytic activation molecule family member 7)

Targeted therapies against SLAMF7 have been developed for the treatment of MM. This glycoprotein receptor, as well known as CD319 or CS-1, can be found on the surface of lymphocytes, and mature DCs but also in both healthy and malignant PC. SLAMF7 is a homophilic receptor that interacts with itself either by binding SLAMF molecules in other cells or by binding its soluble form. When activated, this receptor boosts PC proliferation[147-149].

However, some therapy resistances have been described for this target. For example, both receptor and soluble forms of SLAMF7 are downregulated by IMiDs. This inhibits tumor progression but masks surface target thus impairing efficacy of SLAMF7-targeted therapies[132]. In

addition, fratricide effects have been described for SLAMF-directed immunotherapies as this molecule is expressed in both NK and T cells[150,151].

2.1.5. Other targets under research

Although not yet approved by medical authorities, there are other targets that are being explored in both a preclinical and clinical setting.

For example, CD138, also known as syndecan-1, is a lineage marker of PC and is highly expressed by MM cells[152]. This protein plays an important role in cell adhesion as it binds to many different integrins and extracellular matrix proteins[153]. CD138 can also bind APRIL promoting tumor growth[154]. However, it is also expressed in liver, bladder, and gastrointestinal tract cells[155] leading to possible toxicities and, as well as BCMA, it can be shed from MM cells in advanced stages of the disease[153,156,157] reducing targeted immunotherapy responses.

Ligands for the NKG2D receptor are of special interest not only for MM but also many different solid and hematologic tumors. There are 8 different known NKG2D-L: MHC class I chain-related proteins A and B (MICA, MICB) and the unique long 16 binding proteins (ULBP) 1 to 6. These ligands are usually induced by cellular stress, DNA-damage, viral infections, inflammation, and chemotherapy[158-162]. Moreover, malignant transformation also induces expression of these ligands in more than 85% of tumor cells, in which MM cells are included[54,163,164]. When these ligands bind to the NKG2D activating receptor, which is expressed in NK cells, $CD8^+$ T cells, γδ T cells and NKT cells[164], NKG2D/DAP10 complex activates PI3K/AKT and Grb2/Vav1 signaling pathways triggering a cytotoxic response[165,166]. Within the drawbacks of NKG2D ligand-targeted therapies it is worth mentioning the potential off-tumor effects as these ligands are expressed in the gastrointestinal epithelium[167]. Besides, MICA, MICB and ULBP2 can be shed from cell surface by A disintegrin and metalloproteases (ADAM10 and ADAM17), ERp5 (Endoplasmic reticulum protein 5), and matrix metalloproteases (MMP9 and MMP14) increasing the levels of soluble ligands that impair NKG2D-mediated NK and T cell cytotoxic activity[161]. Importantly, it has been demonstrated that the efficacy of α-NKG2D-L CAR T cells is not interrupted by supraphysiological levels of soluble MICA (sMICA)[168].

Another appealing target for MM immunotherapy is Fc receptor-homolog 5 (FcRH5 or CD307), an orphan receptor that is expressed in B cells along different development stages, including memory B cells and PC and it has been reported to augment cell proliferation. FcRH5 is upregulated in MM cells from patients with 1q21 gain and it is associated with high-risk MM[169]. Possible toxicities that have been suggested may affect skin, eyes and gastrointestinal tract[170,171].

CD19, a member of the Ig superfamily, is a BCR co-receptor molecule that, similarly to FcRH5, is expressed in the B cell lineage. However, its expression is diminished in late stages such as PC being only expressed in MM stem-like cells[172,173]. As a consequence, CD19-targeted therapies have not shown efficacy as monotherapy although they seem to synergize with other BCMA-targeted therapies and ASCT + melphalan treatments[174-176].

Finally, CD44v6 (CD44 variant domain 6) has also been proposed as a potential MM target. This protein is a spliced isoform of the CD44 protein that promotes cell migration and tumor cell survival in response to different interactions with extracellular proteins and growth factors such as VEGF and HGF (hepatocyte growth factor)[177-179]. This aberrant protein is expressed in different tumors, including MM[180,181]. However, it is also expressed in keratinocytes. Of note, although side toxicities affecting skin have been reported for CD44v6-target therapies[182], this has not been observed with CD44v6 CAR T cells[183]. A unique feature of this target is that some macrophages and monocytes which are associated with cytokine release syndrome (CRS) also express CD44v6 and, therefore, CD44v6-targeted products may potentially reduce the severity of this side effect[184,185].

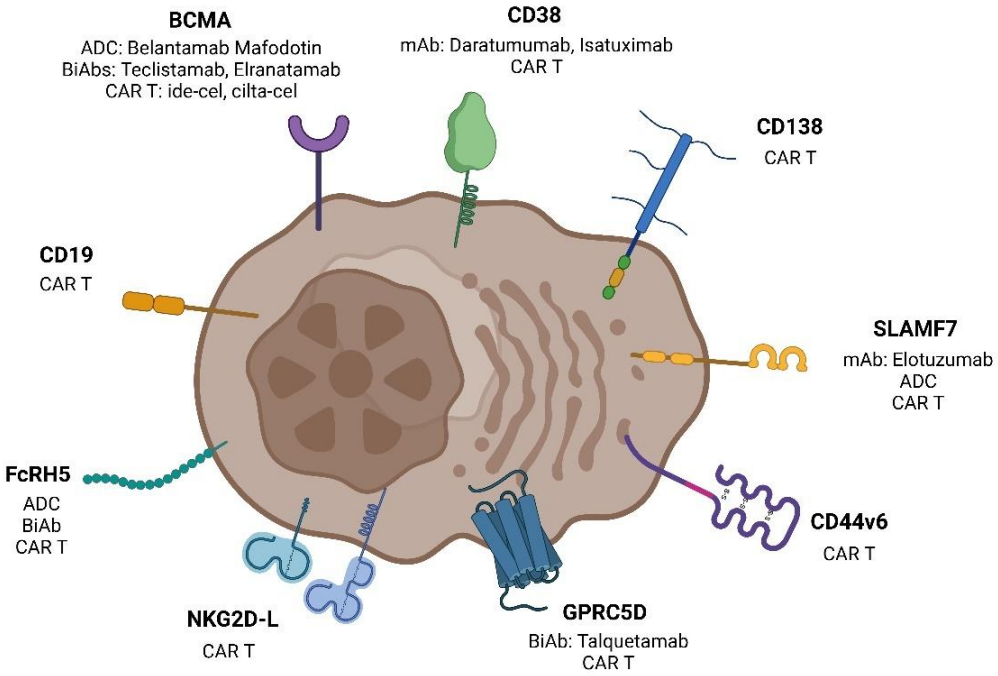

Figure 6. Main antigens used for MM-targeted immunotherapy. Immunotherapy strategies that are under development or have been approved by medical agencies against each target are indicated. BCMA: B-cell maturation antigen; SLAMF7: signaling lymphocyte activation molecule family member 7; CD44v6; CD44 variant domain 6; GPRC5D: G protein-coupled receptor class C group 5 member D; NKG2D-L: ligands for the natural killer group 2 member D receptor; FcRH5: Fc receptor-homolog 5; mAb: monoclonal antibody; ADC: antibody-drug conjugate; BiAb: bispecific Ab; CAR T: chimeric antigen receptor T cells; ide-cel: idecabtagene vicleucel; cilta-cel: ciltacabtagene autoleucel. Created with BioRender.com.

2.2. Monoclonal antibodies (mAbs)

mAbs are recombinant proteins engineered to specifically recognize antigens expressed on tumor cells. There are different mechanisms by which mAbs exert their antitumor response: antibody-dependent cellular cytotoxicity (ADCC), antibody-dependent cellular phagocytosis (ADCP), complement-dependent cytotoxicity (CDC), and direct tumor killing[186] .

Up to date, only daratumumab, isatuximab, and elotuzumab are mAbs approved by medical agencies for the treatment of MM although there are others such as siltuximab (α-IL-6), SEA-BCMA (α-BCMA) and the HexaBody-CD38 are being tested in clinical trials[186,187].

2.2.1. Daratumumab

Daratumumab is a human α-CD38 IgG1κ mAb. It was the first mAb to be approved by FDA as a first-line treatment in combination with other drug treatments. It is also included in RRMM treatment regimens, where it has been shown to improve OS and PFS when combined with other drugs compared to drug-only regimens[1,188,189].

Apart from the classical killing mechanisms described above, daratumumab also modulates TME. It decreases ADO production and, consequently, reduces $CD38^+$ Tregs, Bregs, and MDSCs at the same time as increases T cell proliferation[141,190].

As it has been mentioned before, CD38 expression can be downregulated after treatment with daratumumab. Although expression can be recovered in 3-6 months after treatment, some $CD38^-$ clones may persist, therefore acquiring resistance to this treatment[191]. Another limitation of daratumumab is that it induces NK fratricide as CD38 is highly expressed on NK cells. Consequently, NK cell numbers decrease, and remaining ones become exhausted impairing ADCC responses. Some groups have proposed the use of CD38 KO NK cells in combination with daratumumab to increase the efficacy of the therapy[192,193].

Regarding daratumumab-associated toxicities, anemia, neutropenia, lymphopenia, thrombocytopenia, pneumonia, and diarrhea have been reported[188,189].

2.2.2. Isatuximab

Isatuximab is a chimeric IgG1 mAb also targeting CD38. It was first approved by medical agencies for the treatment of RRMM patients in combination with other drugs, also improving efficacy of drug-only combinations[194-196]. Remarkably, results from the IMROZ clinical trial (NCT03319667), led to the recent FDA approval for its use as first-line treatment in combination with BTZ, lenalidomide and dexamethasone for patients who are not eligible for ASCT[114].

Within the adverse effects associated with isatuximab treatment is worth mentioning infusion reactions, respiratory infections, and HVB reactivation[194,197].

2.2.3. Elotuzumab

Elotuzumab is a α-SLAMF7 humanized IgG1κ mAb approved by the regulatory authorities for the treatment of RRMM. It has demonstrated greater efficacy compared to treatment regimens that rely solely on drug medications[198-200]. Importantly, few adverse effects have been reported for elotuzumab including anemia, neutropenia, and respiratory infections[200].

In addition to classical mAbs action mechanisms, elotuzumab can also impair MM cell adhesion to BM MSCs[201,202]. However, in the same trend as α-CD38 antibodies, elotuzumab produces NK cell fratricide as its target is also expressed on this immune subset[203].

2.3. Antibody-drug conjugates (ADCs)

ADCs are recombinant mAbs that are conjugated to small cytotoxic molecules such as DNA damaging agents, topoisomerase I inhibitors, RNA polymerase II inhibitors, or tubulin inhibitors. When they bind to their specific target, they are endocytosed and release the toxin inside the target cell after lysosomal cleavage[186,204].

Belantamab mafodotin is the only ADC approved for the treatment of RRMM. Other promising ADCs such as AMG 224 and CC-99712 (α-BCMA) or TAK-573 (α-CD38) are being tested in clinical trials. On the contrary, some other ADCs such as lorvotuzumab mertansine (α-CD56), MEDI2228 (α-BCMA), DFRF4539A (α-FcRH5), and azintuxizumab vedotin (α-SLAMF7) were discarded because of their low efficacy and high toxicity[205].

2.3.1. Belantamab mafodotin

This ADC is a humanized α-BCMA mAb conjugated to mafodotin, a microtubule polymerization blocker. It was approved by FDA in 2020 for RRMM treatment after showing promising results in DREAMM-2 clinical trial[204,206]. However, the subsequent Phase III trial (DREAMM-3) showed no efficacy improvements in PFS leading to a provisional withdrawal of this ADC[207]. Recently, FDA and the European Medicines Agency (EMA) have accepted a review for further reapproval of this therapy based on the clinical outcomes of DREAMM-7 and DREAMM-8 clinical trials. In Spain, belantamab mafodotin is still being used and its efficacy is still being tested in different clinical trials[208].

Regarding toxicities, keratopathies, especially irreversible ocular toxicities and blurred vision, as well as anemia and thrombocytopenia were described in DREAMM-2 study[204].

2.4. Bispecific T-cell engagers (BiTEs) and bispecific antibodies (BiAbs)

BiTEs and BiAbs are recombinant molecules designed to favor the interaction between immune and tumor cells. BiTEs consist of two different single chain variable fragments (scFvs) linked together, with one scFv typically targeting CD3 on T cells and the other targeting a tumor-associated antigen. This design enhances immune synapse formation between T cells and malignant cells, thereby promoting T cell activation and tumor elimination. BiAbs are recombinant antibodies with two epitope-binding sites and one common Fc region. One binding site can recognize CD3, allowing the BiAb to function similarly to a BiTE, or it may target a different antigen, acting solely as a mAb. As BiAbs contain an Fc region, they trigger antibody-dependent killing mechanisms (**Figure 7**)[209,210].

Up to date, three different BiAbs have been approved for the treatment of RRMM patients, targeting CD3 and GPRC5D or BCMA[114]. Other BiAbs targeting these molecules or other targets, such as FcRH5 (cevostamab)[211,212] or CD38, as well as some BiTEs are still under study[209].

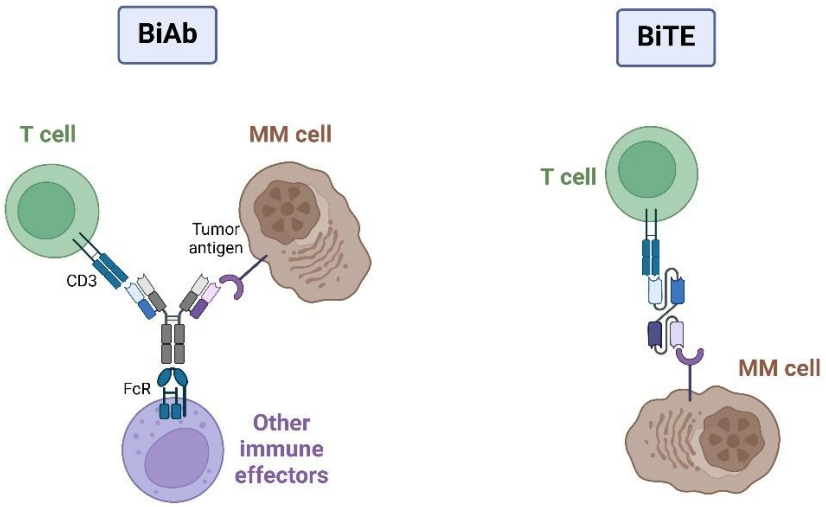

Figure 7. Bispecific antibodies (BiAb) vs bispecific T-cell engagers (BiTE). MM: multiple myeloma; FcR: Fc receptor. Adapted from Rampotas et al. Ther Adv Hematol. 2021[210]. Created with Biorender.com.

2.4.1. Teclistamab

Teclistamab is a humanized IgG4 BiAb targeting BCMA and CD3. It improves T-cell mediated cytotoxicity against MM cells both *in vitro* and *in vivo* and is not inhibited by sBCMA[213]. First clinical trials (MajesTEC-1) have demonstrated efficacy of this BiAb with some toxicities such as neutropenia, thrombocytopenia, neurotoxicity, and CRS[214].

2.4.2. Elranatamab

Elranatamab is another humanized IgG2a BiAb targeting both BCMA and CD3. It was recently approved in 2023 after the good results of MagnetisMM-3 clinical trial. Although some toxicities such as anemia, neutropenia, infections and CRS have been found, they can be reduced by sequential administration of lower doses[215].

2.4.3. Talquetamab

Talquetamab, a humanized BiAb that targets GPRC5D and CD3, was also approved in 2023 by medical authorities. Preclinical studies have shown that it augments T cell-mediated cytotoxicity against MM cells and fosters T cell proliferation. However, its efficacy may be hindered by the presence of BM MSCs and Tregs[136,216]. MonumenTAL-1 clinical trial demonstrated the efficacy of this BiAb in RRMM patients with some adverse effects such as neutropenia and skin-related toxicities. Nowadays, it is being tested in combination with daratumumab and teclistamab[138,217].

2.5. CAR T immunotherapy

Despite the promising results of the aforementioned immunotherapeutic approaches for MM, their efficacy relies on the activity of patients' immune cells which are usually repressed in an immunosuppressive TME. In this context, cell adoptive therapies using chimeric antigen receptors (CAR) have revolutionized the treatment of cancer patients, especially with B-cell lymphoproliferative hematological malignancies. CAR immunotherapy consists on the *ex vivo* modification of immune effector cells to express CAR molecules on their surface and their following activation and expansion to be later administered to the patient. Inside the patients, activated CAR cells target cancer cells and exert their antitumor response (**Figure 8**).

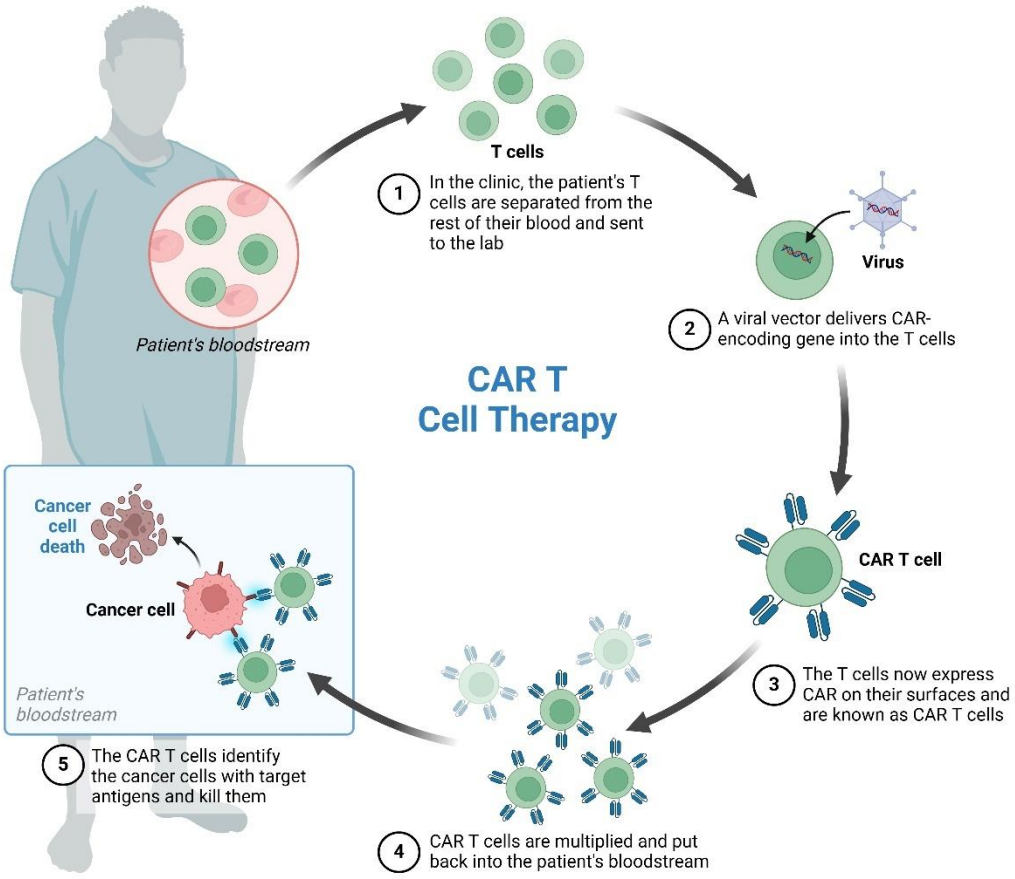

Figure 8. Vein-to-vein process of autologous chimeric antigen receptor (CAR) T cell therapy. Obtained from BioRender.com repository.

CAR molecules are recombinant proteins designed to target tumor cells and trigger an activating response in the effector cell. They contain a recognition region consisting of either a scFv from a mAb that recognized a tumor antigen or a fragment of an endogenous receptor whose ligand is expressed on tumor cells. Then, a hinge region and a transmembrane domain connect the recognition region with the signaling intracytoplasmic domain. Depending on the structure of the signaling endodomain, CAR molecules are classified into 5 groups as described in **Figure 9**. First-generation CAR molecules only contain the CD3ζ signaling chain from the T-cell receptor (TCR) while second- and third-generation additionally contain one or two costimulatory domains, respectively. Most common costimulatory domains used for CAR design are extracted from 4-1BB, CD28, OX40, CD27, CD40 and ICOS, among others. Fourth-generation CARs, also called "armored" CARs, are second-generation molecules that also include a bicistronic transgene for the expression of a cytokine expression inductor or a cytokine. Recently, the new fifth-generation has emerged incorporating a signaling domain of a cytokine receptor (usually IL-2) to activate JAK/STAT pathway[218-220].

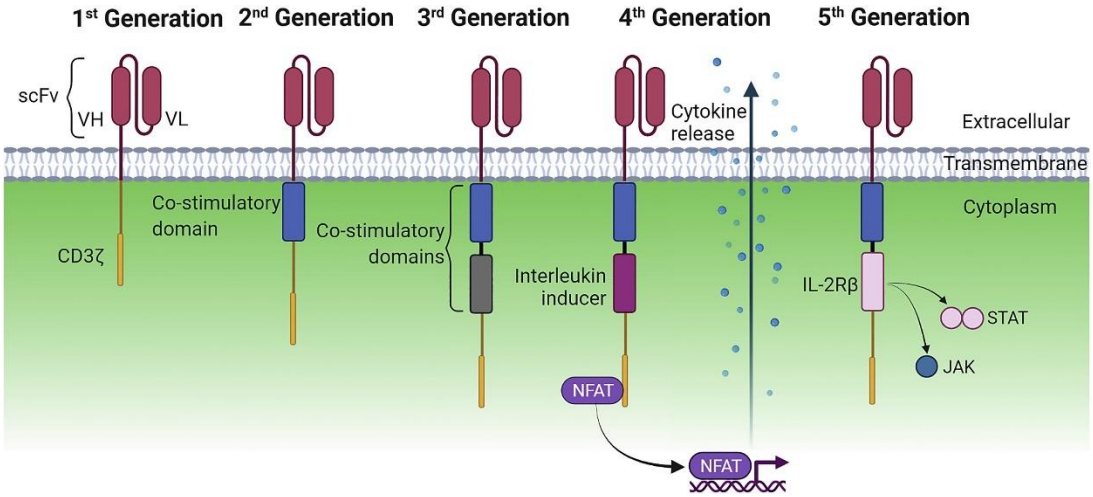

Figure 9. Schematic representation of the different CAR generations. scFv: single chain variable fragment; NFAT: nuclear factor of activated T-cells; IL-2Rβ: interleukin 2 β receptor; JAK: Janus kinase; STAT: signal transducer and activator of transcription. Obtained from Yeo et al. Mol Ther Oncolytics. 2022[220].

In terms of the immune effector cells used in CAR adoptive cell therapies, T cells were the pioneering effectors to be used as CAR hosts. However, not only T cells are good candidates and other immune cells such as NK, iNKT, γδ T cells, macrophages, and DCs have been efficiently modified to express CAR sequences (**Figure 10**)[221].

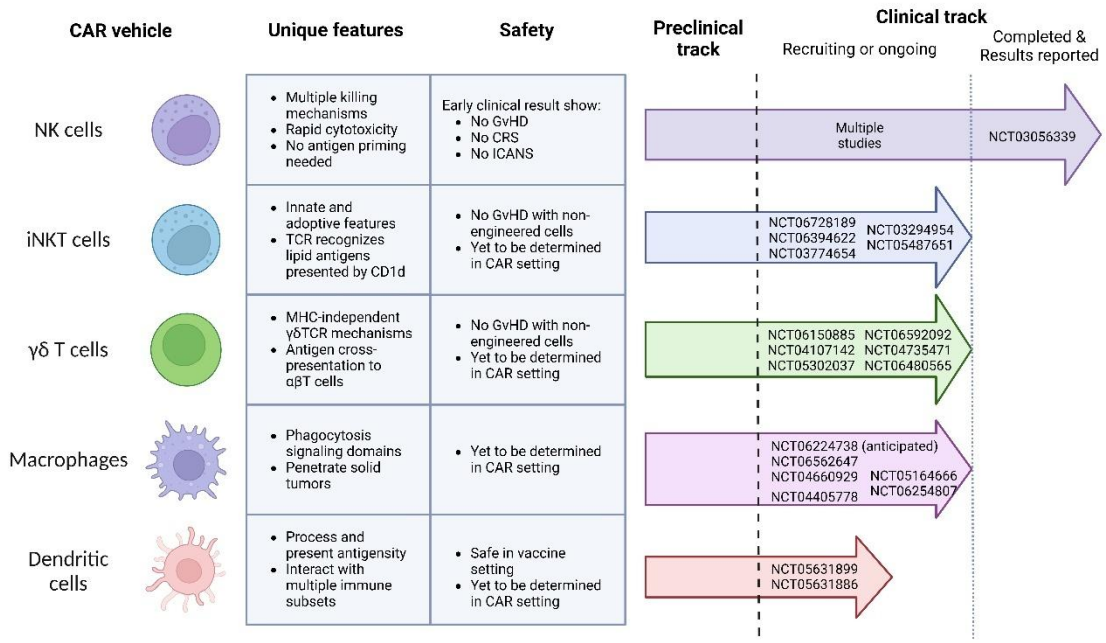

Figure 10. CAR immune effector cells against tumors in preclinical and clinical studies. GVHD: graft versus host disease; CRS: cytokine release syndrome; ICANS: immune effector cell-associated neurotoxicity syndrome; DC: dendritic cell; CAR: chimeric antigen receptor; MHC: major histocompatibility complex; TCR: T cell receptor. Adapted from Daher and Rezvani, Cancer Discov. 2021[221]. Created with Biorender.com.

The first CAR T immunotherapy to be approved by the FDA was tisagenlecleucel, a CAR T product targeting CD19, for the treatment of children and young adults with relapsed or refractory B cell acute leukemia (B-ALL)[222,223]. Since this landmark in the CAR T immunotherapy field in 2017, a total of 6 products have been globally approved by medical authorities, all of them targeting CD19 or BCMA[224]. Additionally, Chinese medicine agency has authorized two other CAR T, also targeting the same antigens and in Spain, ARI-0001 αCD19 CAR T product (Vermicabtagene autoleucel) was authorized under the "hospital exemption" approval pathway by the Spanish Agency of Medicines and Medical Devices (AEMPS). These revolutionary achievements have paved the way for the development of new CAR T therapies, not only for hematological malignancies, but also for solid tumors such as glioblastoma, in which promising clinical outcomes have been reported[225,226].

Regarding MM, there are two medically authorized α-BCMA CAR products for the treatment of RRMM patients: idecabtagene vicleucel (ide-cel) and ciltacabtagene autoleucel (cilta-cel)[114]. Early and long-term efficacies as well as safety of the already approved and other CAR T immunotherapies are currently being tested in around 220 clinical trials. Among the specificities that are being explored besides BCMA, GPRC5D, SLAMF7, CD38, FcRH5, NKG2D-L, and CD138 are the main targets[227].

2.5.1. Idecabtagene vicleucel (ide-cel) and ciltacabtagene autoleucel (cilta-cel)

Ide-cel contains a α-BCMA scFv as CAR recognition region. This CAR T product was approved in 2021 by FDA and later by EMA after the pivotal KarMMa-1 trial outcomes, being indicated for the treatment of RRMM patients after ≥4 lines of therapy including an immunomodulatory agent, a proteasome inhibitor, and an α-CD38 mAb. Recently, the Phase III KarMMa-3 trial reported 71% of responses and a median PFS of 13.3 months being quite superior to the 4.4 obtained for patients treated with drug regimens. Grade 3 and 4 toxicities were observed in 93% of patients, mainly CRS and immune effector cell-associated neurotoxicity (ICANS)[228]. Based on these results, this CAR T therapy was approved for RRMM after ≥2 prior lines of treatment.

In 2022, regulatory authorities gave green light for the use of cilta-cel in RRMM patients who had undergone 4 or more treatment regimens including a proteasome inhibitor, an immunomodulatory agent, and an α-CD38 mAb. This decision was based on the results from CARTITUDE-1 clinical trial which reported 89% OS and 77% 12-month progression-free rates[229]. Although this product also targets BCMA, recognition region of cilta-cel CAR molecule consists of two VHH antibody fragments, differently to ide-del. More recent results from Phase III trial CARTITUDE-4 revealed an 84.6% OS with a 37.1% CR. Although 76.1% of patients showed

adverse therapy-related effects, only 4.5% suffered severe neurotoxicity and just 1.1% severe CRS[230]. After these promising results, the use of cilta-cel was extended to RRMM who have received at least one prior line of therapy, including a proteasome inhibitor and an immunomodulatory agent.

2.5.2. CAR T therapy resistances and limitations

Despite showing promising efficacy in clinical trials, no *plateaus* have been observed in the survival curves of patients treated with α-BCMA CAR T therapies, and relapses still occur[231]. The lack of stability in the responses might be caused by CAR effector-dependent and tumor-dependent resistances.

CAR structure constitutes a key point in the design and development of CAR T therapies. Most scFv used to generate CAR molecules are derived from mice or are not fully human. As a consequence, the patient's immune system can secrete human anti-mouse antibodies and trigger an immunological response against CAR T cells, limiting their expansion and compromising the efficacy of subsequent treatment doses. To reduce the scFv immunogenicity, recognition sequences can be substituted by fully human scFv or a natural receptor or ligand that binds the target cells. Another solution that has been implemented is the use of a lymphodepleting conditioning treatment before CAR T cell infusion[232].

Another important limitation of CAR T cells is their exhaustion. This is a reversible state in which T cells highly express inhibitory receptors (i.e. PD-1, TIM-3, LAG-3, TIGIT, and CTLA-4) and show impaired functional responses. This phenotype has been observed in most of the non-responder patients treated with CAR T cells. CAR structure is also implicated in T cell exhaustion. For example, some scFv, when overexpressed on membrane, can aggregate resulting in a tonic signaling that triggers T cell exhaustion. Moreover, CD28 costimulatory domain has been described to induce T cell exhaustion compared to other domains such as 4-1BB or ICOS[233-235]. Therefore, adequate selection of each of the CAR elements is important to overcome CAR T cell resistances.

Regarding tumor-dependent resistances, antigen escape is one of the most relevant ones. Many tumors can downregulate the expression of the CAR-target antigen as a response to the treatment (i.e. CD38) or clones that do not express the specific antigen can appear, having greater fitting after treatment and therefore a selective advantage. In order to solve these limitations, the expression of two CAR molecules with different specificities (dual-CARs) has been proposed. Another strategy is changing the specificities of the CAR T cells depending on the antigens expressed on the tumor cell[236,237]. Antigen cleavage is another shortcoming related to

antigen loss. In the context of MM, some targets such as BCMA can be shed from cell surface by proteases, as it was mentioned before. This leads to the release of sBCMA that can bind CAR T cells thus impairing their cytotoxic activity. As a possible solution, the use of γ-secretase inhibitors has been proposed to avoid BCMA cleavage[135].

Another tumor-derived therapy resistance is the TME. Most tumors, including MM, create an immunosuppressed environment that not only affects the immune cells of the patient but also can restrain the efficacy of adoptive cell therapies. The release of cytokines such as TGF-β or IL-10, the expression of inhibitory ligands (i.e. PD-1L) and the presence of immunosuppressive cells impair T cell functionality and expansion and can induce T cell exhaustion which, in the end, compromise CAR T cell therapy. Strategies targeting TME or gene editing of CAR T cells have been proposed to enhance the efficacy of CAR T cells[218,234,235,238].

Besides therapy resistances, there are other relevant limitations of CAR T therapies. The major one is treatment-derived toxicities such as CRS, ICANS and on-target off-tumor toxicities. Almost all patients treated with CAR T cells develop CRS which causes fever, and in severe cases, hypotension, hypoxia and/or organ dysfunction although these symptoms are normally controlled by treatment with α-IL-6R mAb. ICANS is also a frequent adverse effect in patients who have experienced CRS and can cause confusion, motor skills impairment or dysphasia but, in severe cases, it can produce seizures, cerebral oedema, or even coma[239]. Prolonged cytopenia[240] and hemophagocytic lymphohistiocytosis[241] are also relevant adverse effects after CAR T treatment. These therapy-related complications prolong hospitalization and increase healthcare costs.

Manufacturing costs and times are also important limitations of CAR T immunotherapy. Most patients have a high tumor burden, which may contaminate final autologous CAR T products, and have impaired T effector cells due to the previous treatment regimens and TME-mediated immunosuppression[242]. This results in a high rate of product failure and prolongs manufacturing times. In most cases, rapid MM progression does not allow such long manufacturing time. Although allogeneic CAR T cells from HD have been proposed to obtain "*off-the-shelf*", universal and efficient CAR T products, they can generate graft-versus-host-disease (GvHD) or host immune rejections. As possible solutions, gene editing strategies, the use of non-αβ T cells or T cells derived from umbilical cord blood (CB) or iPSC banks, and conditioning lymphodepletions have been proposed[243].

In this scenario, there is an emerging need to find alternative CAR effectors to improve their persistence and efficacy, avoiding severe toxicities, immunosuppression and antigen loss consequences.

3. CAR NK immunotherapy in MM

CAR NK cells have emerged as strong and safer candidates due to their singular biological properties that outperform CAR T cells. Among them, it is worth mentioning their low toxicity and the possibility of being used in both an autologous and allogeneic context without previous engineering, because its response is not HLA-restricted. Moreover, their killing mechanisms through innate receptors guarantee CAR NK cell efficacy even if the CAR target is downregulated, overcoming some of the CAR T cell resistances.

3.1. Native properties of NK cells over T cells for CAR immunotherapy

NK cells are innate cytotoxic lymphocytes that represent 5-15% of total lymphocytes in peripheral blood (PB). They originate from an NK cell precursor in BM that differentiates along 6 maturation stages in BM and primary lymph organs. During the final stages of maturation in secondary lymph organs, NK cells acquire a $CD56^{bright}$ and highly proliferative phenotype. Differentiation involves transcriptional and epigenetic changes in the receptor profile towards a more cytotoxic one in which receptors such as CD56, CD62L, NKG2A, CCR7, and CXCR3 are downregulated while expression of activating receptors like CD16 and NKG2D, as well as perforin, granzymes and KIRs (killer-cell immunoglobulin-like receptors), is increased. These $CD56^{dim}$ $CD16^{bright}$ NK cells preferentially circulate into the bloodstream accounting for 90-95% of circulating NK cells (**Figure 11**)[244]. Of note, cytotoxic $CD56^{dim}$ $CD16^{bright}$ NK cells, when activated *ex vivo*, can upregulate CD56 expression but do not resemble the "traditional" regulatory functions of the $CD56^{bright}$ $CD16^{-}$ subset[245]. In addition to the $CD56^{bright}$ $CD16^{-}$ and $CD56^{dim}$ $CD16^{bright}$ classical NK cell populations, a new $CD56^{-}$ $CD16^{bright}$ $NKp46^{+}$ NK cell population has been identified which usually represents a minor proportion of circulating NK cells but is upregulated during viral infections[246].

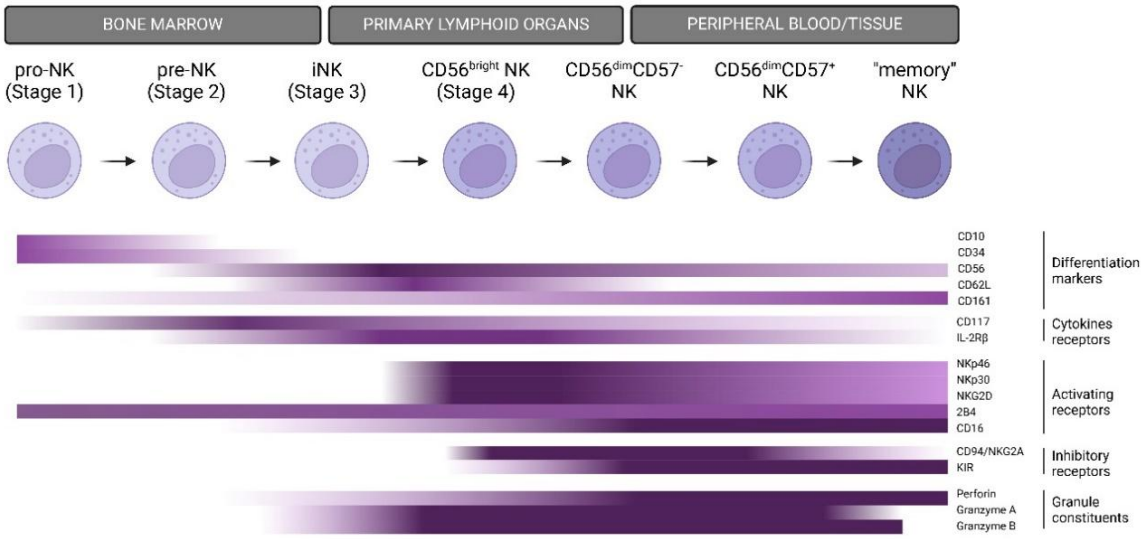

Figure 11. Schematic representation of NK cell differentiation and maturation. Adapted from Cichocki et al. Front Immunol. 2013[244]. Created with BioRender.com.

3.1.1. Germ-line NK cell receptors that mediate CAR-independent killing

The main function of NK cells is to identify and quickly eliminate abnormal, stressed, virally infected, or senescent cells as well as to control tumor and metastatic cells[247,248]. NK cells can eliminate target cells through ADCC, the secretion of granzymes and perforin that mediate direct cytotoxic killing, or by engaging death receptors such as TRAIL or FasL, which trigger apoptotic responses in target cells. Additionally, NK cells secrete immunomodulatory cytokines such as TNF-α and IFN-γ. They act in a similar way to $CD8^+$ T cells but without needing prior antigen sensitization[242,249] (**Figure 12**).

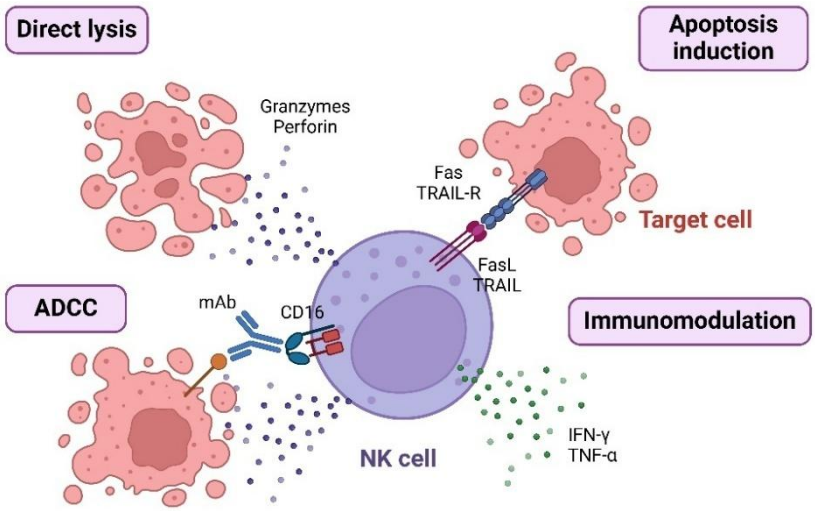

Figure 12. NK cell responses against target cells. ADCC: Antibody-dependent cell-mediated cytotoxicity; mAb: monoclonal antibody; IFN-γ: interferon γ; TNF-α: tumor necrosis factor α; TRAIL: TNF-related apoptosis-inducing ligand; TRAIL-R; TRAIL receptor; FasL: Fas Ligand. Created with BioRender.com.

NK function is mainly modulated by KIRs. These receptors are encoded by 15 different gene loci with allelic variants resulting in a high polymorphic family with a great diversity of receptors. Most KIRs contain ITIM motifs on their cytoplasmic tail which trigger inhibitory responses by recruiting phosphatases although a small proportion of KIRs do not have ITIM motifs and interact with DAP12 (which contains ITAM motifs) instead, thus inducing activating responses in NK cells[250]. KIRs recognize human leukocyte antigen (HLA), also known as major histocompatibility complex (MHC). During their maturation, NK cells are educated or "licensed" to recognize HLA class I molecules in the own healthy cells through their KIR receptors. When NK cells encounter cells that do not express or have downregulated HLA-I, which is the case of altered and tumor cells, they are recognized as "*non-self*" or "*missing-self*" cells and lack of KIR binding triggers a killing response. Apart from HLA-I recognition, NK cell function can be also induced by the recognition of specific ligands in stressed or damaged cells (including tumor cells) that bind other NK cell activating receptors ("*induced-self*" mechanism)[251,252]. (**Figure 13**).

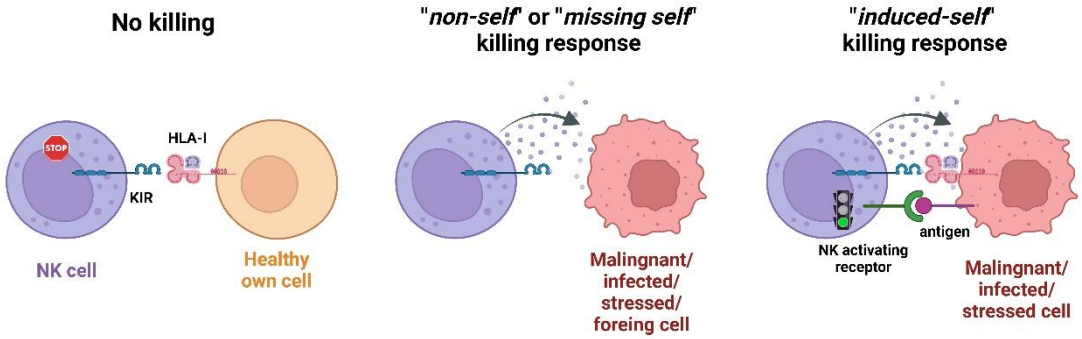

Figure 13. NK-mediated killing responses based on KIR and activating receptor recognition. KIR: killer-cell immunoglobulin-like receptor; HLA-I: human leukocyte antigen class I. Created with BioRender.com

However, regulation of NK cell immune responses is not as simple as this and requires the integration of different signals. In the end, the final NK cell function will depend on the balance between activating and inhibitory signals generated by KIRs and several other surface germ-line receptors[250] (**Figure 14**).

NKG2 receptor family plays a central role in NK cell modulation. These are C-type lectin-like receptors expressed on NK and cytotoxic T cells. Depending on the ITIM or ITAM motifs that each member contains, they are classified into activating (NKG2C, NKG2D and NKG2E) or inhibitory (NKG2A and NKG2B) receptors. They form heterodimers with CD94 with the exception of NKG2D which is a homodimer. As it was previously described, NKG2D recognizes MICA/B and ULBP1-6 ligands in stressed or malignant cells and signaling transduction is mediated by interaction with DAP10. NKG2A, NKG2B, NKG2C, and NKG2E, on the contrary, recognize the non-classical HLA-I

molecule HLA-E with different affinities. NKG2A signaling plays a dominant role in inhibiting NK cell response and will be described in more detail later[250,253].

Natural cytotoxicity receptors (NCR) comprise NKp30, NKp44, and NKp46 proteins. They belong to the Ig superfamily and contain intracellular ITAM motifs thus triggering activating signals in NK cells when bind to their multiple ligands. Additionally, signaling transduction is mediated by the intracellular interaction of NCRs with FcεRIγ and CD3ζ (NKp30 and NKp46) and DAP12 (NKp44)[250,254].

CD16, also known as Fc γ receptor III (FcγRIII), is expressed under two isoforms: A and B. CD16A is highly expressed on mature and activated NK cells and interacts with CD3ζ and FcεRIγ. On the contrary, isoform B is expressed on neutrophils. CD16A can recognize Fc domains of IgG1 and IgG3 and, when binding, induces an activating response in NK cells that promotes ADCC responses and cytokine secretion to mediate target killing. Importantly, CD16 expression in NK cell is regulated by ADAM17 shedding[250,255].

Another important activating and adhesion receptor is DNAM-1 (CD226). This receptor interacts with Nectin-2 (CD112) and poliovirus receptor (PVR, CD155) competing with CD96 and TIGIT. Its tyrosine and asparagine-based motif in the cytoplasmic domain is responsible for triggering activating signals that induce both cytotoxicity and cytokine secretion in NK cells[250,256].

NK cell function is also regulated by inhibitory receptors such as TIGIT, CD96, KLRG1, TIM-3, and PD-1, which are also expressed on T cells and other immune subsets.

TIGIT (T cell immunoreceptor with Ig and ITIM domains) and CD96 (TACTILE) are homology-shared receptors that bind PVR and Nectin-2 (similarly to DNAM-1) but exert an inhibitory response in NK cells. Tumor-infiltrating NK cells showed enhanced TIGIT expression suggesting that this receptor plays an important role in tumor immunosuppression[257,258].

TIM-3 (T cell immunoglobulin and mucin-domain containing-3) is an inhibitory receptor from the TIM family. When binding to its ligands, galectin-9 and CEACAM-1, it interacts with BAT3 regulating NK cell immune response. Importantly, TIM-3 expression in NK cells is considered a prognostic factor in solid tumors and has been related with impaired IFN-γ and granzyme production[258,259].

KLRG1 (Killer cell lectin-like receptor G1) is an ITIM-containing inhibitory receptor that binds to E-, N- and R-cadherin. After binding it impairs AKT phosphorylation leading to proliferative dysfunction in NK cells. Expression of this receptor has been associated to final maturation and even senescent stages of effector cells[260].

Finally, PD-1 (Programmed death 1) receptor also mediates inhibitory responses, especially in the cancer context as tumor cells usually express PD-1 ligands (PD-L1 and PD-L2). PD-1 is one of the main inhibitory checkpoint of T cell activity although its role in NK cells has not been completely elucidated[261]. However, induction of PD-1 expression in expanded NK cells[262] as well as trogocytosis-mediated PD-1 acquisition[263] in the presence of tumor cells have been described, suggesting that PD-1 plays relevant regulatory roles in the tumor context.

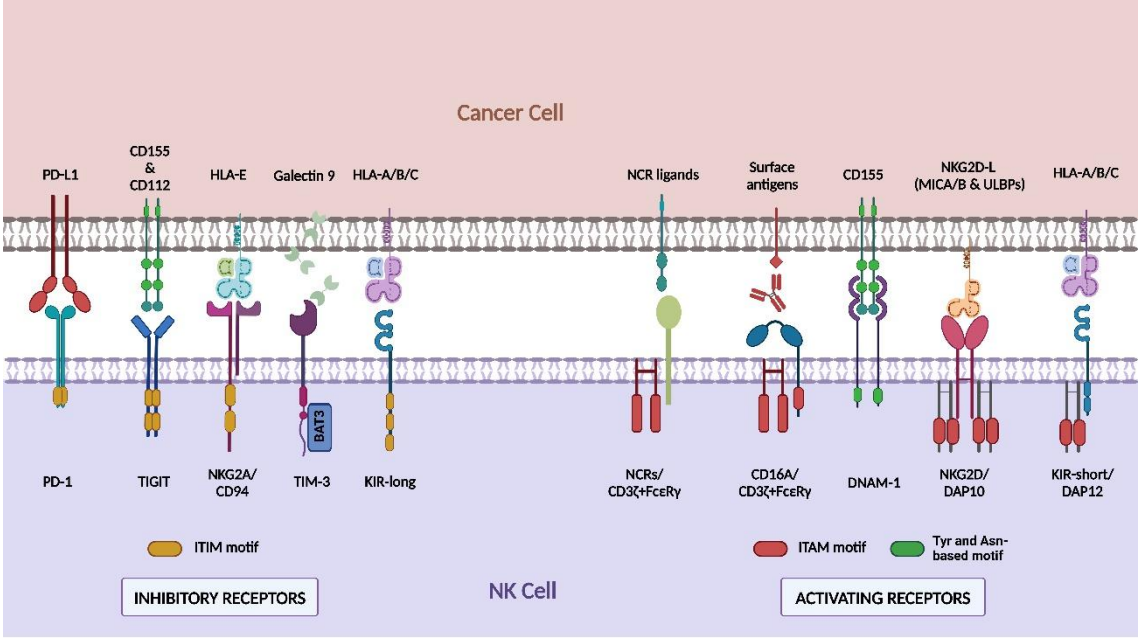

Figure 14. Major endogenous inhibitory and activating NK receptors and their ligands that modulate NK cell responses. PD-L1: programmed cell death ligand 1; HLA: human leukocyte antigen; NCR: natural cytotoxicity receptors; NKG2D: natural killer group 2 member D; NKG2D-L: NKG2D ligands; MICA/B: major histocompatibility complex class I chain-related protein A/B; ULBP: unique long 16 binding protein; KIR: killer-cell immunoglobulin-like receptor; DAP10/12: DAP10: DNAX-activating protein 10/12; DNAM-1: DNAX accessory molecule-1; TIM-3: T cell immunoglobulin domain and mucin domain-3; NKG2A: natural killer group 2 member A; TIGIT: T cell immunoreceptor with Ig and ITIM domain; PD-1: programmed cell death 1; ITIM: immunoreceptor tyrosine-based inhibitory motif; ITAM: immunoreceptor tyrosine-based activation motif; Tyr- and Asn- based motif: tyrosine- and asparagine-based motif. Modified from Valeri et al. Front Immunol. 2022[242]. Created with BioRender.com

NK cells *per se* have great antitumor potential which synergizes with the expression of CAR molecules that redirect NK cells towards tumors. These native receptors potentially guarantee tumor killing even in a "tumor escape" context characterized by CAR antigen downregulation or loss, thus remarking a great advantage over CAR T cells, whose activity is limited to CAR signaling.

Importantly, another relevant feature of CAR NK cells over CAR T effectors is that on-target off-tumor toxicities using CAR NK cells are minimal[264], probably due to the short half-life of circulating CAR NK cell effectors (approximately 2 weeks) and KIR inhibiting mechanisms that control CAR NK cell killing. This avoids the need of introducing suicide genes to control CAR NK response and proliferation[242,265].

3.1.2. Safer cytokine-release profile with low probability of producing severe adverse effects

Contrary to CAR T cells that mainly release IL-6, IL-8, and IL-1β cytokines upon activation that usually unleash severe CRS in patients, CAR NK cells exert their function through IFN-γ, GM-CSF, TNF-α, and IL-3 secretion, reducing the probability of generating a CRS. Additionally, the short *in vivo* lifespan of CAR NK cell effectors may contribute to this advantage over CAR T cells. Moreover, clinical studies have not yet reported ICANS in CAR NK treated patients[242,252]. On the other hand, CAR NK cells have high expression of chemokine receptors and usually release chemokines such as CCL2, CCL3, CCL4, CCL5, and CXCL1 that promote NK and other immune effector trafficking to tumor niches[266,267].

3.1.3. "Off-the-shelf" product from different NK cell sources

CAR NK cells can be generated from multiple primary NK sources such as PB, CB, or placenta[268] or can be derived from undifferentiated progenitors like HSPCs, human embryonic stem cells (hESC), or induced pluripotent stem cells (iPSC). Additionally, there are NK cell lines which can also be used for CAR NK adoptive immunotherapy (**Figure 15**).

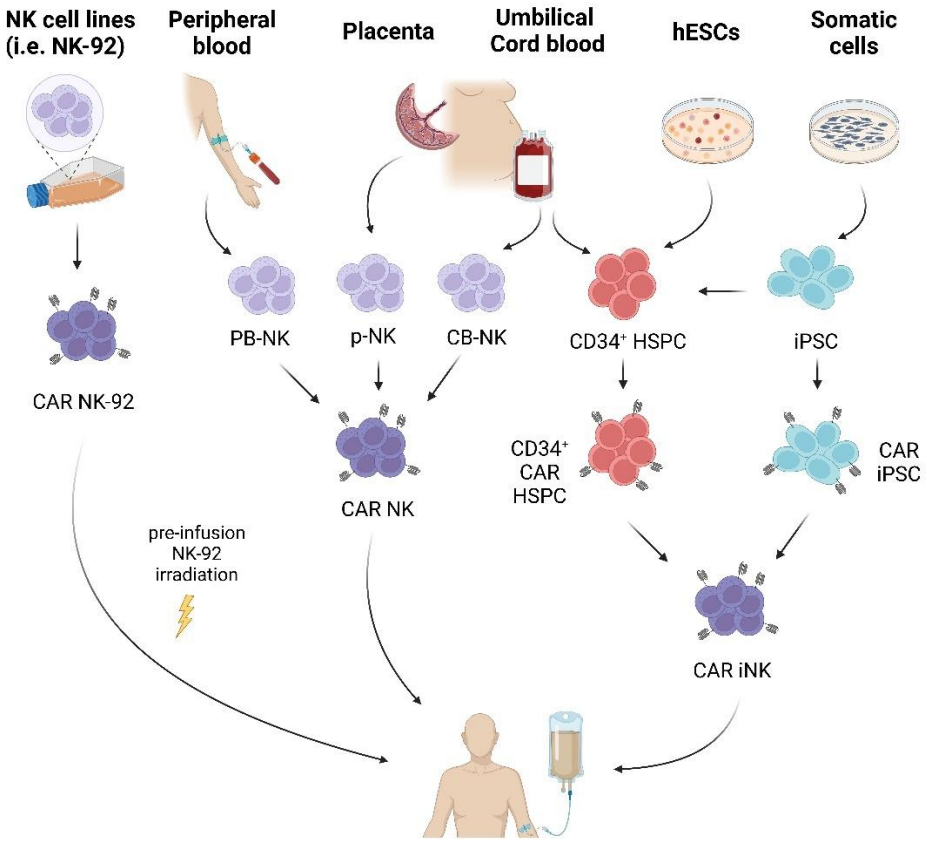

Figure 15. NK cell sources for CAR NK cell adoptive immunotherapy. PB: peripheral blood; p: placental; CB: cord blood; HSPC: hematopoietic stem progenitor cell; hESC: human embryonic stem cells; iPSC: induced pluripotent stem cell; CAR: chimeric antigen receptor. Created with BioRender.com.

Most of CAR NK cell products are applied in an allogeneic context due to the low probability of NK cells to produce GvHD, as they lack TCR. This facilitates the preparation and manufacturing of "*off-the-shelf*" products which supposes a great advantage over the expensive and length procedures to obtain autologous CAR T cells[250,269].

The majority of CAR NK cell preclinical and clinical studies have used NK cells derived from PB and CB. Although circulating PB-NK cells only represent 5-15% of total blood lymphocytes, PB mononuclear cells (PBMCs) from large blood samples (i.e. apheresis and buffy coats) can be expanded using artificial antigen presenting cells (aAPCs) and/or cytokines promoting NK cell activation and proliferation thus obtaining clinical doses of NK cell effectors. Activated PB-NK cells have a potent cytotoxic and heterogenous profile with high expression of activating receptors like CD16, DNAM-1, NKG2D, and NCRs as well as TRAIL death-inducing ligand. However, they also present a mature phenotype with high expression of CD57 and KIRs and are highly refractory to lentiviral vector transduction due to NK-antiviral mechanisms that limit CAR transference. Additionally, it has been reported that long PB-NK cultures drive telomere shortening which may compromise CAR NK cell persistence[270-273].

NK cells derived from CB samples represent an alternative to PB-NK cells with some advantages, such as better lentiviral transduction efficiencies and lower GvHD risk because of the lower percentage of T cells in CB samples compared to PB, which reduces the probability of T contamination in final products. Moreover, CB-NK cells can be cryopreserved which facilitates the creation of cell banks that allow rapid therapy preparation and even creation of multiple doses from the same donor[272,274]. Although resting CB-NK cells have an immature phenotype with lower KIR expression and less activating receptors such as DNAM-1 or CD16[272,274-276], when activated *in vitro* with aAPCs and/or cytokines, they have similar killing capacity as PB-NK cells[272,274,275,277]. Moreover, CB-NK cells express higher levels of CXCR4 which facilitates their migration to BM, thus enhancing efficacy against BM-resident tumors[274,275]. Of note, NKG2A immune checkpoint is highly expressed on resting CB-NK cells which may impair their functionality within the TME as will be later described[274,276,278].

NK cell lines can be also used for CAR immunotherapy. Although different cell lines are being investigated, NK-92 cell line, immortalized from an NK lymphoma donor, is the only NK cell line approved by FDA for clinical purposes. Despite presenting some clear advantages over primary NK cell sources, such as homogeneity, easy genetic modification, and unlimited culture expansion, irradiation of NK-92 cells is necessary prior infusion to avoid tumorigenesis and, as a consequence, its cytotoxic potential and persistence *in vivo* are diminished[245,272,276].

Finally, other emerging sources for CAR NK manufacturing are *in vitro* differentiated NK (iNK) cells from $CD34^+$ HSPCs, hESCs or iPSCs. Among the advantages of using these NK sources, it is worth mentioning the homogeneity of the final product, the easy genetic manipulation, and the possibility of generating unlimited doses from the same donor. However, the manufacturing process is significantly longer compared to CB- or PB-NK cells and requires specialized expertise. Moreover, the final iNK cells express a reduced variety of NK cell killing receptors, are immunogenic and, in the case of iNKs derived from hESCs or iPSCs, potentially harbor a high risk of malignant transformation[245,272,276]. Nevertheless, up to date, no teratoma appearance has been observed in current iNK clinical trials (NCT05182073, NCT04555811)[227,279].

3.2. CAR NK cells targeting MM in preclinical studies and clinical trials

Numerous preclinical studies have demonstrated the great efficacy of CAR NK cell effectors obtained from different sources for cancer treatment, especially in hemato-oncologic patients.

In the context of MM, different CAR NK approaches have been proposed with promising efficacy results. The first strategies were developed using NK-92 cell line targeting CS-1[151] and CD138[280]. However, although these studies showed both *in vitro* and *in vivo* efficacy, as it was aforementioned, these targets are not specific from malignant MM PCs which leads to off-tumor toxicities and NK cell fratricide (CS-1) and, as a consequence, difficult their clinical application. With a similar potential fratricide effect, a few years later, α-CD38 CAR NK-92 cells also demonstrated antitumor activity against MM[281]. NK-92 cells expressing a CAR directed to the *gold-standard* BCMA antigen have shown as well preclinical anti-MM efficacy alone[282] or in combination with other genetic modifications (TRAIL overexpression) and drug therapies[283]. Moreover, the easy genetic manipulation of this cell line has facilitated the development of therapeutic strategies combining two different CAR specificities within the same cell effector. Examples of these include dual CAR NK-92 targeting BCMA and CD19[284], CD138 and CD19[285], and BCMA and NKG2D-L[286].

Primary CAR NK cells derived from PB, CB, and iPSCs have also been designed against MM, some of them including genetic modifications to improve their antitumor responses or surpass certain therapy-related limitations. For example, the expression of a CAR targeting BCMA has demonstrated enhanced cytolytic activity of PB-NK cells against MM cell lines[287]. Some groups have gone further and have developed more sophisticated α-BCMA CAR PB-NK cell products incorporating CXCR4, which enhances NK migration towards BM[288], or an inducible IL-15 expression cassette to potentiate CAR NK proliferation and killing potential[289]. Our laboratory has also engineered BCMA-targeting PB-NK cells (unpublished results[290]) and NKG2D CAR PB-NK cells

targeting NKG2D-L with demonstrated efficacy against MM both *in vivo* and *in vitro*[164]. Another target that has been explored for CAR PB-NK immunotherapy against MM is CD38. To avoid CAR-derived fratricide effects, Edri *et al.* eliminated the expression of endogenous CD38 in PB-NK cells carrying an α-CD38 CAR[291]. A similar strategy has been used in preliminary experiments in CAR CB-derived NK cells by Brophy *et al.*[292] and Duggal *et al.*[293], who also included a simultaneous *CISH* knock-out (KO) to enhance CAR NK cell persistence. Although many different CB-NK immunotherapies have been evaluated against different hematological tumors, regarding CB-derived effectors targeting MM, no other preclinical studies have been reported yet. However, our group has developed both α-BCMA and α-NKG2D-L CAR CB-NK cells that show encouraging efficacy results against MM (unpublished results[290]). With respect to CAR NK cells derived from iPSCs, O'Neal *et al.*[294] have reported *in vivo* antitumor efficacy against MM of α-BCMA CAR iNK cells. Moreover, two other innovative iNK products have been already developed, FT555[295] and FT576[296], carrying CAR molecules targeting GPRC5D and BCMA, respectively. Both CAR iNK cells contain additional genetic modifications including the addition of a non-cleavable CD16 receptor to enhance ADCC, *CD38* knock-out to avoid NK fratricide when used in combination with daratumumab and the addition of a membrane-bound IL-15/IL-15R fusion protein to boost CAR iNK cell persistence and function. Noteworthy, FT576 is currently being tested in clinical studies.

When moving to the clinic, there are a total of 85 clinical trials testing CAR NK cells efficacy and safety, most of them in early Phases (I and II) and targeting hematologic malignancies. Among them, only 9 are focused on MM treatment (**Table 4**) with only released preclinical supporting data from FT576 iNK product.

Product	NCT	NK source	Phase	Study start	Status
α-BCMA CAR NK	NCT05652530	Unknown	I	2022	Recruiting
α-BCMA CAR NK	NCT06045091	Unknown	I	2023	Recruiting
α-BCMA CAR NK	NCT06242249	Unknown	I/II	2024	Not yet recruiting
α-BCMA CAR NK + Fludarabine + cytoxan	NCT05008536	CB	I	2021	Unknown
ACT-001 CAR NK cell (α-BCMA/ α-GPRC5D bispecific CAR NK)	NCT06594211	Unknown	N/A	2024	Not yet recruiting
α-BCMA CAR NK	NCT03940833	NK-92	I/II	2019	Active, not recruiting
NKG2D CAR NK	NCT06379451	Unknown	I	2024	Not yet recruiting
FT576 (α-BCMA CAR NK)	NCT05182073	iPSCs	I	2021	Active, not recruiting
LUCAR-B68 (α-BCMA CAR NK)	NCT05498545	Unkown	I	2022	Not yet recruiting

Table 4. Current clinical trials testing CAR NK cells for the treatment of MM. CB: cord blood; iPSCs: induced pluripotent stem cells. Data obtained from Clinicaltrial.gov. database.

Regarding hematological tumors in general, only 6 clinical trials have reported preliminary efficacy and safety results, one of them testing FT576 for MM treatment (NCT05182073). The first trial using CAR NK cells was reported for the treatment of $CD19^+$ malignancies by Rezvani's group (NCT03056339), who tested the safety and efficacy of a α-CD19 CAR CB-NK product which was additionally engineered to express ectopic IL-15 and an iCas9 safety switch. The first reported results showed complete responses (CR) in 7 of 11 patients and CAR NK persistence in some patients was observed after 12 months[297]. A most recent update from 37 patients showed 68% and 32% of 1-year overall response (OR) and PFS rates. Despite these improvable efficacy parameters, the most encouraging outcome was the absence of notable toxicities such as CRS, neurotoxicity or GvHD[298]. The lack of therapy-derived toxicities was also reported in the other five studies confirming the safety of these immune effectors over CAR T therapies. However, regarding efficacy, these trials, including the one testing FT576 product, have demonstrated disappointing results[279,299,300], highlighting the urgent need for new strategies to enhance CAR NK cell efficacy.

3.3. Combinatorial strategies to overcome CAR NK limitations

With the aim of improving CAR NK cell efficacy the use of small inhibitors (i.e. GSK3)[301] or receptor agonists such as 2B4, 4-1BB, and SLAMF7[245] which activate CAR NK cell function has been proposed. Moreover, both IMiDs and HDAC inhibitors, despite targeting tumor cells, are able to induce expression of activating receptors in NK cells and, consequently, boost CAR NK activity[302]. In the same line, the use of mAbs such as daratumumab in combination with CAR NK

cells can enhance ADCC responses (NCT05182073). In a similar way to its application in CAR T therapy, another strategy to facilitate CAR NK-tumor interactions and thereby potentiate NK killing, is the use of bispecific killer cell engagers (BiKEs) or BiAbs such as NKG2DxBCMA[174] and CD16xBCMA[303] for MM, or NKG2DxErbB2[304] and CD16xIL13Rα2[305] for breast cancer and glioma, respectively. Additionally, NK cell redirection towards the tumor niche has been also achieved by the engineering of α-BCMA-CAR NK cells to express CXCR4 receptor[288].

However, although those strategies can enhance CAR NK cell activity, the final efficacy outcome remains constrained by several critical factors, including fratricide induction, the immunomodulatory checkpoints in NK cells and the surrounding immunosuppressive TME that limit NK cell function, as well as the reduced *in vivo* persistence of the effector cells which compromise long-term tumor control[242].

3.3.1. Avoiding NK fratricide

Ex vivo expansion of CAR NK cells can be difficult due to an NK cell fratricide effect by which NK cells recognize receptors or ligands on their siblings and kill themselves in response. This undesired effect can be provoked by the manufacturing protocol *per se*. One of the main killing mechanisms of NK cells is apoptosis induction through FasL signaling. However, cytokine or feeder-cell stimulation protocols implying IL-2, IL-15 and IL-21 stimulation can upregulate the expression of Fas receptor that, when binds to NK-expressed FasL, trigger an apoptosis response in the effector cells, decreasing final effector cell numbers. Moreover, as it will be later described, FasL expressed within the TME can decrease CAR NK efficacy. Some other studies have associated cytokine stimulation as well as trogocytosis of tumor cells with increased expression of NKG2D-L in NK cells which could be recognized by endogenous NKG2D receptor. Thus, special care in cell expansion protocols should be taken into account when manufacturing CAR NK effectors[242].

On the other hand, CAR-related fratricide is of special relevance for CAR NK cell design. The use of CAR molecules targeting antigens that are also expressed on the effector cells could trigger fratricide responses that reduce CAR NK cell numbers and therefore, its antitumor efficacy and manufacturing yield. In the context of MM, this happens with CAR NK products targeting CD38 and CS-1. To solve this problem, genome editing has been proposed to eliminate expression of CD38 in CAR NK cells targeting MM cell lines[291-293], as has been previously mentioned, and acute myeloid leukemia (AML)[306] and expression of CD70[307] in CAR NK cells against other hematological malignancies. Besides, CAR-targeted antigen expression can be transferred from tumor cells to CAR NK cells through trogocytosis resulting in lower tumor density antigen as well as CAR NK fratricide. To overcome this limitation, Rezvani's group has proposed the generation of dual CAR

NK cells expressing an activating CAR against the tumor antigen and an inhibitory CAR (containing ITIM intracellular domains) targeting an NK-self antigen (such as CS-1) to counteract the killing response against CAR NK cells that had acquired the tumor antigen[308].

3.3.2. Counteracting NK cell checkpoint inhibitors

As has been described before, in physiological conditions, NK cell activity is highly controlled by inhibitory receptors, also known as checkpoint receptors, that counteract the activating signals to avoid toxicity against healthy cells. However, a high expression of these inhibitory receptors in CAR NK cells decreases their antitumor activity. In this context, strategies based on the use of blocking mAbs or genome editing of specific receptors have been proposed to boost both NK and CAR NK adoptive cell therapies (**Figure 16**).

KIRs are the principal inhibitors of NK cell activity. Notably, KIR expression is upregulated on NK cells from MM patients and impairs antitumor capacity of these effector cells within the tumor niche[309]. A monoclonal antibody against KIR2D, known as IPH2101 or lirilumab, was proposed to be used in combination with lenalidomide or daratumumab to enhance their antitumor response of patient endogenous NK cells against MM and other hematologic tumors. Although preclinical *in vitro* studies showed promising results[310,311], only objective clinical responses were observed in patients when used in combination with lenalidomide but not as monotherapy[312-314]. Importantly, NK cells isolated from patients treated with this mAb, showed less degranulation and cytokine production probably due to trogocytosis-mediated KIRD2 loss in NK cells or a lack of NK cell licensing produced by sustained KIR inhibition[315,316]. The potential use of IPH2101 or other mAbs targeting KIRs in combination with adoptive NK cell transfer, remains to be investigated.

PD-1/PD-1L immune checkpoint has also been targeted to improve NK cell functionality. In an autologous context, pidilizumab (CT-011), a mAb targeting PD-1, boosted NK activity against MM cells synergizing with lenalidomide treatment which reduces PD-L1 expression in tumor cells[317]. However, when pembrolizumab, another α-PD-1 mAb, was tested in clinical trials against MM, controversial outcomes were reported. Some studies demonstrated the efficacy of this antibody, but others reported lack of long-term responses and high therapy-related adverse effects[318-320]. When applied in a CAR NK cell context, although PD-1 expression is low in *ex vivo* expanded NK effectors[321], Yang *et al.* have reported preliminary results supporting the use of an α-PD-L1 mAb in combination with dual αBCMA/αGRPC5D CAR NK cell to better target MM[322]. Of note, a Phase II clinical trial is already underway combining CAR NK with pembrolizumab (NCT04847466), although it is currently indicated for the treatment of solid tumors. Additionally, CRISPR/Cas9

genome editing also represents a useful tool to address this target as Pomeroy *et al.* described for NK cell effectors[323].

In MM, expression of TIGIT ligands (PVR and Nectin-2) is increased after BTZ treatment which impairs NK cell activity. Liu *et al.* demonstrated that TIGIT blockade could enhance NK cell activity against MM cells, in an autologous context[324]. In a similar trend, this strategy has been followed in other tumors[325,326]. Regarding adoptive NK or CAR NK therapies, it has also been reported a higher antitumor efficacy of NK cells using mAbs[327] or after disrupting TIGIT expression in NK effectors by CRISPR/Cas9 genome editing[328-330], although these strategies have not been yet applied in MM.

Despite not yet combined with CAR immunotherapy, the use of mAbs that block TIM-3 has also demonstrated efficacy in increasing NK cell anti-MM efficacy[331] as well as CRISPR/Cas9 genome editing has proven to be a feasible tool to eliminate TIM-3 expression and increase NK cell efficacy against glioma cells[332].

Apart from those inhibitory receptors, HLA-E/NKG2A is a dominant immune checkpoint in cancer, including MM, and constitutes one of the major breaks in CAR NK effector cell activity.

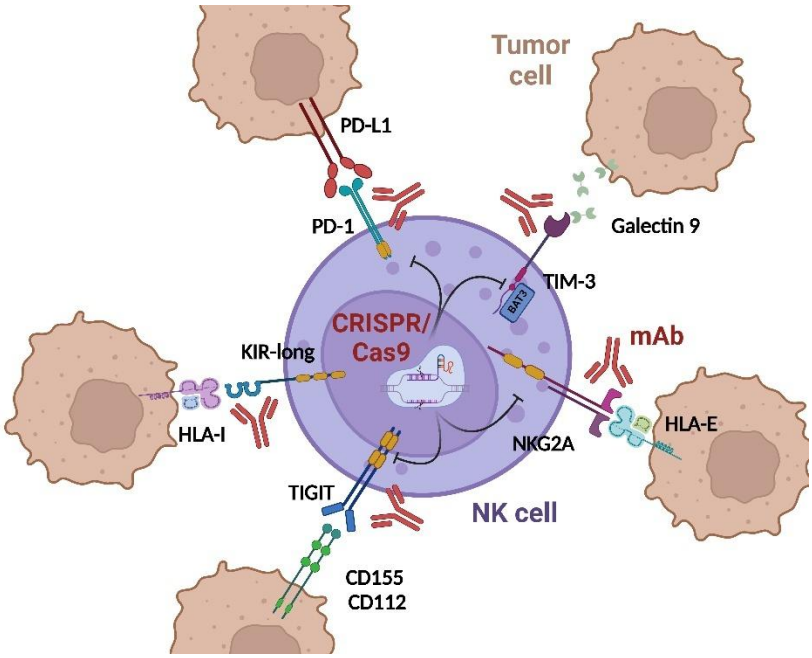

Figure 16. Proposed strategies to avoid immunocheckpoint-mediated inhibitory signals in adoptive NK cellular therapy. PD-L1: programmed cell death ligand 1; PD-1: programmed cell death 1; TIM-3: T cell immunoglobulin domain and mucin domain-3; mAb: monoclonal antibody; HLA: human leukocyte antigen; NKG2A: natural killer group 2 member A; TIGIT: T cell immunoreceptor with Ig and ITIM domain; KIR: killer-cell immunoglobulin-like receptor. Created with BioRender.com

3.3.2.1. NKG2A/HLA-E axis

HLA (or MHC) class I molecules comprise two different groups of molecules: Ia and Ib. HLA class Ia molecules are highly polymorphic molecules that allow selection of T cell repertoire and mediate antigen-specific T cell responses. On the contrary, class Ib comprise the low polymorphic proteins HLA-E, -F, -G, MICA, and MICB molecules and CD1 antigens[333]. *HLA-E* gene consists of 8 exons and is located in the MHC complex on the chromosome 6. HLA-E molecules are less diverse than HLA class Ia counterparts but, although two dominant alleles represent 99% of the total frequency with one single nucleotide variation, recent studies have reported the existence of up to 256 *HLA-E* encoding for 110 HLA-E proteins[334], which challenges its low polymorphism.

HLA-E is nearly structurally identical to HLA class Ia molecules requiring binding to an invariant B2M and specific peptides for stable surface expression[334]. However, peptides binding to HLA-E are limited, in contrast to the wide variety of peptides that interact with HLA class Ia. Most of them are derived from intracellular proteins or pathogens, amino acid residues 3-11 from other HLA molecules (A, B, C, and G) or Hsp60. These peptides are generated in the cytosol by proteasome degradation and require the correct functionality of a transporter associated with antigen processing (TAP). Moreover, peptide sequence influences the binding affinity to HLA-E[335-337].

HLA-E is expressed at low levels in almost all nucleated healthy cells, except for placenta trophoblasts and ductal epithelial cells in the testis and epididymis and some immune cells, which express high levels of this protein, thus suggesting the importance of this molecule for immune tolerance. However, under pathological conditions, such as autoimmune diseases, stem cell transplantation or cancer, HLA-E protein expression can be highly upregulated and impairs the correct functionality of NK and $CD8^+$ T lymphocytes. Related to cancer, high levels of HLA-E have been described in different solid and hematologic tumors, including MM. In some of these cases, its expression is correlated with a worse prognosis[100,337,338].

Regarding MM, a preliminary study by Lagana *et al*. demonstrated increased HLA-E mRNA expression in PC from newly diagnosed MM patients which correlated with a lower PFS[339] and, in the same trend, Yang *et al.* reported a high correlation between HLA-E expression and advanced ISS stages and high-risk cytogenetics[53]. Recently, HLA-E protein expression was also confirmed in PC from MGUS and MM patients[340]. Moreover, our group has analyzed the expression of HLA-E protein in PC from MM patients, finding higher expression of this protein in pathologic PC compared to normal PC within the same patient, especially at progression (unpublished results[341]).

HLA-E expression can be modulated by different drugs used for the treatment of MM patients. For example, BTZ treatment impairs proteasome degradation, which not only alters the protein metabolism of MM cells but also reduces the amount of stabilizing HLA-E-binding peptides and, therefore, compromises stable HLA-E expression[96]. Although it has not been described in MM, the treatment with IMiDs such as pomalidomide has been shown to reduce the expression of HLA-E in AML cells[342] and Selinexor has been reported to reproduce the same effect in B lymphoma cells[116]. Other drugs used to treat other tumors, such as selenite or cyclin-dependent kinase (CDK) inhibitors (dinaciclib) can also downmodulate HLA-E expression in tumor cells[343,344].

On the contrary, it has been reported that IFN-γ, a cytokine found in high levels in MM patients[345], induces HLA-E expression in MM via JAK/STAT1 signaling[346,347] and other tumor cells[348-350]. As a consequence, IFN-γ activating agents such as IMiDs (pomalidomide and lenalidomide), as well as panobinostat can enhance HLA-E expression in MM cells[340]. Importantly, combined treatment of proteasome inhibitors (BTZ or carfilzomib) with IMiDs decreased HLA-E expression, suggesting a dominant effect of proteasome inhibitors over IFN-γ-inducing agents and, adding a rationale to the combination drug regimens[340]. Another dominant regulator that has been described for HLA-E and is related with JAK/STAT1 signaling is CREB1 (cAMP responsive element binding protein 1). This transcription factor directly binds to HLA-E promoter and also induces STAT1 and IRF9, enhancing HLA-E expression through both direct and indirect mechanisms. Inhibition of this protein reduced the expression of HLA-E in MM cells even in the presence of IFN-γ stimulation[340,351].

HLA-E binds to the NKG2 family members A, B, C, and E, but does not interact with KIRs. Importantly, it binds with much higher affinity to NKG2A (inhibitory receptor) than to NKG2C and NKG2E (activating receptors), mainly triggering an inhibitory response[335,338,352].

NKG2A protein is encoded by *KLRC1* gene, which consists of 7 exons and localizes in chromosome 12. NKG2A is expressed on NK cells, invariant NKT, activated $CD8^+$ T cells, and γδ T cells and constitutes an important immune checkpoint inhibitor that modulates immune responses. NKG2A forms heterodimers with CD94 protein, which lacks intracellular signaling domains. On the contrary, NKG2A intracellular domain contains ITIM domains that, upon HLA-E binding, get phosphorylated and recruit SHP1 and SHP2 phosphatases, which dephosphorylate and inactivate proteins such as SYK (spleen tyrosine kinase), Vav1, ZAP70 (zeta-chain-associated protein kinase 70), Fyn, and LCK (lymphocyte-specific protein tyrosine kinase) impairing the formation of immune synapsis with target cells and, as a consequence, reducing NK and T cell activity[353-355] (**Figure 17**). Additionally, besides controlling NK cell responses, NKG2A plays an important role in NK cell licensing alongside with KIRs and it has been reported in murine models

that long-term suppression of NKG2A may result in deficient NK cell cytotoxicity and IFN-γ production[356].

The interaction of HLA-E and NKG2A is modulated depending on the peptides loaded on HLA-E. For example, HLA-G peptides induce a stronger inhibition in NK cells than HLA-A, B and C, while Hsp60 peptides impair NKG2A binding to HLA-E[357].

Between 20-50% of circulating NK cells express NKG2A, being increased in the $CD56^{bright}$ NK cell population compared to $CD56^{dim}$ subset. It has been reported that some drugs such as dasatinib, used for CML treatment, can inhibit GATA-3 transcription factor thus reducing NKG2A expression. On the contrary, some cytokines used in NK cell expansion methods (i.e. IL-21 and IL-15) can upregulate NKG2A expression, highlighting the importance of this modulation axis in adoptive NK cell therapies, including CAR immunotherapy. Other cytokines such as IL-10 and TGF-β, which are usually present within the TME, also increase NKG2A expression in NK cells. Of note, NKG2A expression has been found to be upregulated in tumor-infiltrating NK cells from different types of solid and hematologic tumors and correlates with a poor prognosis[352,353]. Moreover, in the context of MM, preliminary results from our lab indicate that BM NK cells from RRMM patients had increased NKG2A expression compared to patients at diagnosis or with MGUS (unpublished results[341]).

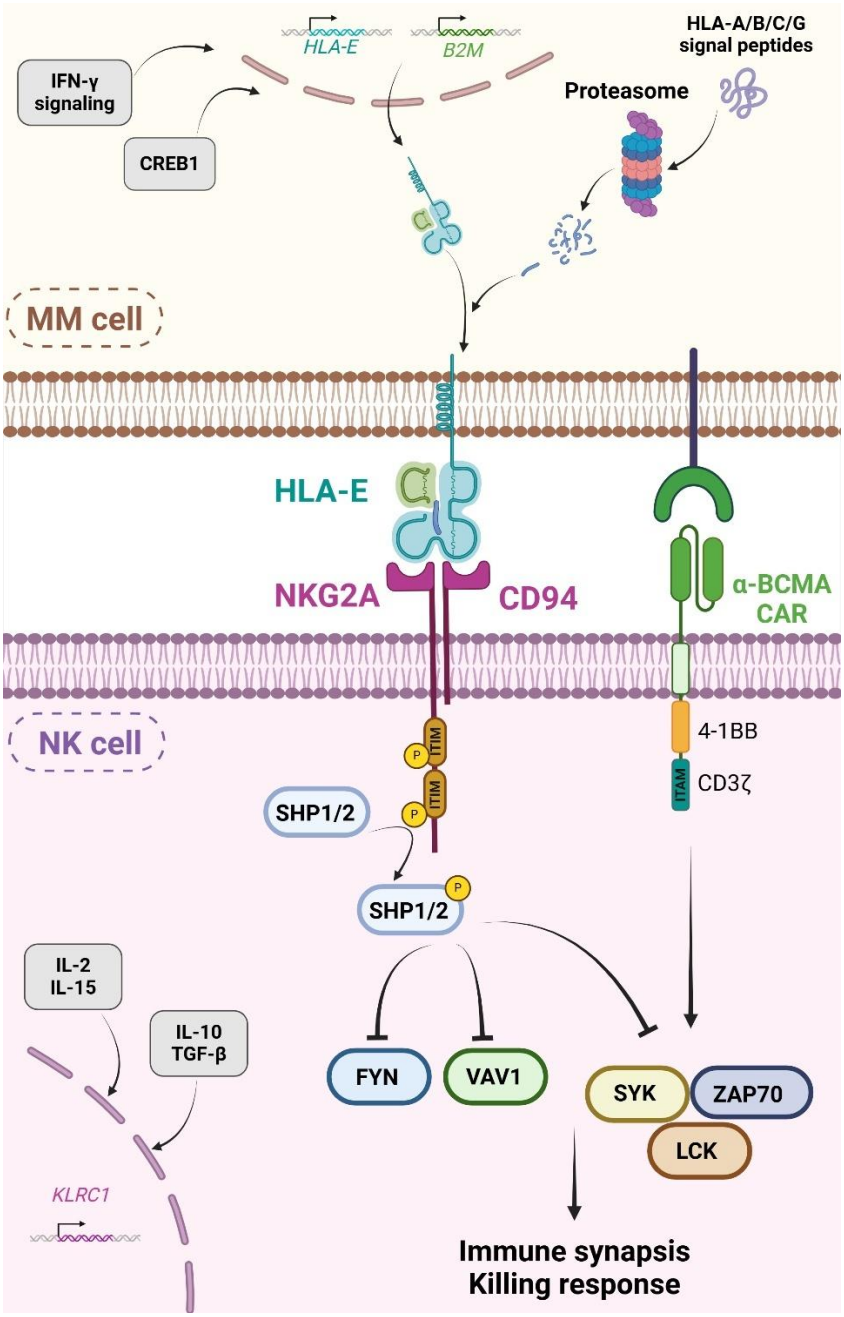

Figure 17. NKG2A/HLA-E signaling pathway and modulation. IFN-γ: interferon γ; CREB1: cAMP responsive element binding protein 1; HLA: human leukocyte antigen; MM: multiple myeloma; NKG2A: NK group 2 member A; BCMA: B cell maturation antigen; CAR: chimeric antigen receptor; ITIM: immunoreceptor tyrosine-based inhibitory motif; ITAM: immunoreceptor tyrosine-based activation motif; SHP: Src homology region 2 domain-containing phosphatase; LCK: lymphocyte-specific protein tyrosine kinase; SYK: spleen tyrosine kinase; ZAP70: Zeta-chain-associated protein kinase 70; IL: interleukin; TGF-β: transforming growth factor β. Created with BioRender.com.

Due to the high expression of both HLA-E in tumors and NKG2A in tumor-infiltrating and *ex vivo* expanded NK cells, many groups have focused their research on the development of strategies targeting this pathway with the goal of potentiating NK antitumor responses in both an autologous and allogeneic context (**Figure 18**).

The combination of chemotherapeutic drugs that reduce HLA-E expression, as was described above, has been proposed to indirectly target HLA-E in tumor cells. Additionally, direct targeting using α-HLA-E mAbs has shown efficacy *in vitro* in reducing HLA-E-mediated NK inhibition and fostering NK-mediated ADCC[353]. However, most of the strategies are focused on the NKG2A receptor.

Preclinical studies have demonstrated that the use of α-NKG2A mAbs such as Z199 (mouse anti-human Ab) or monalizumab (humanized IgG4 Ab) increases NK cell antitumor efficacy against different solid and hematologic tumor cells[245,348,349,358-361]. Regarding MM, Mahaweni *et al.* suggested that Z199 mAb did not provide cytotoxic improvement to *ex vivo* expanded NK cells, despite expressing high levels of NKG2A[362]. However, another study from the same year published by Tognarelli *et al.* demonstrated opposite results supporting the use of Z199 mAb to potentiate cell immunotherapy against MM[346]. In accordance with this, our group has also demonstrated the efficacy of both Z199 and BMS-986315 α-NKG2A mAbs in enhancing CAR NK antitumor potential (unpublished results[341]).

Other strategies are focused on reducing NKG2A surface expression in NK cells. For example, Kamiya *et al.* designed a protein expression blocker (PEBL) for NKG2A using fragments from Z199 and ER-retention domains. This PEBL efficiently retained NKG2A protein in the ER, resulting in a lower surface expression and an increased NK cytotoxicity against HLA-E^+ tumors, even with higher efficacy than α-NKG2A antibodies[350]. Using a different approach, Figuereido *et al.* demonstrated that NKG2A silencing with siRNAs enhanced NK cell cytotoxicity against B lymphoblastoid cells[363]. With the emergence of CRISPR genome editing technology, some groups have disrupted *KLRC1* expression in PB-NK cells to improve their antitumor potential against hematologic malignancies, including MM[347,364-366], and solid tumors[367]. When considering CAR NK cell effectors, there are controversies about the functional effects of knocking-out NKG2A. Some authors have reported that elimination of NKG2A expression in CAR NK-92[368] and CAR iNK[369] cells do not improve their antitumoral potential against melanoma and B-ALL, respectively. On the contrary, a recent study from Bexte *et al.* with CAR PB-NK cells has demonstrated that *KLRC1* KO in α-CD33 CAR NK cells increases killing potential against primary AML cells and cell lines, compared to wild-type CAR NK effectors. These results were confirmed in an immunodeficient xenograft mouse model of AML[370].

Despite all those preclinical studies, up to date, only the use of monalizumab as monotherapy or in combination with other blocking antibodies or chemotherapy has been tested in clinical trials. Most of these studies have been focused on solid tumors. As monotherapy, monalizumab showed short-term disease control against gynecologic malignancies[371] but failed to achieve

expected responses in head and neck squamous cell cancer (HNSCC) (1.7 months PFS)[372]. Therefore, monalizumab efficacy has been tested in combination with other mAbs against HNSCC achieving PFS that ranged from 4.5 to 6.9 months, depending on the mAb regimen. Some adverse effects that were found in these patients were dermatitis acneiform, dry skin, pruritus, rash, asthenia, mucosal inflammation, and infusion-related reactions[373,374]. Another study in non-small cell lung cancer (NSCLC) patients showed a beneficial effect of using monalizumab in combination with durvalumab (PFS 15.1 months) but also some adverse effects such as cough, dyspnea, pneumonitis, and pruritus were observed[375]. Monalizumab has been also combined with trastuzumab for the treatment of $HER2^+$ breast tumors but no objective responses were achieved[376]. Regarding hematologic tumors, first short-term results from a Phase I trial using monalizumab after ASCT in patients with AML, myelodysplastic syndrome (MDS), lymphoma, chronic lymphocytic leukemia (CLL), and myelofibrosis revealed CR in 13 out of 15 patients, with no side effects[377].

These results suggest that monalizumab monotherapy is not able to restore NK and T cell effector cytotoxicity, especially in solid tumors, but can show great utility when combined with adoptive cell therapies such as ASCT or CAR immunotherapy. Although no clinical studies have been reported in the context of MM, preclinical results demonstrate the importance of addressing NKG2A/HLA-E axis to boost CAR NK efficacy against malignant PC.

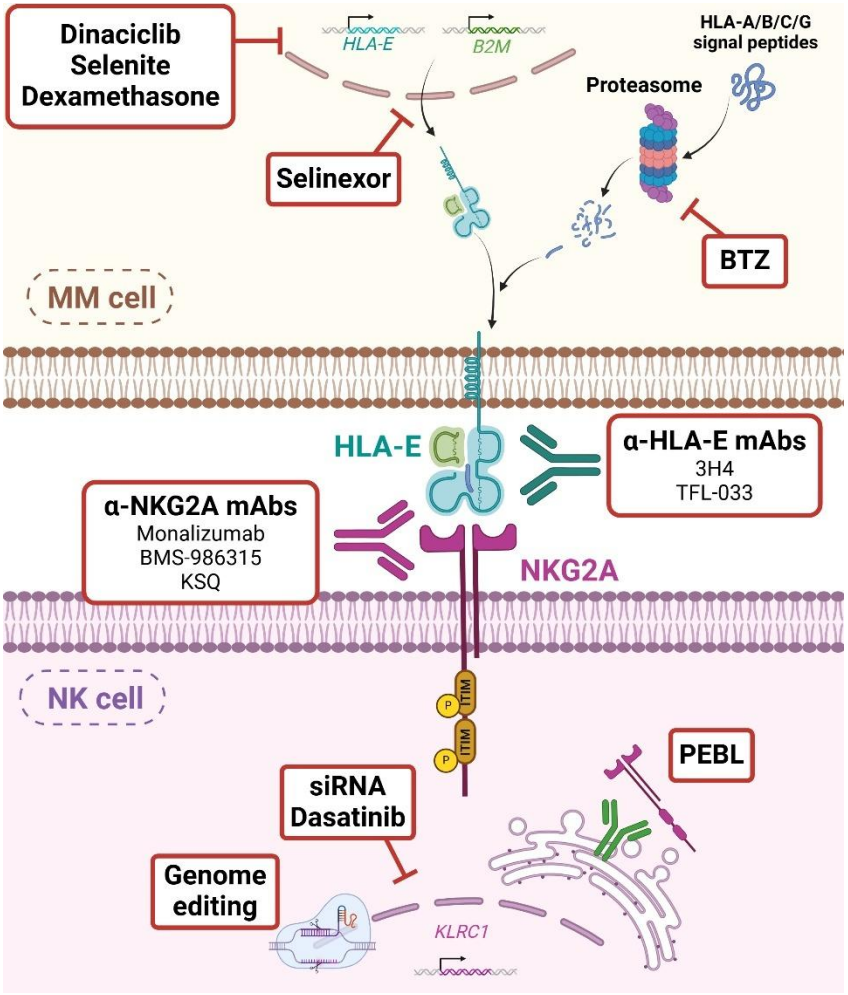

Figure 18. Therapeutical strategies targeting NKG2A/HLA-E signaling. HLA: human leukocyte antigen; MM: multiple myeloma; NKG2A: NK group 2 member A; ITIM: immunoreceptor tyrosine-based inhibitory motif; mAbs: monoclonal antibodies; PEBL: protein expression blocker; siRNA: small interfering RNA. Created with BioRender.com.

3.3.3. Overcoming immunosuppressive TME

Tumor microenvironment is another key factor that not only diminishes the antitumor capacity of patient's immune effectors favoring tumor evasion, but also compromises the cytotoxic efficacy of adoptive CAR NK and CAR T therapies. While the presence of an immunosuppressive TME is one of the hallmarks for tumor development in both solid and hematologic tumors, in MM there is a notorious immunosuppression that is especially associated with disease progression.

As previously mentioned, MM cells express high levels of surface proteins (HLA class I, HLA-E, PD-L1, and CD80/86) that interact with immune checkpoint inhibitors which are upregulated in NK and T cells from MM patients (KIR, NKG2A, PD-1, CTLA-4, TIGIT, TIM-3), impairing their functionality. In addition to these cell-cell interactions, high levels of IL-6, IL-10, TGF-β, INF-γ

together with other inhibitory factors such as sMICA, ADO, and indoleamine-pyrrole 2,3-dioxygenase (IDO) have been found in MM patients[59,345,378]. These inhibitory molecules diminish cytotoxic responses of immune cells as well as recruit other immune cells that contribute to immunosuppression[59,379] (**Figure 19**).

For example, IL-6, produced by MM PC, BM MSC as well as MDSCs not only enhances tumor proliferation but also diminishes NK cell function[59,380] and inhibits DC differentiation, which consequently reduces T cell stimulation[381]. MM PCs along with recruited M2-polarized TAMs and Tregs secrete IL-10 which hampers effector T cell proliferation and inhibits production of IFN-γ in NK cells, impairing their antitumor capacity[59,382]. Moreover IL-10 also induces NKG2A expression in NK cells[352,353]. These cells also secrete TGF-β which reduces NK and T cell function, as will be described later in more detail. High levels of IFN-γ induce PD-L1 and HLA-E expression in MM plasma cells thus contributing to NK and T cell inhibition and/or exhaustion[346,347,383]. In addition, ADO release from MM cells, which is mediated by CD38 ectoenzyme, also limits NK and cytotoxic T cells[59,379,384,385]. On the other hand, IDO activity converts tryptophan into kynurenine. Excessive IDO levels in MM reduce tryptophan availability leading to cell cycle arrest and apoptosis of T cells, which require this amino acid for survival. Kynurenine also impairs interactions between DCs and T and NK cells[386,387]. IDO can also downregulate NCR and NKG2D expression in NK cells thus reducing their killing capacity[250,388]. Apart from these molecules, high levels of sMICA, which is correlated with a poor prognosis in MM, neutralize NKG2D receptor function diminishing NK efficacy[378,389].

MM cells and BM MSCs secrete chemokines that promote M2 polarization of macrophages and factors such as type I IFN, APRIL, and ADO, that together with IDO activity, induce Treg activation and recruitment into the tumor niche[59,379]. Moreover, BTZ treatment promotes TAMs accumulation in BM from MM patients[390]. TAMs, Tregs, and MDSC secrete factors that promote angiogenesis and tumor growth but, at the same time, release IL-10, TGF-β, and ADO contributing to NK and T cell inhibition[59,379]. Importantly, several studies have correlated high levels of M2 macrophages with poor prognosis and worse response to chemotherapy and ASCT[391-393]. Besides, an increased proportion of Tregs is associated with shorter PFS in MM patients[394].

Altogether, the TME is characterized by multiple interactions mediated by cell-cell contacts and secretion of soluble factors that support MM progression and immune evasion. These interactions create an immunosuppressive niche that can reduce the efficacy of adoptive CAR immunotherapy.

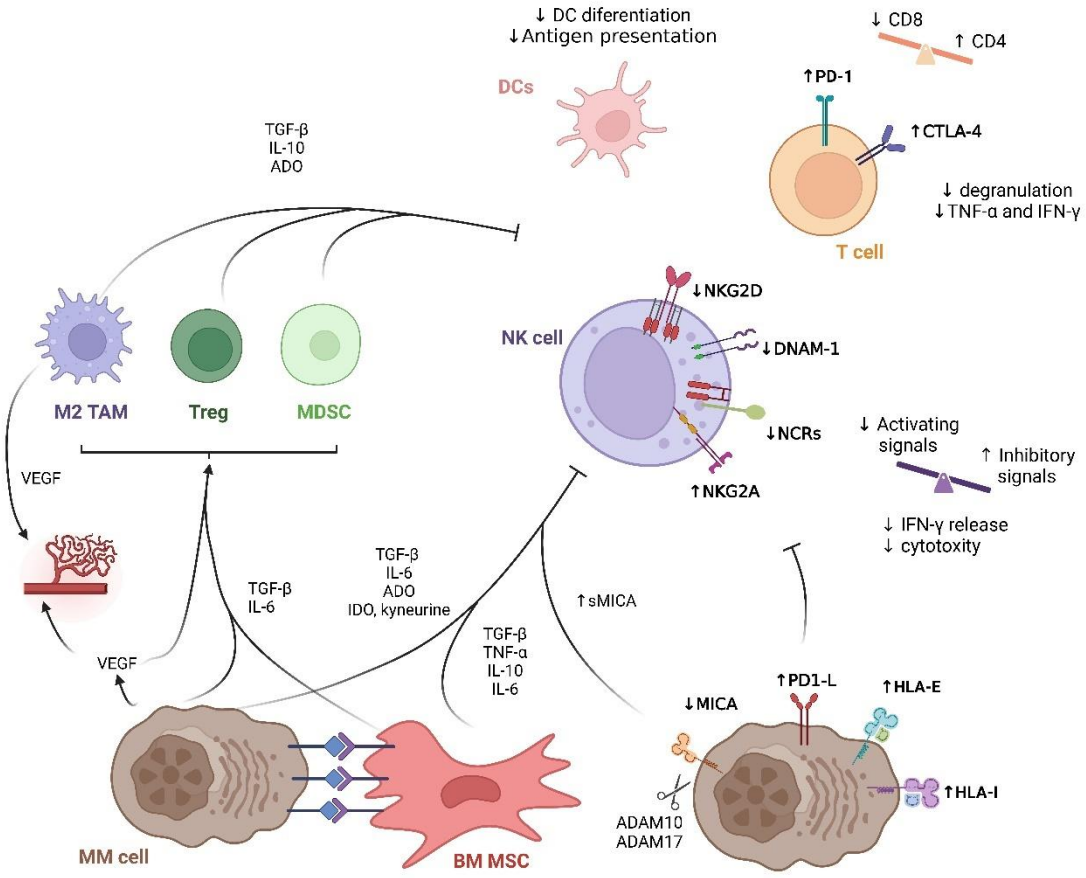

Figure 19. Immunosuppressive signals from TME in MM. DC: dendritic cell; TGF-β: transforming growth factor-β; IL: interleukin; ADO: adenosine; CTLA-4: cytotoxic T-lymphocyte antigen 4; PD-1: programmed cell death 1; TNF-α: tumor necrosis factor α; NKG2A/D: N natural killer group 2 member A/D; DNAM-1: DNAX accessory molecule-1; NCR: natural cytotoxicity receptors; M2 TAM: M2-polarized tumor-associated macrophages; Treg: regulatory T cell; MDSC: myeloid derived suppressor cells; VEGF: vascular endothelial growth factor; IDO: indoleamine-pyrrole 2,3-dioxygenase; MM: multiple myeloma; BM MSC: bone marrow mesenquimal stromal cell; MICA: major histocompatibility complex class I chain-related protein A; sMICA: soluble MICA; ADAM: A disintegrin and metallopeptidase; PD-1L: programmed cell death ligand 1; HLA: human leukocyte antigen. Created with BioRender.com.

Different strategies have been proposed to enhance antitumor activity of effector cells by directly targeting TME immunosuppressor cells. For example, concerning MM, the use of JAK1/2 inhibitors (ruxolitinib) or CSF1R receptor blocking mAbs in a preclinical setting has demonstrated efficacy in reducing M2 polarization and decreasing TAMs survival and proliferation[395,396]. The use of the inhibitor FL118 was found to inhibit multiple antiapoptotic proteins from the inhibitor of apoptosis (IAP) family (Survivin, XIAP, cIAP2) and from the BCL-2 family (MCL-1) while inducing the expression of pro-apoptotic proteins such as BAX and BIM in BM MSCs thus inhibiting BM MSC-mediated resistance to CAR T therapies[397]. Moreover, Tregs in MM can potentially be targeted with α-CD38 CAR effectors, which not only recognize MM cells but also $CD38^{+}$ Tregs[398]. Using a similar strategy, α-CD25 CAR NK cells may have the same effect against Tregs, although they have not yet been applied in MM[399]. Other strategies proposed for solid tumors that could

potentially be translated to MM, focus on preventing the release of soluble factors to the TME. For example, specific mAbs targeting the MICA α3 domain have shown to inhibit the shedding of this ligand from tumor cells boosting NK cell-mediated cytotoxicity[400].

Nevertheless, many other groups have focused their research on strategies that directly target TGF-β signaling pathway, as it represents one of the major immunosuppressive agents in the TME not only in MM but also in other tumors.

3.3.3.1. TGF-β signaling

The soluble factor TGF-β (transforming growth factor β) belongs to a cytokine family comprised of 33 members that, besides TGF-β isoforms, include other cytokines such as bone morphogenetic proteins (BMPs), growth and differentiation factors (GDFs), activins, inhibins, and nodal and anti-Müllerian hormone (AMH)[401]. There are three different isoforms of TGF-β (1, 2, and 3) that are encoded by three different genes (*TGFB1*, *TGFB2,* and *TGFB3*) and share between 71-79% identity[402]. The three TGF-β isoforms play essential functions during embryonic development, wound healing, and adult tissue and immune homeostasis[403].

During TGF-β biosynthesis, initial TGF-β monomers contain a signal peptide, a latency-associated peptide (LAP), and the mature TGF-β protein. During post-translational processing in the ER and Golgi, signal peptide is removed and mature TGF-β monomers dimerize through disulfide bonds. Additionally, LAP is cleaved but still remains associated with de TGF-β dimer forming the latent TGF-β complex (LTC) that is secreted by the cell. After secretion, LTC interacts with extracellular proteins that anchor LTC to cell surface or to ECM. In order to become a mature cytokine that triggers signal transduction, LTC needs to be activated by removal of LAP. This process is modulated by pH, reactive oxygen species, integrins, trombospondin-1, and MMP. After processing, active TGF-β homodimers can bind to their cognate receptors[403].

There are also different receptors that recognize with different specificities the members of TGF-β family. The three TGF-β isoforms bind with different affinities to TGF-β receptors I, II, and III which are codified by *TGFBR1*, *TGFBR2,* and *TGFBR3* genes, located in different chromosomes (9, 3, and 1, respectively). Moreover, TGF-β can also be recognized by activin receptor-like kinase (ALK)-1, which is expressed on endothelial cells. Importantly, TGF-βRII and III only bind to TGF-β isoforms while TGF-βRI (also known as ALK-5) shows a more promiscuous binding profile and recognizes other ligands of the family[401].

TGF-βRI and II are enzyme-linked receptors with Ser/Thr kinase and Tyr kinase activity while TGF-βRIII lacks signaling motifs and acts as a coreceptor that further enhances recognition by the other two receptors. TGF-β1 and TGF-β3 bind to TGF-βRII homodimers with high affinity. In

contrast, TGF-β2 shows higher affinity for TGF-βRIII receptor. TGF-β binding promotes heterotetramerization of TGF-βRI/II. Canonical TGF-β signaling is mediated via SMAD2/3 signaling. Upon the formation of the heterotetrameric complex, TGF-βRII phosphorylates TGF-βRI which recruits and activates SMAD2/3. However, apart from the SMAD-dependent pathway, non-canonical pathways can trigger ERK, JAK/STAT3, RHO GTPase, p38, JNK, NF-κB, and PI3K/AKT signaling. As a result of this great variety of signaling cascades, TGF-β modulates a wide diversity of processes that modulate survival, growth, differentiation, movement, metabolism, and immune responses[401,403] (**Figure 20**).

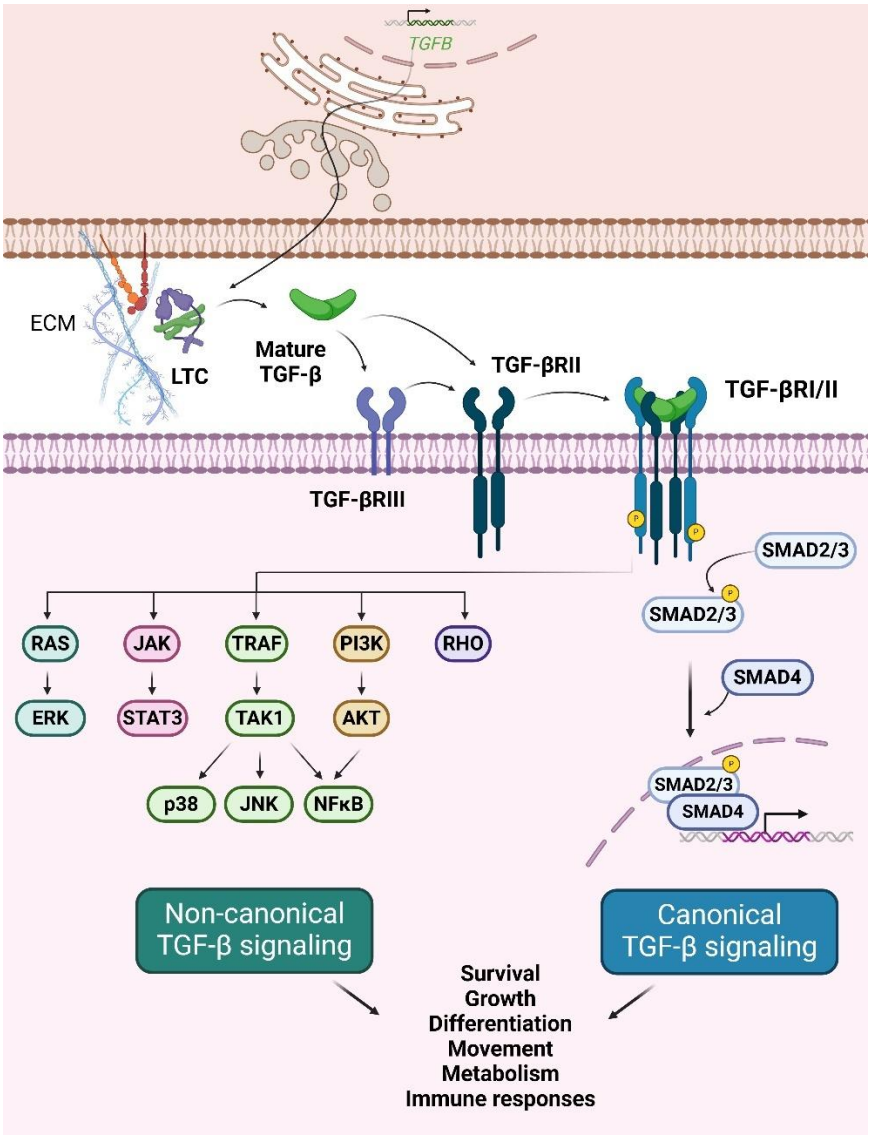

Figure 20. Canonical and non-canonical TGF-β signaling pathways. ECM: extracellular matrix, LTC: latent TGF-β complex; TGF-β: transforming growth factor β; TGF-βR: TGF-β receptor; ERK: extracellular signal-regulated kinase; JAK: Janus kinase; STAT: signal transducer and activator of transcription; TRAF: TNF receptor associated factor; TAK1: Transforming growth factor β-activated kinase 1; JNK: c-Jun N-terminal kinase; NFκB: nuclear factor-κB; PI3K: Phosphoinositide 3-kinase. Created with BioRender.com.

In physiological conditions, many different cell types secrete TGF-β and/or express their receptors. However, during pathological processes, TGF-β dysregulation may contribute to developmental defects, aberrant wound healing, fibrotic and inflammatory diseases, as well as tumor progression[403].

In the context of MM, TGF-β is highly secreted by MM PCs and triggers IL-6 and VEGF secretion by BM MSCs, thus promoting tumor growth and angiogenesis. Moreover, TGF-β/SMAD signaling can regulate the expression of the proteasome subunit PSMB5, which is associated with resistance to proteasome inhibitors[404]. This soluble factor also stimulates Treg and MDSC differentiation and activation, which in turn, secrete more TGF-β and other cytokines that exert inhibitory control over other antitumor immune cells. Besides, TGF-β can also promote M2 macrophage polarization[10,16,51,403,404].

TGF-β also regulates immune cell activity in the MM TME and suppresses immunosurveillance by directly targeting T, NK, and DC effector cells. For example, TGF-β downregulates MHC class II molecules in DCs impairing antigen presentation. Moreover, TGF-β suppresses expression of T-BET and GATA-3 transcription factors which are essential for Th1/Th2 differentiation. On the other hand, secretion of cytolytic factors, FasL, and IFN-γ by $CD8^+$ T cells is diminished in response to TGF-β/SMAD signaling. Additionally, TGF-β may induce T cell exhaustion[403,404].

Regarding NK cells, increased TGF-β levels affect the cytolytic potential of tumor surrounding NK cells in different ways. TGF-β downregulates T-BET expression in NK cells in a SMAD3-dependent manner and therefore inhibits CD16-induced INF-γ production[405]. Moreover, granzyme A and B as well as perforin expression were also downregulated by the same mechanism, impairing cytotoxic activity of NK cells[405,406]. It has also been reported that TGF-β downregulates NK cell activating receptors such as CD16, NKG2D, DNAM-1, and NKp30[406-409]. Additionally, some studies have reported that TGF-β alters NK cell metabolism affecting glycolysis and phosphorylation[410,411] (**Figure 21**).

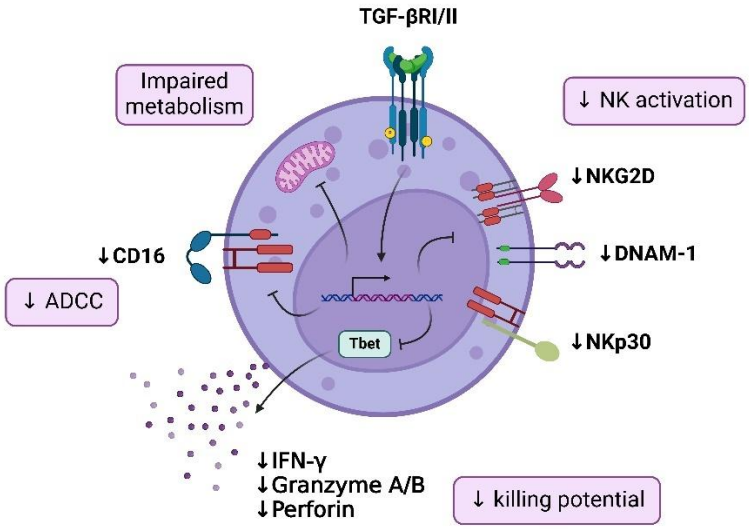

Figure 21. Immunomodulatory effects of TGF-β signaling in NK cells. TGF-βR: transforming growth factor β receptor; ADCC: antibody-dependent cell-mediated cytotoxicity; NKG2D: natural killer group 2 member D; DNAM-1: DNAX accessory molecule-1; IFN-γ: interferon γ. Created with BioRender.com.

Due to the high relevance of this axis in tumor progression and immune surveillance, many strategies have been designed to directly target both TGF-β and their receptors in cancer patients (**Figure 22**). For example, antisense RNAs alone or in tumor vaccines targeting TGF-β mRNA (Trabedersen and belangenpumatucel-L) or mRNAs encoding for proteins implicated in TGF-β processing (gemogenocatucel-T), have been proposed for the treatment of different solid tumors with promising clinical outcomes. Similarly, other mAbs (SRK-181; PIIO-1 and Abituzumab) and inhibitors (cilengitide) targeting the LTC and the proteins that mediate its processing, prevent TGF-β activation and are being investigated against solid cancers. Different antibodies (Fresolimumab and NIS793) and ligand traps (AVID200) targeting the active form of TGF-β are able to inhibit ligand-receptor interactions and are being tested in clinical trials[403,412]. Related to ligand traps, a new generation of bifunctional antibody-ligand traps recognizing both TGF-β and PD-L1 (bintrafusp alfa and BR102) are being tested against solid tumors in a clinical and preclinical setting and have inspired the development of CAR T cells secreting PD-1/TGF-β traps to enhance CAR T efficacy against $CD19^+$ cell lines[403,412,413].

On the other hand, other groups have focused on targeting TGF-β receptors. With that aim, different small kinase inhibitors such as vactosertib and galunisertib have been proposed for both solid and hematologic tumors[403,412]. Notably, Vactosertib has been tested in a Phase Ib clinical trial in combination with pomalidomide in RRMM patients. Preliminary results showed objective responses in 75% of patients and 6-month PFS in 82%. Adverse effects were manageable although one patient died from a grade 4 hepatotoxicity[414]. Other TGF-βRI inhibitors

that have shown preclinical efficacy in restoring osteoblast differentiation in MM are SB-431542 and Ki26894[415].

Those approaches have been mainly designed to directly inhibit tumor growth and potentiate patients' immunosurveillance. However, regarding NK cells, reported results from Shaim *et al.* are of special relevance. These authors remark that the use of TGF-βR inhibitors (galunisertib and LY2109761) efficiently increases HD NK cell cytotoxicity against glioblastoma cells preventing TGF-β-mediated inhibition but, importantly, fails to re-activate inhibited tumor-infiltrating NK cells[416]. Moreover, a recent publication from the same group reported that TGF-β-mediated inhibition of NK cells from AML patients was also persistent due to a deep epigenetic reprogramming triggered by BATF, which is one of the targets of the TGF-β/SMAD pathway[417]. These results highlight the importance of developing NK and CAR NK adoptive cell therapies to treat both solid and hematologic cancer patients. On the other hand, it has been reported that *ex vivo* expanded PB- and CB-NK cells are also susceptible to TGF-β inhibition[418] which indicates that combinatorial strategies directly targeting TGF-β signaling are necessary, not only to restore patient's immune cell activity, but also to boost the efficacy of adoptive NK immunotherapy.

In this context, Otegbeye *et al*. have demonstrated that the use of the TGF-β receptor inhibitor LY2157299 mitigates the TGF-β-mediated impairment of *ex vivo* expanded HD NK cells and increases their antitumor potential against AML and colon cancer cell lines[419]. Shaim *et al.* also demonstrated that the use of galunisertib or cilengitide (which targets αβ integrins necessary for LTC processing) potentiates NK cell killing against glioblastoma cell lines both *in vivo* and *in vitro*[416]. Using another approach applied in CAR T[420,421], Bollard's group has expressed a dominant negative TGF-β receptor II (DNR) in CB-NK by retroviral transduction. These DNRs are mutant receptors that lack kinase domain but bind with high affinity to TGF-β, thus acting as anchored ligand traps that impair TGF-β binding to the wild-type receptors. DNR-expressing CB-NK cells were phenotypically similar to non-transduced peers. However, in the presence of TGF-β, they maintained perforin and IFN-γ secretion as well as NKG2D and DNAM-1 expression and showed increased efficacy against glioblastoma and medulloblastoma[422,423]. A similar strategy was followed by Yang *et al.* in NK-92 cells against lung cancer cells using nucleofection[424] and, more recently, by Thangaraj *et al.* in iNK cells for hepatocellular carcinoma treatment using the Piggybac transposon system[425].

As CRISPR editing technology emerged, different groups have efficiently disrupted *TGFBR2* in NK cells to be used against both solid and hematologic tumors. Naeimi *et al.* were the pioneers in disrupting this receptor in PB-NK cells using CRISPR/Cas9 which conferred resistance to TGF-β-mediated inhibition of cytotoxicity against a medulloblastoma cell line[426]. Rezvani's group,

besides demonstrating the efficacy of galunisertib in combination with PB-NK cell infusion for the treatment of glioblastoma and AML, also targeted TGF-β pathway by disrupting *TGFBR2* in PB-NK cells. Of note, knock-out of *TGFBR2* increased antitumor efficacy of NK cells *in vivo* and even outperformed TGF-βRII inhibition by galunisertib[416,417]. Zhang *et al.* have also efficiently eliminated TGF-βRII expression in PB-NK cells through the development of a highly efficient version of AsCas12 enzyme. *TGFBR2* KO NK cells did not show SMAD phosphorylation in response to TGF-β treatment and their cytotoxic potential against ovarian tumor spheroids was not diminished in the presence of this soluble factor[427]. Moreover, preliminary results from Gerew *et al.* also demonstrated the feasibility of knocking-out *TGFBR2* in combination with *CISH* in iNK cells to generate an allogeneic NK product with higher efficacy against ovarian cell line models and less susceptibility to IL-15 exhaustion and TGF-β inhibition[428]. In the CAR NK immunotherapy field, up to date, only two groups have eliminated *TGFBR2* expression by CRISPR/Cas9 in CAR NK effectors. Guo *et al.* eliminated this receptor in α-CD19 CAR PB-NK cells showing preliminary data of function improvement[429] and Thangaraj et al. have recently demonstrated that *TGFBR2* KO in two different CAR iNK effectors increased their persistence as well as their antitumor efficacy *in vivo* in hepatocellular carcinoma xenograft mouse models[425].

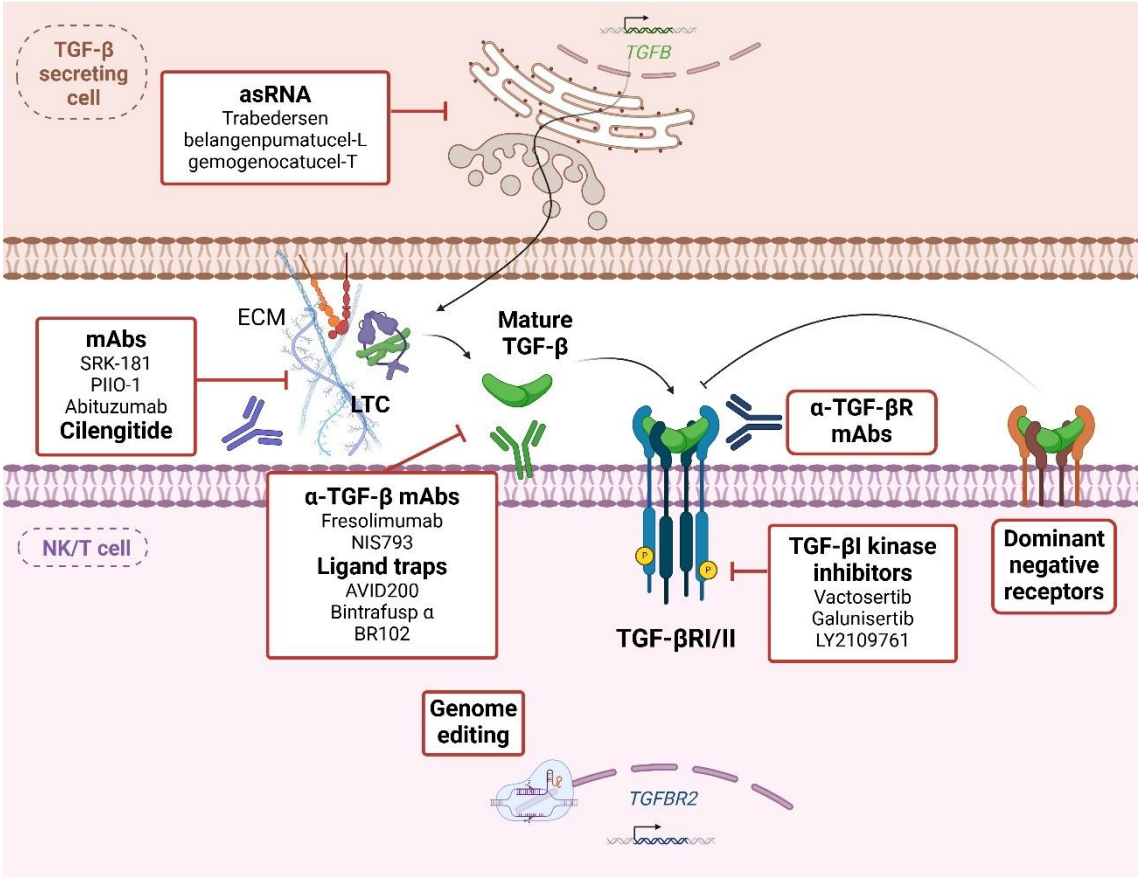

Figure 22. Therapeutical strategies targeting TGF-β signaling pathway. TGF-β: transforming growth factor β; asRNA: antisense RNA; mAbs: monoclonal antibodies; ECM: extracellular matrix; LTC: latent TGF-β complex. Created with BioRender.com.

3.3.4. Improving NK cell *in vivo* persistence

Another major limitation that compromises long-term efficacy of CAR NK cell effectors is their short lifespan. Although this low persistence avoids the generation of uncontrolled immune responses and reduces the possibility of oncogenesis, it also diminishes antitumor efficacy. Better clinical responses have been correlated with higher *in vivo* persistence of NK and CAR NK after adoptive transfer[298,430].

One of the main reasons behind the reduced persistence of CAR NK cell effectors is T cell allorejection. Although allogeneic NK cells do not produce GvHD, the host immune system can recognize exogenous CAR NK cells. The creation of universal cell banks with HLA-typed CAR NK products may facilitate the election of haploidentical CAR NK cells to mitigate host allorejection. The first approaches to increase NK persistence proposed multiple cell injections, but the NK cell numbers in circulation were even lower after second infusion[431]. To reduce allorejection, Hoerster *et al*. have introduced two genetic modifications in PB-NK cells. First, they knocked-out *B2M* gene to eliminate expression of HLA-I in NK cells thus not being recognized by alloreactive

T cells. Second, to avoid NK cell fratricide by "*missing-self*" recognition, they introduced a single-chain HLA-E molecule that binds to NKG2A receptor. These modifications overcame $CD8^+$ T cell alloreactivity while maintaining NK cell killing potential against AML cell lines[432]. Noteworthy, Century Therapeutics has implemented these modifications in a multi-engineered α-CD19 CAR iNK product (CNTY-101), which is being tested in a clinical trial (NCT05336409), along with the disruption of CIITA (class II major histocompatibility complex transactivator) to further circumvent $CD4^+$ allorejection[433,434].

Another explanation for the reduced *in vivo* persistence of CAR NK cells is the lack of cytokine support. Most *ex vivo* NK cell expansion protocols rely on a continuous administration of non-physiological doses of interleukins which efficiently contribute to cell activation. However, NK cells can become "cytokine-dependent", limiting their survival *in vivo* after cytokine withdrawal[435]. In this context, the combined IL-2 systemic administration together with allogeneic NK cells was firstly proposed to sustain NK cells *in vivo*, but this cytokine also activated endogenous Tregs that counteracted NK cell activation[436]. Moreover, systemic IL-2 administration showed severe toxicities such as capillary leak syndrome[437,438]. As an alternative, the use of engineered IL-15 agonists such as ALT-803[439] and NKTR-255[440] has been considered to potentiate NK cell activity. Despite no clinical outcomes have yet been reported in combination with NK cell adoptive therapy, some studies have found cytokine-related toxicities such a CRS or neutropenia after systemic IL-15 administration in humans[441] and non-human primates[442], respectively. *In situ* IL-15 secretion has been tested by engineering CAR NK cells to avoid undesired effects of systemic administration. For example, Liu *et al.* developed an α-CD19 CAR CB-NK product with autocrine secretion of IL-15. This NK cell product showed high cytotoxicity *in vitro*[443] and enhanced persistence in a Phase I/II clinical trial, without systemic IL-15 increase in patients[297]. In a similar trend, other armored CAR NK cell products have been developed against solid and hematologic tumors[289,444,445]. Importantly, one of these CAR NK products has shown systemic toxicity in an AML mouse model[444]. Going one step beyond, Soldierer *et al.* engineered α-CD19 CAR PB-NK cells with an IL-15/IL-15Rα fusion protein, which increased CAR NK antitumor capacity and persistence *in vivo*, compared to IL-15 secreting CAR NK cells[446]. This construction has been included in multi-edited CAR iNK cells against MM (FT576)[279] and B cell malignancies (FT596)[299].

Cytokine support of NK cells with IL-2 or IL-15, besides inducing cell activation, can also trigger NK cell exhaustion through the activation of suppressors of cytokine signaling (SOCS). SOCS family comprises SOCS1-7 members as well as CIS (cytokine-inducible SH2-contianing protein; encoded by *CISH* gene). These proteins are upregulated in response to cytokine signaling and act

as negative feedback regulators by impairing JAK/STAT cytokine cascades[447,448]. Naeimi *et al.* showed preliminary results of increased antitumor efficacy of PB-NK cells after deletion of *SOCS3* by CRISPR/Cas9[449]. However, the most exploited SOCS member is CIS. Many different groups have successfully eliminated *CISH* expression in PB-NK, iNK and NK cell lines alone or in combination with other genes (*TGFBR2, TIPE2,* or *B2M*) resulting in higher sensitivity to IL-15-mediated activation, improved metabolic fitness, longer *in vivo* persistence and enhanced antitumor capacity against different solid and hematologic cancer models[428,450-455]. Others have taken a step further by disrupting this gene in CAR NK effectors derived from PB, CB, and iPSCs[456-458]. Among them, it is worth mentioning the combined strategy followed by Daher *et al.* in which the ablation of *CISH* in α-CD19 CAR CB-NK effectors synergized with the effects of autocrine secretion of IL-15[458]. There are other cytokine-induced modulators that can decrease sensitivity of NK cells to IL-induced expansion. In this sense, BLIMP1 constitutes a promising target to improve NK cell persistence, as will be described later.

Independently of cytokine support, *ex vivo* activated and expanded PB-NK cells can eventually become unresponsive to stimulation and undergo senescence after 15 weeks of continuous *in vitro* proliferation[459]. Regarding CAR CB-NK effectors, Liu *et al.* also showed a decrease in NK fold expansion after 3 weeks of *in vitro* culture using IL-15 armored CARs[443]. In the clinical use, although α-CD19 CAR CB-NK effectors demonstrated increased persistence, their detection in PB by flow cytometry was limited to the first three weeks after therapy infusion, despite IL-15 autocrine support and previous lymphodepletion[297]. This suggests that NK, and consequently CAR NK, effectors are short-lived cells and may undergo senescence induction, likely influenced by the expansion methods[242]. In this setting, some groups have proposed ectopic expression of hTERT (human telomerase reverse transcriptase) in NK cells to improve their expansion capacity and persistence and therefore, increase their therapeutic potential, as it has been described for CAR T cells[460]. For example, a pioneer study from Campana's lab demonstrated that overexpression of hTERT in both NK and CAR NK from PB could restore replicative potential up to one year maintaining their cytotoxic potential although these cells still required continued stimulation and were not capable of growing autonomously in an immunodeficient mouse model[459]. More recently, Streltsova *et al.* corroborated that hTERT ectopic expression in PB-NK cells boosted their expansion capacity and lifespan without completely immortalizing the cells. These promising studies support the use of this strategy to enhance NK cell proliferative potential[461].

Finally, another strategy to improve NK cell persistence is to induce a memory-like phenotype by a brief cytokine priming with IL-12, IL-15, and IL-18 that induces epigenetic reprogramming and

phenotype changes in NK cells that are transferred to the progeny. These cytokine-induced memory-like NK (CIML NK) effectors secrete more INF-γ and have decreased KIR, thus acquiring more cytotoxic potential. Moreover, they have increased proliferative capacity and higher expression of CD25 (IL-2Rα) and nutrient transporters being more responsive to IL-2 stimulation and showing enhanced metabolic activity that favors their *in vivo* persistence. Many preclinical and clinical studies are evaluating the efficacy and safety of this approach against both hematological and solid tumors and even designing combinatorial strategies to increase clinical outcomes, including CAR molecules[242,462]. Regarding MM, up to date, there is one ongoing clinical trial testing CIML NK cells in combination with an α-CD38 antibody recruiting molecule in RRMM patients[463].

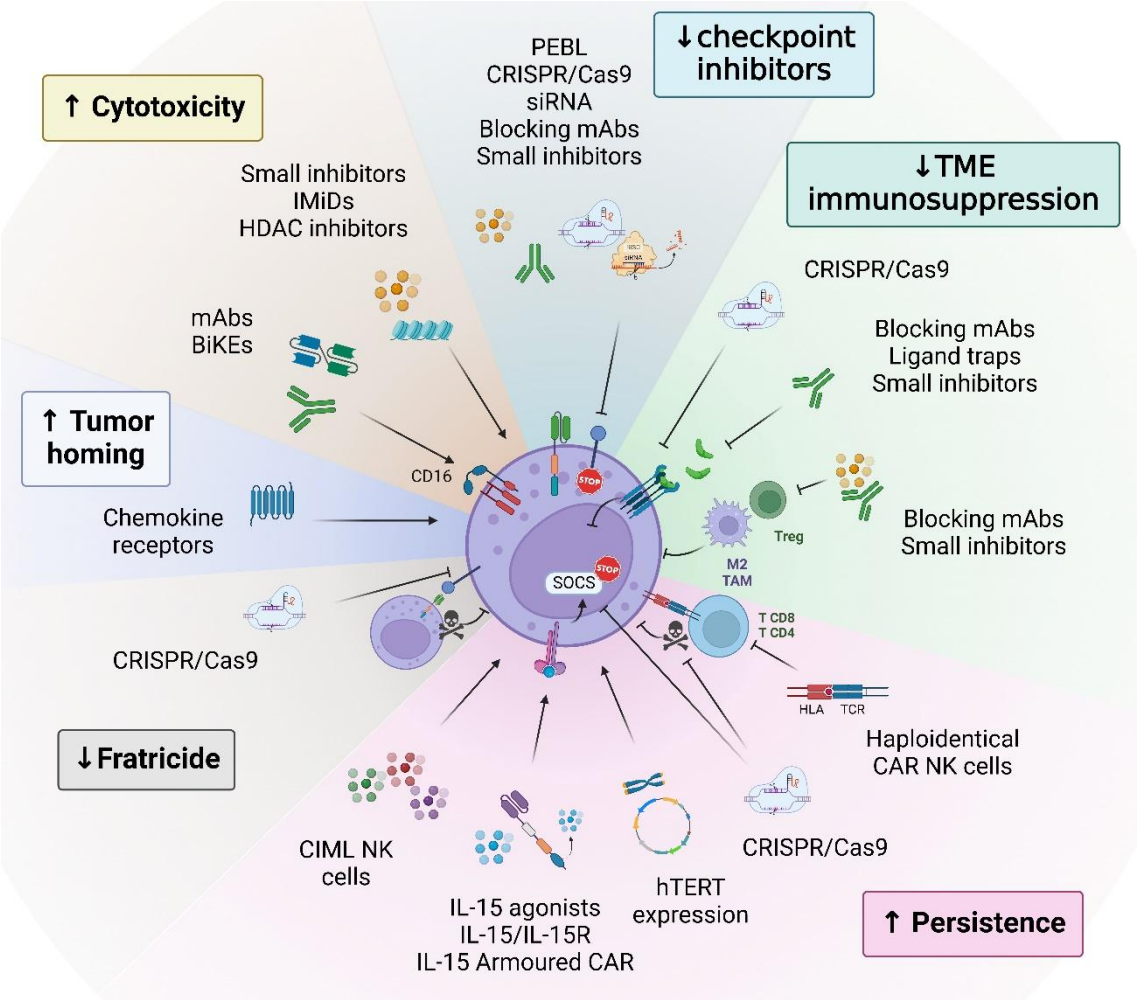

Figure 23. Summary of strategies proposed to increase CAR NK cell efficacy, persistence, and tumor homing, as well as to reduce CAR-mediated fratricide and inhibitory signals from immunomodulatory checkpoint inhibitors and from the immunosuppressive TME. PEBL: protein expression blocker; siRNA: silencing RNA; mAbs: monoclonal antibodies, IL-15: interleukin 15; IL-15R: IL-15 receptor; CAR: chimeric antigen receptor; CIML NK: cytokine-induced memory-like NK cells; BiKEs: bispecific NK engagers; HDAC: histone deacetylase; IMiDs: immunomodulatory drugs; Treg: regulatory T cells; M2 TAM: M2-polarized tumor-associated macrophages; HLA: human leukocyte antigen; TCR: T cell receptor; hTERT: human telomerase reverse transcriptase. Created with BioRender.com.

3.3.4.1. The master transcriptional regulator BLIMP1

BLIMP1 (B-lymphocyte-induced maturation protein 1), also known as PRDI-BF1 (positive regulatory domain 1 binding factor 1) is a transcription factor encoded by *PRDM1* gene, comprising 7 exons and located in chromosome 6. BLIMP1 binds DNA target through five Zn domains at the C-terminus of the protein. When binding to DNA, BLIMP1 recruits chromatin-modifying factors such as TLE1 (Transducin-like enhancer protein 1) and histone deacetylases through a proline-rich region at the N terminal side of the protein, enabling chromatin modifications to repress target gene transcription[464].

There are two main isoforms of the protein encoded by two different promoters: a full-length protein (BLIMP1-α) and a truncated form that lacks exons 1-3 (BLIMP1-β). Despite BLIMP1-β is the predominant expressed form in primary NK cells, this isoform has reduced repressive ability compared to BLIMP1-α, due the lack of the PR domain and N terminal domain[465,466] (**Figure 24**). Moreover, another isoform (BLIMP1-αΔ6), a splice variant of BLIMP1-α with an intermediate molecular weight, has been identified in primary NK cells[466].

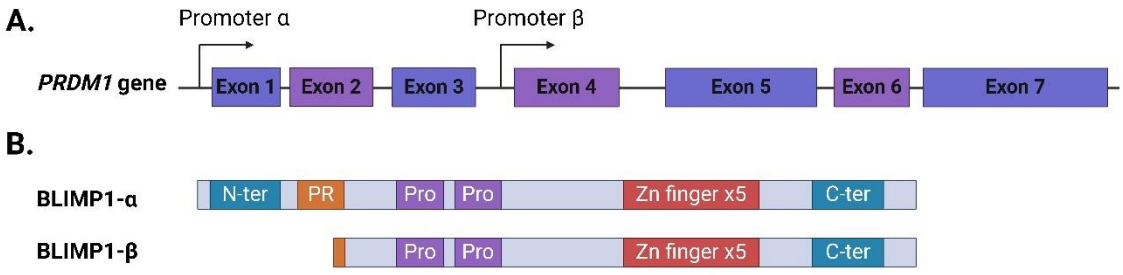

Figure 24. Schematic representation of *PRDM1* gene (A) and main BLIMP1 protein isoforms (B). N-ter: acidic N-terminal domain; Pro: Proline-rich domain; C-ter: C-terminal domain. Adapted from Nadeau et al. Front Immunol. 2022[464]. Created with BioRender.com.

BLIMP1 is expressed in a wide variety of cells and constitutes a master regulator during embryonic development and terminal differentiation of numerous cell lineages, including immune cells. The role of BLIMP1 is essential for terminal differentiation and mAb secretion in plasma cells, whereas in T cells this transcription factor regulates terminal functional differentiation and modulates cytokine gene expression and T cell homeostasis. Moreover, BLIMP1 has also been described as participating in DC maturation[464,467].

Regarding NK cells, Kallies *et al.* studied the role of BLIMP1 mouse homolog (Blimp1) in NK cell development and maturation using different transgenic mouse models and *in vitro* assays. They described that Blimp-1 was dependent on IL-15 stimulation and T-bet expression and regulated

NK cell homeostasis by promoting cell differentiation and maturation while restricting proliferation, without having direct control over NK cell cytotoxicity capacity[467].

At the same time, Smith *et al.* were the first to provide a functional description of BLIMP1 in human NK cells. BLIMP1 expression was preferentially expressed in the $CD56^{dim}CD16^{+}$ population after cytokine stimulation (i.e. IL-2, IL-12, and IL-18). Chromatin immunoprecipitation (ChIP) experiments revealed that BLIMP1 binds to target-gene promoters in a cell type-specific manner, regulating transcriptional network differently compared to other cell types. They demonstrated that BLIMP1 binds to *INFG* and *TNF* regulatory sequences in NK cells and negatively controls the production of these cytokines in response to NK cell activation. However, this transcription factor does not have a significant role in regulating perforin-mediated direct cytotoxicity[466]. More recent preliminary results from another group revealed that *PRDM1* targets different genes that restrict NK cell activation as well as other genes important for NK development and homeostasis[468].

On the other hand, *PRDM1* has been described as a tumor suppressor gene that is usually inactivated in NK cell malignancies by a combination of monoallelic deletions and hypermethylation. Moreover, non-functional and truncation mutations in *PRDM1* have been observed in different NK cell lines[469-471]. *In vitro* studies from Küçük *et al.* and Karube *et al.* demonstrated that reconstitution of *PRDM1* in *PRDM1*-null NK cell lines led to cell-cycle arrest, increased apoptosis, and a strong negative selection in culture, especially when IL-2 concentration was limited[469,470]. Additionally, *PRDM1* overexpression was associated with lower expression of *MYC*, *TNFα,* and *4-1BBL* and upregulation of some negative regulators of the cell cycle. On the contrary, knock down of *PRDM1* expression in primary PB-NK cells conferred a growth advantage on the cells. Moreover, *PRDM1* mRNA levels inversely correlated with *MYC* expression in activated PB-NK cells[469]. Dong *et al.* recently confirmed that BLIMP1, besides controlling multiple regulation pathways, also represses genes associated with cell cycle and proliferation such as *MYC* and *MYB* in PB-NK cells. As a consequence, *PRDM1* elimination in PB-NK cells reduced apoptosis and conferred increased proliferative potential on the cells, which could be maintained in culture up to 3 months upon cytokine stimulation. Altogether, these studies corroborate that BLIMP1 represses NK cell proliferation and the loss of *PRDM1* expression is associated with malignant transformation. However, no studies have demonstrated that *PRDM1* acts as a tumor-driver gene in NK cell malignances[472].

Another BLIMP1-targeted gene of special relevance for *ex vivo* expansion of NK cells is CD25 (IL-2Rα). Apart from the multiple roles attributed to BLIMP1 in NK cell homeostasis, BLIMP1 seems to act in a similar way to SOCS. It has been reported that *in vitro* stimulation of PB-NK cells

increased CD25 expression during the first two weeks of expansion, progressively decreasing after that point through BLIMP1-mediated repression. Indeed, malignant NK cells which harbor genetic or epigenetic alterations that inactivate *PRDM1* expression, express high levels of CD25, being more responsive to low IL-2 doses[473].

All reported studies in which *PRDM1* was knocked-out in NK cells are focused on understanding the roles of this gene in NK cell homeostasis, differentiation, and malignant transformation. However, it may also represent a potential target to improve the persistence of CAR NK cells as it has been described in CAR T cells, in which *PRDM1* ablation promoted the expansion of less differentiated "memory-like" CAR T *in vivo* thus enhancing both persistence and therapeutic efficacy in different tumor models without increasing the risk of oncogenesis transformation [474,475].

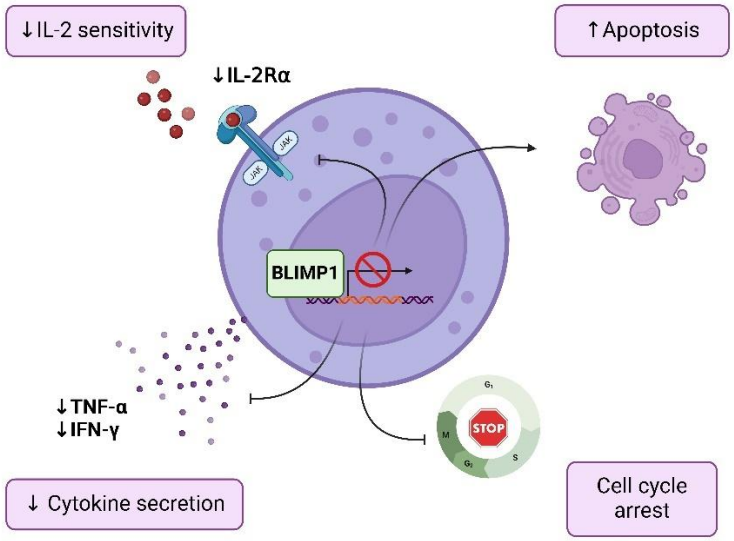

Figure 25. Biological BLIMP1 functions in mature NK cells. IL-2: interleukin 2; IL-2R: IL-2 receptor; TNF-α: tumor necrosis factor α; IFN-γ: interferon γ. Created with BioRender.com.

4. CRISPR/Cas9 genome editing in NK cells

4.1. CRISPR/Cas9 technology

CRISPR/Cas was originally discovered as an adaptative immune defense mechanism in *Bacteria* and *Archaea* to eliminate foreign nucleic acids from viruses or plasmids[476,477]. This system consists of the clustered regularly interspaced short palindromic repeats (CRISPR) loci, which are composed of short (30-40 bp) repetitive sequences separated by a series of palindromic repeats (25-35 bp each), and the CRISPR-associated (Cas) nucleases genes. CRISPR/Cas defense comprises two different steps. First, during the immunization step, new spacer sequences

(protospacers) are acquired from foreign genetic elements and incorporated into the CRISPR array, only when they are located next to a specific protospacer-adjacent motif (PAM). Then, when the same foreign DNA re-infects the bacteria, CRISPR/Cas system is activated to eliminate it. During this defense step, the protospacer sequence is transcribed into a CRISPR RNA (crRNA) that, after being processed hybridizes with a transactivating CRISPR RNA (tracrRNA) and binds to Cas nucleases. Cas nucleases use this crRNA as a probe to specifically recognize the invading DNA, cleaving the complementary target DNA sequence only if they are adjacent to the PAM (**Figure 26**). PAM-restricted activity ensures system safety, by preventing Cas nucleases from destroying their own CRISPR/Cas machinery[478,479]. CRISPR/Cas systems can be divided into two classes depending on the usage of multiple nucleases (class I) or a unique nuclease (class II) for DNA degradation. Moreover, depending on the CRISPR loci architecture and the Cas protein mechanism of action, class I systems can be subdivided into type I, III, and IV, while class II systems into type II, V, and VI.[478].

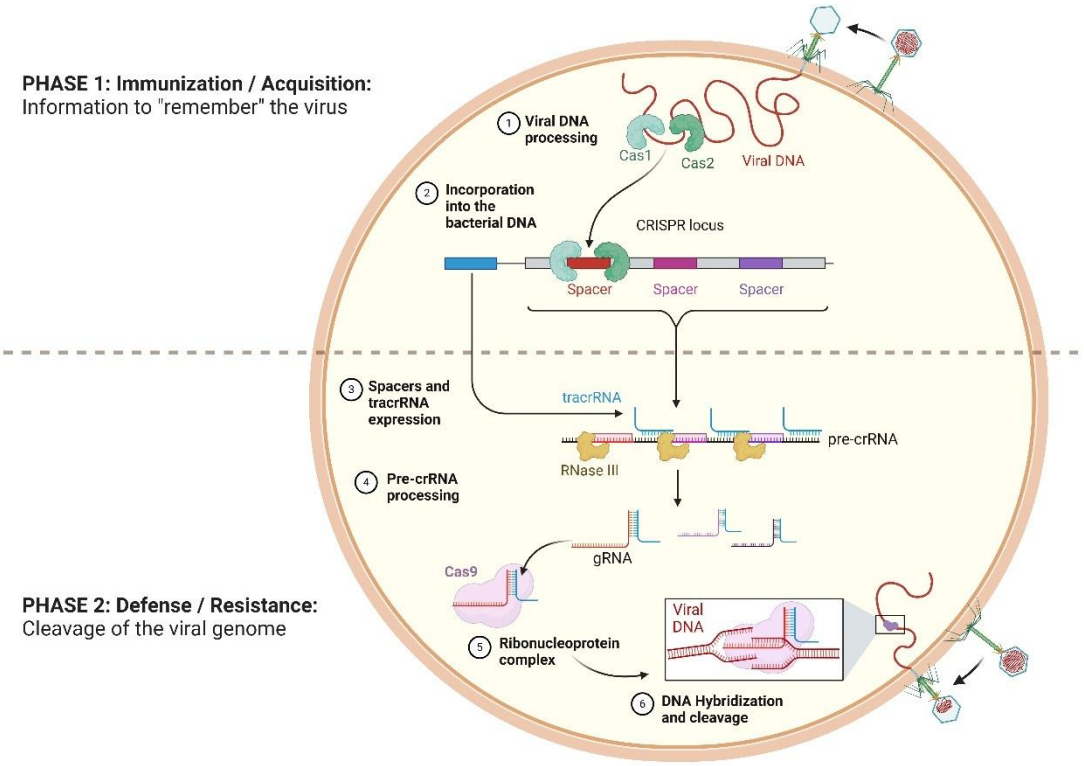

Figure 26. CRISPR-Cas9 adaptive immune system of *Streptococcus pyogenes* against bacteriophages. After viral infection, Cas1 and Cas2 proteins incorporate short fragments of viral DNA within the CRISPR array in the bacterial genome. CRISPR locus is then transcribed as a pre-crRNA (CRISPR RNA) which is processed and hybridized with a tracrRNA (transactivating CRISPR RNA) forming a gRNA (guide RNA) that binds with Cas9. Upon viral re-infection, gRNA recognizes complementary segments of the invading genome favoring Cas9-mediated DNA cleavage. Obtained from BioRender.com repository.

Many different gene editing tools have been developed using different Cas nucleases for multiple applications. Among them, the class II type II *Streptococcus pyogenes* Cas 9 (SpCas9) is the most exploited one, due to its relatively simple structure and mechanism of action[480,481]. Cas9 nuclease recognizes specific 5'-NGG-3' PAM sequences (N can be A, T, G, or C), which are highly abundant in the human genome, and requires a crRNA and a tracrRNA to be "guided" to target sites. When Cas9 recognizes the PAM sequence adjacent to the target site, it generates a double-strand break (DSB) in the DNA which will be repaired by the cell machinery. To facilitate the applicability of Cas9 in genome editing protocols, single-guide RNAs (sgRNA) have been developed by the fusion of the crRNA and the tracrRNA[482].

4.2. Repair of Cas9-induced double-strand breaks

After DSB, cells activate their DNA repair machinery to preserve genome integrity. In general, mammals have developed four different DNA repair pathways, including two major pathways, which are classical non-homologous end joining (C-NHEJ) and homology-directed repair (HDR), and two alternative pathways, alternative NHEJ (A-NHEJ) and single-strand annealing (SSA) which represent back-up mechanisms for the major ones (**Figure 27**)[483].

The first and preferentially activated DNA repair mechanism is C-NHEJ which acts in all stages of the cell cycle. This pathway is initiated by the recognition of Ku70/Ku80 heterodimers that bind to broken ends and recruit the catalytic subunit DNA-dependent protein kinase complex (DNA-PKcs). This complex recruits different proteins including Artemis nuclease, λ and μ DNA polymerases, DNA ligase IV, XRCC4 (X-ray repair cross complementing protein 4), and XLF (XRCC4-like factor). The coordinated action of these proteins removes damaged nucleotides and ligates blunt DNA ends. During this process, different bases can be randomly added or included by the action of the polymerases and nucleases. Therefore, small indels may appear in the repaired DNA leading to frameshift and non-sense mutations which, if they occur in the coding sequence, most commonly result in disruption of gene expression. This is the basis of NHEJ-based error-prone editing, which constitutes a highly efficient mechanism to induce gene knock-outs[483,484].

On the other hand, during S/G2 phases, when a sister chromatid is available to act as a homology donor, cells can activate the HDR pathway. DSBs are recognized by the MRN complex (MRE11-RAD50-NBS1) that recruits CtIP (C-terminal binding protein interacting protein) and other nucleases that generate a single-strand (ss) DNA end. With the assistance of recombination mediators such as breast cancer proteins (BRCA) 1 and 2 and RAD51, ssDNA end invades the DNA template generating a displacement loop (D-loop) and forming Holliday junctions with the other

DSB. Finally, polymerases, ligases, and resolvases terminate the repair process using the donor DNA as template. This repair mechanism is the basis of HDR-based precision editing tools which combine Cas9 nuclease with a donor DNA template to introduce specific DNA modifications in the genome. This system has been widely used to specifically replace disease-causing mutations[483,484].

A-NHEJ, also known as microhomology (MH)-mediated end-joining (MHEJ), shares features of both NHEJ and HDR and repairs DNA DSBs by annealing 2-20 bp long MH sequences internal to the broken ends. This pathway involves the initial resection of DSBs through MRN and CtIP, similar to HDR, to expose the internal MH sequences to the ends. Exposed MH then anneal, flaps are removed, and ssDNA regions are filled and ligated by the combined action of XPF/ERCC1, the low fidelity θ polymerase, XRCC1, PARP-1 (poly ADP-ribose polymerase 1), and DNA Ligase III. A-NHEJ is always mutagenic because one of the two MH regions, and the inter-MH region, will be deleted from the repair product. During the initial steps of the cell cycle, Ku70/80 inhibits PARP-1 thus C-NHEJ prevails over A-NHEJ. During S and G2 phases, the length of the resection usually determines the continuity of HDR (extensive resection) or the activation of A-NHEJ (short resection)[485,486].

Finally, the SSA repair mechanism serves as a back-up of HDR, when RAD51 is suppressed, and utilizes homologous repeats to bridge DSB ends but, contrary to HDR, it is regarded as a mutagenic process that can generate DNA deletions between the DNA repeats[483].

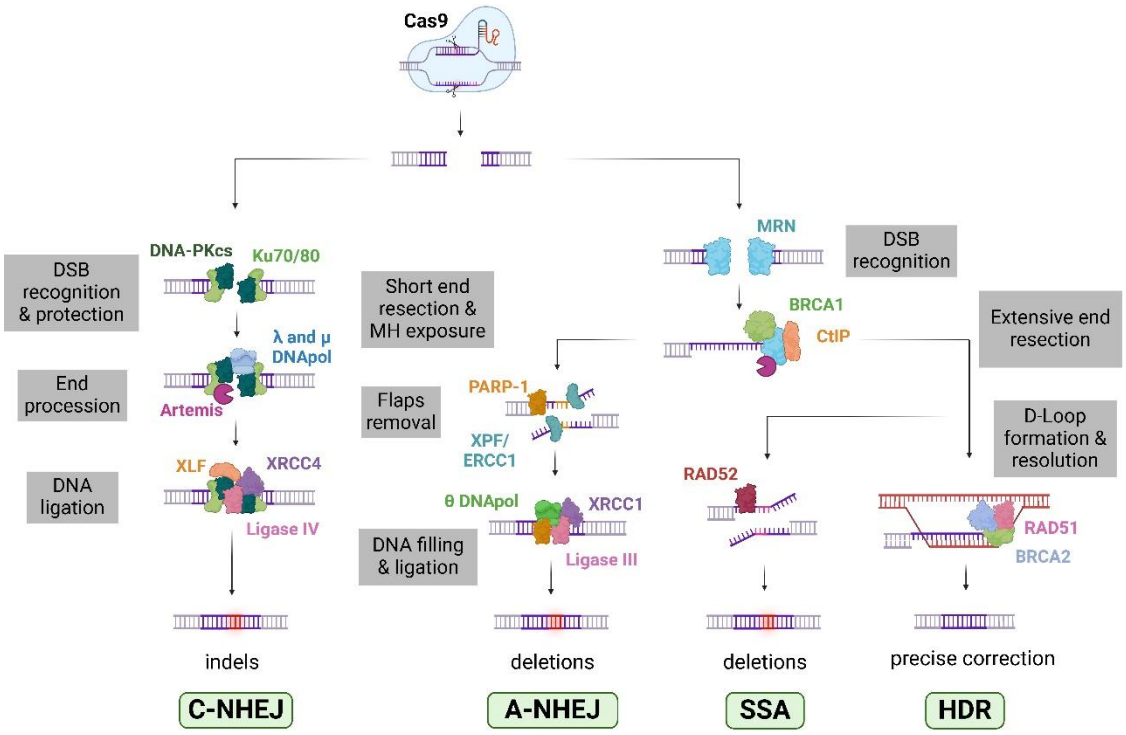

Figure 27. DNA repair mechanisms after double strand Cas9-mediated cleavage in mammals. C-NHEJ: canonical non-homologous end joining; A-NHEJ: alternative non-homologous end joining; SSA: single strand annealing; HDR: homology-directed repair; DNA-PKcs: DNA-dependent protein kinase catalytic subunit; DSB: double-strand break; MH: microhomology; XRCC: X-ray repair cross complementing protein; XLF: XRCC4-like factor; MRN: MRE11-RAD50-NBS1 complex; CtIP: C-terminal binding protein interacting protein; BRCA1/2: breast cancer protein 1/2. PARP-1: poly ADP-ribose polymerase 1. Adapted from Yang et al. Int J Mol Sci. 2020[483]. Created with BioRender.com.

After a DSB, a rapid signaling cascade is triggered by the cell to efficiently respond to the DNA damage. Upon DNA breaks, ATM (ataxia telangiectasia mutated) and ATR (ataxia telangiectasia and rad3-related) damage-sensing kinases are activated and phosphorylate γH2AX protein that spreads throughout the DSB area and recruits different proteins to initiate DNA repair responses. During G1 phase, 53BP1 (TP53-binding protein 1) binds to the complex, inhibiting DNA resection and consequently HDR. During G2 phase, BRCA1 replaces 53BP1 and promotes HDR[483]. Importantly, if DNA breaks are not repaired, ATM/ATR signaling, via Chk1/2 phosphorylation, can activate p53/p21 pathway and inactivate cyclin-dependent kinases to induce cell cycle arrest, senescence, or apoptosis[487,488] (**Figure 28**).

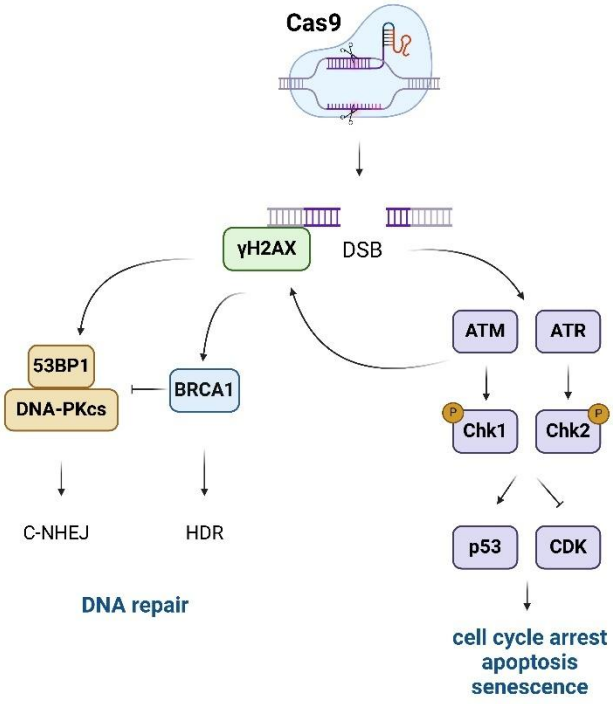

Figure 28. Activated signaling pathways in response to DSBs. DSB: double-strand break; 53BP1: TP53-binding factor 1; DNA-PKcs: DNA protein kinase catalytic subunit; C-NHEJ: classical non-homologous end joining; HDR: homology-directed repair; ATM: ataxia telangiectasia mutated; ATR: ataxia telangiectasia and rad3-related; CDK: cyclin-dependent kinase. Adapted from Ouellette et al. Diagnostics. 2022[488]. Created with BioRender.com.

4.3. Applications of CRISPR/Cas9 genome editing in CAR NK immunotherapy

Since the development of the first CRISPR/Cas9 editing tool in 2012, this technology has been broadly applied to biomedicine research constituting a feasible tool to modulate gene expression (gene knock-out or knock-in (KI), gene silencing (CRISPRi) or activation (CRISPRa)), to generate multiple research *in vitro* and *in vivo* models and to perform high-throughput screening assays, but also has emerged as a promising therapeutic approach to correct specific mutations causing genetic diseases[489]. Besides, CRISPR/Cas9 has revolutionized the field of cell adoptive immunotherapy, offering a simple and versatile platform to eliminate expression of specific genes in T, NK, and even macrophages, to augment their efficacy and avoid therapy resistances and toxicities[490]. Of course, CAR NK immunotherapy has similarly benefited from these advancements. For instance, as previously described, CRISPR/Cas9 has been used to knock-out specific genes (i.e. *CD38*[291,306] and *CD70*[307]) in CAR NK cells to avoid CAR-targeted fratricide. Moreover, disruption of *KLRC1*[370], *TIGIT*[328,491], or *CBLB*[491] genes eliminate inhibitory signals from immunomodulatory checkpoints therefore boosting CAR NK efficacy. Another example is the elimination of *ADAM17* in CAR NK cells to reduce CD16 shedding and potentiate ADCC responses[492]. This technique has also been used to eliminate expression of *TGFBR2* in CAR iNK

cells targeting hepatocellular carcinoma, providing them with resistance to TME-derived immunosuppressive soluble factors such as TGF-β[425]. Additionally, other groups have knocked-out cytokine-induced suppressors, such as *CISH,* to increase CAR NK persistence[456,458].

Over the last decade, various strategies for delivery of Cas9 and sgRNA to target cells have been developed, such as physical methods, viral vectors, and non-viral vectors, expanding the versatility of the system[489,493]. In the context of *ex vivo* adoptive NK cell manufacturing, as these cells are highly refractory to viral transduction and double-strand (ds) DNA molecules or plasmids[494,495], the electroporation of pre-transcribed sgRNA-Cas9 protein in the form of ribonucleoprotein (RNP) complexes represents the most exploited and efficient method to generate knock-outs in CAR NK cell effectors[291,306,370,425,458,491].

Combined or multiplex gene editing is another possibility that offers CRISPR/Cas9 technology to target several loci at the same time. In 2020, Huang *et al.* were the first to demonstrate that both double and triple knock-out through electroporation of pre-transcribed RNP complexes was feasible and efficient to eliminate the expression of *CD96*, *NCR1,* and *KLRC1* in NK-92 cell line[496]. Later, Ureña-Bailén *et al.* simultaneously disrupted *KLRC1*, *TIGIT,* and *CBLB* in α-CD276 CAR and α-CD19 CAR NK-92 cells[491]. Regarding primary PB-NK cells, only two groups have demonstrated efficient simultaneous gene disruption. After publishing their work in NK-92 cell line, Huang *et al.* were the pioneers to generate double and triple knock-out of *CD96*, *TIGIT,* and *CD226* in primary PB-NK cells by RNP electroporation[497]. These authors also described the potential appearance of chromosomal translocations within the on-target sites due to simultaneous DSBs which could limit the application of this technique[496,497]. More recently, Bi *et al.* have reported a synergistic antitumor efficacy improvement against K562 cells after the combined disruption of *CISH* and *TIPE2* in PB-NK cells[452]. In the context of CAR NK from PB or CB, no multiplexed gene editing approach, in which two or more genes are disrupted simultaneously, has been reported.

CRISPR/Cas9 technology has also been applied to introduce transgenes (including CAR molecules) in NK cells for adoptive immunotherapy. Although knock-in strategies that require DNA donor templates can be potentially challenging in the case of NK cells, different groups have demonstrated efficient gene editing of NK cells using the combination of adeno-associated vectors (AAV) and electroporation methods. For example, Pomeroy *et al.* and Naeimi *et al.* introduced a non-cleavable CD16 version or a CAR molecule, respectively, in the *AAVS1* safe harbor locus in PB-NK cells[323,498]. Going a step further, Clara *et al.* designed a two-in-one KO/KI strategy to disrupt CD38 expression by introducing a non-cleavable version of CD16[499].

Taken together, CRISPR/Cas9 technology is a versatile tool applicable to all NK sources to overcome most of the limitations faced by CAR NK immunotherapy.

4.4. Advantages of CRISPR/Cas9 genome editing over other combinatorial strategies to improve CAR NK effectors

In the context of CAR immunotherapy, one of the main advantages of CRISPR/Cas9 over blocking mAbs refers to the toxicity. As it has been described before, combined administration of mAb or small molecule inhibitors together with CAR T and CAR NK effectors can improve their antitumor efficacy and represents an easier strategy in terms of manufacturing compared to CRISPR/Cas9 genome editing. However, the systemic administration of these mAbs or molecules may lead to off-target or on-target off-tumor adverse effects. For example, different clinical trials testing the safety and antitumor efficacy of α-PD-1/PD-L1 mAbs as monotherapy have reported different grade 3-4 adverse effects in some patients including fatigue, dermatologic toxicities (i.e. rash, pruritus), hepatic toxicities (i.e. AST/ALT elevation) and pneumonitis, among others. Moreover, toxicities increase when two mAbs are used in combination[500]. Adverse effects such as fatigue, diarrhea, anemia, lymphopenia, altered biochemical values, dermatitis, pruritus, or pneumonitis have been also associated to the administration of monalizumab (α-NKG2A) alone or in combination with other antibodies in patients with different cancers[371-375]. Something similar happens with the systemic use of small-molecule inhibitors such as vactosertib or galunisertib (TGF-βRI inhibitors) which show drug-related toxicities such as fatigue, alopecia, pruritus, rash, increased lipase and amylase nausea and even leukopenia, pneumonitis, hepatotoxicity or pancreatitis in some patients[414,501,502].

On the other hand, CRISPR/Cas9 technology has demonstrated to outperform mAbs and inhibitors in terms of efficacy. For example, two independent studies from Prof. Rezvani's laboratory showed that *TGFBR2* KO NK cells had increased tumor control compared with the combination of non-edited counterparts and galunisertib treatment in AML and glioblastoma *in vivo* models[416,417]. Furthermore, a recent publication by Gong *et al.* exhaustively compares the use of α-NKG2A mAbs with *KLRC1* gene editing in PB-NK cell effectors, demonstrating that the latter is a more effective approach for targeting NKG2A/HLA-E suppressive pathway and enhancing NK cell antitumor potential against both solid and hematologic tumors[365].

Another advantage of CRISPR/Cas9 mediated knock-out is that, at a single-cell level, protein expression is totally abrogated while treatment with mAbs only downregulates or masks the surface protein. Moreover, CRISPR/Cas9 mediated knock-out of checkpoints and inhibitory receptors confers stable protection for CAR effectors. On the contrary, monoclonal antibodies

have short half-lives and repeat dosing would be required to achieve the same benefit[490] which would increment therapy costs as well as increase therapy-related toxicities due to dose accumulation. Indeed, the study from Gong *et al.* reported that serial administration of α-NKG2A mAb to mice increased mAb serum levels but showed no improvement in tumor control[365].

Importantly, permanent and complete gene disruption can become a double-edged sword. The elimination of inherent checkpoints, signaling molecules and transcription factors involved in multiple biological networks may alter the functionality or viability of CAR NK effectors. For example, the preliminary results from Kanaya *et al.* in iNK cells suggest that *KLRC1* deletion probably impedes NKG2A-mediated NK licensing or education process, resulting in impaired CAR NK effector function[369]. Moreover, depleting tumor suppressors in CAR NK cells augments the risk of uncontrolled lymphoproliferation *in vivo*. Therefore, rigorous study to efficacy and safety of each approach should be considered when designing knock-out strategies in CAR NK immunotherapy.

4.5. CRISPR/Cas9 off-target activity

Despite the highly precise gene editing capacity of Cas9 nuclease, tolerant mismatches between DNA and sgRNA sequences can result in the recognition of multiple genomic sites by the CRISPR/Cas9 system leading to unintended or off-target editing events. The generation of unintended DSBs in the genome may trigger gene activation, silencing, or genomic rearrangements, among other adverse outcomes[503,504] and therefore represents a significant challenge for the clinical use of CRISPR/Cas9. Consequently, extensive research has been dedicated to predict and detect potential off-target sites and to develop CRISPR/Cas9 variants with greater precision.

Off-target activity mainly relies on the sgRNA specificity although it can be influenced by the delivery method, cell type, nuclease exposure time, and target site accessibility. Nowadays, multiple algorithms enable the *in silico* prediction of off-target activity based on the sgRNA sequence, thus optimizing sgRNA design and selection, and allowing site-directed sequencing analysis of editing events. Taking a step further, many groups have developed cell-independent (i.e. DIG-seq, CIRCLE-seq, or SITE-seq) and cell-based strategies (such as GUIDE-seq, CAST-seq, UDiTaS™, BLISS, and BLESS) to precisely detect potential off-target activity across the whole genome and analyze the safety of gene editing approaches prior to clinical application[505 506].

Besides these design and detection technologies, different modified Cas9 proteins have been developed to reduce off-target activity[507] such as the HiFi Cas9 which retains high on-target

activity of wild-type Cas9 while reducing off-target editing when transiently delivered in RNP complexes[508].

4.6. New CRISPR/Cas editing approaches for CAR NK cells

Despite the great versatility and efficacy of CRISPR/Cas9 tools to edit CAR NK cells, new editing technologies could overcome some of the Cas9-related limitations and are recently emerging to be applied in the CAR immunotherapy field.

For example, Zhang *et al.* have proposed the use of an improved AsCas12a class II type V nuclease with higher efficiency than the wild type one. This nuclease offers an alternative to Cas9 nuclease, reducing off-target editing rates due to its lower tolerance for guide-target mismatches. The authors obtained around 90% KO efficiencies for different genes (*CIITA*, *PD-1*, *CISH,* and *TGFBR2*) in T and NK cells. Moreover, they showed a proof-of-concept for the introduction of a CAR molecule within the *TRAC* locus in PB-NK cells. Although efficiencies were still modest, this could represent a promising tool for dual KO/KI strategies in the future[427].

On the other hand, DSB-independent methods such as base editing and prime editing may overcome the generation of undesired insertions/mutations, translocations, and p53 activation thus emerging as a promising approach for multiplex gene editing of CAR NK effectors. Base editing is a precise gene editing tool to introduce base modifications in a genomic locus without the need of DSBs. This system is composed of a Cas9 nickase variant (nCas9) fused to a ssDNA deaminase enzyme which is guided to a specific locus by a specific sgRNA. Base editors are classified into adenine base editors (ABEs), which convert A:T base pairs to G:C base pairs, and cytosine base editors (CBEs) that promote conversion of a C:G pair to a T:A pair[509,510]. Importantly, this technology is not exempt from undesired editing events. It has been described that base editors can also induce 'bystander' deaminations proximal to the editing window or even induce indels in addition to the nucleotide substitution. Additionally, they can induce single-nucleotide mutations at off-target DNA and even RNA sites[509,511,512], in most cases independently of the sgRNA. With the aim of optimizing the efficacy and safety of base editors, multiple improvements in protein architecture and modifications have been incorporated into the system to develop the new generation of base editors[509,510]. Ongoing preclinical and clinical studies with these new base editors will confirm their efficacy and safety.

CRISPR prime editing is another DSB-free method that allows the introduction of a wide range of base substitutions, insertions, and deletions. Prime editors consist of an nCas9 fused to an engineered reverse transcriptase together with a modified prime editing guide RNA (pegRNA) which serves as a specific-site guide as well as a template for the transcriptase. Reverse

transcriptase will polymerize a correct DNA sequence in the editing site that will be later introduced in the cell genome. One of the main advantages of this system is the reduced Cas9 off-target activity due to the minimal DSB generation and to the specific requirement of a sequence of molecular events between the prime editor and the target DNA for productive editing outcome[513,514]. Despite some improvements in this technology are still required in terms of efficacy, this tool represents a promising safe strategy more versatile than base editing and potentially more efficient than DNA template-dependent CRISPR/Cas9 methods, which are quite limiting in CAR NK immunotherapy[490].

HYPOTHESIS & OBJECTIVES

Despite the wide range of therapeutic approaches already approved for MM, most patients eventually progress, often with increasingly shorter response periods, defining MM as an incurable disease. The development of innovative-targeted cellular therapies such as CAR T cells has transformed the treatment landscape for hematologic malignancies although cumbersome manufacturing, severe toxicities such as CRS, neurotoxicity and prolonged cytopenia, as well as suboptimal non-stable responses caused by T cell-dependent resistances, highlight the need for alternative CAR effectors. In this context, allogeneic CAR NK cells have emerged as a safer, "*off-the-shelf*", and cost-effective alternative to CAR T cells. Nevertheless, although the limited *in vivo* persistence of CAR NK effectors reduces the probability of uncontrolled immune responses and oncogenesis, the short lifespan of these cells could dampen their long-term clinical efficacy. In addition, the inhibitory immune checkpoints and the immunosuppressive TME that surround MM, especially at progression, may reduce the persistence and antitumor activity of CAR NK effectors, therefore compromising clinical responses. Both HLA-E/NKG2A axis as well as TGF-β signaling represent two of these dominant mechanisms of CAR NK resistance in MM. Antagonistic antibodies or small molecule inhibitors as monotherapy targeting these pathways did not show efficacy in the clinical setting, and, although non-adoptive combinatorial strategies blocking these axes have shown promise in efficacy, systemic administration of these treatments can lead to life-threatening adverse effects. Several preclinical studies have demonstrated that the use of antibodies or small molecule inhibitors increases NK activity against different tumors. However, combining these agents with CAR NK cells may also raise concerns regarding toxicity. In this scenario, CRISPR/Cas9 genome editing has arisen as a versatile technology to disrupt the expression of proteins involved in CAR therapy resistance, potentially offering a safer and more efficient alternative to monoclonal antibodies and drug inhibitors to overcome CAR NK limitations.

1. Hypothesis

Multiplexed CRISPR/Cas9 genome editing in CAR NK effectors can increase their *in vivo* persistence and enhance their antitumor potential against MM.

2. Objectives

Considering the current challenges in CAR NK immunotherapy in the context of hematological malignancies, the main objective of this doctoral thesis is the application of CRISPR/Cas9 genome editing tool to improve the therapeutic efficacy of α-BCMA CAR CB-NK cells against MM.

The specific objectives of this thesis are:

1. To generate and characterize double knock-out α-BCMA CAR CB-NK cells by the combined disruption of *KLRC1* and *TGFBR2* and to analyze their persistence and cytotoxic potential against MM both *in vitro* and *in vivo*.
2. To elucidate the possible mechanisms underlying the changes of CAR NK antitumor activity after *KLRC1* and *TGFBR2* knock-out.
3. To investigate *PRDM1* knock-out as a feasible strategy to optimize the expansion and persistence of α-BCMA CAR CB-NK cells without compromising their cytotoxic capacity.
4. To explore the potential and safety of a multi-edited triple knock-out α-BCMA CAR CB-NK product to improve antitumor efficacy against MM without increasing therapy-related toxicities.

MATERIALS & METHODS

1. Cell lines and primary samples

1.1. Cell lines

1.1.1. MM cell lines

MM cell line RPMI-8226 (ACC 402) was purchased from DSMZ (Leibniz Institute, Germany). U-266B1 (TIB-196; from here on U-266) and MM.1S (CRL-2974) were purchased from ATCC. XG-1 cell line was kindly provided by Dr. Joshua Epstein (Arkansas Cancer Research Center, Arkansas, USA). Cell line integrity was tested through short tandem repeat (STR) analysis in the Genomic Unit from Cancer Research National Center (CNIO), Madrid.

For *in vivo* experiments, U-266B1 cell line was transduced with a ffLuc-GFP lentiviral vector (U266 ffLuc-GFP) to constitutively express luciferase and GFP (green fluorescence protein), therefore allowing tumor burden detection by bioluminescence imaging (BLI) and flow cytometry. Non-treated 24-well plates were coated with 2 µg/cm^2 retronectin (TakaraBio) 24 hours before their use and stored at 4°C. On the day of transduction, U-266 cells were seeded on these plates at a concentration of 1 x 10^6 cells/mL and ffLuc-GFP lentiviral vector was added at a multiplicity of infection (MOI) of 10. Plates were centrifuged at 400 ×g for 20 minutes at 24°C and incubated at 37°C for 16-20 hours. Transduced cells were then washed with PBS and medium was replaced. Cells were maintained for one week in culture and then GFP$^+$ cells were sorted using BD FACSAria™ Fusion Cell Sorter (BD Biosciences).

All MM cell lines were cultured in Roswell Park Memorial Institute (RPMI)-1640 medium (Lonza) supplemented with 10% fetal bovine serum (FBS; Hyclone), 2 mM L-glutamine (Lonza) and 100 IU/mL penicillin/streptomycin (P/S; Lonza) at 37°C in a humidified atmosphere with 5% CO_2. Additionally, XG-1 cell line medium was supplemented with 1 ng/mL recombinant human IL-6 (Miltenyi). Medium was replaced every two-three days. Polymerase Chain Reaction (PCR) was regularly performed to test the absence of mycoplasma in the culture supernatant using DreamTaq PCR Master Mix (Thermofisher) according to manufacturer's instructions. Forward (5'-GGCGAATGGGTGAGTAACACG-3') and reverse (5'-CGGATAACGCTTGCGACCTATG-3') primers were used for mycoplasma amplification.

1.1.2. Artificial antigen presenting cell lines

K562-mb21-41BBL cell line (Clone 9.mbIL21 or CSTX002) was kindly provided by Dr. Dean A. Lee (Nation Wide Children, Ohio, USA). This cell line derives from K562, an erythroleukemic cell line with positive Philadelphia chromosome, which was genetically modified to constitutively express membrane-bound IL-21, 4-1BB ligand (4-1BBL or CD137-L), CD64, CD86 and truncated CD19. This

cell line was used as an aAPC to activate NK cells *in vitro* as both IL-21 and 4-1BBL promote NK cell activation[515]. K562-mb21-41BBL cell line was cultured as described for MM cell lines (section 1.1.1) and irradiated under 100 Gy before co-culture with NK cells.

1.1.3. Cell lines for lentiviral production

HEK293T cell line (CRL-11268) was purchased from ATCC and was used as the packaging cell to generate lentiviral vector concentrates and titrate them. It is an embryonic human kidney cell line modified to express SV40 T antigen which allows episomal replication of plasmids that contain the SV40 replication origin[516] thus enhancing transfection efficiency. This cell line was cultured in Iscove´s Modified Dulbecco´s Medium (IMDM; Lonza) supplemented with 10% FBS and 100 IU/mL P/S at 37°C in a humidified atmosphere with 5% CO_2 and 21% O_2. Every two-three days, cells were detached using a Trypsin- ethylenediaminetetraacetic acid (EDTA) solution (Lonza) and diluted in fresh medium.

1.2. Primary cells

Umbilical cord blood samples from HD were provided by Centro de Transfusiones de la Comunidad de Madrid. HD PB samples and MM patient BM aspirates were obtained from Hospital 12 de Octubre. Both healthy donors and MM patients gave their written informed consent to collaborate in the study (nº20/326) which was previously approved by the Hospital 12 de Octubre ethics committee, in accordance with the Declaration of Helsinki protocol. All primary samples were processed according to the arrival order at the hospital.

2. Integration-competent lentiviral vectors

2.1. CAR molecule design

Second generation α-BCMA CAR molecule was generated by modifying the NKG2D-CAR transfer plasmid (pTRPE_NKG2D-ECD_4-1BBz) which was kindly provided by Daniel J. Powell Jr. (Perelman School of Medicine, Pennsylvania, USA).

A cloning sequence flanked by Nhe I and Nde I restriction sites and containing the κLC signal peptide followed by clone 4ZFO α-BCMA scFv (mouse/human chimera J22.9-xi mAb) and the hinge and transmembrane domain of the CD8α receptor was designed using SnapGene™ software and synthetized by GeneArt (Thermofisher).

Using Nhe I and Nde I restriction enzymes (New England Biolabs) and T4 DNA Ligase (New England Biolabs), a one-step cloning was performed according to manufacturer's instructions to

replace the region containing the signal peptide, the NKG2D ectodomain and, the hinge and transmembrane domain from the pTRPE_NKG2D-ECD_4-1BBz with our cloning sequence. Ligation product was transformed into One Shot™ Stbl3™ chemically competent *E.coli* (Thermofisher) by heat shock. Transformed bacteria were cultured overnight at 37°C in plates containing 2% (p/v) Luria Bertani (LB) agar (Condalab) and 50 µg/mL ampicillin. Ampicillin-resistant colonies were isolated and cultured overnight at 37°C in 3 mL liquid LB medium (Condalab) supplemented with ampicillin in an orbital shaker. Plasmid DNA from bacteria was purified using Plasmid Mini Kit (Qiagen) following manufacturer's instructions and verified by enzyme restriction analysis (New England Biolabs) and Sanger sequencing (Stabvida) to select clones containing the correct pTRPE_BCMA_4-1BBz transfer plasmid.

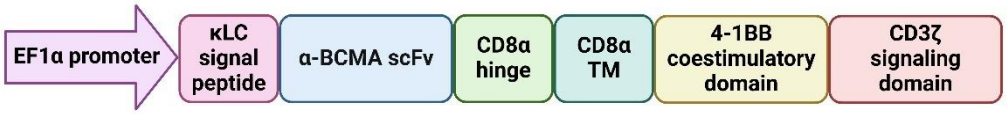

Figure 29. Schematic representation of the α-BCMA CAR. κLC: kappa light chain; TM: transmembrane domain. Created with BioRender.com.

2.2. Plasmids amplification

Both pTRPE_BCMA_4-1BBz and pRRL_Luc_EGFP (kindly provided by Dr. Jerónimo Blanco) transfer plasmids and pAdvantage™ helper plasmid (Promega Biotech) were transformed into One Shot™ Stbl3™ chemically competent *E.coli* by heat shock for amplification. Transformed bacteria were cultured overnight at 37°C in LB agar plates with 50 µg/mL ampicillin. Ampicillin-resistant colonies were isolated and cultured overnight at 37°C in 250 mL of liquid LB medium supplemented with ampicillin in an orbital shaker. Plasmid DNA from bacteria was purified using EndoFree Plasmid Maxi Kit (Qiagen) following manufacturer's instructions and verified by enzyme restriction analysis. Plasmid DNA quantity and quality were measured using a Nanodrop ND-1000 Spectrophotometer (Thermo Fisher Scientific).

Packaging and envelope plasmids used for lentiviral vector production were purchased from Addgene and amplified by PlasmidFactory (Bielefeld, Germany).

2.3. Lentiviral vector production

Integration-competent lentiviral vectors (LV) containing α-BCMA CAR or ffLucGFP transgenes were generated by a third-generation packaging system in which HEK293T cells were co-transfected with the transfer plasmid, two packaging plasmids, a helper plasmid and the VSV-G (vesicular stomatitis virus glycoprotein G) envelope plasmid (**Table 5, Figure 29**).

Plasmid type	Name	Description
Transfer plasmid	pTRPE_BCMA_4-1BBz	Contains the second generation α-BCMA CAR construct
	pRRL_Luc_EGFP	Contains the luciferase and GFP reporter genes
Packaging plasmid	pMDLg/pRRE	Contains HIV-1 *gag* and *pol* genes
	pRSV-Rev	Contains HIV-1 *Rev* gene
Helper plasmid	pAdVAntage™	Enhances transient protein expression by increasing translation initiation.
Envelope plasmid	pMD2.VSV.G	Contains the glycoprotein G of Vesicular Stomatitis Virus

Table 5. Plasmids used for production of third-generation lentiviral vectors.

The day before transfection, 9 x 10^6 HEK293T cells were seeded in 150 mm culture-treated plates. When cells reached 70% confluence, culture medium was refreshed and two hours later, cells were transfected using the $CaCl_2$ DNA precipitation method. Plasmid mixture was prepared by adding 36 µg transfer plasmid, 12.5 µg pMDLg/pRRE, 6.5 µg pRSV-Rev, 9 µg pMD2.VSV.G and 15 µg pAdVantage™ plasmid to a final volume of 1 mL 0.1X Tris-EDTA buffer/dH_2O (2:1) per plate and mixed during 15 minutes at room temperature (RT). Then 150 µL of 2.5 M $CaCl_2$ (Sigma) were added. After mixing for another 15 minutes, 1250 µL of 2X HBS buffer (100 mM HEPES, 281 mM NaCl, 1.5 mM Na_2HPO_4, pH 7.14) were added drop by drop to the plasmid/$CaCl_2$ mixture while vortexing at full speed. Immediately, transfection mix was added to HEK293T cells. Culture medium was refreshed 16 hours later, and LV supernatants were collected 30 hours after transfection, 0.45µm-filtered and concentrated by ultracentrifugation at 25,000 rpm for 2 hours. Viral pellets were resuspended in RPMI-1640 medium, aliquoted and stored at -80°C.

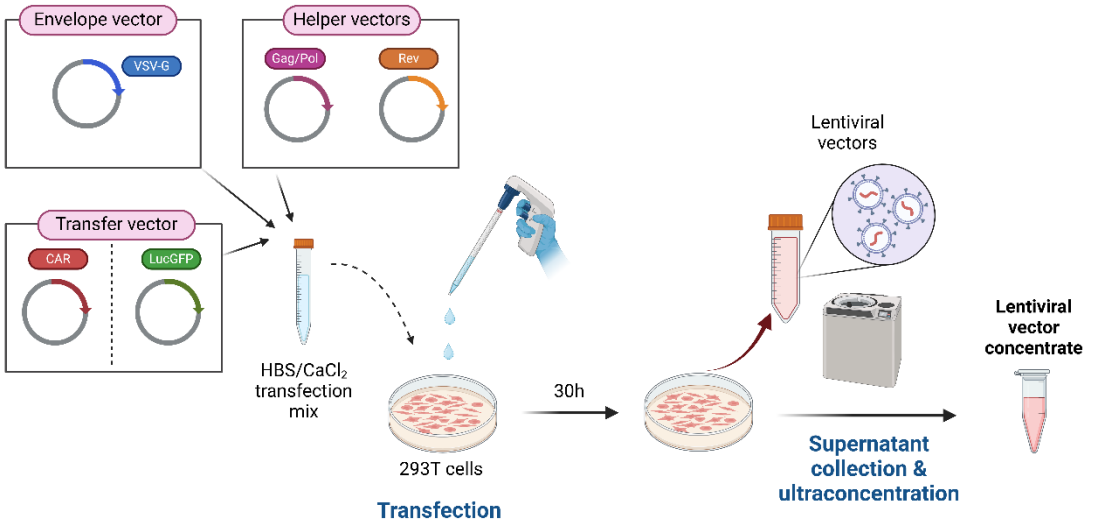

Figure 30. Schematic representation of third-generation lentiviral vector production. Created with BioRender.com.

2.4. Lentiviral vector titration

LV titer was determined by transduction of HEK293T cells with serial dilutions of vector supernatants. 1 x 10^5 HEK293T cells were seeded in culture-treated 24-well plates 24 hours before transduction. Then, serial dilutions from vector supernatants ranging from 10^{-3} to 10^{-6} were prepared in culture medium and added to the cells. Initial cell number was determined the same day of transduction. Transduced cells were maintained in culture for 7 days and then collected for flow cytometry analysis as described in section 6. Transduction percentage was measured for each dilution using a recombinant human BCMA protein (rhBCMA) or GFP fluorescence. LV titers (transducing units/mL) were determined considering the initial cell number and assuming one copy of vector per transduced cell according to the following formula:

$$\text{Titer}\left(^{\text{TU}}/_{\text{mL}}\right) = \frac{\text{initial cell number} \times \%\ \text{transduced cells} \times \text{dilution factor}}{100}$$

3. Single-guide RNA design

Single-guide RNAs (sgRNAs) were designed using CRISPOR.org web tool[517]. Target exons for each gene used as input sequence were selected based on published data. Two sgRNAs were chosen for each target gene (**Table 6**), based on the best specificity score and less off-target activity[518]. Modified synthetic sgRNAs were purchased from Synthego with specific modifications at 5' and 3' sites (2'-O-methyl and 3' phosphorothioate) that increase stability and protection against exonuclease activity to improve editing efficiency.

Gene	sgRNA name	Target exon	Sequence (5' to 3')
KLRC1	*KLRC1* sg1	Exon 2	GGTCTGAGTAGATTACTCCT
	KLRC1 sg2	Exon 2	ACTGCAGAGATGGATAACCA
TGFBR2	*TGFBR2* sg1	Exon 3	CACATGAAGAAAGTCTCACC
	TGFBR2 sg2	Exon 3	TCCAGAATAAAGTCATGGTA
PRDM1	*PRDM1* sg1	Exon 4	ATTGTCAGCTCTCCGGGATA
	PRDM1 sg2	Exon 5	GCTTACTTGAACGCGTCCTA

Table 6. sgRNAs selected for gene editing experiments.

4. Generation of edited CAR cord blood-derived NK cells

4.1. NK cell isolation and expansion

CB samples were diluted 1:2 with Phosphate-Buffered Saline (PBS; Gibco) and added 2:1 over Ficoll-Paque (Sigma-Aldrich). Mononuclear cell (MNC) fractions were collected after centrifugation at 400 ×g for 20 minutes (acceleration 6; deceleration 3), washed with PBS, and centrifuged at 350 ×g for 10 minutes. MNC samples were then lysed with ACK lysis buffer (Lonza) to remove the remaining erythrocytes. After a washing step to eliminate lysis buffer, NK cells were isolated by immunomagnetic depletion with a Human NK cell Isolation Kit (Miltenyi) following manufacturer's instructions. Purified NK cells were then co-cultured with K562-mb21-41BBL aAPC, previously irradiated with 100 Gy, at a ratio of 1:1.5 (NK:APC) in Stem Cell Growth Medium (SCGM; CellGenix) supplemented with 20% human AB serum (Sigma-Aldrich), 2 mM L-glutamine, 100 IU/mL P/S, 500 IU/mL human IL-2 (Miltenyi) and 140 IU/mL human IL-15 (Miltenyi). Henceforth, this culture medium will be referred as CB-NK medium. Fresh CB-NK medium was added every three days to the culture for 10-12 days.

4.2. Activated and expanded CB-NK cell transduction

After ten to twelve days of expansion, NK cells were transduced with the α-BCMA CAR LV. Non-treated 12-well plates were coated with 2 µg/cm^2 retronectin 24 hours before their used and stored at 4°C. The day of transduction, NK cells were washed with PBS and resuspended in fresh SCGM supplemented with 10% human AB serum, 2 mM L-glutamine, 100 IU/mL P/S, 500 IU/mL hIL-2 and 140 IU/mL hIL-15 at a concentration of 1.33 x 10^6 cells/mL. α-BCMA CAR LVs were added at an MOI of 10. Then, 750 µL (1 x 10^6 cells) of the vector-cell mix were added per well in retronectin-coated plates. Plates were centrifuged at 400 ×g for 20 minutes at 24°C and incubated at 37°C for 16-20 hours. Transduced cells were then washed with PBS and prepared for electroporation.

4.3. CAR NK cell electroporation

4.3.1. Single, double, and *one-shot* triple gene editing of CAR NK cells

Modified synthetic sgRNAs were resuspended in nuclease-free water (Synthego) to a final concentration of 3.2 µg/µL and stored at -80°C. To form the pre-assembled ribonucleoprotein (RNP) complex, Alt-R™ S.p. HiFi Cas9 Nuclease (IDT) was mixed with specified sgRNA and incubated at RT for 10 minutes. For multiplexed genome editing experiments, RNP complexes for each sgRNA were formed separately.

After transduction, CAR NK cells were washed with PBS, centrifuged at 200 ×g for 10 minutes and resuspended in P3 Primary Cell electroporation solution (Lonza). Cells were electroporated with pre-formed RNP complexes using an Amaxa 4-D nucleofector (Lonza).

To test sgRNA editing efficacy, P3 Primary Cell 4D X Kit S (Lonza) was used according to manufacturer's instructions. 5 x 10^5 CAR NK cells were resuspended in 20 µL electroporation solution and electroporated with RNP complexes composed of 500 pmol sgRNA and 16.2 µg Cas9, 100 pmol sgRNA and 6 µg Cas9 or 50 pmol sgRNA and 3 µg Cas9 using nucleofection programs CM-137 or EN-138.

After optimal sgRNA selection, P3 Primary Cell 4D X Kit L (Lonza) was used following manufacturer's instructions for further experiments. 2.5 x 10^6 CAR NK cells were resuspended in 100 µL electroporation solution and electroporated with RNP complexes composed of 500 pmol sgRNA and 30 µg Cas9 (for *TGFBR2* and *PRDM1* sgRNAs) and/or 250 pmol sgRNA and 15 µg Cas9 (for *KLRC1* sgRNA) using program CM-137.

After electroporation, cells were incubated for 10 minutes at 37°C and collected in pre-warmed SCGM supplemented with 20% human AB serum, 2 mM L-glutamine, 500 IU/mL hIL-2, and 140 IU/mL hIL-15. Cells were seeded at a density of 2 x 10^6 cells/mL and co-cultured with 100 Gy-irradiated aAPC at a ratio of 1:1.5 (NK:aAPC). Gene-edited CAR NK cells were maintained in culture by adding fresh CB-NK medium every three-four days. Gene editing efficiency was analyzed by Sanger sequencing as detailed in section 5 at different times of culture. Additionally, TGFBR2 and NKG2A expression was analyzed by flow cytometry (see section 6) and BLIMP1 expression was detected by Western blot (see section 7).

In all experiments, two control conditions were included: non-nucleofected CAR NK cells (NN) and CAR NK cells receiving an electroporation pulse without any RNP complex (mock).

4.3.2. *Sequential* triple gene editing of CAR NK cells

To generate *sequential* triple knock-out CAR NK cells, sequential electroporation steps were performed. First, cells were electroporated with *PRDM1* sgRNA RNP complex following the protocol described in 4.3.1. Then, 8 days after the first electroporation, cells were nucleofected again with *KLRC1* sgRNA and *TGFBR2* sgRNA RNP complexes following the same protocol and re-challenged with aAPC. Gene editing efficacy was analyzed by Sanger and NGS sequencing (see section 5), flow cytometry (see section 6) and Western blot (see section 7).

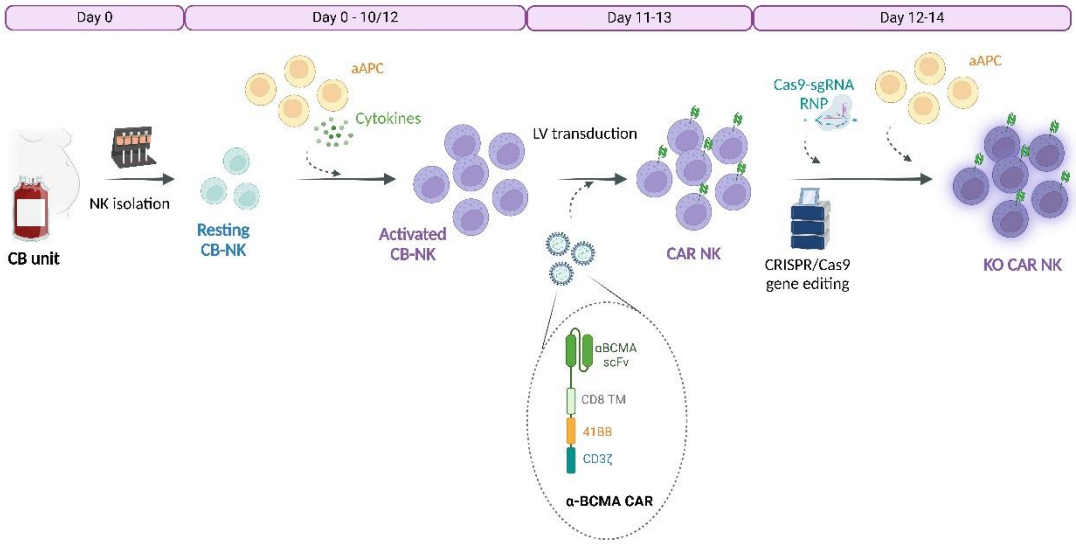

Figure 31. Protocol to generate edited CAR CB-NK cells. Schematic representation of the protocol designed to generate edited CAR CB-NK cells from HD cord-blood samples. CB: cord blood; aAPC: artificial antigen presenting cell; LV: lentiviral vector; RNP: ribonucleoprotein; KO: knock-out. Created with BioRender.com.

5. Gene editing analysis

5.1. Sanger sequencing

To extract DNA from control and edited CAR NK cells, 2 x 10^5 cells were collected and washed with PBS. Pellets were resuspended in 50 µL of QuickExtract™ DNA Extraction Solution (Lucigen) and incubated at 65°C in a heat block for 15 minutes. Then, samples were vortexed and incubated at 95°C for another 15 minutes. DNA was used as template to amplify on-target sites by PCR using Herculase II fusion DNA polymerase (Agilent). Primers used for each on-target site and PCR conditions are indicated in **Tables 7 and 8**, respectively. All primers contained forward and reverse Illumina adapter sequences (Fw: 5'-ACACTCTTTCCCTACACGACGCTCTTCCGATCT-3'; Rv: 5'GACTGGAGTTCAGACGTGTGCTCTTCCGATCT-3') for further Next Generation Sequencing (NGS) analysis. PCR products were subjected to Sanger sequencing using Stabvida sequencing services. Forward primers listed in **Table 7** without Illumina adapters were used for sequencing.

On-target site	Primer	Sequence (5' to 3')	Tm (°C)	PCR product size (bp)
KLRC1 exon 3	Fw	CGTTCTCCACCTCACCCTTT	60	297
	Rv	GCAGTGATAGGTTTTGTCATTCC		
TGFBR2 exon 3	Fw	AGGAGAAAGAATGACGAGAACA	60	300
	Rv	CACAGATCTCAGGTCCCACA		
PRDM1 exon 4	Fw	ATGCGCTATGTGAATCCAGC	60	243
	Rv	GCAGAACCGACATTACTGGC		
PRDM1 exon 5	Fw	AAGAAGCAGCCCCGACCAAA	60	222
	Rv	AACTTGGGGTAGTGAGCGTT		

Table 7. Primers used for PCR amplification. Fw: forward; Rv: reverse.

Herculase II fusion Polymerase		
95°C	10'	
94°C	30''	40 cycles
60°C	30''	
72°C	30''	
72°C	10'	
4°C	hold	

Table 8. Herculase II fusion PCR conditions.

5.2. Interference of CRISPR edits

Chromatograms obtained from Sanger sequencing were analyzed with Synthego Interference of CRISPR Edits (ICE) analysis web tool that provides a quantitative assessment of genome editing. Percentage of indels produced in chromatograms from edited samples was used to calculate genome editing rates. Mock control was used as control input sequence.

5.3. Next-generation sequencing

Genomic DNA from control and edited CAR NK cell samples was extracted using DNeasy Blood & Tissue Kit (Qiagen) according to manufacturer's instructions. sgRNA on-target sites were amplified by PCR using Q5® High-Fidelity DNA Polymerase (New England Biolabs) and the same primers as for Sanger sequencing (**Table 7**). PCR conditions are listed in **Table 9**. PCR products were then purified using DNA Clean & Concentrator kit (Zymo Research) and quantified by Qubit™ Fluorometer (Thermofisher) with Qubit™ dsDNA BR Assay Kit (Thermofisher). Illumina NovaSeq (PE250) NGS was then performed using Biomarker Technologies (BMKGENE) sequencing services. Sequence cleaned data was analyzed with CRISPRessoV2[519], using GRCh38 genome reference sequences and default settings for Cas9 editing tool.

Q5® High-Fidelity DNA Polymerase		
95°C	30''	
95°C	10''	35 cycles
Tm*	30''	
72°C	90''	
72°C	2'	
10°C	hold	

Table 9. PCR conditions used for off-target NGS analysis. Tm* varied depending on primers used.

6. Multiparametric flow cytometry analysis

For antibody staining, 2-5 x 10^5 cells were collected, washed with PBS and resuspended in 100 µL antibody cocktail prepared in PBS. Cells were stained for 30 minutes at 4°C in darkness and then washed with PBS and resuspended in 100 µL PBS with 0.2 µg/mL 4',6-diamidino-2-phenylindole (DAPI, Sigma-Aldrich). All antibodies and reagents as well concentrations used for staining are listed in **Table 10**.

Cells were analyzed using a FACSCanto™ II cytometer (BD Biosciences) which contains 3 different laser lines (405nm, 488nm, and 633nm) and detects 8 different fluorescence channels. FACSDiva v.8.0.1 software was used to exclude debris by Forward Side Channel-Area (FSC-A) vs Side Scatter Channel-Area (SSC-A) and select single cells by FSC-A and FSC-Height (FSC-H). Alive cells were then gated by $DAPI^+$ cell exclusion. A range of 10,000-30,000 alive cell events were acquired per tube. Unstained and single-stained controls were used to set laser voltages and compensate for the spectral overlap among fluorochromes. Fluorescence minus one (FMO) controls were included to identify the additive effect of spreading from multiple fluorochromes in the fluorochrome of interest. Data analysis was later performed using FlowJo V10 software (BD Biosciences). Relative fluorescence intensity (RFI) was then calculated as the mean fluorescence intensity (MFI) of Ab staining divided by the FMO, isotype, or unstained.

Antigen	Clone	Fluorochrome	Source	Catalog number	Dilution
CD3	UCHT1	PE/Cy7	BioLegend	300420	1:100
CD16	3G8	APC/Cy7	BioLegend	302018	1:100
CD19	SJ25C1	APC/Cy7	BioLegend	363010	1:100
CD25	BC96	APC	BioLegend	302610	1:100
CD34	4H11	PE/Cy7	Invitrogen™	25-0349-42	1:50
CD34	4H11	APC	Invitrogen™	17-0349-42	1:50
CD38	H-B7	FITC	BioLegend	356610	1:100
CD45	2D1	PerCP/Cy5.5	BioLegend	368504	1:100
CD45	HI30	APC/Cy7	BioLegend	304014	1:100
CD56 (NCAM)	HCD56	APC	BioLegend	318310	1:100
CD56 (NCAM)	HCD56	PerCP/Cy5.5	BioLegend	318322	1:100
CD56 (NCAM)	HCD56	PE	BioLegend	318306	1:200
CD138	MI15	PE/Cy7	BioLegend	356514	1:100
CD138	MI15	Brilliant Violet 421™	BioLegend	356516	1:100
NKG2A (CD159a)	Z199	PE	Beckman Coulter	IM3291U	1:100
NKG2C (CD159c)	134591	Alexa Fluor 488	R&D Systems	FAB138G	1:100
DNAM-1 (CD226)	TX25	FITC	BioLegend	337104	1:100
TRAIL (CD253)	RIK-2	PE	BioLegend	308206	1:100
NKG2D (CD314)	149810	PE	R&D Systems	FAB139P	1:100
NKp44 (CD336)	P44-8	PE	BioLegend	325108	1:100
NKp30 (CD337)	P30-15	PE	BioLegend	325208	1:100
KLRG1	14C2A07	PE	BioLegend	368610	1:100
TIGIT	A15153G	PE	BioLegend	372704	1:100
Ki67	Ki-67	Brilliant Violet 421™	BioLegend	350506	1:50
BCMA (CD269)	19F2	PE	BioLegend	357504	1:100
HLA-E	3D12HLA-E	APC	Invitrogen™	17-9953-42	1:100
TGFβ-RII	W17055E	APC	BioLegend	399706	1:50
Biotinylated rhBCMA (CD269)	-	-	Adipogen	ANC-519-030	1:200
Streptavidin	-	PE	BD Biosciences	554061	1:200
Streptavidin	-	PE/Cy7	Invitrogen™	SA1012	1:100
IgG1, κ	P3.6.2.8.1	APC	Invitrogen™	17-4714-42	1:100
IgG2a, κ	MOPC-173	PE	BioLegend	400211	1:100
Annexin V	-	APC	BioLegend	640920	1:40

Table 10. Antibodies and other reactants used for flow cytometry. FITC: Fluorescein isothiocyanate; PE: Phycoerythrin; PerCP/Cy5.5: Peridinin chlorophyll protein-Cyanine5.5; PE/Cy7: PE-Cyanine7; APC: Allophycocyanin; APC/Cy7: APC-Cyanine7.

6.1. Immunophenotyping

Multiparametric flow cytometry was used to characterize the phenotype of CAR NK effector cells, MM cell lines and BM mononuclear cells (BMMCs) from MM patients.

For α-BCMA CAR detection in CAR NK cells and lentiviral vector titration, biotin-fused rhBCMA protein (Adipogen) was added to the antibody cocktail. Following the primary staining step, cells were washed with PBS and incubated with fluorescent conjugates of streptavidin (strep) for 30 minutes. After completing secondary staining, cells were washed again with PBS and resuspended in 100 µL PBS with DAPI. Untransduced controls were used to set CAR^+ population gates.

The following expression markers were also studied on CAR NK effector cells:

- Activating receptors: NKG2D, NKG2C, NKp30 and NKp44
- Inhibitory or exhaustion receptors: NKG2A, TIGIT and KLRG1
- ADCC receptors: CD16
- Adhesion receptors: DNAM-1
- Cytokine receptors: CD25 (IL-2Rα) and TGF-βRII
- Markers of apoptosis induction: TRAIL

The percentage of positive cells and RFI of each marker within NK cell population ($CD56^+$) was calculated over FMO controls.

Immunophenotyping of control and edited CAR NK cells was also used to analyze the functionality of *TGFBR2* KO in these effector cells. For this purpose, 10 ng/mL of soluble human TGF-β1 (R&D Systems) was added to NK cells for 48 hours before flow cytometry analysis. RFI of each marker was relativized to untreated controls.

HLA-E and BCMA expression was studied in different MM cell lines. Isotype controls were used to calculate the percentage of positive cells and calculate RFI.

We also characterized BMMCs from MM patients used for cytotoxicity and toxicity assays (section 10.2). Percentage of PC ($CD138^+$ $CD38^+$) and $CD34^+$ cells was determined for each sample. HLA-E and BCMA expression within $CD138^+$ $CD38^+$ population was calculated using FMO controls. Additionally, the phenotype of MM PC was characterized by flow cytometry (CD45, CD56, CD19, CD38 and CD138 expression).

6.2. Cell apoptosis analysis

Phosphatidylserine is normally found on the intracellular part of the plasma membrane in healthy cells but, during early apoptosis, it can be translocated to the external part. Annexin V protein binds phosphatidylserine and can be used as a indirect method to quantify cell apoptosis[520].

To analyze apoptosis on control and edited CAR NK cell cultures, 5 x 10^5 cells were collected and washed twice with cold PBS. Cell pellets were then resuspended in 100 µL of Annexin Binding Buffer (BioLegend) and stained with 2 µL of Annexin-V (BioLegend) for 15 minutes. 0.05% of Propidium Iodide (PI, Sigma-Aldrich) was added to the mix before flow cytometry analysis. Single-stained and unstained controls were used for gating strategy. Apoptotic cells were calculated as Annexin V^+ cells.

6.3. Senescence-associated β-Galactosidase activity analysis

Senescence-associated β-galactosidase (SA-β-Gal) activity is a well-known senescence marker that can be quantify in an indirect manner using 9H-(1,3-Dichloro-9,9-Dimethylacridin-2-One-7-yl) β-d-Galactopyranoside (DDAOG) substrate. DDAOG is cleaved by SA-β-Gal to produce 7-hydroxy-9H(I,3-dichloro-9,9-dimethylacridin-2-one) (DDAO). DDAO generates a far-red-shifted fluorescent signal that can be measured by multiparametric flow cytometry[521].

We used this method to analyze SA-β-Gal activity on control and edited CAR NK cells. 6 x 10^5 cells were collected, washed with PBS and resuspended in 600 µL SCGM medium without any supplement. Bafilomycin A1 (MedChemExpress) was added at 0.1 µM and cells were incubated for 90 minutes at 37°C without CO_2 to induce lysosomal alkalinization. Cells were then separated equally into two tubes. DDAOG substrate (Invitrogen™) was added to one of the tubes at 10 µg/mL while the other tube remained as unstained control. After 1-hour incubation at 37°C without CO_2, cells were washed twice with 0.05% Bovin Serum Albumin (BSA, Sigma-Aldrich) in PBS and resuspended in a final volume of 100 µL PBS with 0.2 µg/mL DAPI for flow cytometry analysis. Percentage of $DDAO^+$ cells was calculated over unstained control.

6.4. Soluble cytokine quantification assay

To analyze cytokine secretion capacity of CAR NK cells, 50,000 cells were co-cultured with different MM target cells (U-266, XG-1, RPMI-8226, and MM.1S) at 1:1 ratio in fresh SCGM supplemented with 20% of AB serum, 2 mM L-glutamine and 100 IU/mL P/S, without cytokines, in non-treated U-bottom 96-well plates (Corning). After 24 hours of co-culture, supernatants were collected and stored at -80°C.

Quantification of soluble cytokines in these supernatants was performed using LEGENDplex™ Human CD8/NK Panel (13-plex) (BioLegend), following the manufacturer´s instructions. This is a bead-based multiplex assay (**Figure 32**) that allows simultaneous quantification of 13 human cytokines and cytolytic proteins including IL-2, IL-4, IL-6, IL-10, IL-17A, IFN-γ, TNF-α, soluble Fas, soluble FasL, Granzyme A, Granzyme B, Perforin, and Granulysin. Flow cytometry data files were analyzed using LEGENDplex™ Data Analysis Software Suite.

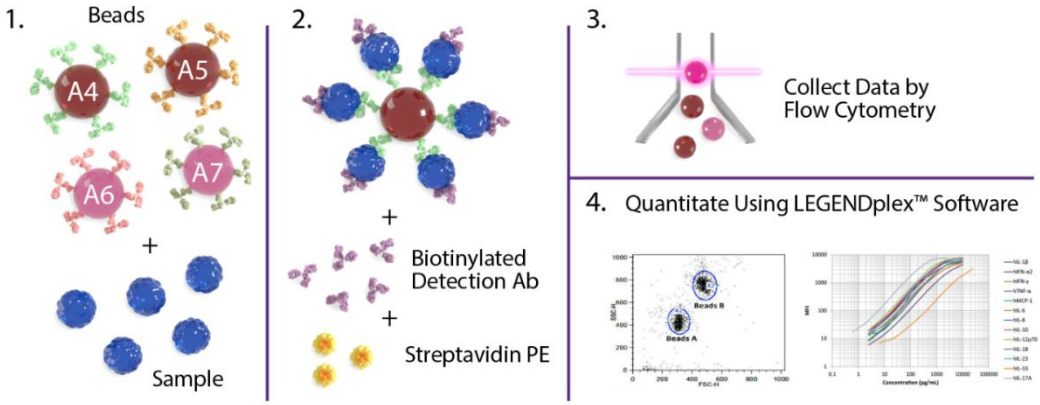

Figure 32. Schematic illustration of the principle of LEGENDplex™ assay. Obtained from BioLegend.

7. Western blot (WB)

To extract proteins from CAR NK effector cells, 3-5 x 10^6 cells were collected and washed with PBS. Cell pellets were then lysed with RIPA lysis buffer (Sigma-Aldrich) supplemented with protease (Roche) and phosphatase inhibitors (Sigma-Aldrich) for 1 hour on ice. Samples were centrifuged at 14,000 ×g for 10 minutes at 4°C. Supernatants were collected and protein concentration was assessed using Quick Start Bradford protein 1x dye (Bio-Rad) following manufacturer's instructions. After protein quantification, 20-30 µg of protein samples were diluted in LaemmLi loading buffer (Bio-Rad) containing sodium dodecyl sulfate (SDS) and 5% β-mercaptoethanol and incubated at 99°C for 10 minutes in a block heater for denaturization.

Proteins were separated following an SDS-polyacrylamide gel electrophoresis (SDS-PAGE) under denaturing conditions. Electrophoresis was performed at constant voltage (140 V) in electrophoresis buffer (25 mM Tris-HCl, 200 mM glycine, 0.1% SDS, pH 8.3). Then, proteins were transferred to nitrocellulose membranes (Amersham) using wet transfer at a constant current of 350 mA for 2 hours. Protein transfer was checked using Ponceau staining solution (Sigma-Aldrich).

Membranes were blocked with 3% BSA in PBS for 30 minutes at RT in agitation. Then, they were incubated overnight at 4°C with primary antibodies diluted in Tris-Buffered-Saline (TBS) buffer with 0.1% Tween20 (TBS-T buffer). Primary Abs and concentration used are listed in **Table 11**. The following day, membranes were washed three times with TBS-T buffer and incubated with anti-mouse or anti-rabbit secondary Abs conjugated to Horseradish Peroxidase (HRP, Cell Signaling) for 45 minutes at RT. After secondary antibody incubation, membranes were washed again three times with TBS-T.

Blots were visualized with a Gel Doc™ EZ Documentation System (Bio-Rad) using Amersham ECL Prime Western Blotting Detection Reagent (Cytiva) or SuperSignal™ West Femto Substrate (Thermofisher). Protein bands were then quantified using Image Lab Software (Bio-Rad).

Antigen	Clone	Host species	Source	Reference	Dilution
BLIMP1/PRDI-BF1	C14A4	Rabbit	Cell Signaling	9115	1:250
β-ACTIN	Polyclonal	Rabbit	Cell Signaling	4967	1:1000
p150 [Glued]	Clone 1	Mouse	BD Biosciences	610474	1:1000
p53	DO-7	Mouse	Dako	M7001	1:500
p16	EP1551Y	Rabbit	Abcam	ab51243	1:1000
Phospho-γH2AX (S139)	JBW301	Mouse	Sigma	05-636-1	1:1000
Phospho-STAT5 (Y694)	C11C5	Rabbit	Cell Signaling	9359	1:1000
STAT5	D3N2B	Rabbit	Cell Signaling	25656	1:1000
Phospho-SHP1 (Y564)	Polyclonal	Rabbit	Abcam	ab192669	1:1000
SHP1	E1U6R	Rabbit	Cell Signaling	26516	1:1000
Phospho-ZAP70 (Y319)/ Phospho-SYK (Y352)	Polyclonal	Rabbit	Cell Signaling	2701	1:1000
ZAP70	99F2	Rabbit	Cell Signaling	2705	1:1000
Granzyme B	D2H2F	Rabbit	Cell Signaling	17215	1:1000
FLC λ	SHL53	Mouse	Leica Biosystems	NCL-L-LAM-578	1:250

Table 11. Primary antibodies used for Western Blotting.

7.1. BLIMP1 detection

BLIMP1 protein was analyzed in NN, mock, *PRDM1* KO, and triple KO CAR NK lysates to verify efficient *PRDM1* disruption at specified times after nucleofection. β-ACTIN was used as loading control. To quantify reduction of BLIMP1 expression, BLIMP1α/β-ACTIN ratio in edited CAR NK cells was relativized to BLIMP1α/β-ACTIN from mock control.

7.2. DNA damage response pathway

Expression of the DNA damage response-associated proteins p16, p53 and, phosphorylated γH2AX was analyzed in NN, mock, *KLRC1* KO, *TGFBR2* KO, double KO, and triple KO CAR NK cell lysates collected on day 19 after first nucleofection. p150 was used as loading control.

7.3. Intracellular activation signaling pathways

To evaluate intracellularly the activation state of CAR NK cells, effector cells were previously stimulated with the U-266 MM cell line. For this purpose, 3 x 10^6 cells from mock, *KLRC1* KO, double KO, and triple KO cell cultures were incubated for 2 hours in RPMI-1640 supplemented with 100 IU/mL and 2% of AB serum. After this time, CAR NK cells were stimulated with U-266 at a 4:1 effector:target (E:T) ratio for 30 minutes. CAR NK cells without stimulation as well as U-266 alone were collected as controls. Pellet samples were processed as previously described and specific Abs were used for detection of phosphorylated STAT5, ZAP70/SYK, and SHP-1 proteins and Granzyme B. Abs against total non-phosphorylated proteins and p150 were utilized as loading controls.

8. Vector copy number (VCN) analysis by quantitative-PCR (q-PCR)

Genomic DNA from CAR NK cell pellets collected on day 14 after nucleofection was extracted using DNeasy Blood & Tissue Kit following manufacturer's instructions. VCN per cell was determined by q-PCR as previously described[522] using TaqMan™ Fast Advanced Master Mix (Applied Biosystems™) according to manufacturer's instructions and 7500 Fast Real Timer PCR system (Applied Biosystems™). The viral packaging signal sequence Psi and human albumin sequence were amplified using probe-labelled primers listed in **Table 12**.

Region	Primer	Sequence (5' to 3')	Probe
Psi	Fw	CAGGACTCGGCTTGCTGAAG	FAM™
	Rv	TCCCCCGCTTAATACTGACG	FAM™
ALBUMIN	Fw	GCTGTCATCTCTTGTGGGCTG	VIC™
	Rv	ACTCATGGGAGCTGCTGGTTC	VIC™

Table 12. Primers used to amplify Psi and human ALBUMIN sequences by q-PCR. Fw: forward; Rv: reverse.

Serial dilutions with a known concentration of a dsDNA fragment containing Psi and human ALBUMIN sequences recognized by our primers were used to generate a standard curve. Both Psi and ALBUMIN quantity were determined by interpolating sample Ct values to the standard

curve. Each sample was analyzed by duplicate and VCN per cell was calculated according to the following formula:

$$\text{VCN} = \frac{\text{Psi quantity}}{\text{human ALBUMIN quantity}} \times 2$$

Final VCN value per sample was determined as the mean of three independent q-PCR analysis.

9. Proliferation assays

9.1. Absolute cell count

To analyze proliferation of control and edited CAR NK cells, cells were counted at different times of culture using a Neubauer chamber (VWR) and 0.4% Typan Blue (Gibco) exclusion method. Fold increase was calculated in each count and then, cumulative fold expansion was calculated over time.

9.2. Cell cycle analysis

To study cell cycle state of CAR NK effectors, 5 x 10^5 cells were collected from culture, washed with PBS, and fixed by adding 2 mL of 70% cold ethanol drop by drop while vortexing for 1 minute and stored at -20°C for at least 12 hours before analysis. Fixed cells were washed twice with PBS, resuspended in 100 µL PBS, and incubated with 0.2 mg/mL RNAse A for 30 minutes at RT. Then, PI was added to each tube at a concentration of 0.04%. DNA content (stained with PI) was then analyzed by flow cytometry on linear scale and percentage of cells in G_1 and S-G_2-M phases were calculated.

9.3. Ki67 staining analysis

Ki67 nuclear protein is used as a cell proliferation marker as it is expressed in cells that are in G_1, S, G_2, and mitosis phases, but not in G_0[523]. To analyze this marker in CAR NK effector cells, 5 x 10^5 cells were collected, washed, and fixed as described in section 9.2. Fixed cells were washed three times with Cell Staining Buffer (BioLegend) and stained for 30 minutes in darkness with Ki67 BV421 antibody (BioLegend) at a concentration of 1:50 in Cell Staining Buffer. After Ki67 antibody labeling, cells were washed twice with Cell Staining Buffer and resuspended in 200 µL of buffer for flow cytometry analysis. Unstained controls were used to set gates and calculate RFI.

10. Cytotoxicity assays

10.1. Calcein-release cytotoxicity/toxicity assay against MM cell lines and HD PBMCs

CAR NK cell cytotoxic activity against MM cell lines and toxicity against HD PBMCs were evaluated *in vitro* through calcein-release assay. Calcein-acetoxymethylester (calcein-AM) is a lipophilic ester that penetrates the plasma membrane and is hydrolyzed in the cytosol by esterase enzymes to a polar green-fluorescent product (calcein). Calcein is retained into cells with intact membrane but when a cell is lysed, this compound is released to the supernatant. Detection of calcein fluorescence in co-culture supernatants can be used as a measure of cell cytotoxicity.

Target MM cell lines (50,000 cells/well) or HD PBMCs (25,000 cells/well) were washed with PBS and stained with 3 µM Calcein-AM (Sigma-Aldrich) during 30 minutes at 37°C in RPMI-1640 medium with 100 IU/mL P/S. Cells were then washed again with PBS and co-cultured with CAR NK effector cells at different E:T ratios in RPMI-1640 medium supplemented with 100U/mL P/S and 10% FBS. Additionally, two control conditions were included: calcein-labelled cells without effector cells to quantify basal lysis and calcein-labelled cells with 1% Triton X 100 (Sigma-Aldrich) to quantify maximum lysis signal. Every condition was carried out per triplicate in a non-treated U-bottom 96-well plate. Plates were centrifuged for 5 minutes at 300 ×g and incubated for 3 hours at 37°C. After this time, plates were centrifuged again and supernatant of each well was collected and transferred into 96-well black microplate (Corning). VICTOR Nivo™ spectrophotometer (PerkinElmer) was used to detect calcein fluorescence (excitation 488 nm; emission 520 nm).

Specific lysis was calculated using the following formula:

$$\text{Specific lysis (\%)} = \frac{\text{sample fluorescence} - \text{basal lysis fluorescence}}{\text{maximun lysis fluorescence} - \text{basal lysis fluorescence}} \times 100$$

To evaluate CAR NK cell cytotoxic activity against MM cell lines in the presence of soluble TGF-β, effector cells were pre-treated with 10 ng/mL of soluble human TGF-β1 for 24 hours before cytotoxicity assay.

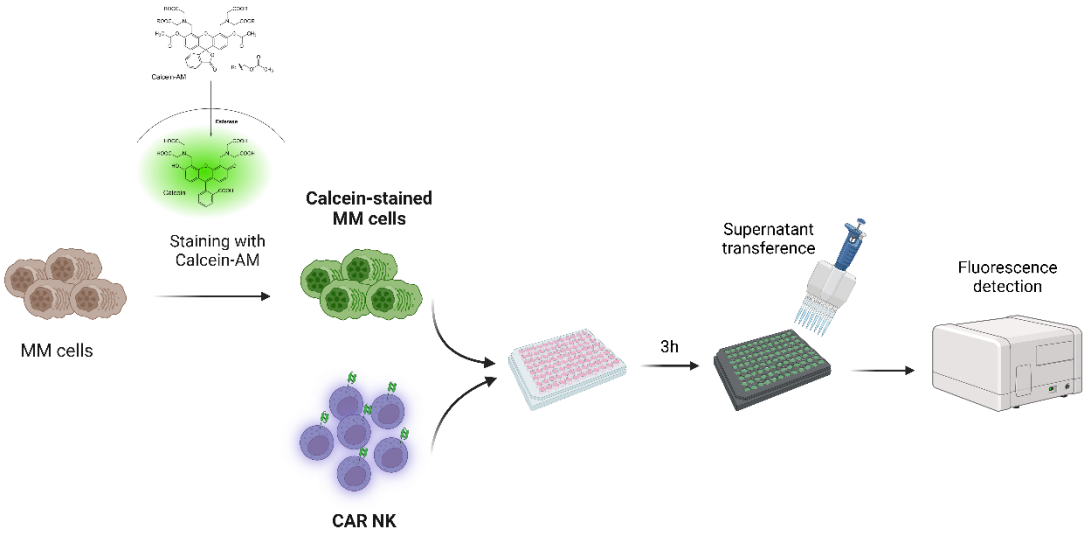

Figure 33. Schematic illustration of calcein-release cytotoxicity assay. MM: multiple myeloma; calcein-AM: calcein-acetoxymethylester; CAR: chimeric antigen receptor. Created with BioRender.com.

10.2. Cytotoxicity assay against primary MM cells and CD34$^+$ cells by flow cytometry

CAR NK cell cytotoxic activity against primary MM cells and toxicity over CD34$^+$ cells were evaluated *in vitro* by flow cytometry after 24 hours of co-culture in a native context.

BM aspirates from MM patients were first centrifuged at 350 ×g for 10 minutes to collect plasma. Then, samples were diluted 1:10 with PBS and added 2:1 over Ficoll-Paque. After a 20 minutes centrifugation at 400 ×g, BMMC fraction was isolated and washed with PBS and centrifuged for 10 minutes at 350 ×g. 2 x 10^5 cells were stained to analyze by flow cytometry the percentage of PC (CD138$^+$ CD38$^+$) in each sample. 30,000 PC were plated per well and cocultured with effector cells at a 5:1 E:T ratio in the absence or presence of 10 ng/mL of soluble TGF-β1. Control wells with BMMCs without effector cells were included to determine the maximum PC survival in each experiment. Each condition was plated per triplicated in non-treated U-bottom 96-well using RPMI-1640 medium supplemented with 100 IU/mL P/S, 10% human AB serum, and 6% of BM plasma to maintain TME present in the patient BM and sustain PC survival. Plates were centrifuged at 300 ×g for 5 minutes and incubated for 24 hours at 37°C.

Plates were then centrifuged at 350 ×g, supernatant was discarded, and cells were stained with CD38 FITC, CD138 PE/Cy7, CD45 PerCP/Cy5.5, CD34 APC and CD56 PE antibodies, as described in section 6. After antibody staining, cells were washed and 30 µL of DAPI and 5 µL of CountBright™ beads (Life Technologies) were added to samples. Whole sample volume was acquired using a FACSCanto™ II cytometer.

Singlets and alive cells were gated as described in section 6 and total number of PC ($CD138^+$ $CD38^+$) and $CD34^+$ events within the alive population ($DAPI^-$) was normalized to the number of CountBright™ beads events. Cytotoxicity of CAR NK cells against PC and toxicity against $CD34^+$ cells was calculated based on cell survival using the following formula:

$$\text{Survival (\%)} = \frac{\text{Number of PC or CD34}^+\text{cells}}{\text{Number of PC or CD34}^+\text{ without effector cells}} \times 100$$

$$\text{Cytotoxicity or toxicity (\%)} = 100 - \text{survival (\%)}$$

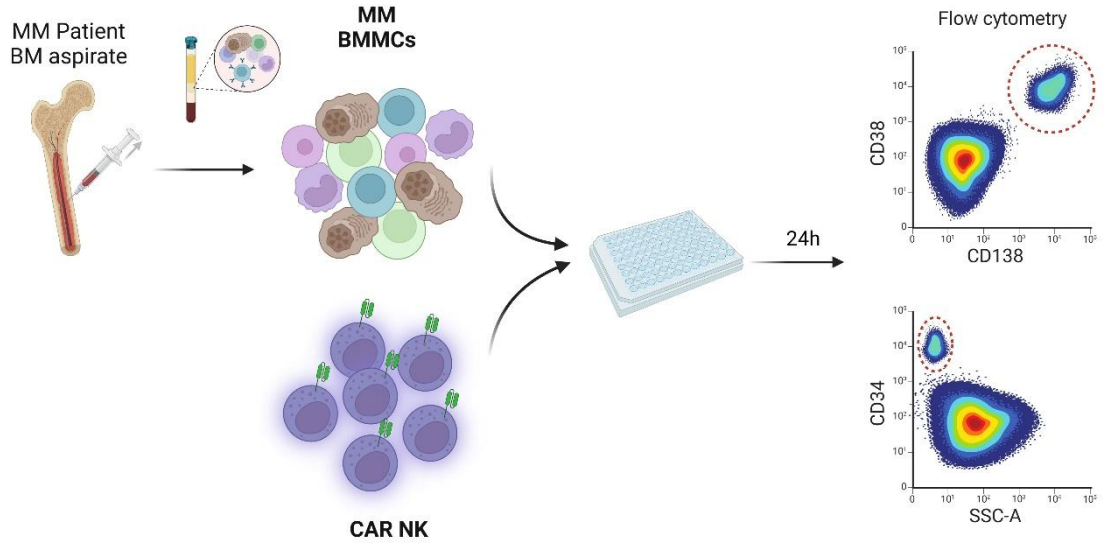

Figure 34. Schematic illustration of flow cytometry cytotoxicity assay against MM BMMCs. MM: multiple myeloma; BM: bone marrow; BMMC: BM mononuclear cells; CAR: chimeric antigen receptor. Created with BioRender.com.

11. Transcriptomic analysis by bulk RNA sequencing (RNA-seq)

11.1. Cell sorting

Mock, *PRDM1* KO, double KO, and triple KO CAR NK cells from three independent CB units were generated as previously described in section 4. In order to reduce heterogeneity and simplify bulk transcriptomic analysis, specific CAR NK populations were sorted 21 days after first nucleofection. A total of 1-2 x 10^7 cells were collected from cell cultures, washed with PBS and stained with CD56 PerCPy5.5, NKG2A PE, TGFBR2 APC and rhBCMA/strep PE as described in section 6. Stained cells were 0.3 µm-filtered and sorted using a BD Influx™ high-speed cell sorter (BD Biosciences).

Two sorting strategies were followed: CD56^{+} CAR^{+} cells were separated from mock and *PRDM1* KO cell cultures and CD56^{+} CAR^{+} TGFBR2^{-} NKG2A^{-} were selected from double KO and triple KO cell cultures. Gating strategy is represented in **Figure 35**. Sorted cells were washed with PBS, centrifuged at 350 ×g and pellets were resuspended in 300 µL Qiazol™ Lysis Reagent (Qiagen) and stored at -80°C for further RNA extraction.

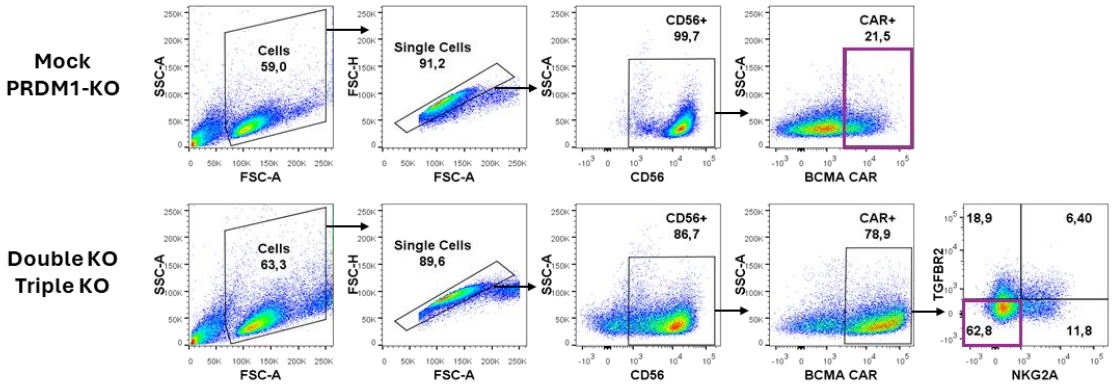

Figure 35. Cell sorting strategy before bulk RNA sequencing. Purple gates indicate cell populations selected for cell sorting. Gating hierarchy is indicated with arrows.

11.2. RNA extraction, library preparation, and RNA sequencing

Qiazol™ cell suspensions were submitted to Genewiz (Leipzig, Germany) for RNA extraction, library preparation, and RNA sequencing. Total RNA was extracted from sorted cells using RNeasy Mini Kit (Qiagen) according to manufacturer's protocol. Libraries were then prepared with Next Single Sell/Low Imput RNA Library Prep Kit (New England Biolabs). Each library received a unique 2x8 bp barcode for multiplexing. Prior to sequencing, library quality was checked by Qubit™ Fluorometer and TapeStation System (Agilent). Sequencing was performed on NovaSeq™ X Plus sequencing system (Illumina). An average of 50 million paired-end reads per sample were obtained.

11.3. Data analysis

The RNA-seq data processing and analysis were carried out by the Translational Bioinformatics Unit at NavarraBiomed Biomedical Research Center following these steps.

First, RNA-seq quality was tested using FastQC v0.11.7[524] and raw reads were trimmed based on quality and length using trimmomatic v0.33. Trimmed reads were mapped to the human genome version GRCh38 using STAR v2.6.1[525].

Genes with a minimum of 10 reads along all the samples were kept for further analysis. Donor bias, based on the observation that there was more than one sample per donor, was corrected

using ComBatseq[526]. Normalization and differential expression analysis were performed using DESeq2[527]. Principal component analysis (PCA) was carried out in all the samples. The two first components were selected for plotting as they expressed the most variability of the samples (**Figure 36**).

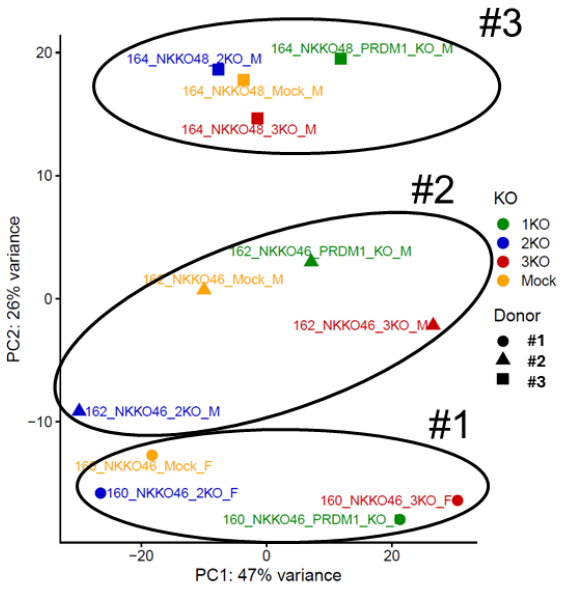

Figure 36. Principal component analysis from RNA sequencing data. Independent donors are indicated with #. 1KO: *PRDM1* KO; 2KO: double KO; 3KO: triple KO.

Genes were considered differentially expressed with p-value < 0.05 after Benjamini-Hochberg (BH) correction for multiple comparisons in each pair-wise comparison. Additionally, only genes with Log_2 fold change values lower than -0.58 or higher than 0.58 were considered differentially expressed. Gene Ontology (GO) and KEGG enrichment analysis for each pair-wise comparison was performed using clusterProfiler (BH p-value adjust < 0.05)[528].

All plots were created in R using ggplot2.

12. Safety profile of edited CAR NK cells

12.1. Next-generation sequencing analysis of potential off-targets

Potential off-target loci of each sgRNA were predicted *in silico* using CRISPOR.org web tool. For each sgRNA, we selected those potential off-target sites in which sgRNA sequence would hybridize with up to 3 mismatches. Specific primers for each of these loci were designed using Primer3 webtool (Primer 3). All primers contained forward and reverse Illumina adapter

sequences (Fw: 5'-ACACTCTTTCCCTACACGACGCTCTTCCGATCT-3'; Rv: 5'GACTGGAGTTCAGACGTGTGCTCTTCCGATCT-3') for NGS analysis.

Genomic DNA from control and edited CAR NK cell samples was extracted using DNeasy Blood & Tissue Kit according to manufacturer's instructions. Off-target sites were amplified by PCR using Q5® High-Fidelity DNA Polymerase or AmpliTaqGold 360 DNA polymerase (Applied Biosystems™). Primers used for each off-target site are listed in **Table 13**. PCR conditions are detailed in **Tables 9 and 14.** PCR products were then purified using DNA Clean & Concentrator kit and quantified by Qubit™ Fluorometer and Qubit™ dsDNA BR Assay Kit. Illumina NovaSeq (PE250) NGS was then performed using Biomarker Technologies (BMKGENE) sequencing services. Sequence clean data was analyzed using CRISPRessoV2. Using GRCh38 genome reference sequences, the percentage of indels as well as single nucleotide substitutions within 5 bp upstream and downstream of the Cas9 cutting site were determined.

Gene		Primer	Primer seq	PCR product size (bp)	Tm (°C)	Polymerase
KLRC1 sgRNA-2	OT1	Fw	TGCCACCAAAATTCAGGAGGA	211	60	Q5
		Rv	CCGCAATACTGTCTGACTTCCT			
	OT2	Fw	CAGGTGCTGTTTATAATTGGTACT	228	62	Q5
		Rv	AAATAATTCCTATGTCAAGCTGGT			
	OT3	Fw	AGAAACATCTGCCCAACAAACG	186	67	Q5
		Rv	CACGCCCAGCCAACAAAG			
	OT4	Fw	TGGGCACAGTGACAATGGAA	192	68	Q5
		Rv	CAAGGTGCTGCTAGGCTTCA			
	OT5	Fw	CCCACTGGAGAGTCTAGATAAAGA	234	66	Q5
		Rv	GTAGTAGGGCTGGAAATTTGAGC			
	OT6	Fw	TCTTCACTCACATTTCCCTGGT	217	63	Q5
		Rv	AAGGGCATGCATTTAGAATACA			
	OT7	Fw	ACACACACAGTATACAAGTCCCC	202	67	Q5
		Rv	TGGCCCCTTATACAGTCTGAGA			
	OT8	Fw	TGTTGCTCACCGTCTTTGTTTC	161	67	Q5
		Rv	TACCTGGAAAAGAAGCTGCCTG			
	OT9	Fw	TGTCTTTTCTTTCTGGCTGCA	164	63	Q5
		Rv	GAGCTCTTTGTGTCATTCCAT			
	OT10	Fw	CAGACCTTTACTGGCCTTGTG	174	67	Q5
		Rv	GTAATCCACTTGCCTCCGCC			
	OT11	Fw	GAGGAAGAAAATGGCAGTTACA	238	63	Q5
		Rv	TGCATAAGTTCAAGGGAGGCA			
	OT12	Fw	CCAAGAGCCAGGACATAGGC	210	69	Q5
		Rv	GCCTGCCTCCCAGATAGTTG			
	OT13	Fw	TGCTCACAAGACCAACCCTT	208	65	Q5
		Rv	TGTATGCACAGTACAGCTTGT			
	OT14	Fw	CCCAATGATCGCAGGTCAGA	266	65	Q5
		Rv	CCCTTGATATGAACAACAGAAGGT			

	OT15	Fw	ACACTTTTGGGCCAGATACACT	181	65	Q5
		Rv	AGTTTTGGGAGTTTGGAGTCT			
	OT16	Fw	TGTATGAGAACTTGCATTCCTG	217	63	Q5
		Rv	ACAGAGACACATTAATGGCAGA			
	OT17	Fw	GAGCGATGTGTCCTCTGCAT	256	68	Q5
		Rv	GCTGCGGTTCTGAACACATC			
TGFBR2 sgRNA-1	OT2	Fw	ACTCTACAAATGACCACCTCCA	203	62	Q5
		Rv	GGTTACTGCTGAAAATTCTGATGG			
	OT3	Fw	TGTCACAGATGCTCTTCAACCA	174	67	Q5
		Rv	GCAAGGAAACATCAGCTCTGTC			
	OT4	Fw	CCTCAGCAAACTCCTGTTGA	190	66	Q5
		Rv	GGCCTGACACATAACGTCCT			
	OT5	Fw	TGGTAGGGAGTTCTGCAGGAA	190	65	Q5
		Rv	AGATTGCTCTTCCTGAAATGCA			
	OT6	Fw	AGCTGTTCTCCAAAAGTAGACT	194	64	Q5
		Rv	TCCTTGAAGTGGCACTATGAGC			
	OT7	Fw	AGAATGTTGCTTAGGGAGTACTCT	176	66	Q5
		Rv	TGAACCTAGGCCTTTGTTGTGA			
	OT8	Fw	CCTGGCCTTGACTCTGCAAT	172	60	Amplitaq
		Rv	CTCGATGTGTTGGATTTGAGGC			
	OT9	Fw	CAGCCGGTGTTTGTTGTAGTTA	256	66	Q5
		Rv	TGTTCTTGTTTCTGCTGCTATGG			
	OT10	Fw	AGAGAAATAGGACGCTTACATGCT	156	60	Amplitaq
		Rv	GCTGAGAGGTCCAAGGTTGAG			
	OT11	Fw	GATTGGGTCTTTTGGCTGTTGG	251	64	Q5
		Rv	ACATGTACGTCCTGATTCCA			
	OT12	Fw	TTTCTTAACTGTGCAGCCTTGG	190	66	Q5
		Rv	TGGTAAGTGGTTGGTAAGTAGTGT			
	OT13	Fw	CTGTTCCCCTCGTCTTCATCAT	175	67	Q5
		Rv	GCCTTGTAGAGAGCAGGTTAAGT			
PRDM1 sgRNA-1	OT1	Fw	TGGCTAATGTGACTCTCTCCTG	180	66	Q5
		Rv	AGGAGAACTGCCATAACGC			
	OT2	Fw	TCTATGTGAGGCTTACTGTGCA	175	64	Q5
		Rv	TGGGACTGTTCTTCTACTCTTT			
	OT3	Fw	GTCTACTCATTTGGTTTCACTCCA	151	60	Amplitaq
		Rv	TGCCTTCCAGTGAACCATTTTA			

Table 13. Primers used for off-target NGS analysis. Fw: forward; Rv: reverse.

AmpliTaqGold 360 DNA polymerase		
95°C	10'	
95°C	30''	35 cycles
Tm*	30''	
72°C	60''	
72°C	7'	
10°C	hold	

Table 14. PCR conditions used for off-target NGS analysis. Tm varied depending on primers used.

12.2. Bionano's Optical Genome Mapping

12.2.1. Genomic DNA isolation

A total of 1.5 x 10^6 NK cells were collected from control and edited CAR NK cell cultures on day 19 after first nucleofection. Cell pellets were resuspended in 40 µL of stabilizer buffer (Bionano Genomics) and stored at -80°C until genomic DNA isolation.

Genomic DNA was isolated using Bionano Prep SP Frozen Cell Pellet DNA Isolation kit (Bionano Genomics) according to manufacturer's instructions. Briefly, cell suspensions were lysed through a 3-minute incubation at RT with 50 µL proteinase K and 20 µL RNase A. Then, 225 µL of Lysis Binding Buffer were added to samples. After a 15-minute incubation at RT, 10 µL of 100mM phenylmethanesulfonyl fluoride (PMSF, Sigma) were added to the mix and samples were incubated for 10 minutes at RT. Then, genomic DNA from cell lysates was extracted by magnetic isolation using 4 mm Nanobind Discs following detailed manufacturer's protocol. Isolated DNA was incubated at RT for 1 hour in a rotational mixer and rested overnight for homogenization. DNA quantification was measured three times for each sample using Qubit™ fluorometer and Qubit™ dsDNA BR Assay Kit.

12.2.2. Genomic DNA enzymatic labeling

Genomic DNA samples were enzymatically labelled using Bionano Prep DLS-G2 Labeling Kit (Bionano Genomics) according to manufacturer's instructions. This consists on an enzymatic approach for direct green fluorescent labelling of ultra-high molecular weight genomic DNA at a 6 bp specific sequence motif (CTTAAG) by the Direct Labeling Enzyme (DLE-1, Bionano Genomics). After DLE-1 labeling, genomic DNA is stained for backbone visualization. As a result, DL-Green fluorophores are seen as green labels on a blue molecule when imaged on the Stratys™ instrument. After staining, labeled and stained genomic DNA was quantified using Qubit™ fluorometer and Qubit™ dsDNA HS Assay Kit (Thermofisher). Importantly, as detailed in Bionano Prep DLS-G2 Labeling Kit protocol, a sonication step is included during quantification process to fragment an aliquot of the labeled genomic DNA to ensure accurate concentration measurements in Qubit™ fluorometer.

12.2.3. Saphyr™ chip loading and Saphyr™ system running

Labeled and stained genomic DNA samples were loaded in Saphyr Chip® G2.3 (Bionano Genomics) following manufacturer's indications. Loaded chips were introduced in Saphyr™ Optical Genome Maping System (Bioanno Genomics) and running was performed.

12.2.4. Data analysis

Data was analyzed and visualized using Bionano ACCESS Software (Bionano Genomics). After checking quality reports for each sample, Rare Variant Analysis was performed using GRCh37 genome assembly as reference. Structural variants present in >0% of control samples were discarded. Circos plots were generated with filtered data for each sample. Structural variants that differed between mock and edited samples were studied in detail. USCS Genome Browser, GeneCards, ClinVar, OMIM, Network of Cancer Genes and Healthy Drivers, and The Cancer Genome Atlas databases were used to search disease-related information from affected genes. Equivalent genome locations for GRCh38 assembly were determined using Ensembl.org.

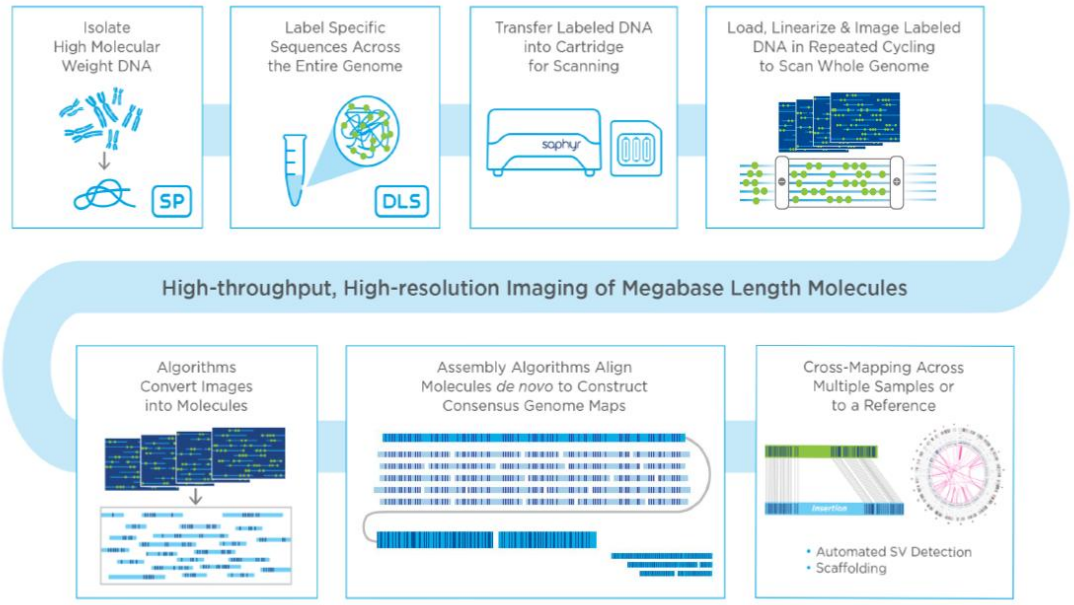

Figure 37. Saphyr™ Optical Genome mapping workflow. Obtained from Bionano Genomics.

13. *In vivo* experiments

Non-obese diabetic (NOD) Cg-Prkdc^{scid} Il2rg^{tm1Wjl} Tg(IL15)1Sz/SzJ (NSG-Tg (Hu-IL15)) mice were purchased from Jackson Laboratory (#030890) and used to study edited CAR NK cell antitumor efficacy *in vivo*. This strain has been modified with a rhIL-15 knock-in to constitutively express physiological concentrations of human IL-15 (7.1 ± 0.3 pg/mL)[529]. All the procedures carried out in these animals were approved by the Comunidad de Madrid (under PROEX 191.2/20) according to the European Union Directive 2010/63/EU and the Spanish Royal Decree-Law RD53/2013. Mice were maintained in pathogen-free conditions at the CIEMAT Laboratory Animal Facility

(registration number ES280790000183). Animals were exposed to 12 hours light:dark (LD) cycles and housed in ventilated cages at 20 ± 2°C, 55 ± 10% relative humidity with *ad libitum* food and water.

At the time of experiments, 6-8 week-old female mice were randomly assigned to the different experiment groups (n=5 mice per group). On day 0, mice were sub-lethally irradiated with a whole-body 1.5 Gy x-ray dose, 4 hours before tumor infusion. Then, 0.5 x 10^6 U266 ffLuc-GFP cells were intravenously (i.v.) injected through tail vein. Three days later, 9 x 10^6 CAR NK effector cells were i.v. infused. Additionally, mice received 3 intraperitoneal (i.p.) injections of 50 ng soluble human TGF-β1 (R&D Systems) on days -1, 7 and 13, and 4 i.p. infusions of 10,000 UI human IL-2 (Miltenyi) on days -1, 3, 7 and 13. One extra control group without cytokine infusions was included to confirm that hTGF-β1 and hIL-2 did not interfere with tumor development.

Mice body weight was monitored weekly. End point criteria were defined as appearance of MM symptoms such as 20% weight loss, asthenia, or paraplegia. At this point, mice were sacrificed by anesthesia (75 µg/gr ketamine and 500 µg/gr dexmedetomidine through intraperitoneal injection) and blood and different tissues were collected for further analysis as described in section 13.3.

13.1. *In vivo* tumor biodistribution analysis by bioluminescence imaging

Tumor burden monitoring was performed every fourteen days by BLI using IVIS Lumina XRMS Series III (Perkin Elmer) until the end of the experiment. Mice were anaesthetized with 2% isoflurane and 200 mg/kg of an aqueous solution of D-luciferin potassium salt (Thermosfisher) was intraperitoneally administered 10 minutes prior to image acquisition. Binning, f-stop, and time exposure were automatically set for each picture. Radiance was expressed in photons per second per cm^2 per steradian (p/s/cm^2/sr) and overlaid on the white light image.

13.2. CAR NK cell infiltration analysis in PB samples

CAR NK effector infiltration in PB was monitored 4, 14, and 30 days after NK cell administration. PB from tail vein was extracted in EDTA tubes and CAR NK cells were detected by flow cytometry. Samples were stained as described in section 6 and lysed with ACK lysis buffer to remove erythrocytes before acquisition. CD138 PECy7, CD45 PerCP/Cy5.5 or APC/Cy7, and CD56 APC or PerCP/Cy5.5 were used for NK cell gating. CD16 APC/Cy7, rhBCMA/strep PE, NKG2A PE, and TGFBR2 APC were used to detect CAR expression and characterize NK phenotype.

13.3. Human population engraftment analysis in PB and BM at necropsy

At the endpoint, mice were necropsied and PB, spleen, femurs and tibias, and cranial dome (CD), were examined. Spleen was smashed in a 0.5% BSA and 2mM EDTA solution in PBS (PBE buffer). BM was flushed out from femurs and tibias into PBE buffer using a syringe. CD was crushed in PBE. Then, cell suspensions were 0.3 µm-filtered and lysed with ACK lysis buffer to remove erythrocytes. Cells were stained as described in section 6. MM cells were detected by GFP expression and CD138 PE/Cy7 staining while NK cells were analyzed as described in section 13.2.

14. Statistical analysis

GraphPad Prism package (version 8, GraphPad Software) was used for all statistical analysis. Data is shown as mean ± Standard Error of Mean (SEM) or Median ± Interquartile Range (IQR). First, Shapiro-Wilk and Kolmogorov-Smirnov tests were conducted to evaluate normal distribution of the samples.

When samples showed a normal distribution, paired or unpaired two-tailed Student t-tests were applied between two parametric groups. To compare more than two groups, one-way or two-way analysis of variance (ANOVA) with post-hoc Tukey's multiple comparison tests were performed, depending on the number of variables to be studied.

In the case of non-parametric samples, two-tailed Mann-Whitney U (unpaired) or Wilcoxon (paired) tests were used to compare two independent groups. To compare more than two groups, Friedman test with post-hot Dunn's multiple comparison tests were carried out.

To compute correlation between VCN and flow cytometry CAR expression data, two-tailed Pearson correlation coefficient analysis was performed, as these variables showed a normal distribution.

In vivo mouse model survival curves were analyzed by applying the Kaplan-Meier method and Mantel-Cox test to compare statistic differences between groups.

Statistical significance was shown as follows: $p<0.05$ (*), $p<0.01$ (**), $p<0.001$ (***), $p<0.0001$ (****).

RESULTS

1. Combined disruption of *KLRC1* and *TGFBR2* improves antitumor efficacy of α-BCMA CAR NK cells but lessens their *in vitro* expansion capacity

1.1. α-BCMA CAR NK cells can be efficiently generated and expanded *in vitro* from umbilical cord blood samples

Different protocols have demonstrated to be successful for the generation of *in vitro* activated and expanded NK cells from CB units[277,443,530,531]. Based on these reported studies, an expansion method was optimized in our laboratory for the generation of CAR CB-derived NK (from here on CAR NK) cells targeting BCMA antigen.

NK cells were isolated from CB samples by Ficoll density gradient and posterior immunomagnetic selection. Although the average percentage of $CD3^+$ cells in CB samples was 28.3 ± 3.8%, after NK cell purification, $CD3^+$ population was lower than 0.3% (**Figure 38A, 38B**). Isolated NK cells were then co-cultured in SCGM with irradiated K562-mb21-41BBL aAPCs and stimulated with IL-2 and IL-15. After 10-12 days of *in vitro* stimulation, activated NK cells were transduced at MOI 10 with a third-generation lentiviral vector containing a second-generation α-BCMA-4-1BBζ CAR transgene and rechallenged again with aAPCs. Flow cytometry analysis 6 days later showed efficient transduction of NK cells (27.2 ± 4.7% CAR^+ cells) (**Figure 38C, 38D**). Of note, after expansion, CAR NK cells acquired a $CD56^{bright}CD16^+$ activation phenotype (**Figure 38C, 38E**).

It has been described that some cytokines used in NK cell expansion methods (i.e. IL-21 and IL-15) can upregulate NKG2A expression[532,533].Moreover, recent studies in our group have demonstrated that IL-15 and the combination of IL-2, IL-21 and 4-1BBL, which is the cocktail of cytokines used in this study, significantly increase NKG2A expression in PB-NK cells (unpublished results[341]). On the other hand, it has been reported that both *ex vivo* expanded PB- and CB-NK cells are also susceptible to TGF-β inhibition[418]. Therefore, we next analyzed the expression of the two dominant inhibitory receptors NKG2A and TGF-βRII (from here on TGFBR2) in our effector cells by flow cytometry. Indeed, both receptors were expressed on CAR NK cells generated using our expansion protocol (95.2 ± 2.3% $NKG2A^+$ and 63.5 ± 4.6% $TGFBR2^+$ NK cells) (**Figure 38F, 38G**).

These results demonstrate the feasibility of generating α-BCMA CAR NK cells from CB samples with a minimal percentage of T cell contamination. Although the CAR NK cell population acquires an activation phenotype, a large proportion of cells expresses the inhibitory receptors NKG2A and TGFBR2, which potentially impact NK cell function.

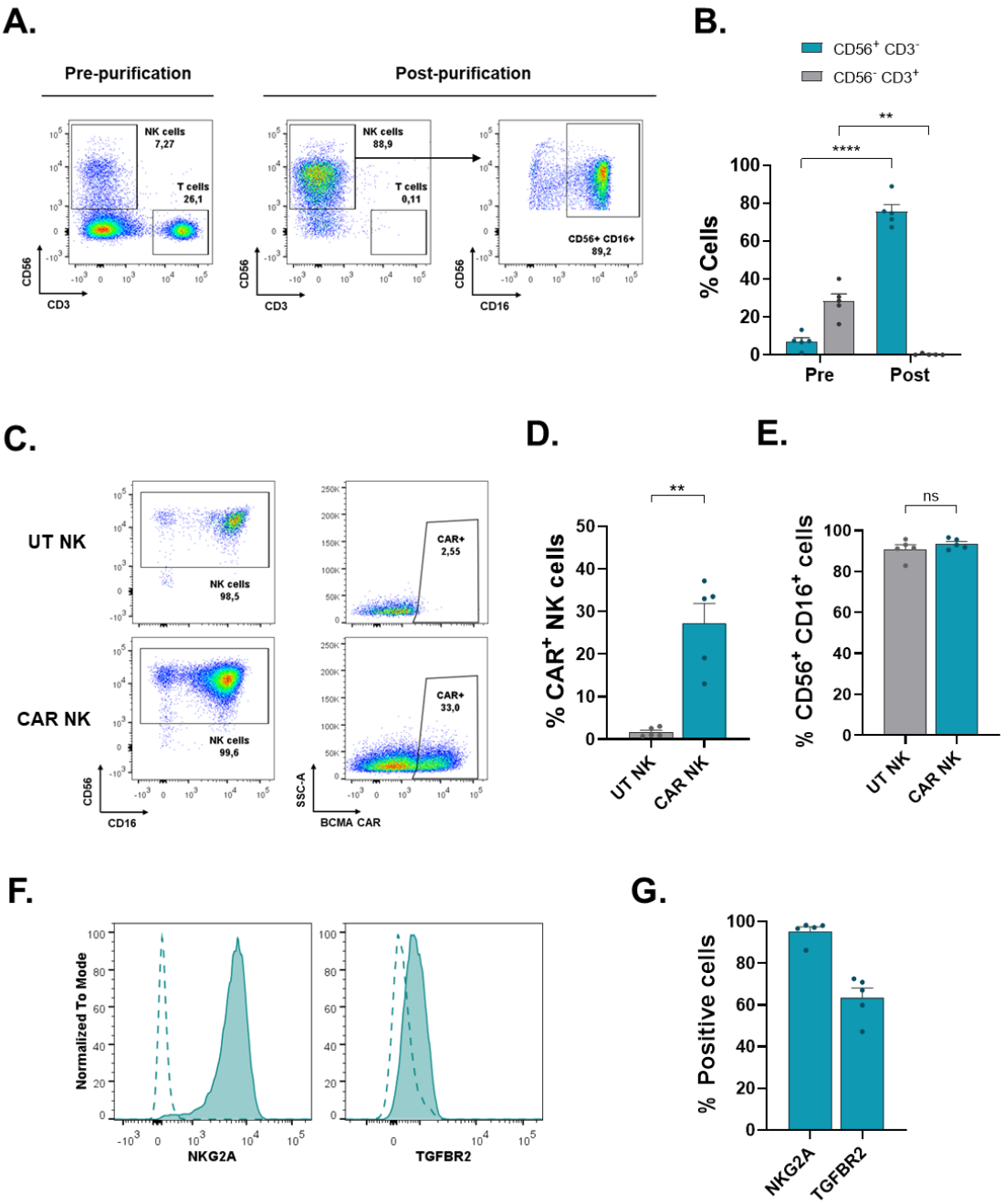

Figure 38. Expanded CAR CB-derived NK cells are efficiently generated *in vitro* and show high expression of NKG2A and TGFBR2. **A.** Representative flow cytometry dot plot of CB samples prior (pre-) or after (post-) purification. **B.** Percentage of NK cells ($CD56^+$ $CD3^-$) and T cells ($CD56^-$ $CD3^+$) analyzed by flow cytometry pre- and post-purification. **C.** Representative flow cytometry dot plot of untransduced (UT NK) and CAR NK cells 6 days after transduction. **D and E.** Percentage of CAR^+ (**D**) and $CD16^+$ (**E**) NK cells analyzed by flow cytometry 6 days after transduction. **F.** Representative flow cytometry histograms of NKG2A and TGFBR2 expression in CAR NK cells 6 days after transduction. **G.** Percentage of $NKG2A^+$ and $TGFBR2^+$ cells measured by flow cytometry. Means ± SEM are shown (n=5). **p<0.01; ****p<0.0001; ns: no significance.

1.2. Optimization of gene editing protocol in CAR NK cells

In order to directly target NKG2A/HLA-E axis, exon 2 from the canonical *KLRC1* (gene encoding for NKG2A) transcript (ENST00000359151.8) was used as the target sequence to design sgRNAs. Two different sgRNAs targeting this region were selected relying on the best predicted efficiency and lower potential off-targets (**Figure 39A**).

Based on previous studies[426,455], Amaxa 4-D nucleofector was used to electroporate sgRNA-Cas9 RNP complexes. To study the most efficient protocol to deliver the sgRNA-Cas9 RNP complexes, two alternative nucleofection programs were used: EN-138 and CM-137.

Firstly, two different doses of each sgRNA were tested (100 and 500 pmol per 0.5 x 10^6 NK cells) using both electroporation programs. Two control conditions were included: non-nucleofected CAR NK cells (NN) and CAR NK cells nucleofected without RNP complexes (mock). Surface NKG2A expression was analyzed by flow cytometry 5 days after nucleofection. Both sgRNAs nucleofected with either electroporation program efficiently reduced NKG2A receptor levels although sgRNA-2 seemed to outperform sgRNA-1 (63.8% KO efficiency for sgRNA-1 vs 81.3% for sgRNA-2 using CM-137 program; 75.7% KO efficiency for sgRNA-1 vs 81.6% for sgRNA-2 with EN-138 program). Independently of the dose used, editing efficiencies were similar (**Figure 39B**). Hence, the lowest dose (100 pmol) was set as the optimal sgRNA concentration.

Once sgRNA concentration was determined, we tested gene editing efficiency with both sgRNAs and nucleofection programs, but also including cell viability analysis by flow cytometry 24 hours and 5 days after nucleofection. EN-138 program reduced the viability of both mock and edited NK cells 24 hours after nucleofection in comparison with non-nucleofected cells, although mock cell culture recovered after 5 days post-nucleofection. By contrast, CM-137 program did not significantly impact on viability of CAR NK cells. Of note, none of the sgRNAs reduced the viability of the edited NK cells compared to mock cells (**Figure 39C, 39D**). Regarding gene editing efficiencies, there were no differences between nucleofection programs. However, as we had previously observed, sgRNA-2 showed higher efficiency than sgRNA-1 (60.2 ± 2.4% for sgRNA-1 vs 76.5 ± 2.3% for sgRNA-2 with CM-137; 66.9 ± 4.4% for sgRNA-1 vs 77.8 ± 1.9% for sgRNA-2 with EN-138) (**Figure 39E, 39F**). Moreover, the percentage of indels calculated by Sanger sequencing and ICE bioinformatic tool showed comparable results to flow cytometry analysis (79.0 ± 3.8% indels for sgRNA-1 vs 92.8 ± 0.9% for sgRNA-2 with CM-137; 78.0 ± 2.0% for sgRNA-1 vs 92.3 ± 0.3% for sgRNA-2 with EN-138) (**Figure 39G**).

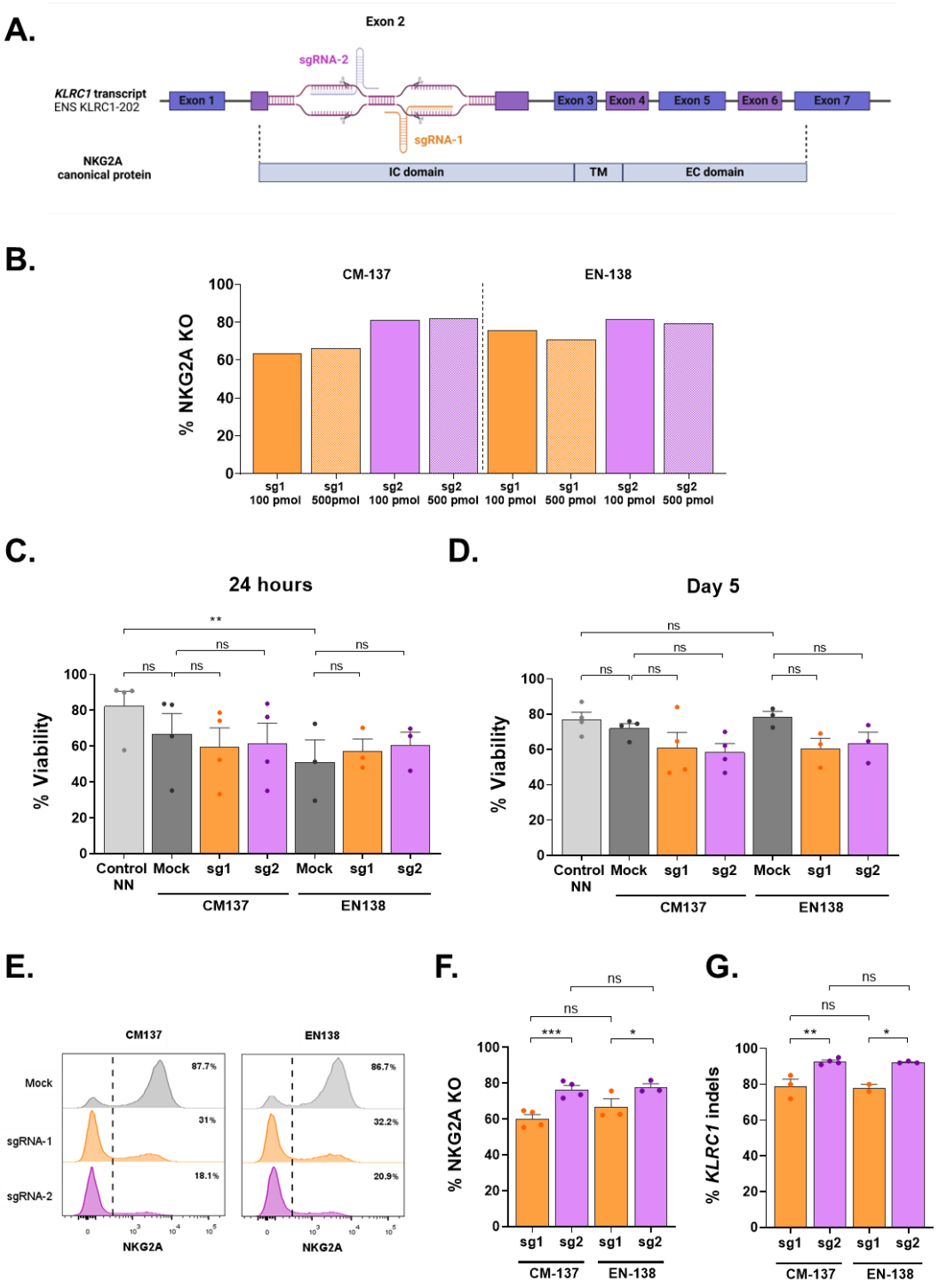

Figure 39. Optimization of nucleofection conditions for *KLRC1* disruption in CAR NK cells. **A.** Schematic representation of the selected sgRNAs to target *KLRC1*. **B.** NKG2A knock-out efficiencies for each tested condition analyzed by flow cytometry 5 days after nucleofection (n=1). **C and D.** Percentage of alive cells in each tested condition analyzed by flow cytometry 24 hours (**C**) and 5 days after nucleofection (**D**) (n=4 for CM-137; n=3 for EN-138). **E.** Representative flow cytometry histograms of NKG2A expression in mock CAR NK and CAR NK cells nucleofected with sgRNA-1 and sgRNA-2 using different electroporation programs. **F.** NKG2A knock-out efficiencies for each tested condition analyzed by flow cytometry 5 days after nucleofection (n=4 for CM-137; n=3 for EN-138). **G.** Percentage of indels in *KLRC1* sgRNA on-target site for each tested condition analyzed by ICE on day 5 after nucleofection (n=4 for CM-137; n=3 for EN-138). sg1: sgRNA-1; sg2: sgRNA-2. Means ± SEM are shown. *p<0.05; **p<0.01; ***p<0.001; ns: no significance.

Due to the higher gene editing efficiency of sgRNA-2, we chose this sgRNA for the generation of the subsequent *KLRC1* KO CAR NK cells. In relation to nucleofection program, although both showed good editing outcomes in CAR NK cells, CM-137 program was selected for further experiments because of the slightly higher cell viability compared to EN-138.

After *KLRC1* sgRNA selection, we then designed and tested two different sgRNAs to directly target TGF-β signaling pathway. Based on reported results[426], exon 3 of the canonical *TGFBR2* transcript (ENST00000295754.10) was chosen as the target sequence (**Figure 40A**). Selected *TGFBR2* sgRNAs were directly tested in combination with *KLRC1* sgRNA-2. Although 100 pmol dose resulted efficient for *KLRC1* disruption, a lower sgRNA concentration (50 pmol per 0.5 x 10^6 NK cells) was additionally tested without altering sgRNA:Cas9 ratio, in order to reduce the total Cas9 amount, which may result toxic for cells. TGFBR2 and NKG2A surface expression was analyzed 5 days after nucleofection by flow cytometry. Combining both sgRNAs, the percentage of NKG2A$^-$ TGFBR2$^-$ NK cells increased compared to non-edited cultures (**Figure 40B, 40C**). *TGFBR2* sgRNA-1 efficiently reduced TGFBR2 expression in a dose-dependent manner. However, *TGFBR2* sgRNA-2 was not as efficient as sgRNA-1 (**Figure 40D, 40E**). As for *KLRC1* sgRNA, the combined disruption approach maintained the same gene editing efficiency and a lower sgRNA dose did not affect the percentage of NKG2A KO (**Figure 40F, 40G**).

Taking all these results together we decided to use *KLRC1* sgRNA-2 at a dose of 50 pmol in combination with *TGFBR2* sgRNA-1 at a dose of 100 pmol per 0.5 x 10^6 cells to generate *KLRC1 TGFBR2* double KO (2KO) α-BCMA CAR NK cells.

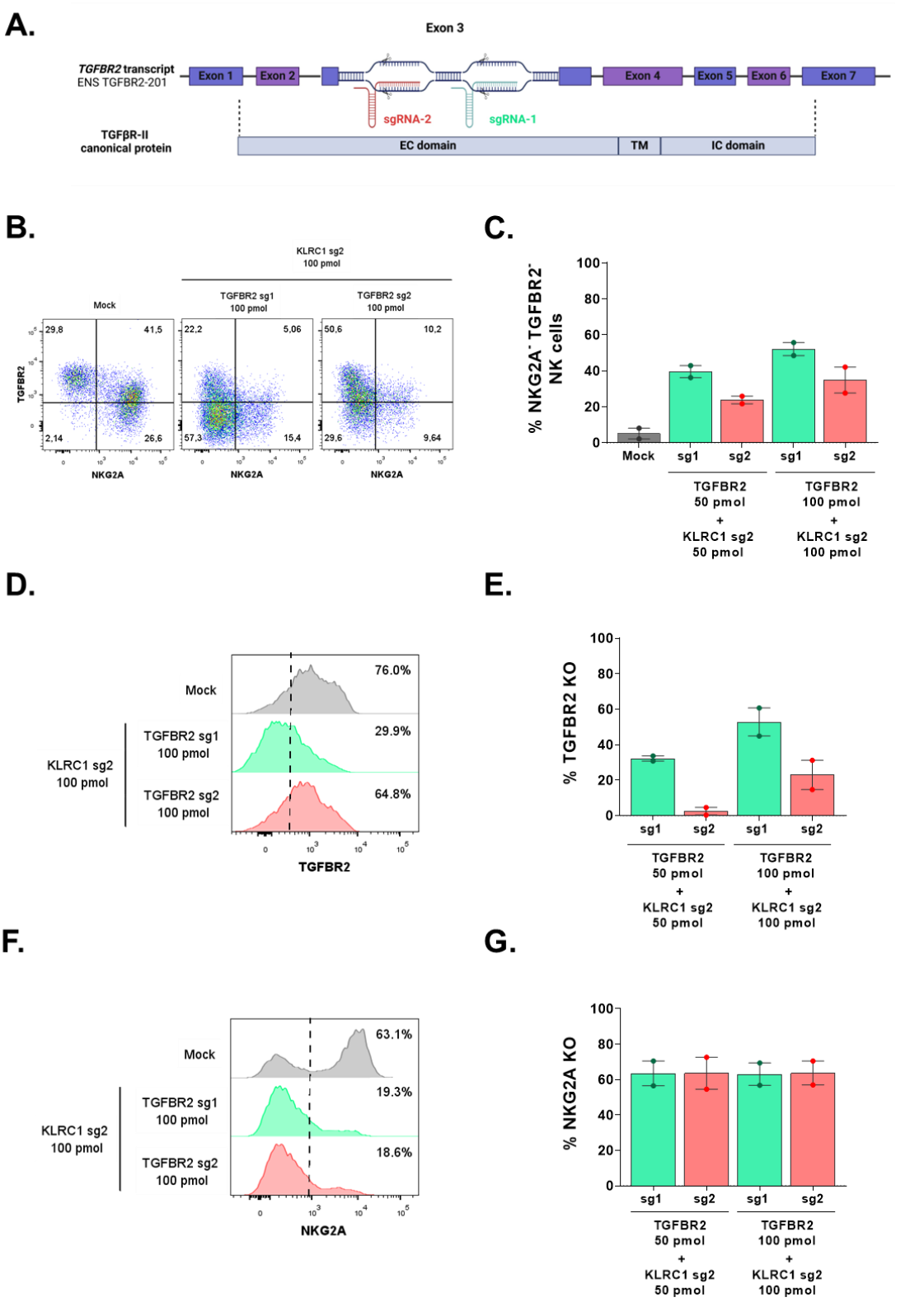

Figure 40. Optimization of nucleofection conditions for the combined disruption of *TGFBR2* and *KLRC1* in CAR NK cells. **A.** Schematic representation of the selected sgRNAs to target *TGFBR2*. **B.** Representative flow cytometry dot plot of mock CAR NK cells and CAR NK cells nucleofected with 100 pmol of *KLRC1* sgRNA-1 and 100 pmol of each *TGFBR2* sgRNA. **C.** Percentage of NKG2A$^-$ TGFBR2$^-$ cells in each tested condition analyzed by flow cytometry 5 days after nucleofection. **D and F.** Representative flow cytometry histograms of TGFBR2 (**D**) and NKG2A (**F**) expression for the same conditions as B. **E and G.** TGFBR2 (**E**) and NKG2A (**F**) knock-out efficiencies calculated for each tested condition analyzed by flow cytometry 5 days after nucleofection. sg1: sgRNA-1; sg2: sgRNA-2. Means ± SEM are shown (n=2).

1.3. Multiplex gene editing efficiently reduces expression of NKG2A and TGFBR2 in CAR NK cells

Once nucleofection conditions were optimized, we generated double KO (2KO) and single KO CAR NK cells to compare gene editing efficiencies and better characterize the CAR NK cell product.

Gene editing efficiency, cell viability, and CAR and CD16 surface expression were analyzed by flow cytometry 5 days after nucleofection. Surface expression of NKG2A and TGFBR2 measured either by percentage of positive cells or by MFI was efficiently reduced in both 2KO and single KO CAR NK cells (**Figure 41A-F**). There was no difference in NKG2A KO efficiency between single KO and 2KO cells (77.6 ± 0.8% and 76.6 ± 1.1%, respectively) (**Figure 41G**). In contrast, TGFBR2 KO percentage was slightly lower in 2KO cells (63.4 ± 3.1%) compared to single *TGFBR2* KO counterparts (69.7 ± 1.6%) (**Figure 41H**). Combining *KLRC1* and *TGFBR2* sgRNAs, the percentage of $NKG2A^-$ $TGFBR2^-$ NK cells increased from 2.8 ± 0.7% to 62.1 ± 2.3% (**Figure 41I, 41J**).

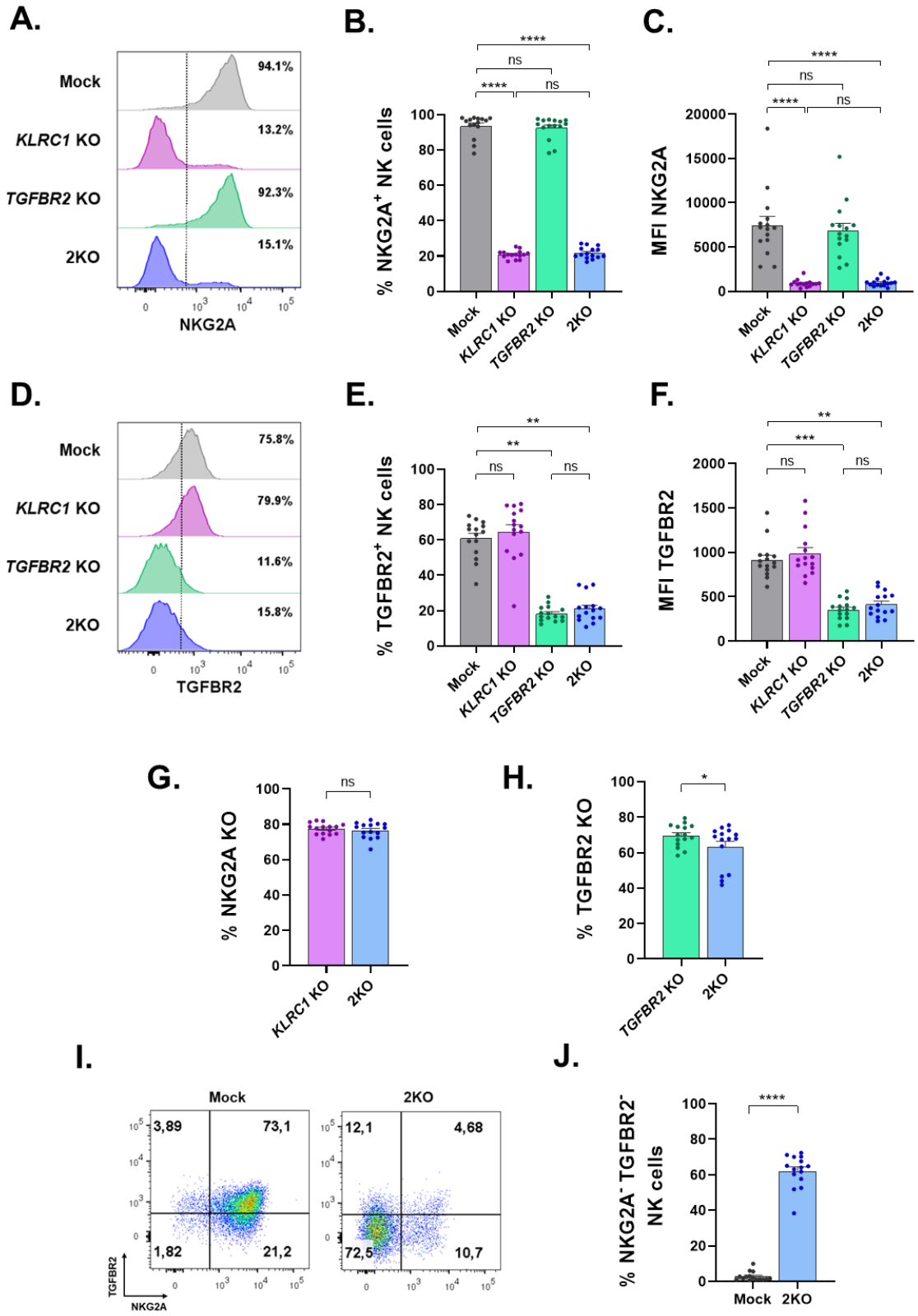

Figure 41. Double KO CAR NK cells show decreased expression of NKG2A and TGFBR2 on day 5 after nucleofection in comparison to non-edited (mock) CAR NK cells. A and D. Representative flow cytometry histograms of NKG2A (**A**) and TGFBR2 (**D**) expression in mock, single KO, and 2KO CAR NK cells analyzed 5 days after nucleofection. Percentage of positive cells is indicated. **B and E.** Percentage of NKG2A$^+$ (**B**) and TGFBR2$^+$ (**E**) NK cells in mock, single KO, and 2KO CAR NK cells analyzed by flow cytometry 5 days after nucleofection. **C and F.** Mean fluorescence intensity of NKG2A (**C**) and TGFBR2 (**F**) in mock, single KO, and

2KO CAR NK cells analyzed by flow cytometry 5 days after nucleofection. **G and H.** NKG2A (**G**) and TGFBR2 (**H**) knock-out efficiencies for single KO and 2KO CAR NK cells on day 5 after nucleofection analyzed by flow cytometry. **I.** Representative flow cytometry dot plot of mock and 2KO CAR NK cells analyzed 5 days after nucleofection. Numbers indicate the percentage of cells in each gate. **J.** Percentage of NKG2A$^-$ TGFBR2$^-$ cells in mock and 2KO CAR NK cells analyzed by flow cytometry 5 days after nucleofection. Means ± SEM are shown (n=15). *p<0.05; **p<0.01; ***p<0.001; ****p<0.0001; ns: no significance.

Concerning CAR NK cell cytotoxic phenotype, disruption of *KLRC1* and *TGFBR2* did not affect the percentage of CD56$^+$ CD16$^+$ or CAR$^+$ cells (**Figure 42A-C**). In contrast, double gene editing significantly reduced the viability of the cells in comparison to non-nucleofected cultures (**Figure 42D**).

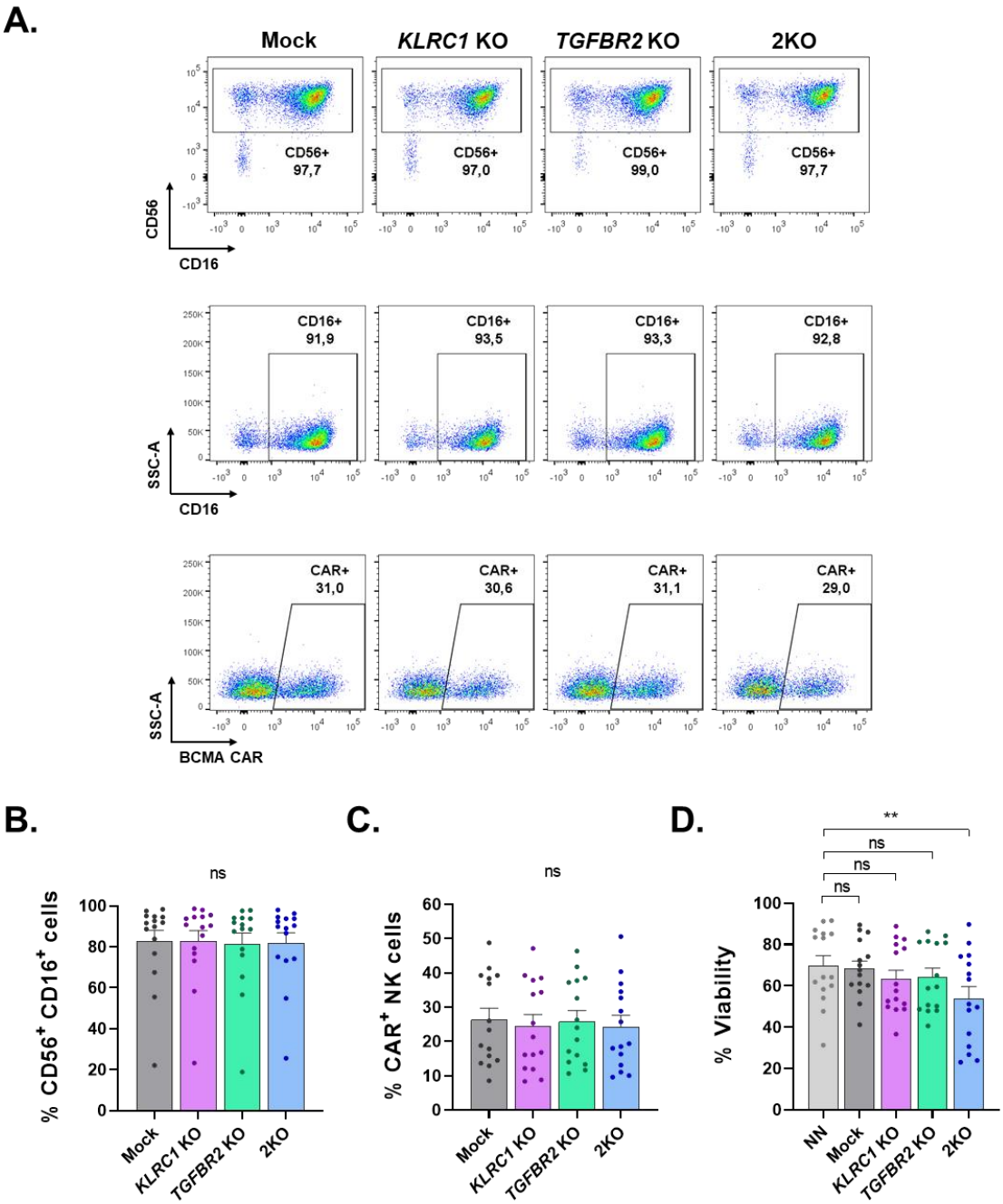

Figure 42. Combined disruption of *KLRC1* and *TGFBR2* does not affect CD16 and CAR expression but reduces the viability of the cells. A. Representative flow cytometry dot plots of mock, single KO, and 2KO CAR NK cells analyzed 5 days after transduction. **B.** Percentage of cytotoxic NK cells in mock, single KO, and 2KO CAR NK cultures analyzed by flow cytometry 5 days after transduction. **C.** CAR expression in mock, single KO, and 2KO NK cells measured by flow cytometry 5 days after transduction. **D.** Percentage of alive cells in mock, single KO, and 2KO CAR NK cultures compared to non-nucleofected (NN) cells analyzed by flow cytometry 5 days after transduction. Means ± SEM are shown (n=15). **p<0.01; ns: no significance.

To confirm flow cytometry editing data, Sanger sequencing of sgRNA on-target sites was also carried out. In general, gene editing efficiencies for *KLRC1* and *TGFBR2* according to percentage of indels were lower than those calculated by flow cytometry. The percentage of indels in *KLRC1* was 71.3 ± 5.8% for single *KLRC1* KO and 58.9 ± 7.6% for 2KO CAR NK cells (**Figure 43A, 43B**) while the percentage of indels in *TGFBR2* was 40.5 ± 6.1% for single *TGFBR2* KO and 27.1 ± 4.8% for 2KO cell cultures (**Figure 43C, 43D**). Due to the discrepancies between flow cytometry and Sanger sequencing results, percentage of indels was analyzed one week later in five donors. In both single KO and 2KO CAR NK cells, percentage of indels in *KLRC1* and *TGFBR2* loci increased considerably (**Figure 43E, 43F**). These differences may be due to the viability and purity of NK cell culture. On day 5 after nucleofection, CAR NK cell cultures still have remaining aAPC debris that contaminate DNA samples, resulting in non-edited sequencing reads that reduced total percentage of indels. Hence, analysis of gene editing efficiency, especially at molecular level, was more precise 12 days after nucleofection.

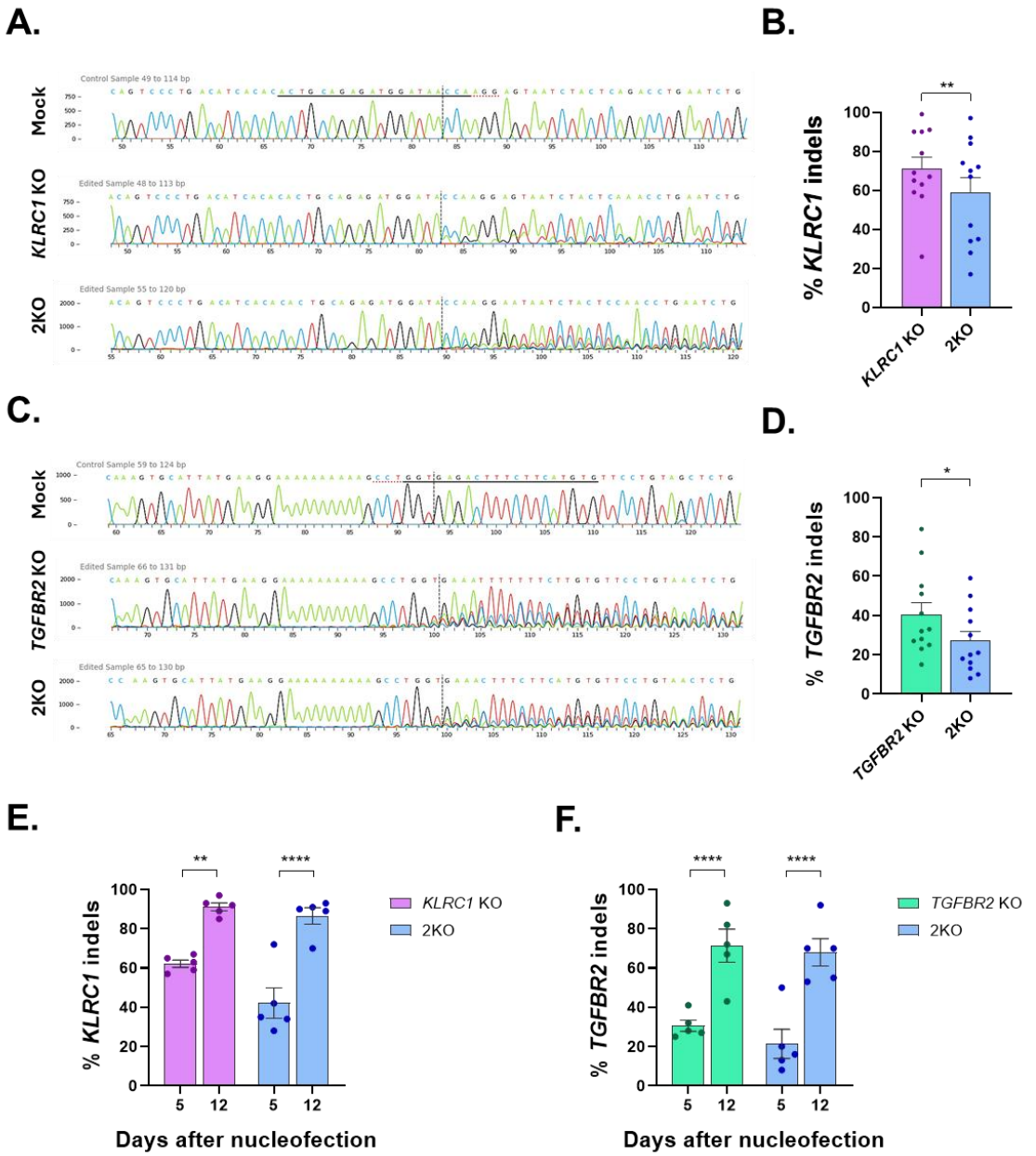

Figure 43. Gene editing efficiencies in CAR NK cells on day 5 after nucleofection by Sanger sequencing. A and C. Representative Sanger sequencing chromatograms of on-target sites for *KLRC1* sgRNA (**A**) and *TGFBR2* sgRNA (**C**) in mock, single KO, and 2KO CAR NK cells analyzed on day 5 after nucleofection. Nucleotides underlined in black correspond to sgRNA binding site. PAM region is indicated with red dashed underlaying. Vertical dashed lines indicate Cas9 cutting site. **B and D.** Percentage of indels in *KLRC1* (**B**) and *TGFBR2* (**D**) sgRNA on-target sites for single KO and 2KO CAR NK cells analyzed by ICE on day 5 after nucleofection (n=12). **E and F.** Percentage of indels in *KLRC1* (**B**) and *TGFBR2* (**D**) sgRNA on-target sites for single KO and 2KO CAR NK cells analyzed by ICE on days 5 and 12 after nucleofection (n=5). Means ± SEM are shown. *p<0.05; **p<0.01; ****p<0.0001; ns: no significance.

To accurately determine gene editing efficiency of 2KO CAR NK cells, a new pool of edited cells was analyzed 12 days after nucleofection. Flow cytometry analysis showed similar results as those obtained on day 5 post-nucleofection. NKG2A and TGFBR2 expression was efficiently reduced in CAR NK cells (**Figure 44A-F**). NKG2A KO efficiency was 75.9 ± 1.2% and 76.8 ± 1.4% for single KO and 2KO CAR NK cells, respectively (**Figure 44G**). With respect to TGFBR2, reduction efficiency was 64.8 ± 3.3% for single *TGFBR2* KO and 61.0 ± 3.5% for 2KO CAR NK cells (**Figure 44H**). Consistent with the flow cytometry analysis on day 5 post-nucleofection, the percentage of $NKG2A^-$ $TGFBR2^-$ cells in 2KO CAR NK cell cultures was 60.6 ± 1.8% on day 12 (**Figure 44I, 44J**).

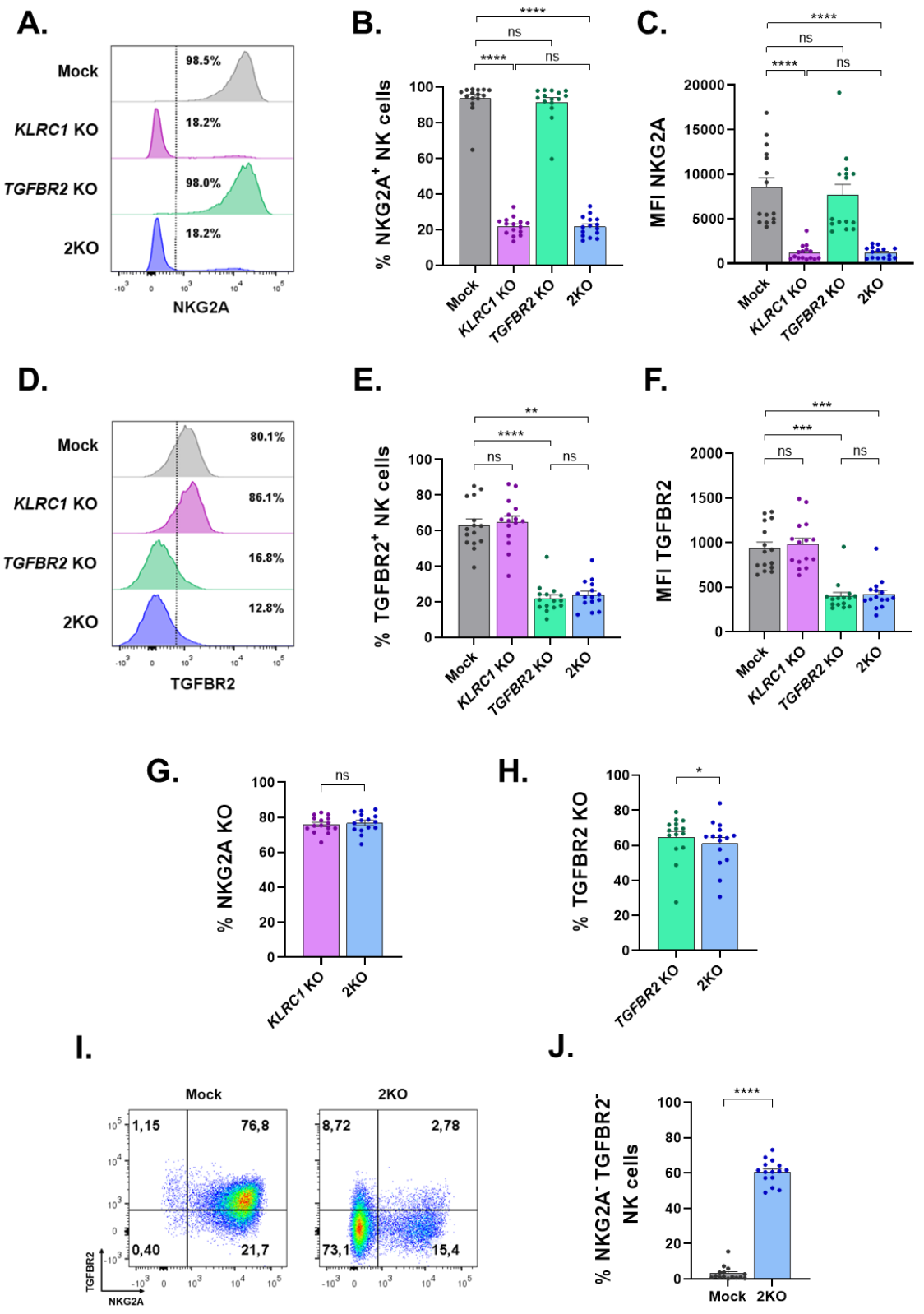

Figure 44. Double KO CAR NK cells maintain NKG2A and TGFBR2 reduction on day 12 after nucleofection. **A and D.** Representative flow cytometry histograms of NKG2A (**A**) and TGFBR2 (**D**) expression in mock, single KO, and 2KO CAR NK cells analyzed 12 days after nucleofection. Percentage of positive cells is indicated. **B and E.** Percentage of NKG2A$^+$ (**B**) and TGFBR2$^+$ (**E**) NK cells in mock, single KO, and 2KO CAR NK cells analyzed by flow cytometry 12 days after nucleofection. **C and F.** Mean fluorescence intensity of NKG2A (**C**) and TGFBR2 (**F**) in mock, single KO, and 2KO CAR NK cells analyzed by flow cytometry 12 days

after nucleofection. **G and H.** NKG2A (**G**) and TGFBR2 (**H**) knock-out efficiencies for single KO and 2KO CAR NK cells on day 12 after nucleofection analyzed by flow cytometry. **I.** Representative flow cytometry dot plot of mock and 2KO CAR NK cells analyzed 12 days after nucleofection. Numbers indicate percentage of cells in each gate. **J.** Percentage of NKG2A$^-$ TGFBR2$^-$ cells in mock and 2KO CAR NK cells analyzed by flow cytometry 12 days after nucleofection. Means ± SEM are shown (n=15). *p<0.05; **p<0.01; ***p<0.001; ****p<0.0001; ns: no significance.

Sanger sequencing results on day 12 post-nucleofection confirmed editing efficiency of both genes and correlated with reduction efficiencies measured by flow cytometry at the same time point (89.5 ± 2.5% and 86.9 ± 2.8% *KLRC1* indels for single KO and 2KO CAR NK cells; 74.2 ± 4.9% and 66.5 ± 4.3% *TGFBR2* indels for single KO and 2KO CAR NK cells, respectively) (**Figure 45**).

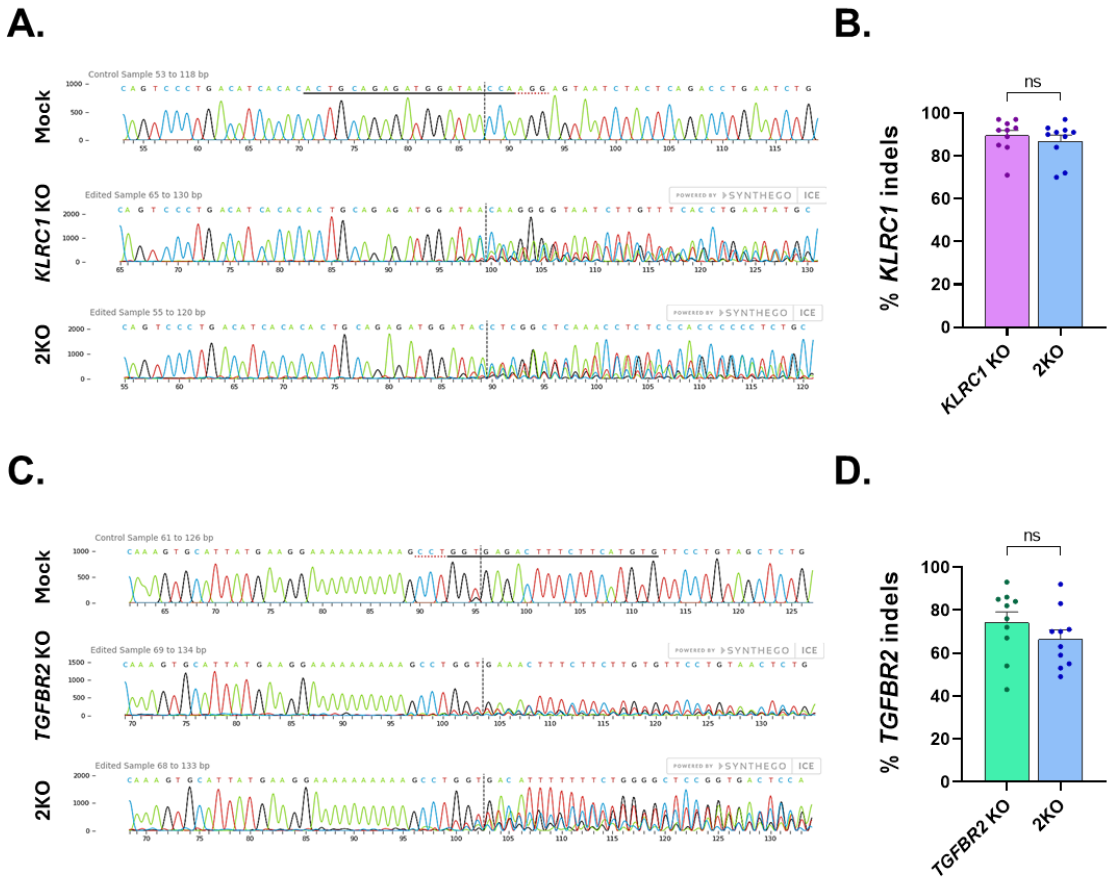

Figure 45. Gene editing efficiencies measured by Sanger sequencing on day 12 after nucleofection. A and C. Representative Sanger sequencing chromatograms of on-target sites for *KLRC1* sgRNA (**A**) and *TGFBR2* sgRNA (**C**) in mock, single KO, and 2KO CAR NK cells analyzed on day 12 after nucleofection. Nucleotides underlined in black correspond to sgRNA binding site. PAM region is indicated with red dashed underlaying. Vertical dashed lines indicate Cas9 cutting site. **B and D.** Percentage of indels in *KLRC1* (**B**) and *TGFBR2* (**D**) sgRNA on-target sites for single KO and 2KO CAR NK cells analyzed by ICE on day 12 after nucleofection. Means ± SEM are shown (n=10). ns: no significance.

Percentage of cytotoxic cells, CAR transduction, and cell viability were also analyzed at this point. As we expected, double gene editing did not affect the proportion of CD16$^+$ cells compared to

mock cells (**Figure 46A, 46B**). CAR expression was neither modified after gene editing (**Figure 46A, 46C**). Moreover, we did not observe any difference in the percentage of alive cells between conditions suggesting that 2KO CAR NK cell culture recovered 12 days after nucleofection (**Figure 46D**).

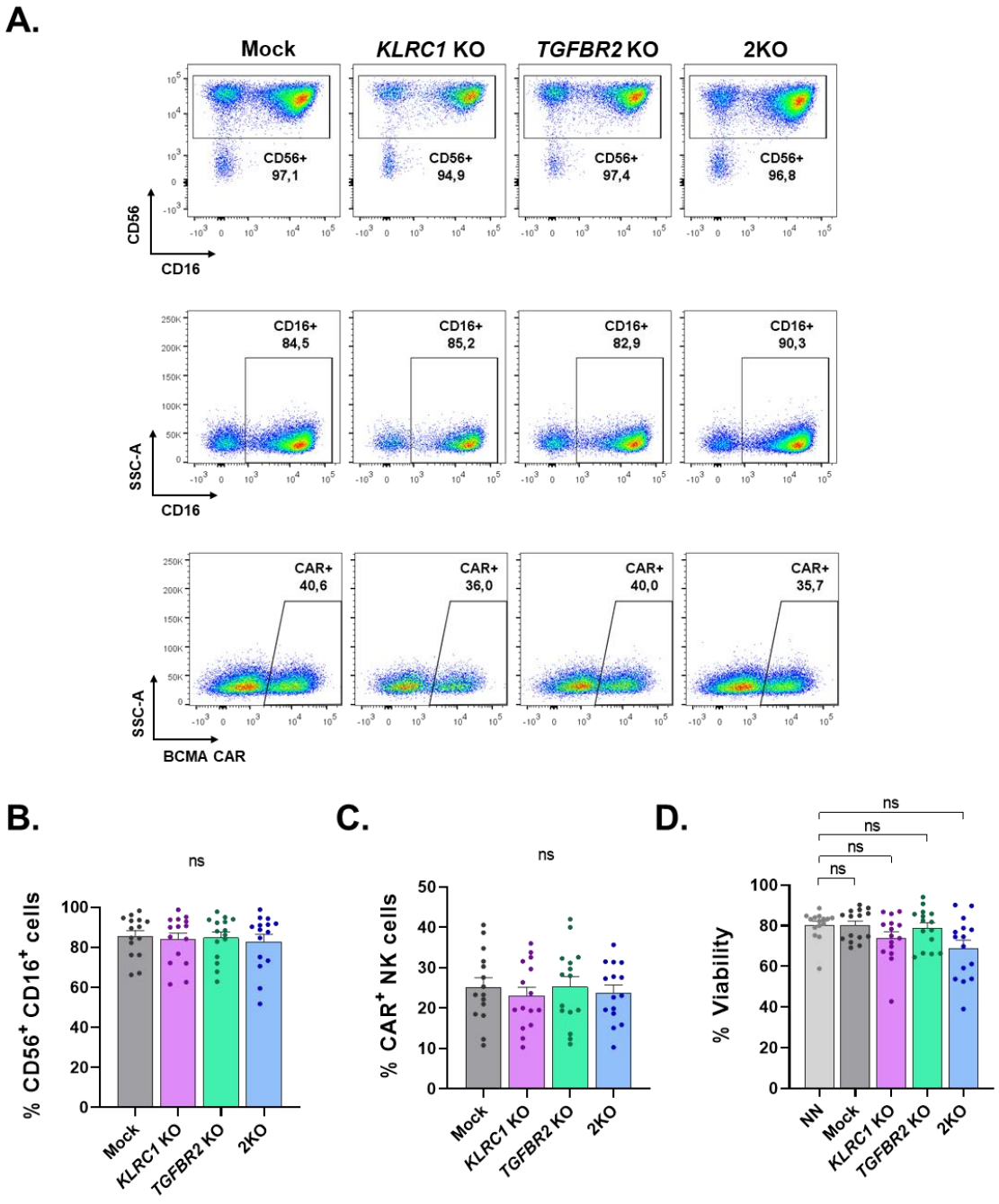

Figure 46. Double knock-out of *KLRC1* and *TGFBR2* does not alter CD16 and CAR expression or viability 12 days after nucleofection. A. Representative flow cytometry dot plots of mock, single KO, and 2KO CAR NK cells analyzed 12 days after transduction. **B.** Percentage of cytotoxic NK cells in mock, single KO, and 2KO CAR NK cultures analyzed by flow cytometry 12 days after transduction. **C.** CAR expression in mock, single KO, and 2KO NK cells measured by flow cytometry 12 days after transduction. **D.** Percentage of alive cells in mock, single KO, and 2KO CAR NK cultures compared to non-nucleofected (NN) cells analyzed by flow cytometry 12 days after transduction. Means ± SEM are shown (n=15). ns: no significance.

Besides analyzing CAR expression by flow cytometry, efficient stable vector integration was also corroborated by q-PCR. 2KO CAR NK cells had 0.53 ± 0.1 copies of vector per cell and showed no differences compared to mock CAR NK control cells (0.49 ± 0.11) (**Figure 47A**). Importantly, VCN quantification correlated with percentage of CAR$^+$ cells analyzed by flow cytometry (**Figure 47B**).

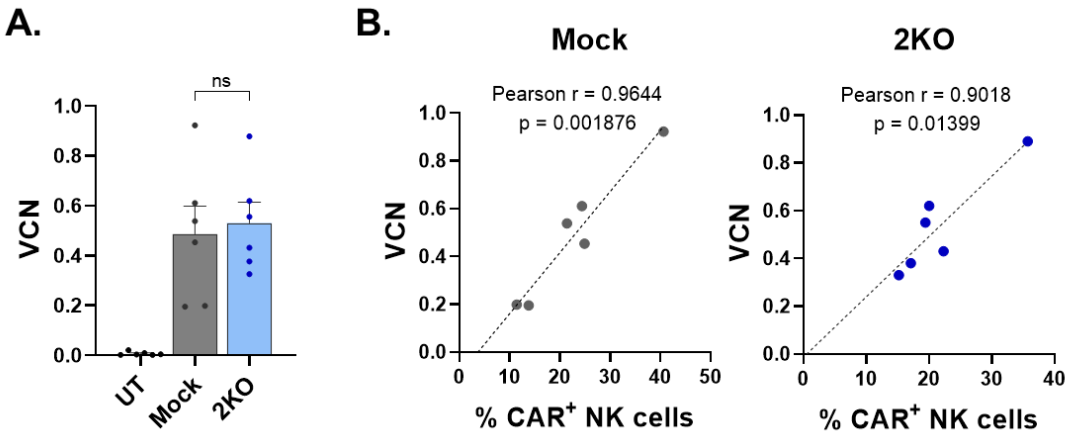

Figure 47. Double knock-out of *KLRC1* and *TGFBR2* does not modify VCN. A. Vector copy number (VCN) quantification by q-PCR of untransduced (UT) NK cells and mock and 2KO CAR NK cells. Means ± SEM are shown (n=6). ns: no significance. **B.** Correlation between VCN quantification by q-PCR and CAR expression by flow cytometry (n=6). Pearson r coefficient and correlation p value are indicated on graph.

To sum up, these data demonstrate that multiplex gene editing allows to generate *KLRC1* and *TGFBR2* double KO CAR NK cells without affecting cell viability, cytotoxic phenotype, CAR expression, and VCN in the final cell product.

1.4. Combined disruption of *KLRC1* and *TGFBR2* does not have a major impact on CAR NK cell immunophenotype

To investigate whether *KLRC1* and *TGFBR2* ablation modified CAR NK cell immunophenotype, the expression of several important NK surface receptors was analyzed by flow cytometry. Only minor phenotypic changes were detected in comparison to mock cells (**Figure 48**). 2KO CAR NK population had lower percentage of cells expressing the activating receptor NKG2D although single *KLRC1* KO counterparts did not. In contrast, the percentage of NKG2C$^+$ NK cells increased in both 2KO and single *KLRC1* KO cells. Regarding inhibitory receptors, the percentage of TIGIT$^+$ cells barely decreased only in 2KO CAR NK cells. Other activating (DNAM-1, NKp30, and NKp44) or death ligand (TRAIL) receptors did not alter their expression among the compared populations.

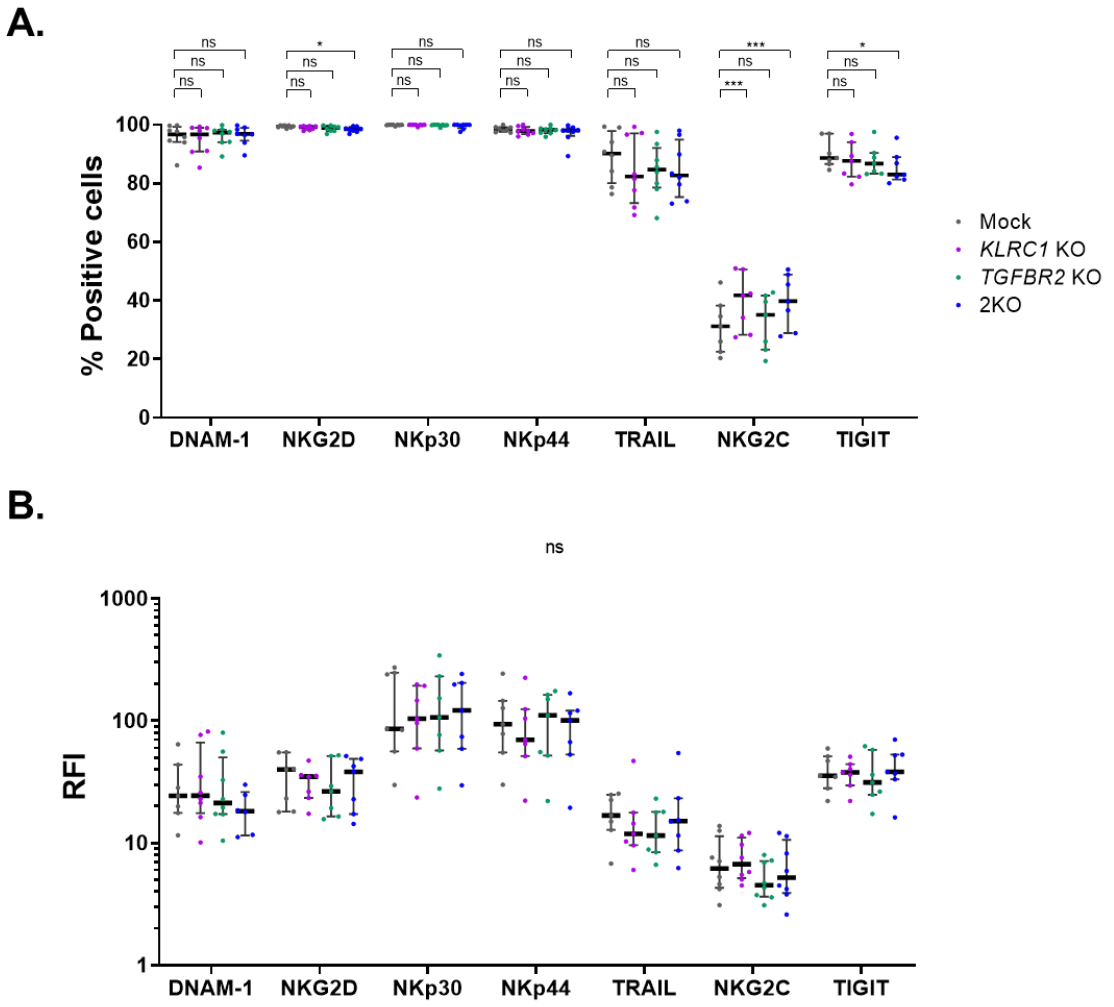

Figure 48. Double KO CAR NK cells show minor immunophenotype changes. A. Percentage of positive cells for each receptor in mock, single KO, and 2KO CAR NK cells analyzed by flow cytometry 12 days after nucleofection. **B.** Relative fluorescence intensity (RFI) of each receptor in mock, single KO, and 2KO CAR NK cells analyzed by flow cytometry 12 days after nucleofection. Data in **B** is presented in logarithmic scale. Medians and IQR are shown (n=6). Statistical analysis shows differences between mock and edited cells. *p<0.05; ***p<0.001, ns: no significance.

1.5. Limited transcriptomic impact of simultaneous *KLRC1* and *TGFBR2* knock-out in CAR NK cells

To further characterize 2KO CAR NK cells, bulk RNA-seq transcriptomic analysis was performed in mock and 2KO CAR NK cells from 3 independent NK donors on day 19 after nucleofection. To reduce potential artifacts associated with culture heterogeneity, CAR NK cells were previously sorted as described in detail in Materials and Methods. Corrections for donor-variability were also performed before comparing RNA-seq data from each group. Surprisingly, we found only 4 genes significantly downregulated and 7 genes upregulated in 2KO CAR NK cells compared to mock CAR NK cells (**Figure 49, Table 15**).

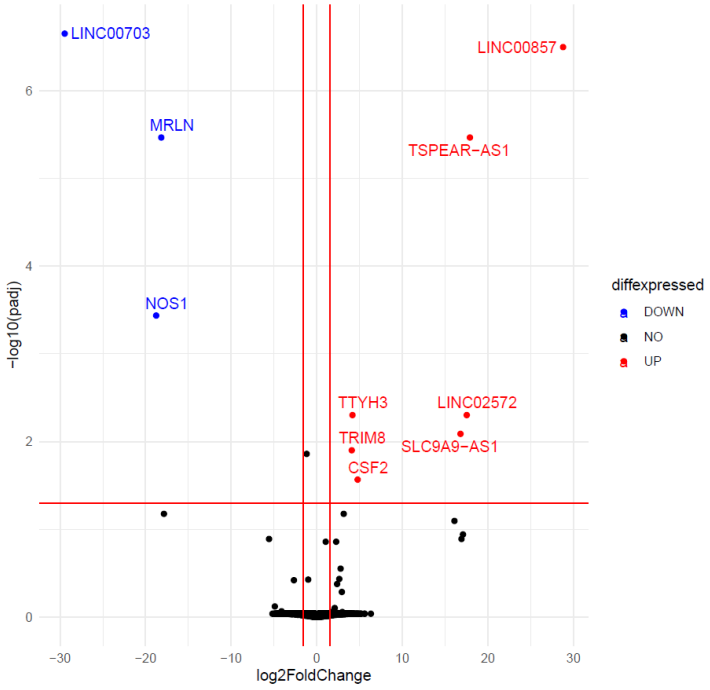

Figure 49. Double KO CAR⁺ NK cells have similar transcriptomic profile to mock CAR⁺ NK cells. Volcano plot of RNA-seq transcriptomic analysis showing upregulated (red) and downregulated (blue) genes in 2KO CAR⁺ NK cells compared to mock CAR⁺ NK cells. Integrated RNA-seq data obtained from 3 independent NK donors.

	ENS entry	Gene name	Log2 Fold Change	Adjusted p
Downregulated	ENSG00000224382	*LINC00703*	-29.454	2.23E-07
	ENSG00000089250	*NOS1*	-18.763	3.66E-04
	ENSG00000227877	*MRLN*	-18.168	3.42E-06
	ENSG00000114013	*CD86*	-1.179	1.38E-02
Upregulated	ENSG00000171206	*TRIM8*	4.091	1.26E-02
	ENSG00000136295	*TTYH3*	4.175	5.00E-03
	ENSG00000164400	*CSF2*	4.779	2.72E-02
	ENSG00000240012	*SLC9A9-AS1*	16.796	8.18E-03
	ENSG00000229536	*LINC02572*	17.527	5.00E-03
	ENSG00000235890	*TSPEAR-AS1*	17.899	3.42E-06
	ENSG00000238246	-	19.913	8.18E-03
	ENSG00000200485	-	23.106	3.66E-04
	ENSG00000237523	*LINC00857*	28.786	3.19E-07

Table 15. List of differentially expressed genes in 2KO CAR⁺ NK cells compared to mock CAR⁺ NK cells. Fold change and adjusted p values are indicated for each gene. Ensembl (ENS) entry codes are referred to GRCh38.p14 genome assembly.

1.6. Double *KLRC1* and *TGFBR2* ablation in CAR NK cells enhances their cytotoxic potential and provides them with resistance to TGF-β-mediated inhibition

Once 2KO CAR NK cells were characterized at immunophenotypic and transcriptomic levels, we sought to assess their cytotoxic potential in the absence and presence of TGF-β inhibition.

To determine if the disruption of *KLRC1* and *TGFBR2* enhanced the antitumor capacity of CAR NK cells, we evaluated cytotoxic potential of edited CAR NK cells against four different MM cell lines: U-266, RPMI-8226, MM.1S, and XG-1. BCMA and HLA-E levels in these cells were analyzed by flow cytometry to confirm the expression of the CAR target and NKG2A ligand. Highest expression of HLA-E was detected in U-266 (16.8 ± 4.8 RFI) compared to RPMI-8226 (6.3 ± 2.5 RFI), MM.1S (8.0 ± 1.4 RFI), and XG-1 (9.3 ± 3.9 RFI). In contrast, RPMI-8226 and MM.1S expressed higher levels of BCMA (10.6 ± 4.9 and 8.6 ± 1.5 RFI, respectively) than U-266 (4.6 ± 1.4 RFI) and XG-1 (4.8 ± 1.8 RFI) (**Figure 50A**). Calcein-release assays demonstrated that *KLRC1* KO significantly increased NK cell cytotoxicity at different E:T ratios against all the tested cell lines, independently of their HLA-E and BCMA expression levels (**Figure 50B**). 2KO CAR NK cells showed similar killing efficiency as single *KLRC1* KO cells.

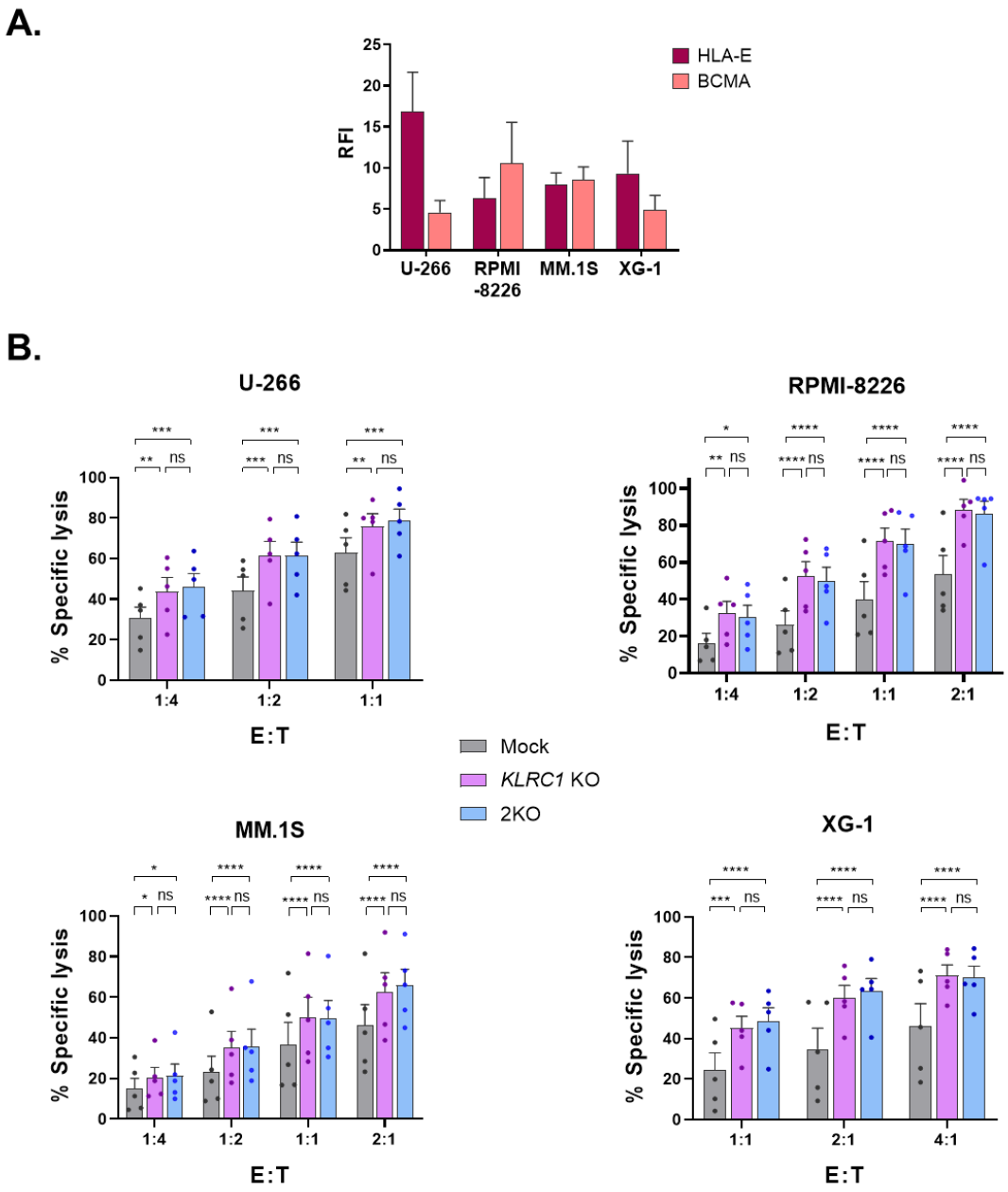

Figure 50. *KLRC1* disruption increases cytolytic potential of CAR NK cells against MM. A. HLA-E and BCMA surface expression in different MM cell lines analyzed by flow cytometry (n=5). Relative expression is calculated over isotype control staining. **B.** Specific lysis of mock, single *KLRC1* KO, and 2KO CAR NK cells against U-266, RPMI-8226, MM.1S, and XG-1 MM cell lines at different E:T ratios, analyzed by 3h-Calcein release assay (n=5). Means ± SEM are shown. *p<0.05; **p<0.01; ***p<0.001; ****p<0.0001; ns: no significance.

Additional disruption of *TGFBR2* did not increase the cytolytic potential of *KLRC1* KO CAR NK cells *per se*. To test the effects derived from *TGFBR2* KO, CAR NK cells were cultured with soluble human TGF-β1 for 48 hours and expression of main NK cell receptors was analyzed by flow cytometry. After treatment with TGF-β, the levels of activating receptors CD16, NKG2D, NKp30, and DNAM-1 were strongly decreased in non-edited and single *KLRC1* KO cells compared to

untreated controls. However, when *TGFBR2* was knocked-out alone or in combination with *KLRC1*, TGF-β treatment was not able to downregulate the expression of these receptors. Interestingly, we found similar results regarding TIGIT expression (**Figure 51**).

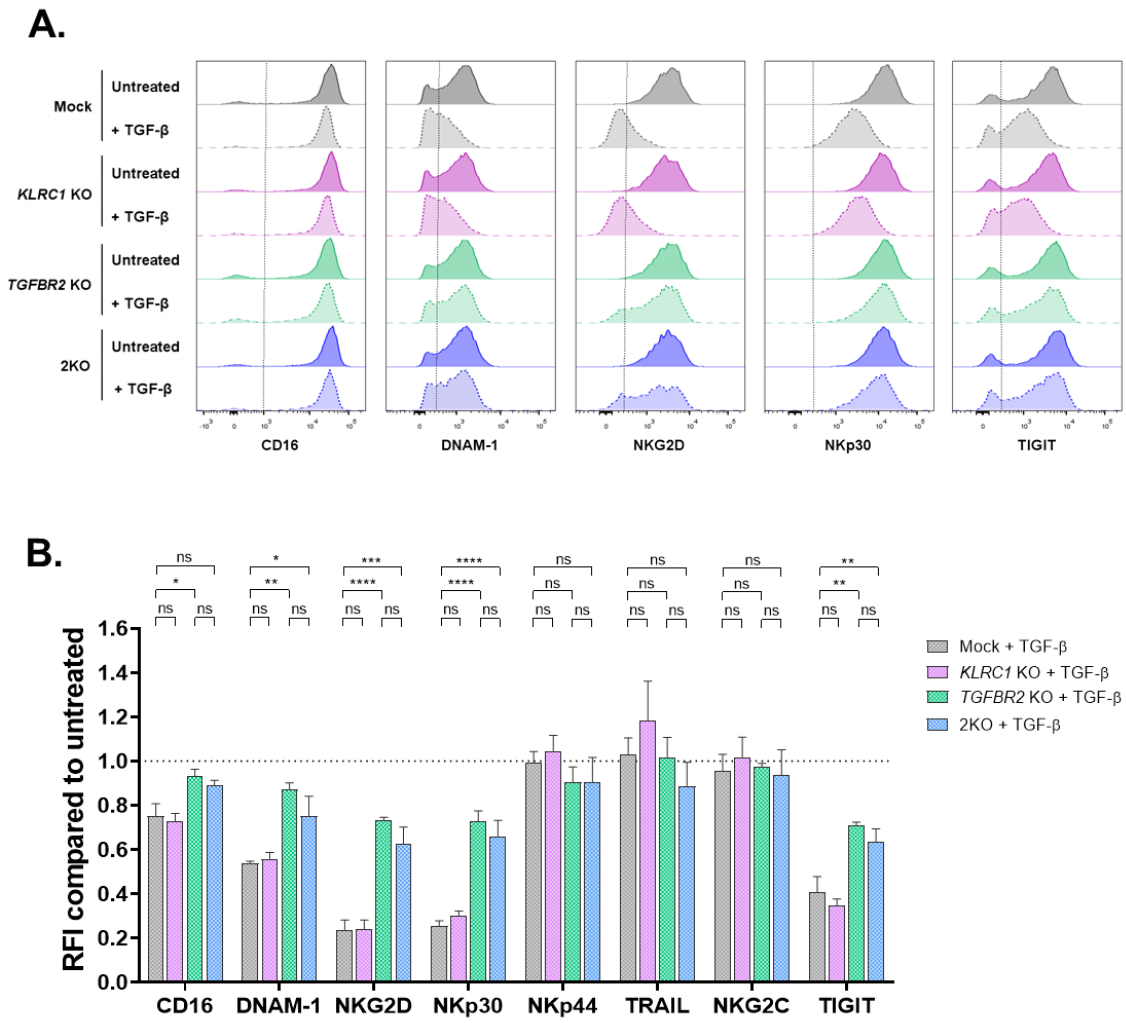

Figure 51. *TGFBR2* knock-out confers CAR NK cells resistance to TGF-β inhibition. A. Representative flow cytometry histograms of different NK cell receptors expressed on mock, single KO, and 2KO CAR NK cells treated or not with 10 ng/ml TGF-β1 for 48 hours. **B.** Expression of different NK receptors in mock, single KO, and 2KO CAR NK cells treated with 10 ng/ml TGF-β1 for 48 hours relativized to untreated controls. Means ± SEM are shown (n=5). *p<0.05; **p<0.01; ***p<0.001; ****p<0.0001; ns: no significance.

Cytotoxic potential of single KO and 2KO CAR NK cells against MM cell lines was also analyzed after treating CAR NK cell cultures with TGF-β. As expected, TGF-β treatment decreased the killing potential of mock and single *KLRC1* KO CAR NK cells against U-266 and RPMI-8226 tumor cells in comparison to untreated controls (**Figure 52**). Nevertheless, single *TGFBR2* KO and 2KO CAR NK cells were resistant to TGF-β inhibition. Importantly, in the presence of TGF-β, 2KO CAR NK cells outperformed non-edited cells *in vitro* at all the different E:T ratios used.

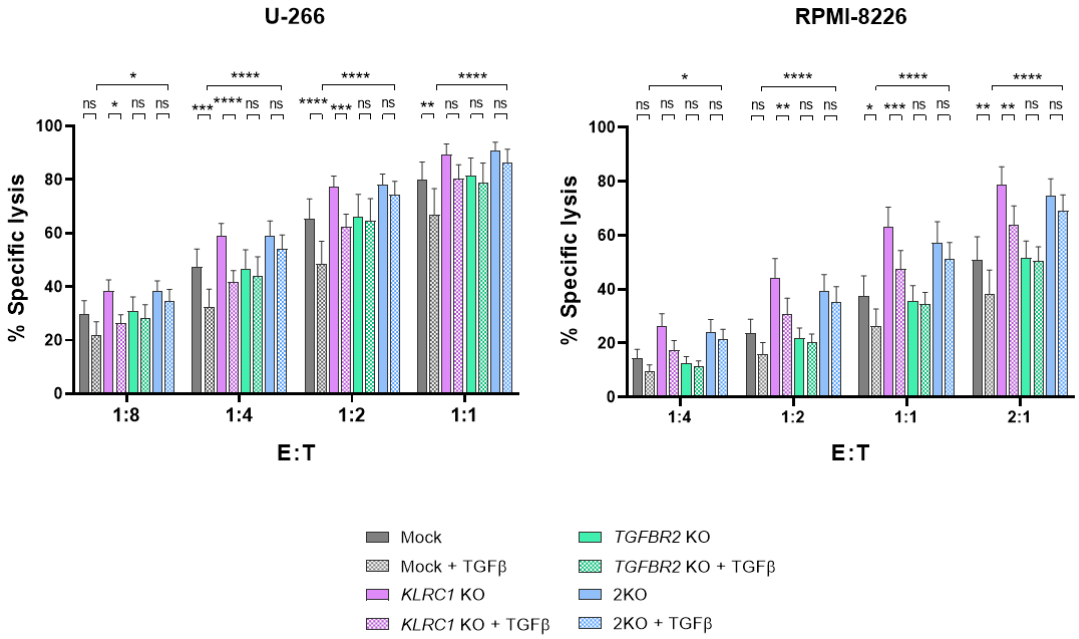

Figure 52. Cytotoxic efficacy of double KO CAR NK cells against MM cell lines is not affected by the presence of TGF-β. Specific lysis of mock, single KO, and 2KO CAR NK cells against U-266 and RPMI-8226 MM cell lines at different E:T ratios, analyzed by 3h-Calcein release assay, after treatment or not with 10ng/ml TGF-β1 for 24 hours. Means ± SEM are shown (n=6). *p<0.05; **p<0.01; ***p<0.001; ****p<0.0001; ns: no significance.

Altogether, these results demonstrated that multiplex gene editing of *KLRC1* and *TGFBR2* in CAR NK cells improves CAR NK cell cytotoxicity against MM and makes cells resistant to TGF-β inhibition.

1.7. Double KO CAR NK cells show limited *in vitro* expansion capacity

Even though the antitumor efficacy of CAR NK cells was improved after multiplex gene editing, we observed that 2KO CAR NK cells had diminished *in vitro* expansion ability in comparison to mock counterparts (**Figure 53A**). Restricted expansion was not an intrinsic consequence of nucleofection process because we did not observe any growth difference between mock and non-nucleofected cells. In contrast, it seems to be associated with the electroporation of RNP and/or the gene editing process. Both single *KLRC1* KO and *TGFBR2* KO CAR NK cells showed lower proliferation than mock cells and when both targets are simultaneously disrupted, this effect is more noticeable.

Although the cell viability of 2KO CAR NK cultures was diminished 5 days after nucleofection (**Figure 42D**), the values were restored one week later (**Figure 46D**). Moreover, transcriptomic RNA-seq analysis did not reveal any change in gene expression associated with diminished

proliferation (**Figure 49, Table 15**). Trying to understand the mechanisms contributing to *in vitro* expansion difficulties of 2KO CAR NK cells, cell apoptosis and senescence state were analyzed by flow cytometry on day 19 after nucleofection, time in which growth differences were prominent.

Apoptosis induction was measured by annexin V staining. In agreement with the cell viability analysis, there was no significant difference in the percentage of annexin V^+ cells between edited and non-edited cultures (mock and non-nucleofected control). In general, the percentage of apoptotic cells for all conditions was low: 17.4 ± 3.4% for *KLRC1* KO, 16.4 ± 3.1% for *TGFBR2* KO and 16.7 ± 4.1% for 2KO cells while for mock control cells was 13.1 ± 2.6% (**Figure 53B, 53C**). Therefore, at least at this time point, the elimination of NKG2A and/or TGFBR2 expression does not induce apoptosis in CAR NK cells.

On the other hand, SA-β-galactosidase activity, which is a well-known marker of senescent cells, was indirectly quantified by flow cytometry using DDAOG substrate. Neither single KO nor 2KO CAR NK cells exhibited increased SA-β-gal activity compared to mock or non-nucleofected control cells thus suggesting that neither single KO nor 2KO induce a senescence state in CAR NK cells (**Figure 53D, 53E**).

Taken together, these results show that 2KO CAR NK cells exhibit a restricted expansion capacity, which is not due to an increase in apoptosis rate or SA-β-galactosidase activity.

Collectively, our data demonstrate that *KLRC1* and *TGFBR2* disruption by multiplex gene editing strengthens antitumor ability and confers resistance to TGF-β inhibition on CAR NK cells, without causing relevant immunophenotypic or transcriptomic modifications but reducing *in vitro* expansion capacity.

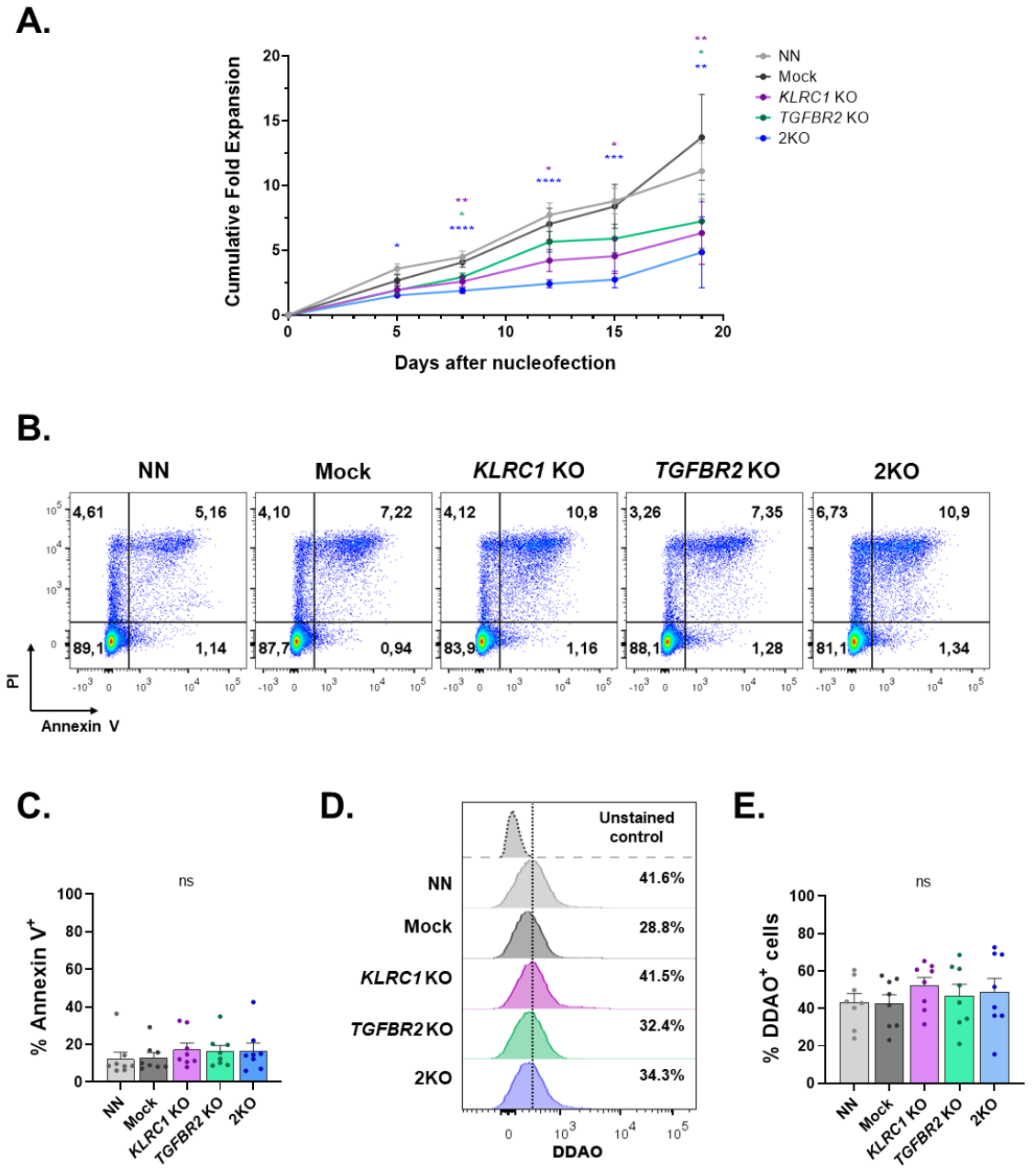

Figure 53. Combined elimination of *KLRC1* and *TGFBR2* in CAR NK cells lessens their *in vitro* expansion capacity. A. Cumulative *in vitro* fold expansion of non-nucleofected (NN), mock, single KO, and 2KO CAR NK cells monitored at different times after nucleofection. Statistical analysis shows differences with respect to mock CAR NK cells. **B.** Representative flow cytometry dot plot of NN, mock, single KO, and 2KO CAR NK cells stained with annexin V and propidium iodide on day 19 after nucleofection. Numbers indicate the percentage of cells in each gate. **C.** Percentage of apoptotic cells in NN, mock, single KO, and 2KO CAR NK cell cultures analyzed by Annexin V flow cytometry staining on day 19 after nucleofection. **D.** Representative flow cytometry histograms of SA-β-gal activity, measured as the percentage of $DDAO^+$ cells, in NN, mock, single KO, and 2KO CAR NK cells 19 days after nucleofection. The percentage of positive cells is indicated. **E.** Percentage of cells showing SA-β-gal activity in NN, mock, single KO, and 2KO CAR NK cells analyzed by flow cytometry on day 19 after nucleofection. Means ± SEM are shown (n=8). *p<0.05; **p<0.01; ***p<0.001; ****p<0.0001; ns: no significance.

2. Knock-out of *PRDM1* enhances the proliferative potential of α-BCMA CAR NK cells maintaining their cytotoxicity against MM

With the aim to increase the expansion and persistence of CAR NK cells, for the third objective of this thesis we proposed *PRDM1* as a potential editing target as disruption or silencing of *PRDM1* in NK cells has been associated with an increased *in vitro* proliferation and reduced apoptotic state of the cells[469,472]. To explore the potential use of this target in CAR NK immunotherapy, single KO of *PRDM1* was first carried out in CAR NK cells to characterize functional consequences derived from this gene modification.

2.1. Gene editing efficiently knocks out *PRDM1* in CAR NK cells

Following the same strategy as for *KLRC1* and *TGFBR2* knock-out, two different sgRNAs targeting exons 4 (sgRNA-1) and 5 (sgRNA-2) from canonical *PRDM1* transcript (ENST00000369096.9) were selected and tested separately (**Figure 54A**). A dose of 100 pmol sgRNA per 0.5 x 10^6 cells was used. Gene editing efficiency was analyzed 12 days after nucleofection by Sanger sequencing. Both sgRNAs showed high efficiency although sgRNA-1 produced a higher percentage of indels (91.6 ± 1.4%) than sgRNA-2 (75.9 ± 4.7%) (**Figure 54B, 54C**). Additionally, protein reduction was analyzed by Western blot to confirm gene editing efficiencies. Both sgRNAs reduced BLIMP1 expression compared to mock cells (**Figure 54D, 54E**). *PRDM1* knock-out was monitored at different time points. As expected, the percentage of indels increased over time in culture and achieved 92.0 ± 1.8% indels for sgRNA-1 and 90.4 ± 1.9% for sgRNA-2 26 days after nucleofection, suggesting that *PRDM1* KO cells had a selective advantage in culture (**Figure 54F**). Although sgRNA-2 showed lower gene editing efficiency at early times from nucleofection, it increased over time being in par with sgRNA-1. Therefore, we continued the functional characterization using both sgRNAs.

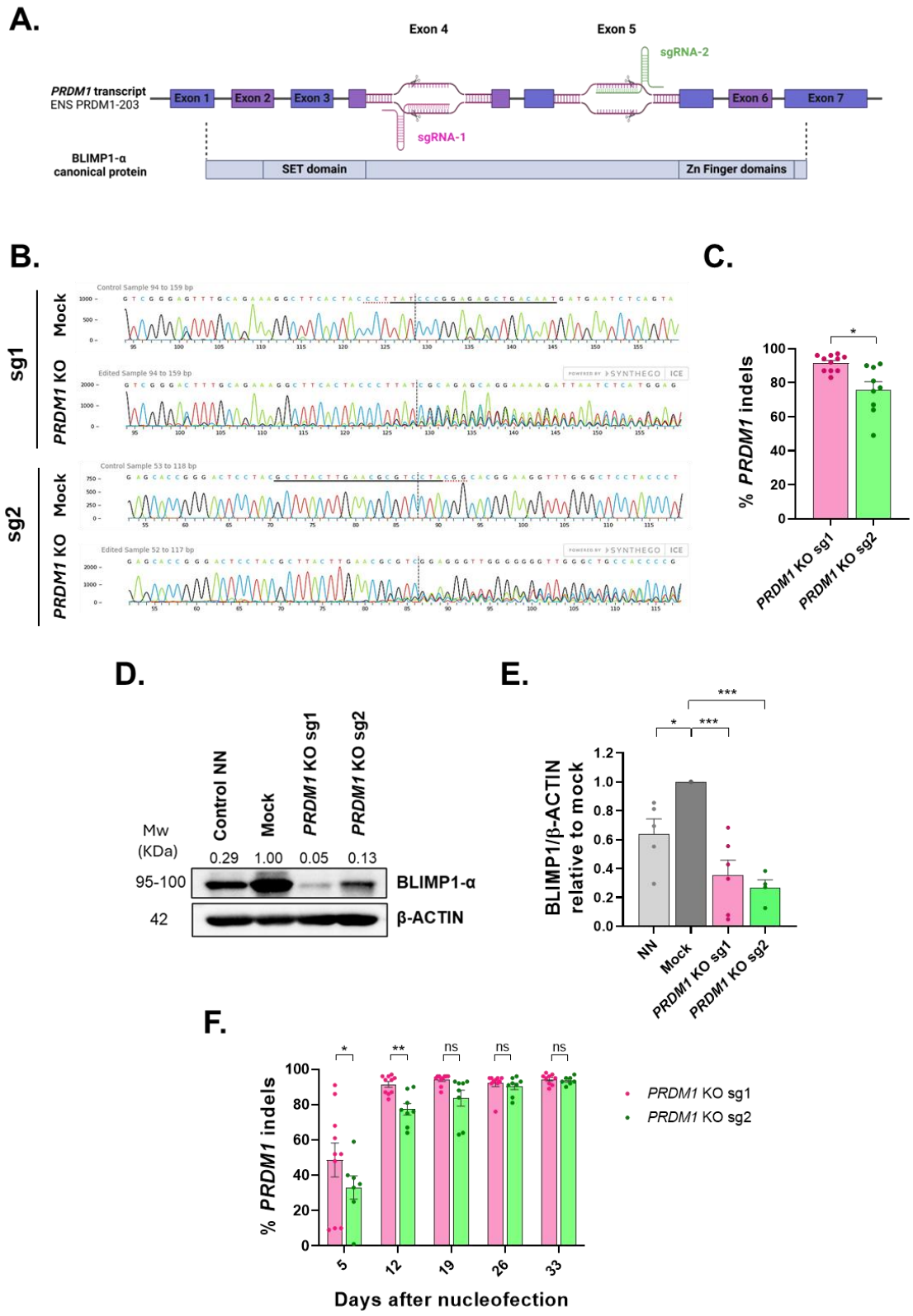

Figure 54. *PRDM1* gene editing in CAR NK cells is highly efficient and increases over time. A. Schematic representation of the selected sgRNAs to target *PRDM1*. **B.** Representative Sanger sequencing chromatograms of *PRDM1* sgRNA on-target sites in mock and edited cells analyzed on day 12 after nucleofection. Nucleotides underlined in black correspond to sgRNA binding site. PAM region is indicated with red dashed underlaying. Vertical dashed lines indicate Cas9 cutting site. **C.** Percentage of indels in *PRDM1* sgRNA on-target sites analyzed by ICE on day 12 after nucleofection (n=11 for sgRNA-1, n=9 for

sgRNA-2). **D.** Representative western blot analysis of BLIMP1 expression in non-nucleofected (NN), mock, and *PRDM1* KO CAR NK cell lysates collected on day 12 after nucleofection. Numbers indicate ratio of BLIMP1/β-ACTIN expression relative to mock control. Molecular weights (Mw) for each protein are indicated on the left. **E.** Quantification of relative BLIMP1 expression in NN and *PRDM1* KO CAR NK cells compared to mock control (n=6 for sgRNA-1; n=4 for sgRNA-2). **F.** Percentage of indels in *PRDM1* sgRNA on-target sites analyzed by ICE at different days after nucleofection (n=10 for sgRNA-1, n=8 for sgRNA-2). sg1: sgRNA-1; sg2: sgRNA-2. Means ± SEM are shown. *p<0.05; **p<0.01; ***p<0.001; ns: no significance

2.2. *PRDM1* disruption confers a higher proliferative capacity to CAR NK cells

The principal objective of knocking-out *PRDM1* was to enhance the proliferative potential of CAR NK cells. Hence, *in vitro* expansion of *PRDM1* KO CAR CB NK cells was analyzed by cell counting. Importantly, *PRDM1* disruption boosted CAR NK culture cell growth. After 33 days following nucleofection, *PRDM1* KO CAR NK cells exhibited a 16.2-fold and 10-fold increased expansion with sgRNA-1 and sgRNA-2 respectively, compared to mock peers (**Figure 55**).

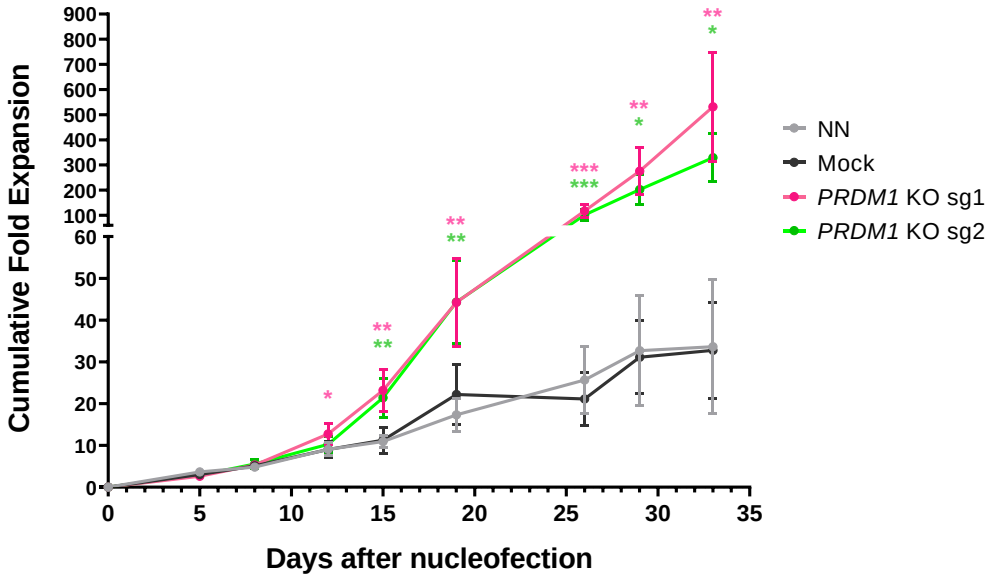

Figure 55. *PRDM1* KO CAR NK cells exhibit higher *in vitro* expansion compared to mock cells. Cumulative *in vitro* fold expansion of non-nucleofected (NN), mock, and *PRDM1* KO CAR NK cells monitored at different times after nucleofection. sg1: sgRNA-1; sg2: sgRNA-2. Means ± SEM are shown (n=12). Statistical analysis shows differences with respect to mock CAR NK cells. *p<0.05; **p<0.01; ***p<0.001.

Proliferative potential of *PRDM1* KO CAR NK cells was measured through two different assays. First, we quantified the percentage of cells that were in the S, G2, and M cell cycle phases. From day 19 forward after nucleofection, the percentage of cells in S-G2-M phase was higher in both *PRDM1* KO cultures compared to mock control cells (**Figure 56A, 56B**). To confirm cycling state of these cells, Ki-67 expression was analyzed in parallel as a direct marker of proliferation. In line with cell cycle analysis, although no differences were detected in Ki-67 expression 12 days after

nucleofection, from day 19 forward, percentage of proliferative cells was higher in both *PRDM1* KO CAR NK cells (58.2 ± 7.1% Ki-67^{+} cells for sgRNA-1 and 54.4 ± 10.9% for sgRNA-2 at day 19 after nucleofection) in contrast to mock CAR NK cells (25.1 ± 5.9%) (**Figure 56C, 56D**). Remarkably, although the proportion of proliferative cells remained higher compared to mock control at different time points, percentage of Ki-67^{+} cells in *PRDM1* KO cell cultures also declined over time suggesting that proliferative advantage was limited in time.

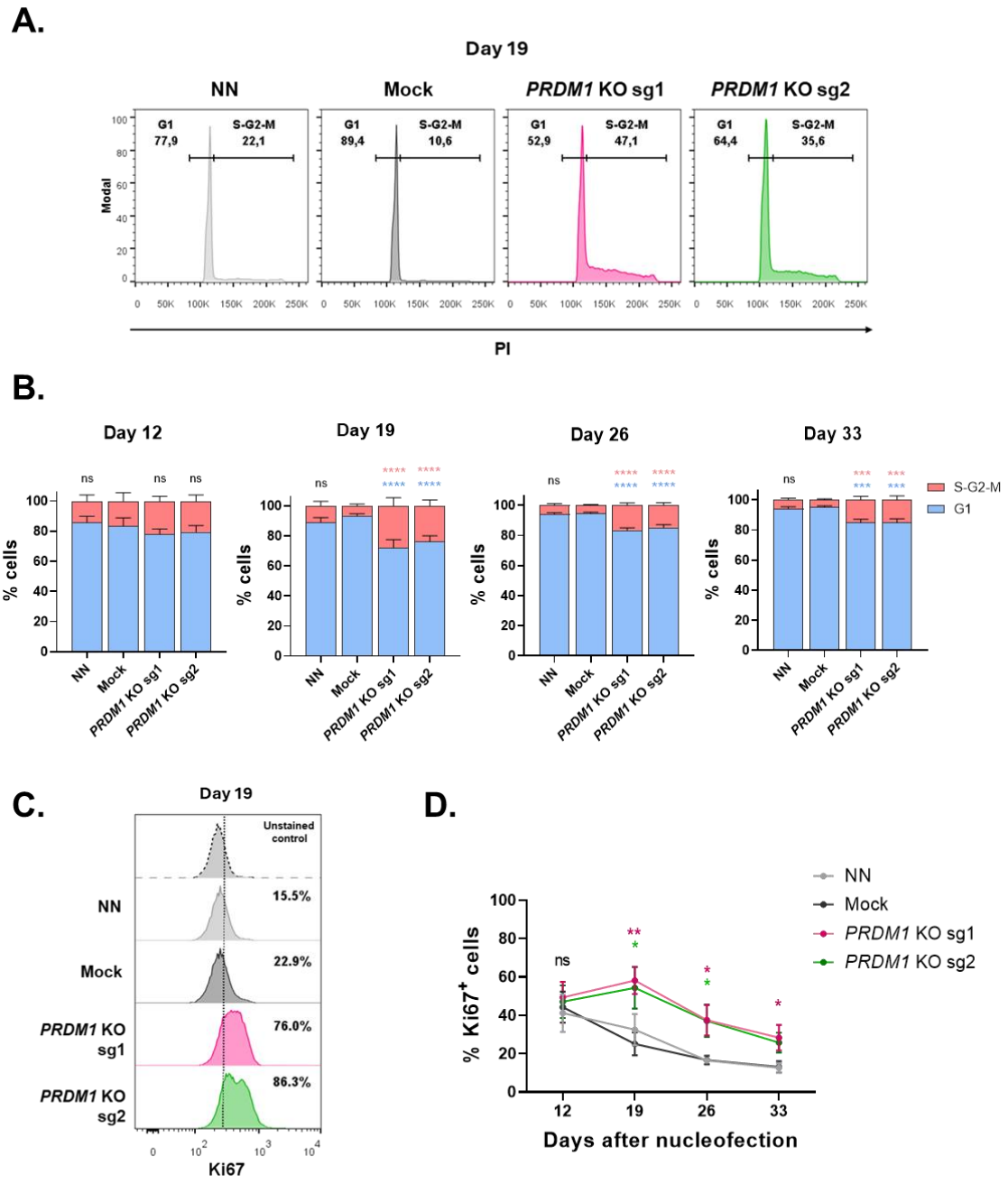

Figure 56. *PRDM1* KO CAR NK cells have increased proliferative potential compared to mock CAR NK cells. A. Representative cell cycle flow cytometry histograms of propidium iodide-stained non-nucleofected (NN), mock, and *PRDM1* KO CAR NK cells analyzed on day 19 after nucleofection. **B.** Proportion of cells in S-G2-M and G1 phases in NN, mock, and *PRDM1* KO CAR NK cells analyzed at different

times after nucleofection. **C.** Representative flow cytometry histogram of Ki-67 staining of NN, mock, and *PRDM1* KO CAR NK cells analyzed on day 19 after nucleofection. The percentage of Ki-67$^+$ cells is indicated on plot. **D.** Percentage of Ki-67$^+$ cells in NN, mock, and *PRDM1* KO cell cultures analyzed at different times after nucleofection. sg1: sgRNA-1; sg2: sgRNA-2. Means ± SEM are shown (n=6). All statistical analyses show differences with respect to mock CAR NK cells. *p<0.05; **p<0.01; ***p<0.001, ****p<0.0001; ns: no significance.

BLIMP1 has also been described as an apoptosis inductor in NK cells. Therefore, we sought to investigate if *PRDM1* disruption may reduce apoptosis in CAR NK cells. With that aim, viability of cell cultures and apoptosis was monitored at different time points by flow cytometry. *PRDM1* ablation did not impact on the cell culture viability. The percentage of alive cells analyzed 12 days after nucleofection was 79.7 ± 5.1% and 77.4 ± 5.9% for *PRDM1* KO cells edited with sgRNA-1 and sgRNA-2, respectively, while mock cells had a viability of 80.8 ± 3.9%. This high viability was maintained over time without showing any differences between edited and mock cells (**Figure 57A**). Accordingly, when percentage of apoptosis was measured through annexin V staining, no differences were found between *PRDM1* KO and mock CAR NK cells (**Figure 57B**).

Altogether, these results demonstrated that the increased *in vitro* expansion capacity of *PRDM1* KO cells is due to a higher proliferative capacity rather than reduced apoptosis.

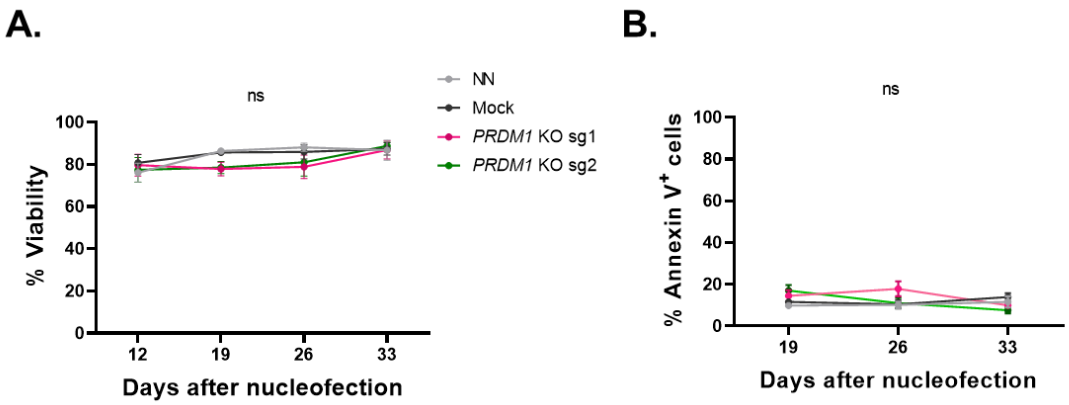

Figure 57. *PRDM1* knock-out does not affect CAR NK cell viability. A. Percentage of alive cells in non-nucleofected (NN), mock, and *PRDM1* KO CAR NK cultures measured by flow cytometry at different times after nucleofection (n=6) **B.** Percentage of apoptotic cells in non-nucleofected (NN), mock, and *PRDM1* KO CAR NK cultures analyzed by Annexin-V flow cytometry staining at different times after nucleofection (n=8 for sgRNA-1; n=5 for sgRNA-2). Statistical analyses show differences with respect to mock CAR NK cells. sg1: sgRNA-1; sg2: sgRNA-2. Means ± SEM are shown. ns: no significance.

2.3. *PRDM1* KO CAR NK cells exhibited delayed senescence induction

BLIMP1 has been reported as a master regulator of T cell terminal differentiation being upregulated in KLRG1$^+$ senescent CD8$^+$ T cells[534,535]. In this context, we wondered if *PRDM1* knock-out in CAR NK cells would delay replicative senescence as well as conferring higher

proliferative potential to the cells. Therefore, we measured SA-β-gal activity in *PRDM1* KO CAR NK cells by flow cytometry as previously described. Non-nucleofected and mock CAR NK cells showed increased SA-β-gal activity over time. Regarding *PRDM1* KO cell cultures, β-gal activity was decreased with sgRNA-1 (31 ± 3.6% $DDAO^+$ cells) compared to mock control (42.2 ± 3.8% $DDAO^+$ cells) after 26 days from nucleofection. However, when it was monitored one week later, no significant differences were found between conditions (**Figure 58**). These observations suggested that *PRDM1* disruption delayed but did not hamper senescence induction in CAR NK effector cells.

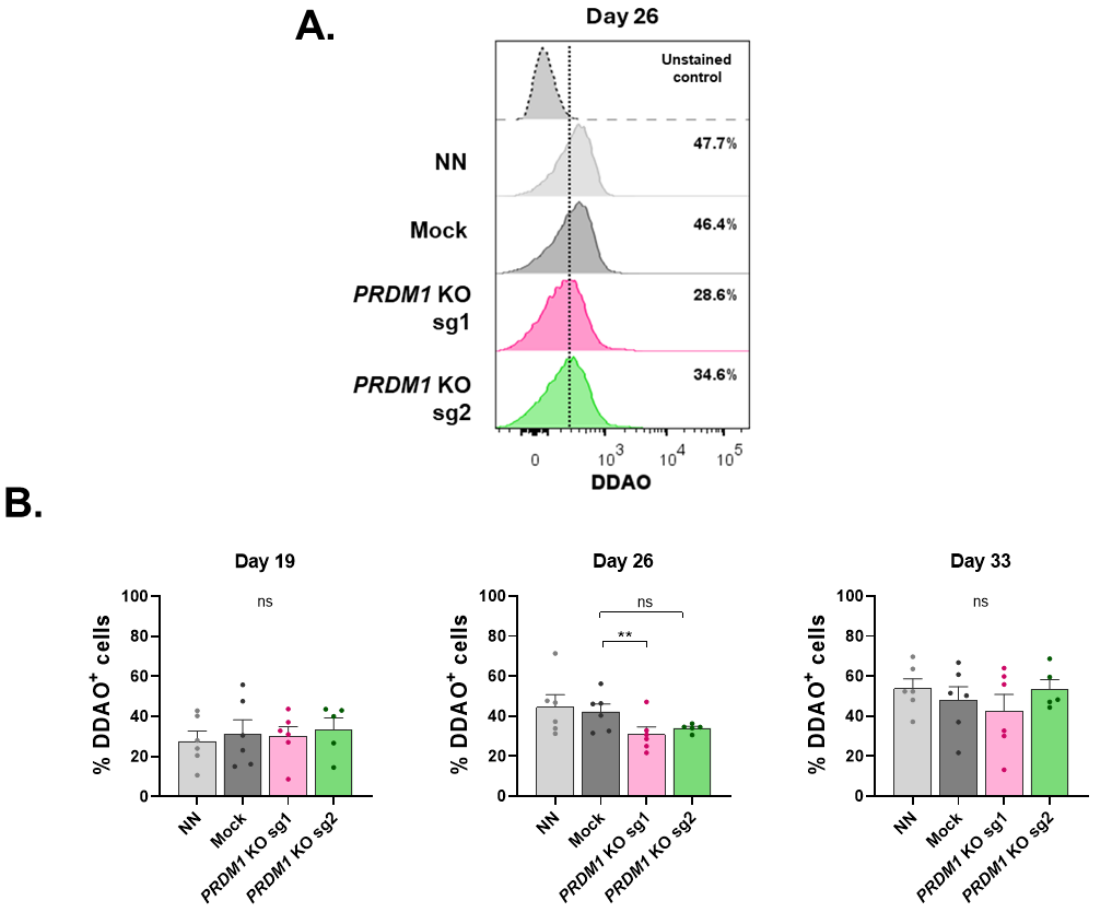

Figure 58. *PRDM1* disruption delays senescence induction in CAR NK cells. A. Representative flow cytometry histograms measuring of SA-β-gal activity in non-nucleofected (NN), mock, and *PRDM1* KO CAR NK cells 26 days after nucleofection. Percentage of $DDAO^+$ cells is indicated on plot. **B.** Percentage of cells showing SA-β-gal activity in NN, mock, and *PRDM1* KO CAR NK cells analyzed by flow cytometry at different times after nucleofection. sg1: sgRNA-1; sg2: sgRNA-2. Means ± SEM are shown (n=6 for sgRNA-1; n=5 for sgRNA-2). Statistical analyses show differences with respect to mock CAR NK cells. **p<0.01; ns: no significance.

2.4. CAR expression of *PRDM1* KO CAR NK cells increases over time

As performed with 2KO CAR NK cells, CAR transduction was analyzed in NK effectors 12 days after nucleofection. CAR expression was higher in CAR NK cells nucleofected with *PRDM1* sgRNA-1 (28.1 ± 4.2% CAR⁺ NK cells) in comparison with mock cells (20.2 ± 2.3% CAR⁺ NK cells). However, we did not observe this difference with *PRDM1* sgRNA-2 (24.7 ± 3.5% CAR⁺ NK cells) (**Figure 59A**). Additionally, CAR expression was monitored over time in a few donors. Interestingly, as *PRDM1* KO cells expanded, the percentage of CAR⁺ cells increased, independently of the sgRNA used. In contrast, the transduction of mock cells remained stable over time, suggesting that *PRDM1* KO CAR⁺ cells acquired a selective advantage *in vitro* (**Figure 59B, 59C**).

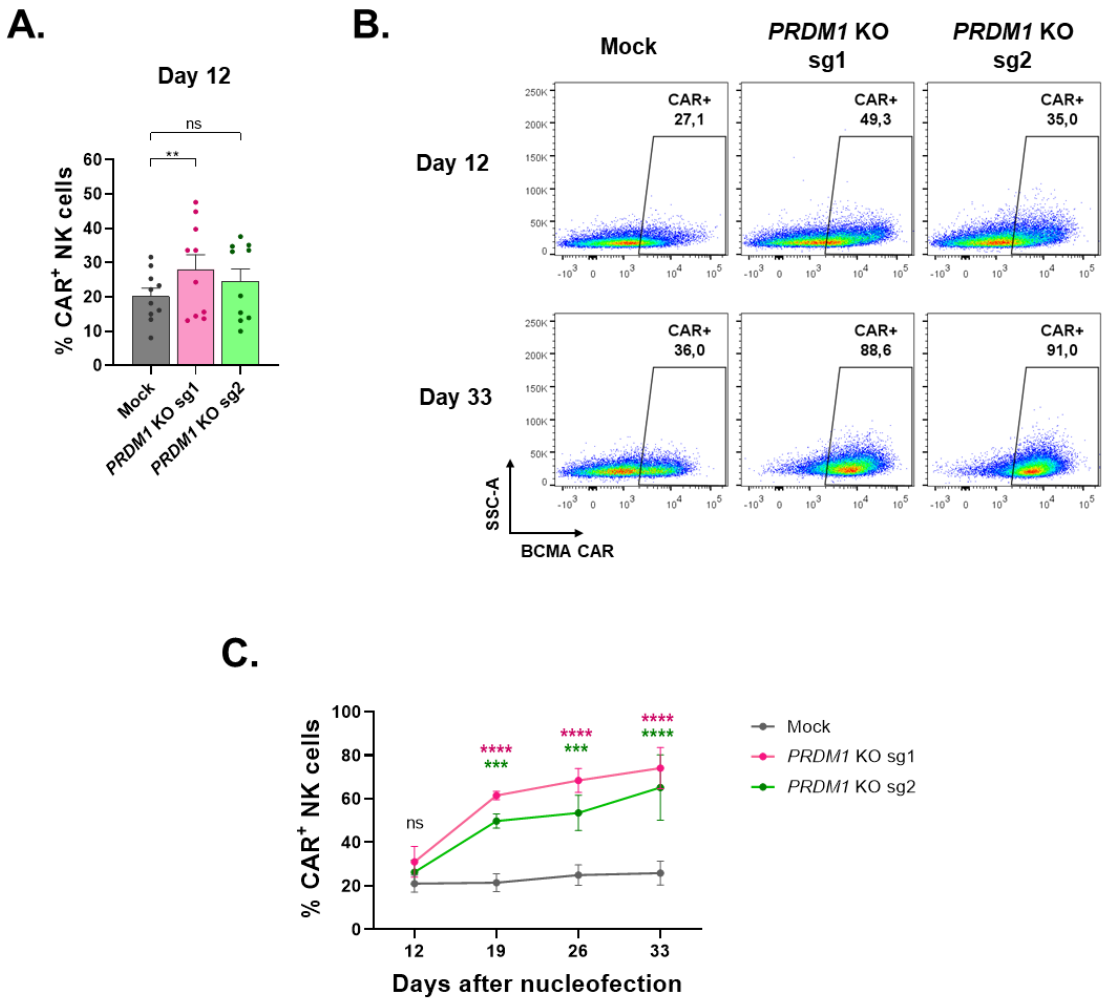

Figure 59. CAR expression in NK cells increases over time after *PRDM1* disruption. A. Percentage of CAR⁺ cells in mock and *PRDM1* KO cell cultures analyzed by flow cytometry 12 days after nucleofection (n=10). **B.** Representative flow cytometry dot plots of CAR expression of mock and *PRDM1* KO CAR NK cells analyzed on days 12 and 33 after nucleofection. Numbers indicate percentage of cells in CAR⁺ gate. **C.** Percentage of CAR⁺ NK cells in mock and *PRDM1* KO NK cell cultures analyzed at different times after nucleofection (n=5). Statistical analyses show differences with respect to mock CAR NK cells. sg1: sgRNA-1; sg2: sgRNA-2. Means ± SEM are shown. **p<0.01; ***p<0.001; ****p<0.0001; ns: no significance.

2.5. *PRDM1* disruption induces immunophenotypic changes in CAR NK cells

To further characterize *PRDM1* KO CAR NK cell immunophenotype, CD16 expression was monitored by flow cytometry. Although the percentage of cytotoxic NK cells was similar in both *PRDM1* KO CAR and mock CAR NK cells at different times in culture (**Figure 60A, 60B**), CD16 RFI was lower in CAR NK cells nucleofected with sgRNA-1 at days 12 and 19 after nucleofection (**Figure 60C**). The same tendency was observed with sgRNA-2 although it was not statistically significant. Interestingly, from day 26 after nucleofection, CD16 expression in *PRDM1* KO CAR NK cells equaled mock control cells.

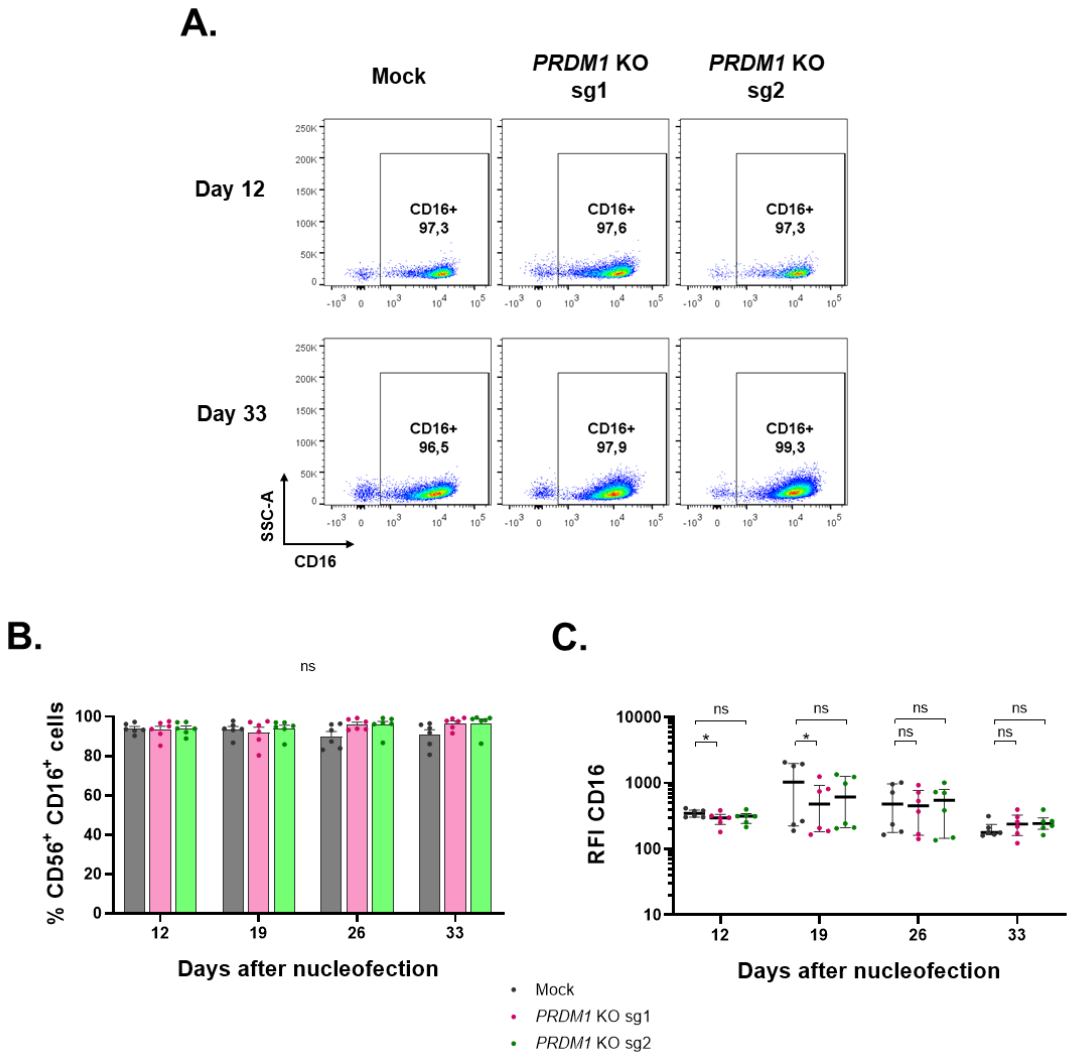

Figure 60. CD16 expression in CAR NK cells is temporarily decreased after *PRDM1* knock-out. A. Representative flow cytometry dot plots of CD16 expression in mock and *PRDM1* KO CAR NK cells analyzed on days 12 and 33 after nucleofection. Numbers indicate percentage of cells in $CD16^+$ gate. **B.** Percentage of cytotoxic $CD16^+$ NK cells in mock and *PRDM1* KO NK cell cultures analyzed by flow cytometry at different times after nucleofection. Means ± SEM are shown (n=6). **C.** Relative fluorescence intensity (RFI) of CD16 in mock and *PRDM1* KO CAR NK cells analyzed by flow cytometry at different times after nucleofection. Medians and IQR are shown (n=6). Data in C is presented in logarithmic scale. sg1: sgRNA-1; sg2: sgRNA-2. All statistical analyses show differences with respect to mock CAR NK cells. *p<0.05; ns: no significance.

Besides CD16, other surface NK receptors were analyzed on day 19 after nucleofection. We found that CD25 expression was higher in *PRDM1* KO CAR NK cells generated with both sgRNAs compared to mock cells. Regarding activating receptors, NKp30 and NKp44 were downregulated in *PRDM1* KO CAR NK cells while DNAM-1 was upregulated. Interestingly, expression of both NKG2A and TGFBR2 inhibitory receptors was reduced after *PRDM1* ablation (**Figure 61**).

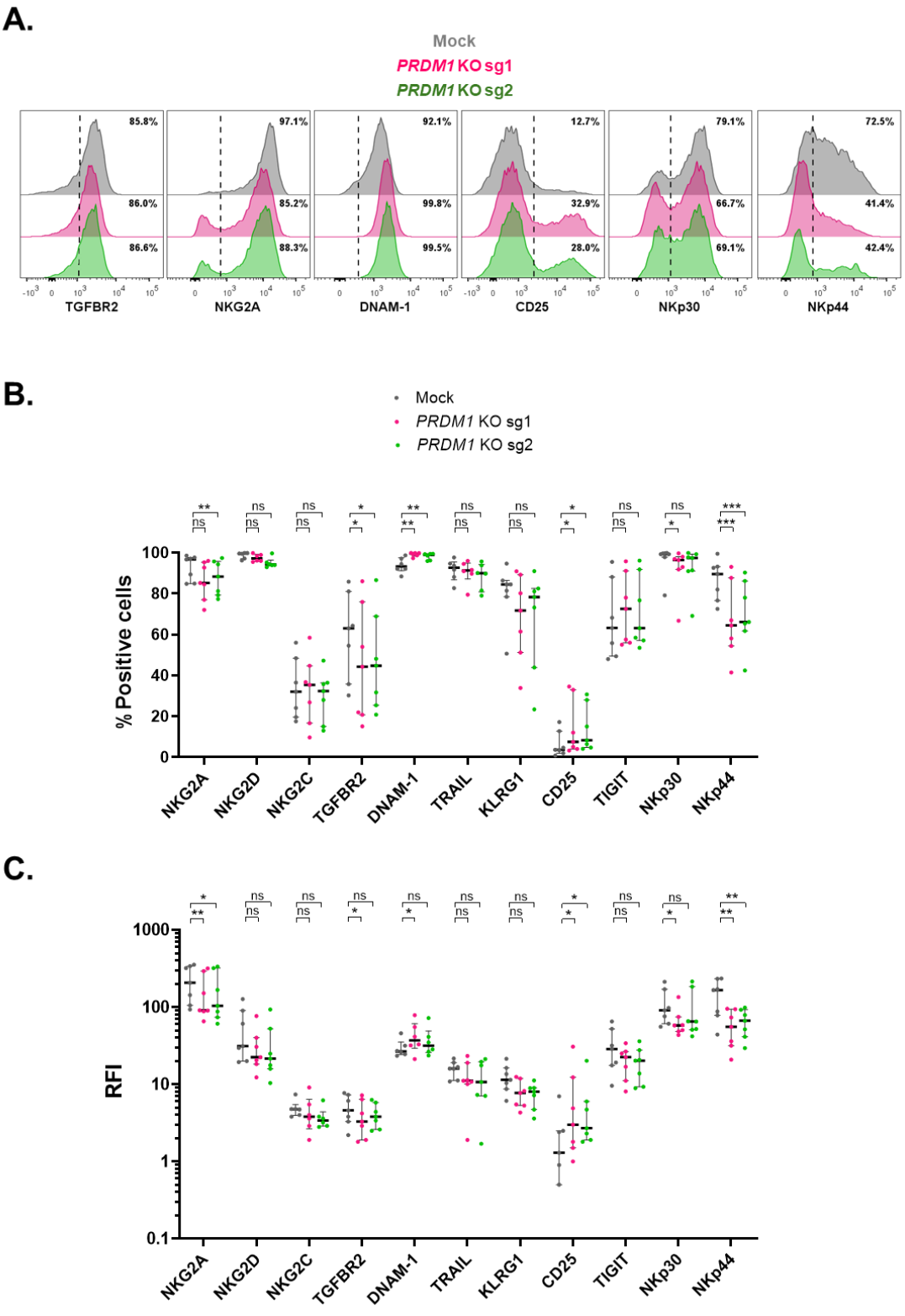

Figure 61. *PRDM1* disruption induces immunophenotypic changes in CAR NK cells. A. Representative flow cytometry histograms of the expression of different NK receptors in mock and *PRDM1* KO CAR NK cells. Percentages indicate the proportion of cells expressing each receptor. **B.** Percentage of positive cells for each receptor in mock and *PRDM1* KO CAR NK cells analyzed by flow cytometry 19 days after nucleofection. **C.** Relative fluorescence intensity (RFI) of each receptor in mock and *PRDM1* KO CAR NK cells analyzed by flow cytometry 19 days after nucleofection. Data in C is presented in logarithmic scale. sg1: sgRNA-1; sg2: sgRNA-2. Medians and IQR are shown (n=6). Statistical analyses show differences with respect to mock CAR NK cells. *p<0.05; **p<0.01; ***p<0.001, ns: no significance.

2.6. *PRDM1* knock-out modifies transcriptomic profile of CAR NK cells

As BLIMP1 is considered a master transcriptional regulator of different pathways, we explored in more detail expression differences between non-edited and *PRDM1* KO CAR NK cells. With that aim, RNA-seq transcriptomic analysis was performed in sorted CAR NK cells from mock and *PRDM1* KO cell cultures from 3 independent donors. Similarly to 2KO CAR transcriptomic analysis, donor-derived variations were corrected before differential gene expression analysis. A total of 244 genes were differentially expressed between *PRDM1* KO and mock CAR NK cells (**Figure 62**). **Table 16** shows some of the genes downregulated and upregulated in *PRDM1* KO CAR NK cells compared to mock control. Among them, we observed upregulation of genes associated with proliferation, survival, and growth (*RALB, CDCA7, JUN, CCNA1, BCAT1, MYB, NCAM2, FGFR1, NKD2,* and *IGFBP4*) as well as implicated in NK cell migration (*CD4, SELL,* and *CCR7*). We also found overexpression of some genes related to IFN-γ and TNF-α signaling (*TNFRSF8, TNFRSF11A,* and *IRF4*). Besides, *PRDM1* knock-out modified the expression of NK cell receptors at transcriptional level. For example, NK activating receptor genes such as *KLRF2, LILRA2, NCR2,* and *NCR1* were downregulated in *PRDM1* KO CAR NK cells compared to mock control while *CD86* and *TLR4* were upregulated. In addition, both *CEACAM1* and *KLRG1*, which encode for inhibitory NK receptors, were also downmodulated. Regarding cytokine and chemokine signaling, *PRDM1* KO CAR NK cells overexpressed genes such as *LIF, CABLES1, IL13* and *IL7R*. Surprisingly, we also observed upregulation of *PRDM1*. To better understand the biological significance of these expression changes, gene set enrichment analysis (GSEA) was performed using GO and KEGG databases, but we could not find any statistically significative enrichment in NK or immune related pathways.

	ENS entry	Gene name	Log2 Fold Change	Adjusted p
Downregulated	ENSG00000172215	*CXCR6*	-2.578	2.44E-09
	ENSG00000256797	*KLRF2*	-2.545	6.89E-04
	ENSG00000079385	*CEACAM1*	-2.502	3.58E-03
	ENSG00000239998	*LILRA2*	-2.236	1.48E-04
	ENSG00000096264	*NCR2*	-1.888	5.92E-07
	ENSG00000184371	*CSF1*	-1.747	1.10E-02
	ENSG00000139187	*KLRG1*	-1.341	2.74E-02
	ENSG00000104998	*IL27RA*	-0.979	9.83E-03
	ENSG00000189430	*NCR1*	-0.869	1.69E-02
Upregulated	ENSG00000144118	*RALB*	0.897	2.17E-02
	ENSG00000114737	*CISH*	1.042	6.67E-03
	ENSG00000114013	*CD86*	1.188	1.17E-03
	ENSG00000144354	*CDCA7*	1.601	7.85E-03
	ENSG00000128342	*LIF*	1.640	4.30E-02
	ENSG00000177606	*JUN*	1.642	4.23E-02
	ENSG00000149212	*SESN3*	1.944	1.51E-02
	ENSG00000120949	*TNFRSF8*	2.579	5.11E-05
	ENSG00000133101	*CCNA1*	2.591	3.74E-03
	ENSG00000060982	*BCAT1*	2.623	2.70E-04
	ENSG00000137265	*IRF4*	2.655	3.58E-03
	ENSG00000106366	*SERPINE1*	2.763	9.58E-04
	ENSG00000134508	*CABLES1*	2.902	1.56E-02
	ENSG00000141655	*TNFRSF11A*	2.967	3.03E-04
	ENSG00000057657	*PRDM1*	3.017	1.02E-14
	ENSG00000118513	*MYB*	3.083	1.66E-02
	ENSG00000010610	*CD4*	3.099	2.33E-03
	ENSG00000154654	*NCAM2*	3.428	2.82E-02
	ENSG00000169194	*IL13*	4.218	3.80E-04
	ENSG00000123685	*BATF3*	4.356	2.38E-10
	ENSG00000077782	*FGFR1*	5.159	5.76E-26
	ENSG00000145506	*NKD2*	5.738	4.71E-02
	ENSG00000188404	*SELL*	5.739	7.25E-25
	ENSG00000227145	*IL21-AS1*	5.850	2.33E-02
	ENSG00000136869	*TLR4*	6.185	4.34E-03
	ENSG00000126353	*CCR7*	6.473	1.07E-04
	ENSG00000141753	*IGFBP4*	7.522	3.80E-04
	ENSG00000168685	*IL7R*	8.354	1.29E-11

Table 16. List of the most relevant genes differentially expressed in *PRDM1* KO CAR NK cells compared to mock CAR NK cells. Fold change and adjusted p values are indicated for each gene. Ensembl (ENS) entry codes are referred to GRCh38.p14 genome assembly.

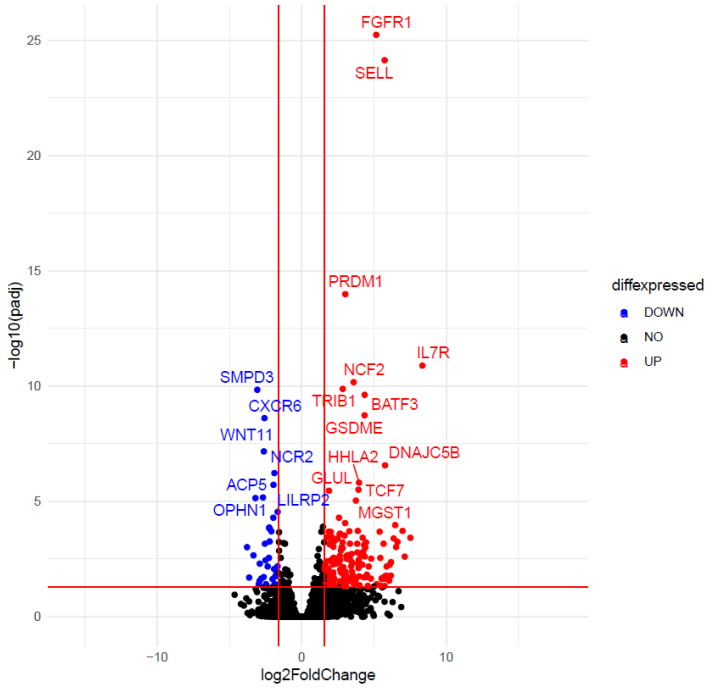

Figure 62. *PRDM1* knock-out induces transcriptomic changes in CAR NK cells. Volcano plot of RNA-seq transcriptomic analysis showing upregulated (red) and downregulated (blue) genes in *PRDM1* KO CAR NK cells compared to mock CAR NK cells. Integrated RNA-seq data obtained from 3 independent NK donors.

2.7. *PRDM1* KO CAR NK cells show the same antitumor efficacy as non-edited CAR NK cells

Although BLIMP1 is not supposed to play a significant role in regulating NK perforin-mediated cytotoxicity[466], we observed that *PRDM1* disruption of this gene downregulates the expression of some important NK cell activating receptors which may compromise NK cell activity. To confirm that *PRDM1* ablation does not negatively impact on CAR NK antitumor efficacy, we analyzed *PRDM1* KO CAR NK cell specific lysis against MM cell lines. Notably, *PRDM1* KO CAR NK cells showed similar killing efficacy as mock peers against U-266, RPMI-8226, MM.1S and XG-1 cell lines at different E:T ratios, corroborating that *PRDM1* disruption does not affect CAR NK antitumor potential (**Figure 63**).

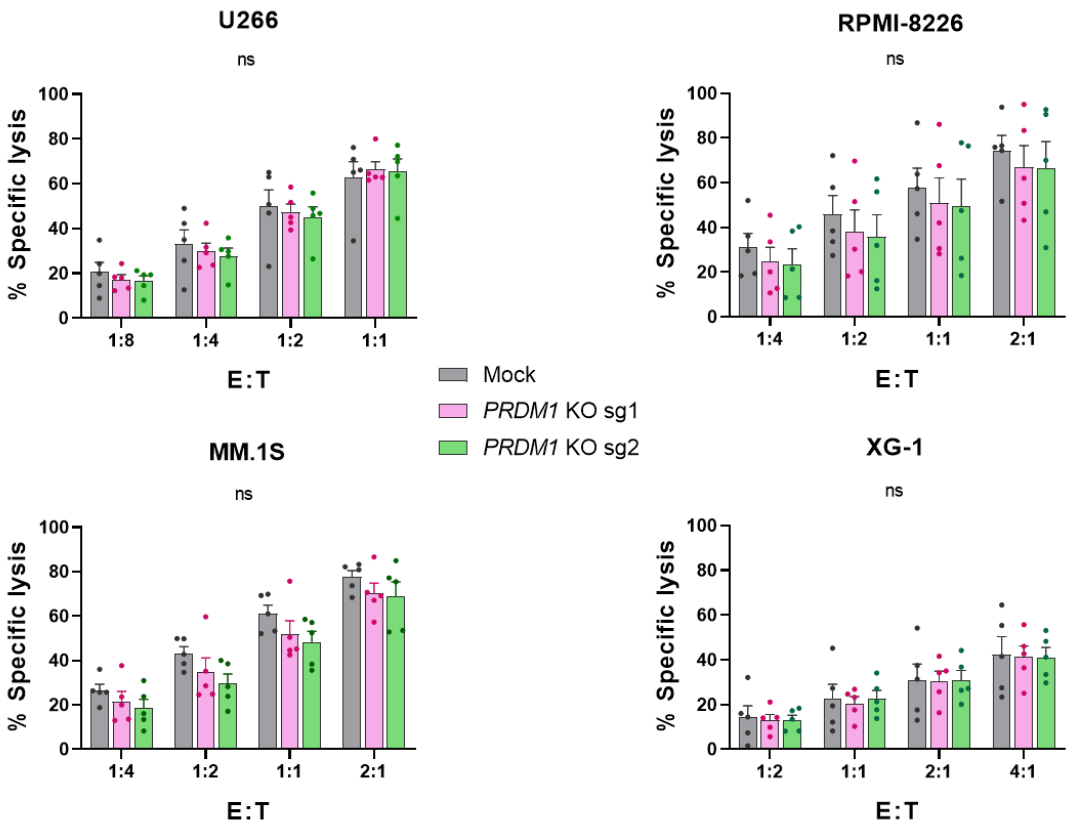

Figure 63. Knock-out of *PRDM1* does not reduce cytotoxic efficacy of CAR NK cells. Specific lysis of mock and *PRDM1* KO CAR NK cells against U-266, RPMI-8226, MM.1S, and XG-1 MM cell lines at different E:T ratios, analyzed by 3h-Calcein release assay (n=5). sg1: sgRNA-1; sg2: sgRNA-2. Means ± SEM are shown. Statistical analysis compares specific lysis of each *PRDM1* KO CAR NK populations in contrast to mock control. ns: no significance.

Despite not affecting direct target killing, BLIMP1 regulates cytokine secretion in NK cells[466]. Therefore, we sought to investigate if *PRDM1* knock-out would affect cytotoxic cytokine or cytolytic protein release profile of CAR NK cell. With this aim, *PRDM1* KO and mock CAR NK cells were cultured alone or with U-266, RPMI-8226, MM.1S, and XG-1 MM cell lines for 24 hours. Supernatants were then collected to measure the release of several cytokines/proteins by a bead-based multiplex flow cytometry assay. We observed that *PRDM1* KO CAR NK cells generated with sgRNA-1 secreted more granzyme A levels in response to MM.1S and XG-1 cells and higher perforin in response to U-266 and RPMI-8226 cell lines, in comparison to mock CAR NK cells. Regarding CAR NK cells nucleofected with *PRDM1* sgRNA-2, only a slight increase in perforin secretion was observed when cultured alone and with RPMI-8226 cells. Concerning the release of other cytotoxic cytokines or cytolytic proteins such as Granzyme B, Granulolysin, TNF-α, sFas, sFasL, and IFN-γ, no differences were found between *PRDM1* KO and mock CAR NK cells either cultured alone or with MM cells (**Figure 64**).

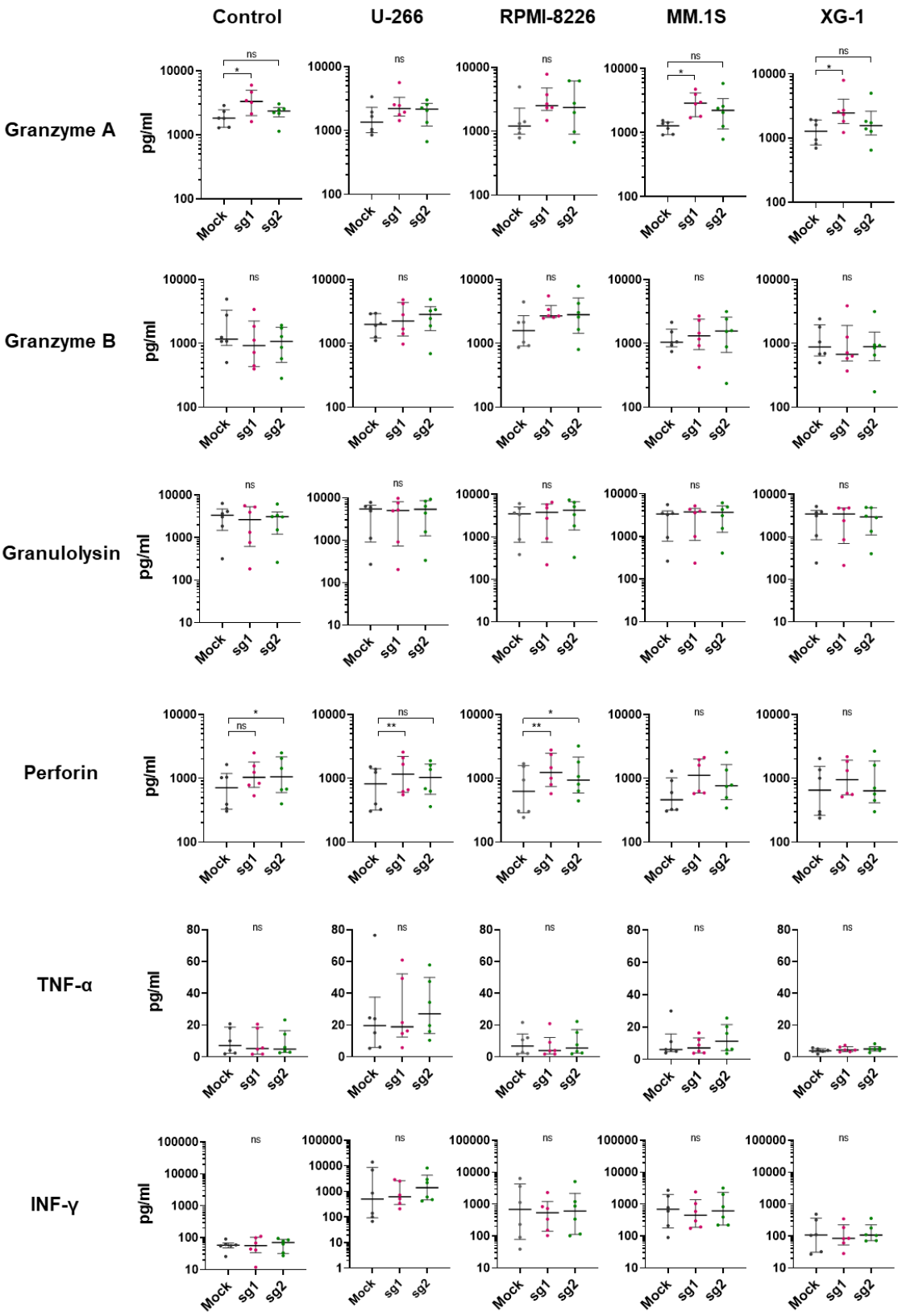
Control
U-266
RPMI-8226
MM.1S
XG-1
Granzyme A
Granzyme B
Granulolysin
Perforin
TNF-α
INF-γ
pg/ml
Mock
sg1
sg2
ns

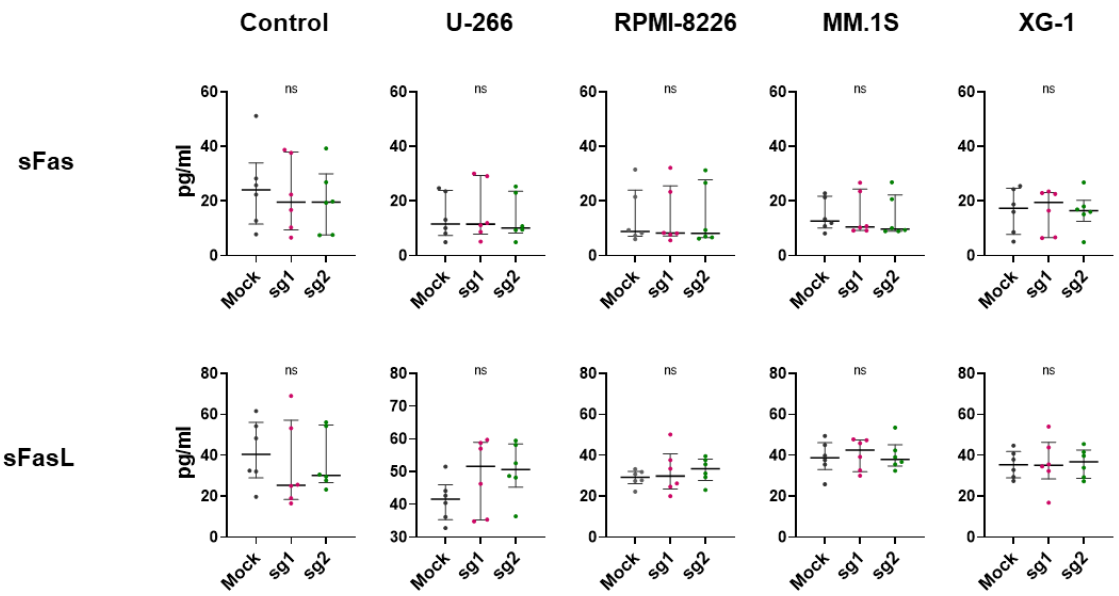

Figure 64. *PRDM1* KO CAR NK cells show similar degranulation profile as mock CAR NK cells. Cytokine quantification in supernatants from mock and *PRDM1* KO CAR NK cells cultured for 24h alone (control) or with U-266, RPMI-8226, MM.1S, and XG-1 MM cell lines at 1:1 E:T ratio, analyzed by LegendPlex bead-based immunoassay. sg1: sgRNA-1; sg2: sgRNA-2. Means ± SEM are shown (n=6). All statistical analyses show differences with respect to mock CAR NK cells. *p<0.05; ns: no significance.

Altogether, these results demonstrate that *PRDM1* ablation enhances the proliferative capacity, delays the senescence induction, and promotes immunophenotypic and transcriptomic changes without modifying the antitumor potency of CAR NK cells.

3. Triple gene editing of *KLRC1*, *TGFBR2*, and *PRDM1* enhances the efficacy of α-BCMA CAR NK cells against MM and increases their expansion *in vitro*.

3.1. Generation of triple KO CAR NK cells by multiplex gene editing is feasible

Once we demonstrated the increased proliferation in CAR NK cells when *PRDM1* was disrupted without compromising the cytotoxic capacity of the cells, we decided to include this target in our multiplex genome editing protocol. For this purpose, CAR NK cells were electroporated simultaneously with RNP complexes targeting *KLRC1*, *TGFBR2,* and *PRDM1* to generate *one-shot* triple KO (*one-shot* 3KO) (**Figure 65A**). Although both *PRDM1* sgRNAs demonstrated high gene editing efficiency, we selected sgRNA-1 for further experiments because it slightly outperformed sgRNA-2 in terms of gene editing and proliferation increase.

NKG2A and TGFBR2 surface expression was analyzed by flow cytometry 12 days after nucleofection. Following this protocol, we efficiently reduced the expression of both receptors in *one-shot* 3KO CAR NK cells compared to non-edited control (19.4 ± 3.0% vs 88.6 ± 5.0% $NKG2A^+$ NK cells and 25.9 ± 4.8% vs 58.8 ± 2.1% $TGFBR2^+$ NK cells) (**Figure 65B-D**). Knock-out efficiencies based on flow cytometry analysis were 78.4 ± 3.0% for NKG2A and 56.6 ± 7.1% for TGFBR2, reaching similar values to those obtained for 2KO CAR NK cells (**Figure 65E**). Without any cell-sorting selection protocol, $NKG2A^-$ $TGFBR2^-$ NK cell population was enriched from 5.8 ± 2.2% to 61.2 ± 3.8% (**Figure 65B, 65F**).

Gene editing was confirmed by Sanger sequencing and ICE analysis (**Figure 65G**). The percentage of indels was 84 ± 3.1% for *KLRC1* and 69.4 ± 6.6% for *TGFBR2*, in accordance with flow cytometry data. *PRDM1* was also efficiently disrupted in *one-shot* 3KO CAR NK cells (74.2 ± 4.4% indels) (**Figure 65H**).

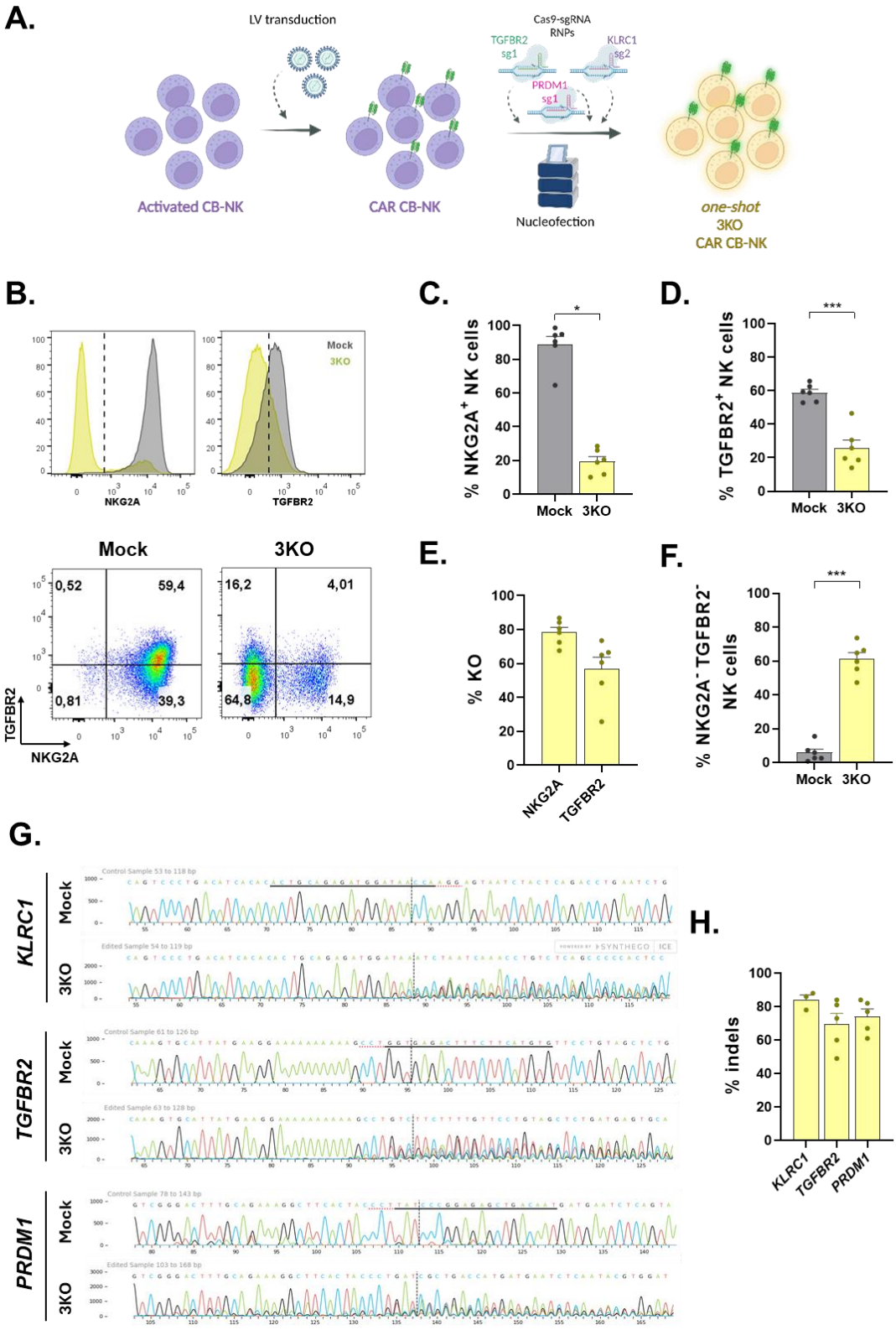

Figure 65. *One-shot* triple gene editing protocol efficiently disrupts *KLRC1*, *TGFBR2,* and *PRDM1* in CAR NK cells. A. Schematic representation of *one-shot* triple gene editing protocol. **B.** Representative flow cytometry histograms (above) and dot plots (below) of NKG2A and TGFBR2 expression in mock and 3KO CAR NK cells analyzed 12 days after nucleofection. Percentage of cells in each gate is indicated. **C and D.** Percentage of NKG2A$^+$ (**C**) and TGFBR2$^+$ (**D**) NK cells in mock and 3KO CAR NK cells analyzed by flow cytometry 12 days after nucleofection (n=6). **E.** NKG2A and TGFBR2 knock-out efficiencies for 3KO CAR NK cells on day 12 after nucleofection analyzed by flow cytometry (n=6). **F.** Percentage of NKG2A$^-$ TGFBR2$^-$

cells in mock and 3KO CAR NK cells analyzed by flow cytometry 12 days after nucleofection (n=6). **G.** Representative Sanger sequencing chromatograms of on-target sites for *KLRC1, TGFBR2,* and *PRDM1* sgRNAs in mock and 3KO CAR NK cells 12 days after nucleofection. Nucleotides underlined in black correspond to sgRNA binding site. PAM region is indicated with red dashed underlaying. Vertical dashed lines indicate Cas9 cutting site. **H.** Percentage of indels in *KLRC1, TGFBR2, and PRDM1* sgRNA on-target sites in 3KO CAR NK cells analyzed by ICE (n=5). Means ± SEM are shown. *p<0.05; ***p<0.001; ns: no significance.

However, despite achieving good editing efficiencies, disruption of the three target genes reduced the culture viability compared to mock CAR NK cells (73.9 ± 3.9% vs 87.1 ± 0.9%) (**Figure 66A**). Moreover, *PRDM1* knock-out in combination with *KLRC1* and *TGFBR2* did not confer a proliferative advantage to the culture, in contrast to single *PRDM1* ablation (**Figure 66B**).

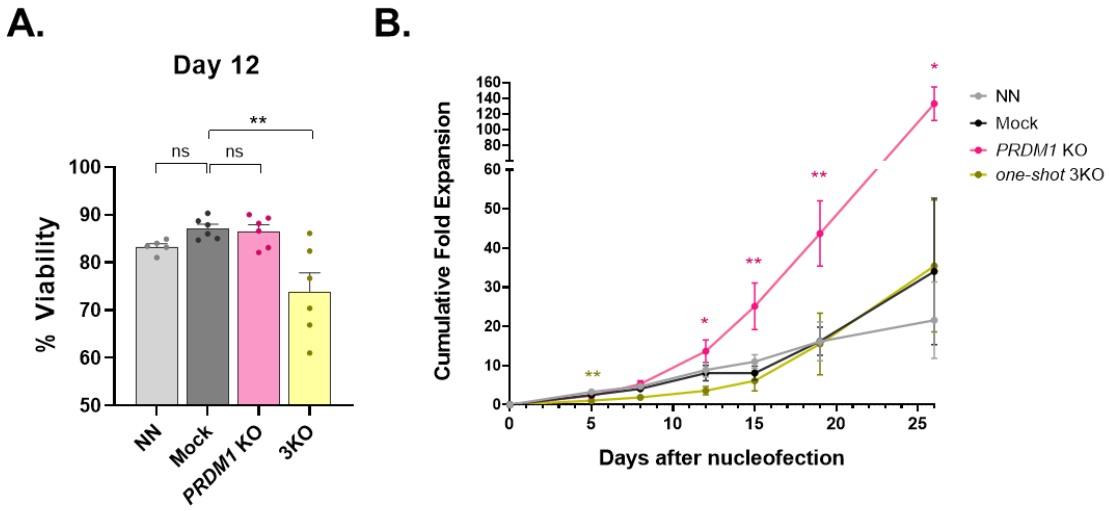

Figure 66. *One-shot* 3KO CAR NK cells do not show increased proliferative potential. A. Percentage of alive cells in non-nucleofected (NN), mock, single *PRDM1* KO, and 3KO CAR NK cultures measured by flow cytometry on day 12 after nucleofection (n=6) **B.** Cumulative *in vitro* fold expansion of non-nucleofected (NN), mock, single *PRDM1* KO, and 3KO CAR NK cells monitored at different times after nucleofection (n=7). Statistical analysis shows differences with respect to mock CAR NK cells. Means ± SEM are shown. *p<0.05; **p<0.01; ns: no significance.

As *one-shot* nucleofection strategy did not turn out to be successful in increasing cell proliferation, we decided to modify our nucleofection protocol for the generation of 3KO CAR NK cells. We proposed firstly to knock-out *PRDM1* in CAR NK cells and one week later, once cells have acquired enhanced proliferative advantage, to disrupt *KLRC1* and *TGFBR2* in a second nucleofection step (**Figure 67A**).

Following this strategy, we generated *sequential* 3KO CAR NK cells. We analyzed gene editing efficiency 11 days after the second nucleofection, which corresponds to 19 days after the first nucleofection. Similarly to *one-shot* protocol, surface expression of both NKG2A and TGFBR2 was reduced in *sequential* 3KO CAR NK cells compared to mock NK cells (15.6 ± 1.7% vs 87.3 ± 3.3%

NKG2A^{+} NK cells and 20.9 ± 3.9% vs 59.1 ± 3.5% TGFBR2^{+} NK cells) (**Figure 67B-D**). Knock-out efficiencies were 82.3 ± 1.6% for NKG2A and 64.6 ± 6.2% for TGFBR2 (**Figure 67E**). The percentage of NKG2A^{-} TGFBR2^{-} NK cells increased up to 67.7 ± 4.1% in *sequential* 3KO CAR NK cells (**Figure 67B, 67F**). Additionally, efficient *PRDM1* disruption was corroborated at protein level by western blot (58.7 ± 5.3% and 79.3 ± 7.4% protein reduction for *PRDM1* KO and *sequential* 3KO CAR NK cells, respectively) (**Figure 67G, 67H**).

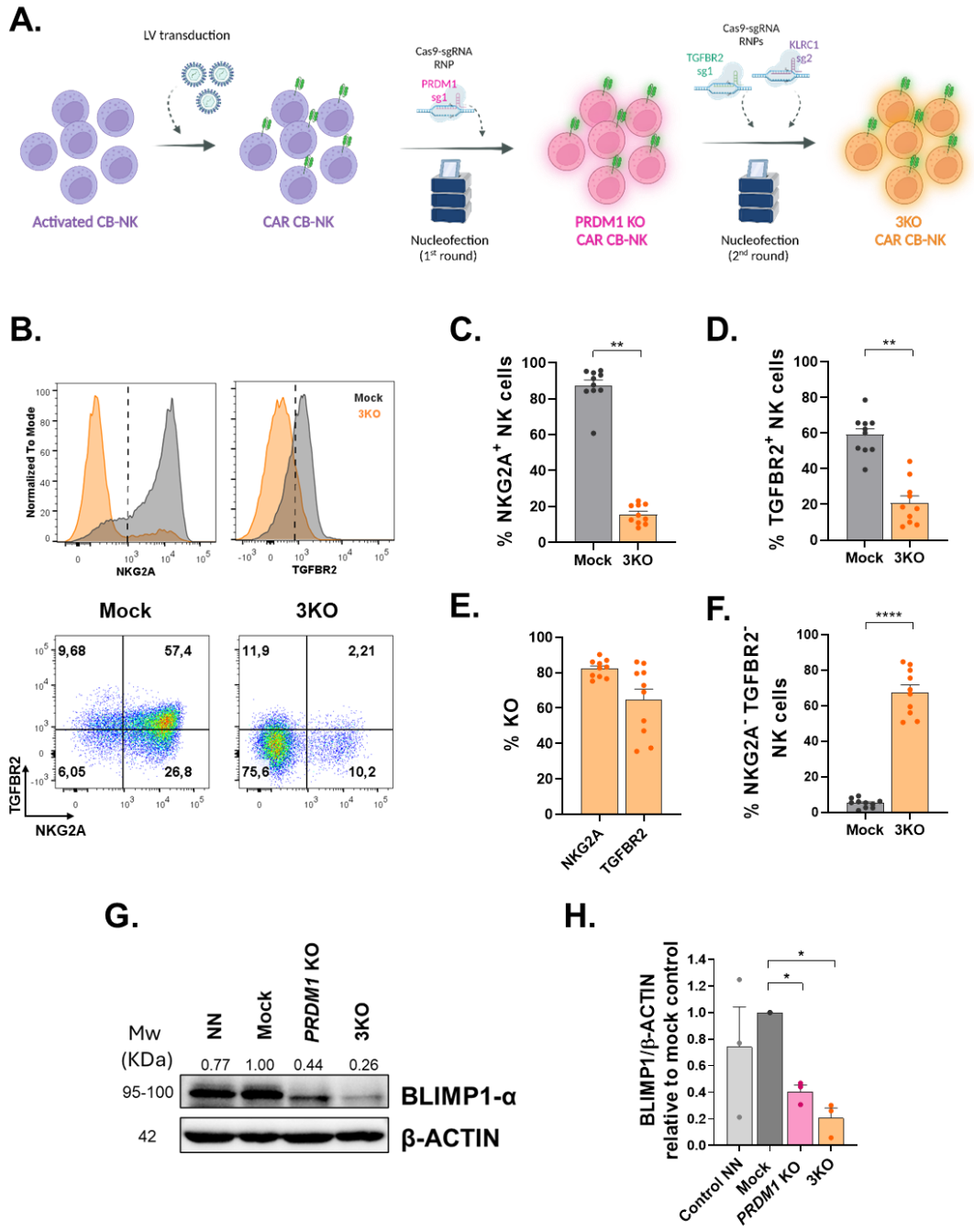

Figure 67. Sequential triple gene editing protocol efficiently reduces expression of NKG2A, TGFBR2, and BLIMP1. A. Schematic representation of sequential triple gene editing protocol. **B.** Representative flow cytometry histograms (above) and dot plots (below) of NKG2A and TGFBR2 expression in mock and 3KO

CAR NK cells analyzed 19 days after first nucleofection. **C and D.** Percentage of NKG2A$^+$ (**C**) and TGFBR2$^+$ (**D**) NK cells in mock and 3KO CAR NK cells analyzed by flow cytometry 19 days after first nucleofection (n=10). **E.** NKG2A and TGFBR2 knock-out efficiencies for 3KO CAR NK cells analyzed by flow cytometry 19 days after first nucleofection (n=10). **F.** Percentage of NKG2A$^-$ TGFBR2$^-$ cells in mock and 3KO CAR NK cells analyzed by flow cytometry 19 days after first nucleofection (n=10). **G.** Representative western blot analysis of BLIMP1 expression in non-nucleofected (NN), mock, single *PRDM1* KO, and 3KO CAR NK cell lysates collected on day 19 after first nucleofection. Numbers indicate ratio of BLIMP1/β-ACTIN expression relativized to mock control. Molecular weights (Mw) for each protein are indicated. **H.** Quantification of relative BLIMP1 expression in NN, single *PRDM1* KO, and 3KO CAR NK cells compared to mock control (n=3). Means ± SEM are shown. *p<0.05; **p<0.01; ****p<0.0001.

Sanger sequencing and ICE analysis confirmed gene editing efficiencies of 89.8 ± 3.4%, 76.2 ± 6.1%, and 89 ± 4.4% for *KLRC1*, *TGFBR2,* and *PRDM1*, respectively (**Figure 68A, 68B**). To validate Sanger sequencing data, deep sequencing analysis of *on-target* sites was performed in four different samples. Percentage of modified reads was 93.4 ± 1.1%, 83.9 ± 3.6%, and 85.33 ± 11.2% for *KLRC1*, *TGFBR2,* and *PRDM1*, respectively, matching with Sanger sequencing analysis (**Figure 68C, 68D**).

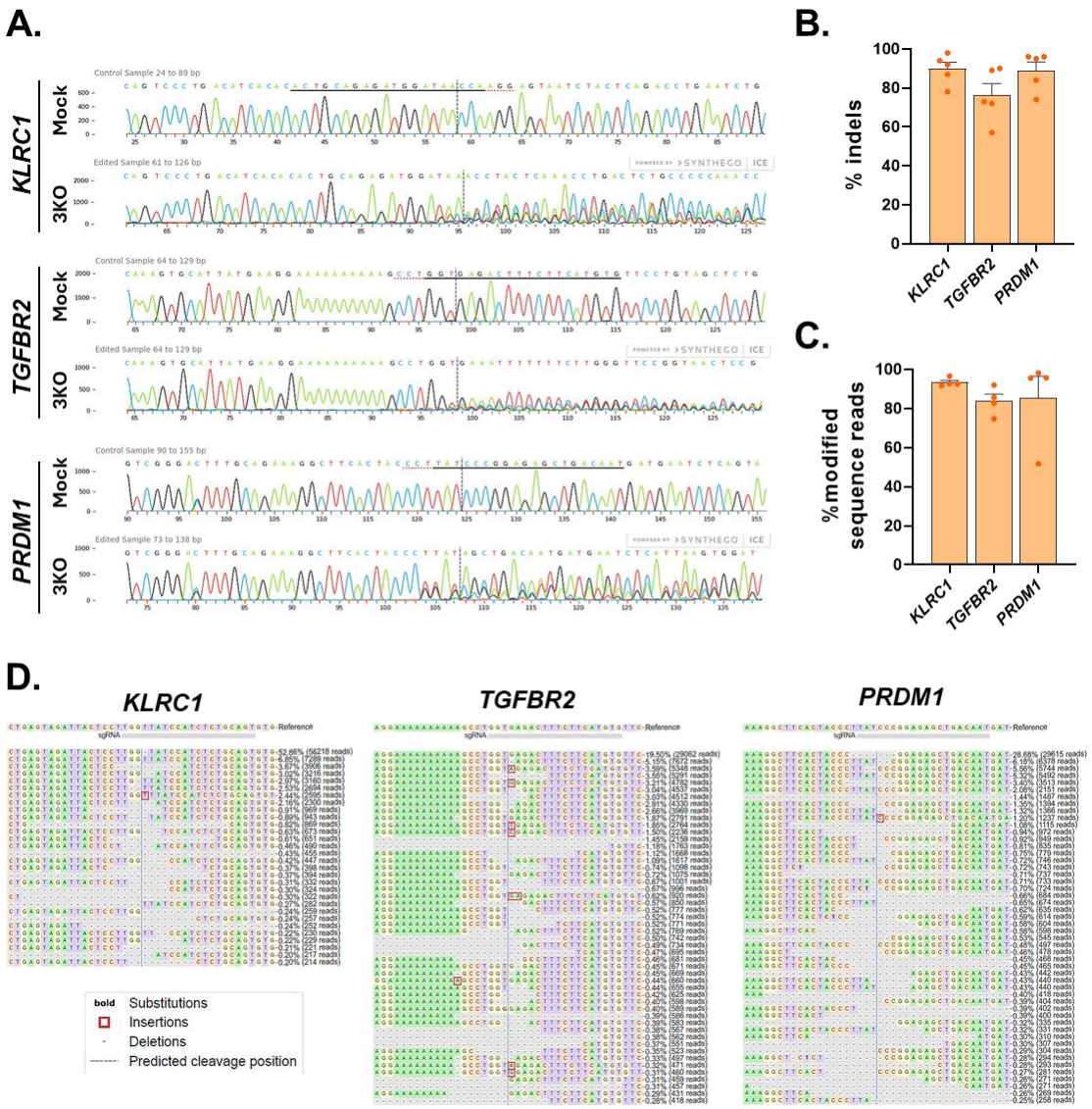

Figure 68. Gene editing efficiencies of sequential triple KO protocol confirmed at the molecular level. A. Representative Sanger sequencing chromatograms of on-target sites for *KLRC1*, *TGFBR2,* and *PRDM1* sgRNAs in mock and 3KO CAR NK cells 19 days after first nucleofection. Nucleotides underlined in black correspond to sgRNA binding site. PAM region is indicated with red dashed underlaying. Vertical dashed lines indicate Cas9 cutting site. **B.** Percentage of indels in *KLRC1*, *TGFBR2,* and *PRDM1* sgRNA on-target sites in 3KO CAR NK cells calculated by ICE (n=5). **C.** Percentage of sequence reads for *KLRC1*, *TGFBR2,* and *PRDM1* that are different to wild type sequences calculated with CRISPResso2 tool from NGS data on day 19 after first nucleofection (n=4). **D.** Representative allele frequency table for *KLRC1*, *TGFBR2,* and *PRDM1* sgRNA on-target sites in 3KO CAR NK cells analyzed on day 19 after first nucleofection. sgRNA target sequence is indicated in gray. Means ± SEM are shown.

After confirming that the three genes had been efficiently targeted, we analyzed viability and proliferative potential of 3KO CAR NK cells. Interestingly, although cell culture viability 19 days after first nucleofection was lower in comparison to non-nucleofected and mock cells (**Figure 69A**), 3KO CAR NK cells generated with two sequential nucleofection steps showed higher *in vitro* expansion, in contrast to mock and *one-shot* 3KO CAR NK cells (**Figure 69B**).

Therefore, we confirmed that our sequential nucleofection protocol was feasible to generate 3KO CAR NK cells with increased expansion capacity.

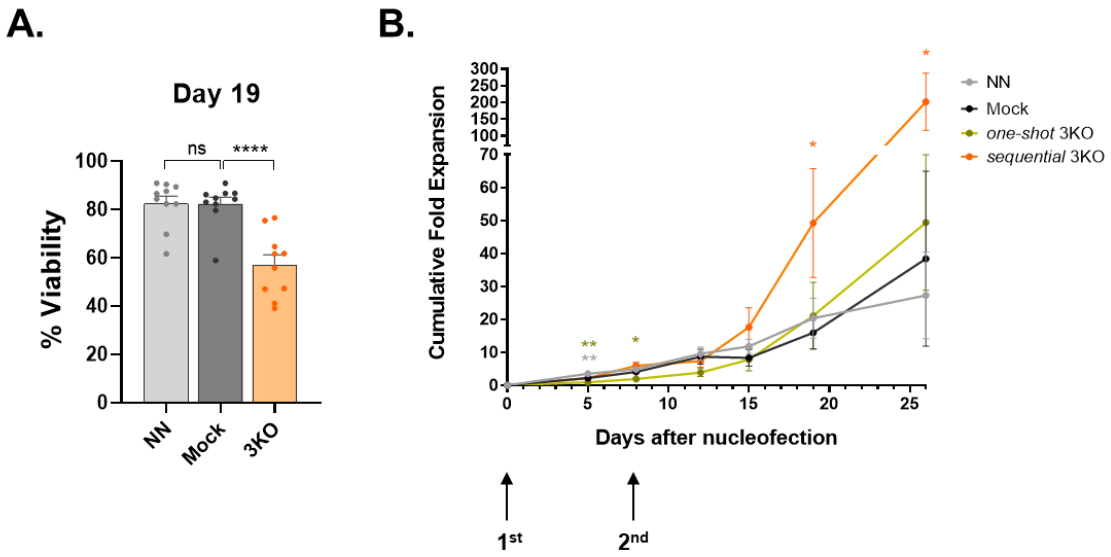

Figure 69. *Sequential* 3KO CAR NK cells have enhanced expansion capacity compared to mock and *one-shot* 3KO CAR NK cells. A. Percentage of alive cells in non-nucleofected (NN), mock, and *sequential* 3KO CAR NK cultures analyzed by flow cytometry on day 19 after first nucleofection (n=10) **B.** Cumulative *in vitro* fold expansion of non-nucleofected (NN), mock, *one-shot* 3KO, and *sequential* 3KO CAR NK cells monitored at different times after nucleofection (n=5). Arrows indicate nucleofection steps for sequential 3KO gene editing protocol. Statistical analyses show differences with respect to mock CAR NK cells. Means ± SEM are shown. *p<0.05; **p<0.01; ****p<0.0001; ns: no significance.

3.2. Triple KO CAR NK cells generated with sequential nucleofection protocol accumulate less DNA damage burden

To understand the growth culture differences between 3KO CAR NK cells generated by *sequential* or *one-shot* protocols as well as with 2KO CAR NK effectors, we indirectly analyzed the DNA damage harbored by each CAR NK effector through the detection of phosphorylated H2AX expression[536]. Preliminary results revealed that elimination of one, two, or three genes using CRISPR/Cas9 increased the levels of DNA damage. However, 3KO CAR NK cells generated with the *sequential* protocol showed reduced phosphorylation of γH2AX compared to 2KO and *one-shot* 3KO CAR NK peers (**Figure 70**). We also analyzed the expression of DNA damage responders p53 and p16. Both 2KO and 3KO cells generated with either protocol had increased expression of p16 compared to non-edited and single KO cells, but this expression was lower in *sequential* 3KO CAR NK cells than in 2KO and *one-shot* 3KO counterparts. Regarding p53, its expression was increased in 2KO and *one-shot* 3KO CAR NK cells compared to mock control. However, *sequential* 3KO cells showed reduced expression of p53 compared to mock cells. Of note, the expression of p53 was higher in mock CAR NK cells with respect to non-nucleofected control. Altogether, these preliminary results suggest that *sequential* 3KO CAR NK cells accumulate less DNA damage and express lower levels of cell cycle controllers than 2KO and 3KO thus giving a possible explanation of expansion capacity variations.

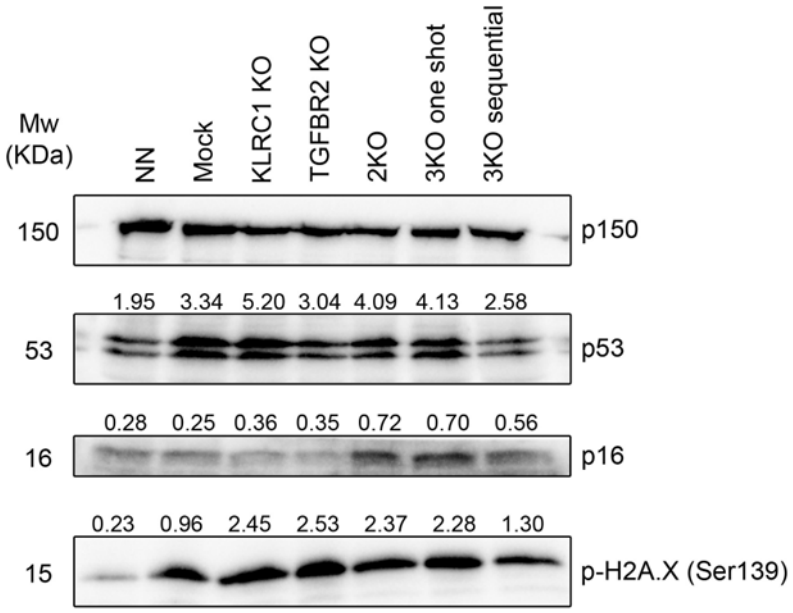

Figure 70. *Sequential* 3KO CAR NK cells show reduced DNA damage compared to 2KO and *one-shot* 3KO CAR NK cells. Western blot analysis of p53, p16, and phosphorylated γH2AX (Ser139) in non-nucleofected (NN), mock, single KO, 2KO, and 3KO CAR NK cell lysates collected on day 19 after first nucleofection. Constitutive expression of p150 was analyzed as protein loading control. Numbers indicate expression of each protein with respect to p150. Molecular weights (Mw) for each protein are indicated (n=1).

3.3. Triple KO CAR NK cells exhibit higher proliferation capacity *in vitro*

After optimizing the protocol to generate 3KO CAR NK cells, we studied the proliferative potential of these cells *in vitro* in comparison with single *PRDM1* KO CAR NK cells. *Sequential* 3KO CAR NK cells (from here on 3KO CAR NK cells) showed similar *in vitro* expansion capacity as single *PRDM1* KO CAR NK cells, reaching a cumulative 10.1-fold expansion in comparison with mock CAR NK cells 33 days after first nucleofection (**Figure 71**). To ascertain the mechanisms underlying the enhanced growth of 3KO CAR NK cell culture, we studied their viability, proliferative capacity, apoptosis, and senescence state at different time points after nucleofection by flow cytometry.

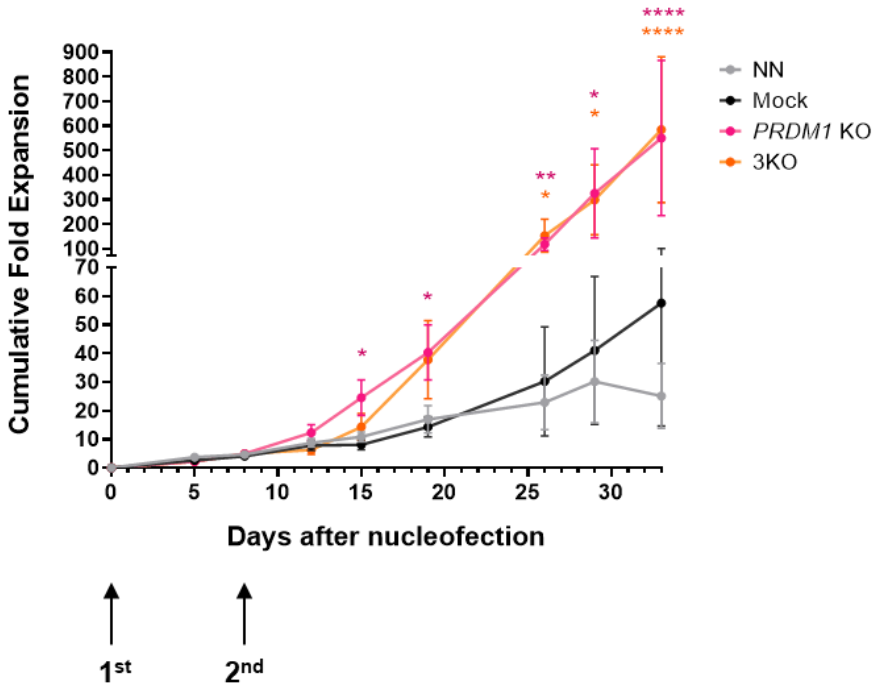

Figure 71. 3KO CAR NK cells have similar expansion capacity as single *PRDM1* KO CAR NK cells. Cumulative *in vitro* fold expansion of non-nucleofected (NN), mock, single *PRDM1* KO, and 3KO CAR NK cells monitored at different times after nucleofection. Arrows indicate nucleofection steps for sequential 3KO gene editing protocol. Means ± SEM are shown (n=7). Statistical analysis shows differences with respect to mock CAR NK cells. *p<0.05; **p<0.01; ****p<0.0001.

As expected, following two nucleofection steps, the viability of 3KO CAR NK cells on day 19 after first nucleofection was reduced (57.2 ± 5.1% alive cells) compared both to mock (82.2 ± 3.1%) and parental single *PRDM1* KO CAR NK cells (77.9 ± 3.3%) (**Figure 72A**). Consitent with this result, the percentage of apoptotic cells in 3KO CAR NK cells was higher than mock cells (**Figure 72B, 72C**). However, the percentage of annexin V^+ cells decreased over time, and, consequently, viability of cell culture was restored (**Figure 72A, 72C**).

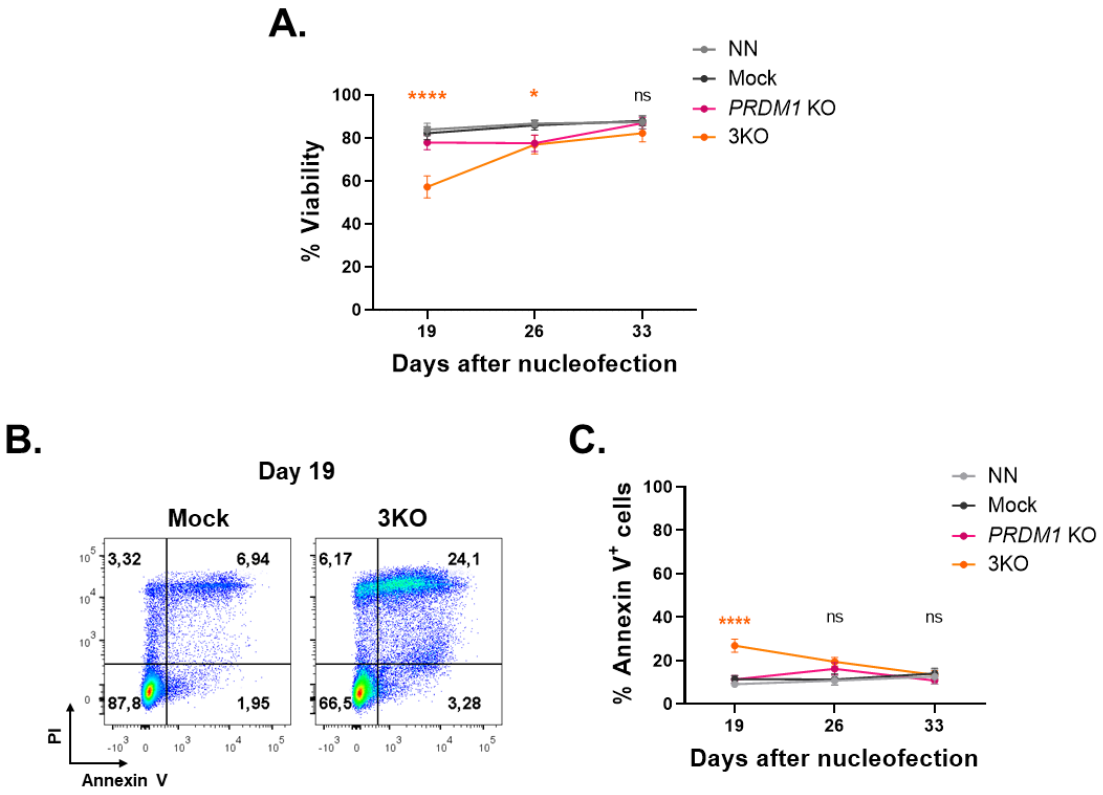

Figure 72. Sequential nucleofection to generate 3KO CAR NK cells does not compromise long-term culture viability. A. Percentage of alive cells in non-nucleofected (NN), mock, single *PRDM1* KO, and 3KO CAR NK cell cultures measured by flow cytometry at different times after nucleofection (n=8) **B.** Representative flow cytometry dot plot of mock and 3KO CAR NK cells stained with Annexin-V and propidium iodide on day 19 after nucleofection. **C.** Percentage of apoptotic cells in NN, mock, single *PRDM1* KO, and 3KO CAR NK cultures analyzed by Annexin-V flow cytometry staining at different times after nucleofection (n=6). Means ± SEM are shown. Statistical analyses show differences with respect to mock CAR NK cells. *p<0.05; ****p<0.0001; ns: no significance.

Besides, the proliferative capacity of 3KO CAR NK cells was measured through cell cycle analysis and Ki-67 expression. From day 19 after first nucleofection, 3KO CAR NK cultures showed higher percentage of cells in S-G2-M compared to mock control, similar to parental *PRDM1* KO CAR NK cells (**Figure 73A, 73B**). In line with these results, the percentage of proliferative cells 19 days after first nucleofection was greater in both 3KO and *PRDM1* KO CAR NK cells (52.4 ± 9.3% and 53.6 ± 8.3% Ki-67$^+$ cells, respectively) compared to mock counterparts (24.9 ± 5.9% Ki-67$^+$ cells). Importantly, as we previously observed in single *PRDM1* KO CAR NK cells (**Figure 56D**), the percentage of Ki-67$^+$ cells in 3KO CAR NK cells, while being superior to mock cells, was reduced two weeks later, suggesting that the proliferative potential is enhanced but not unlimited (**Figure 73C, 73D**).

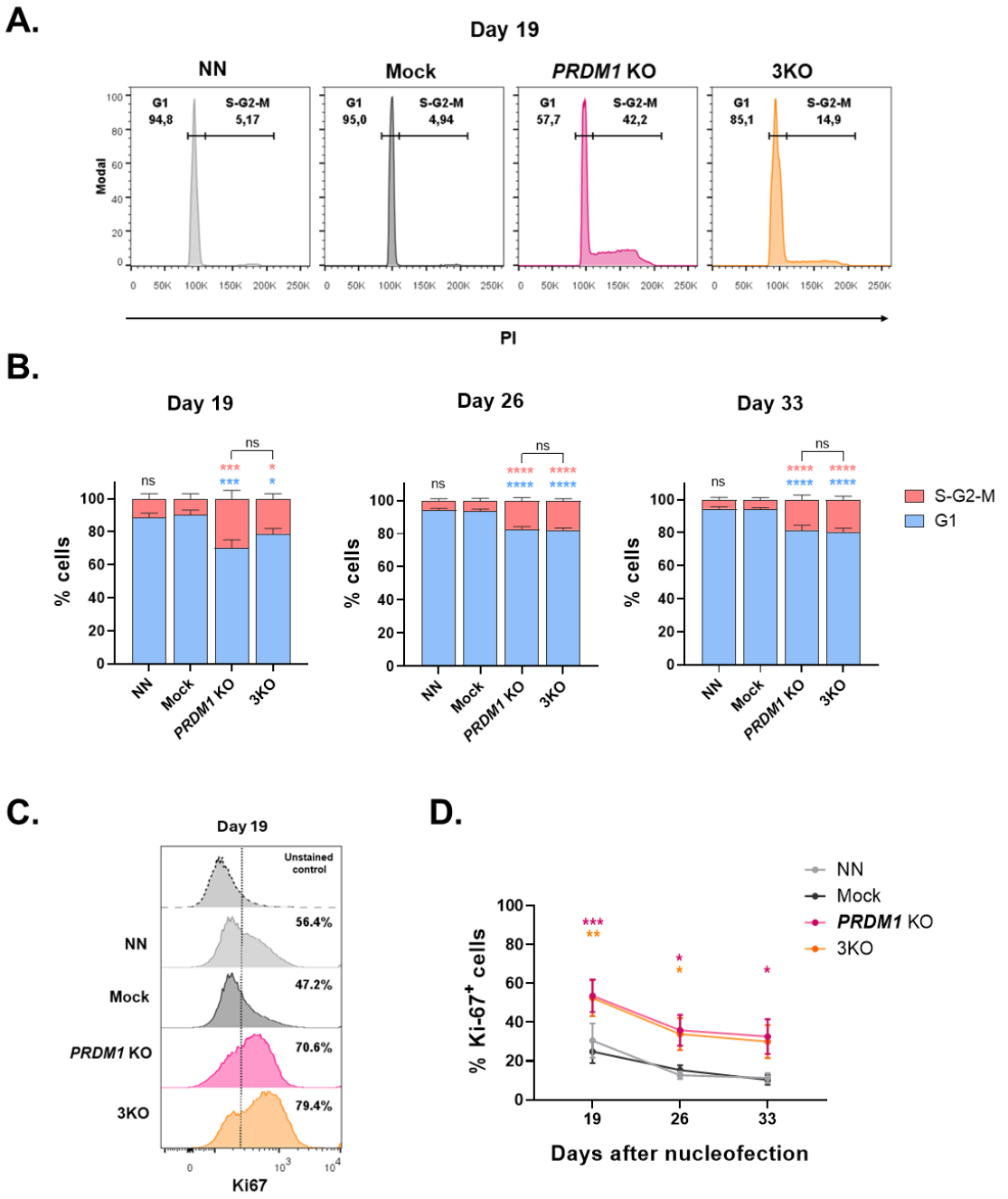

Figure 73. Triple KO CAR NK cells have increased proliferative potential compared to mock CAR NK cells. **A.** Representative cell cycle flow cytometry histograms of propidium iodide-stained non-nucleofected (NN), mock, single *PRDM1* KO, and 3KO CAR NK cells analyzed at day 19 after nucleofection. **B.** Proportion of cells in S-G2-M and G1 phases in NN, mock, single *PRDM1* KO, and 3KO CAR NK cells analyzed at different times after nucleofection. Statistical analysis shows differences with respect to mock control and between single *PRDM1* KO and 3KO CAR NK cells. **C.** Representative flow cytometry histogram of Ki-67 staining of NN, mock, single *PRDM1* KO, and 3KO CAR NK cells analyzed at day 19 after nucleofection. The percentages of Ki-67$^+$ cells are indicated on each histogram. **D.** Percentage of Ki-67$^+$ cells in NN, mock, single *PRDM1* KO, and 3KO CAR NK cell cultures analyzed at different times after nucleofection. Statistical analysis shows differences with respect to mock CAR NK cells. Means ± SEM are shown (n=6). *p<0.05; **p<0.01; ***p<0.001, ****p<0.0001; ns: no significance.

Finally, as we had previously observed that *PRDM1* ablation may impact the senescence state of CAR NK cell cultures, we analyzed SA-β Gal activity in 3KO CAR NK cells. Similar to *PRDM1* KO CAR NK cells, from day 26 after first nucleofection, 3KO cells exhibited less SA-β Gal activity than mock cells (33.2 ± 5.2% vs 49.4 ± 5.3% DDAO$^+$ cells) (**Figure 74**).

Taken together, *PRDM1* disruption resulted in an increased proliferation rate and a reduced senescence state, which conferred 3KO CAR NK cells a controlled enhanced *in vitro* expansion capacity.

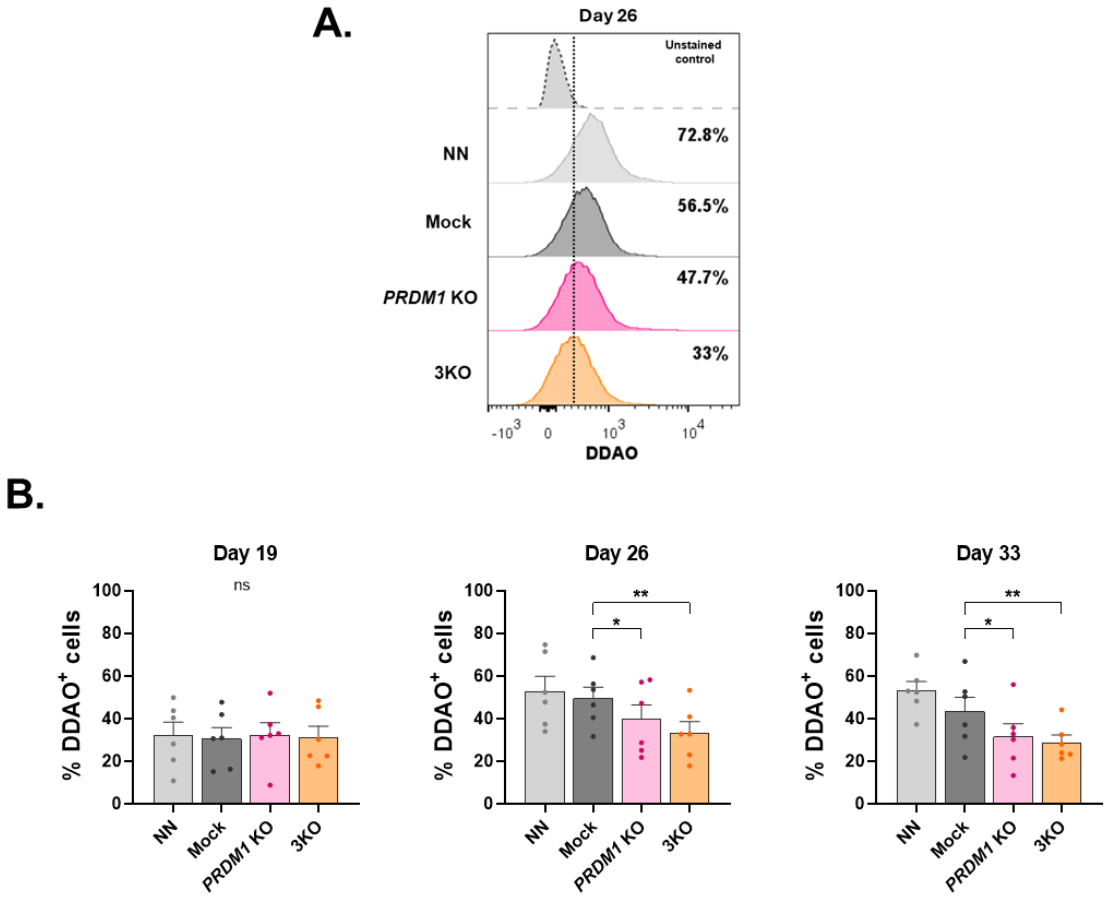

Figure 74. Senescence is reduced in triple KO CAR NK cells in comparison with mock CAR NK cells. A. Representative flow cytometry histograms of measurement of SA-β-gal activity in non-nucleofected (NN), mock, single *PRDM1* KO and 3KO CAR NK cells 26 days after nucleofection. The percentage of DDAO$^+$ cells is indicated on each histogram. **B.** Percentage of cells showing SA-β-gal activity in NN, mock, single *PRDM1* KO, and 3KO CAR NK cultures analyzed by flow cytometry staining at different times after nucleofection. Means ± SEM are shown (n=6). Statistical analyses show differences with respect to mock CAR NK cells. *p<0.05; **p<0.01; ns: no significance.

3.4. Triple gene editing in CAR NK cells is maintained over time

Since *in vitro* expansion of CAR NK cells could result in clonal selection of specific edited populations, we analyzed gene editing efficiency during the *in vitro* expansion. On day 33 after first nucleofection, the percentage of NKG2A$^-$ TGFBR2$^-$ NK cells was 66.72 ± 4.3% in 3KO CAR NK cell cultures, almost identical to percentage observed at day 19 (66.3 ± 4.3%) (**Figure 75A**). Both NKG2A and TGFBR2 KO efficiencies were maintained on day 33 (75.9 ± 3.5% and 59.2 ± 5.4%, respectively), showing no significant differences to day 19 (81.9 ± 1.7% and 63.4 ± 6.9%) (**Figure 75B**). Moreover, the percentage of indels in sgRNA on-target sites remained invariable after two weeks of expansion (87.6 ± 5.5% for *KLRC1*, 72.6 ± 6.3% for *TGFBR2,* and 91 ± 3.8% for *PRDM1*) (**Figure 75C**). Therefore, we corroborated that the proportion of edited CAR NK cells remain invariable over time.

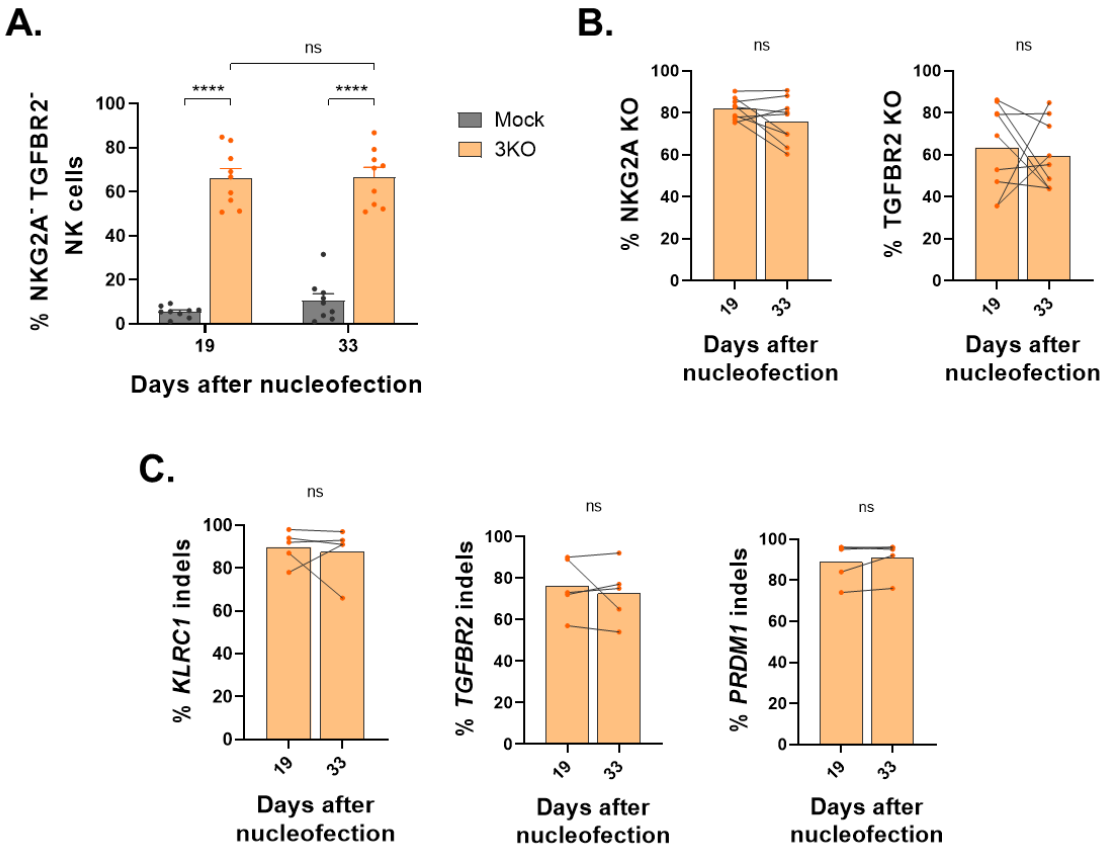

Figure 75. Triple KO gene editing efficiencies are stable over time. A. Percentage of NKG2A$^-$ TGFBR2$^-$ NK cells in mock and 3KO CAR NK cell cultures analyzed by flow cytometry on day 19 and 33 after first nucleofection (n=9). **B.** Knock-out efficiencies for NKG2A (left) and TGFBR2 (right) in 3KO CAR NK cells analyzed by flow cytometry on day 19 and 33 after first nucleofection (n=9). **C.** Percentages of indels in *KLRC1* (left), *TGFBR2* (middle), and *PRDM1* (right) sgRNA on-target sites analyzed by ICE on days 19 and 33 after first nucleofection (n=5). Means ± SEM are shown. ****p<0.0001; ns: no significance.

3.5. Triple KO CAR NK cells show higher CAR expression

Single *PRDM1* KO CAR NK cells showed increased CAR expression over time. For this reason, we further analyze CAR transduction in 3KO CAR NK cells. Twenty days after lentiviral transduction (19 days after first nucleofection) percentage of CAR$^+$ NK cells was higher in 3KO CAR NK cells (51.2 ± 7.6%) than in non-edited CAR NK cells (25.0 ± 2.9%). This percentage was similar to parental single *PRDM1* KO CAR NK cells (57.2 ± 6.2%) (**Figure 76A, 76B**). Moreover, as we observed in *PRDM1* KO CAR NK cells, the analysis of CAR expression over time showed that CAR$^+$ population is enriched in 3KO CAR NK cells two weeks later while remaining invariable in mock CAR NK cells (**Figure 76B**). To further confirm lentiviral vector integration, VCN was analyzed on day 19 by q-PCR in the next batch of experiments. We found a positive correlation between CAR expression and VCN quantification (**Figure 76D**).

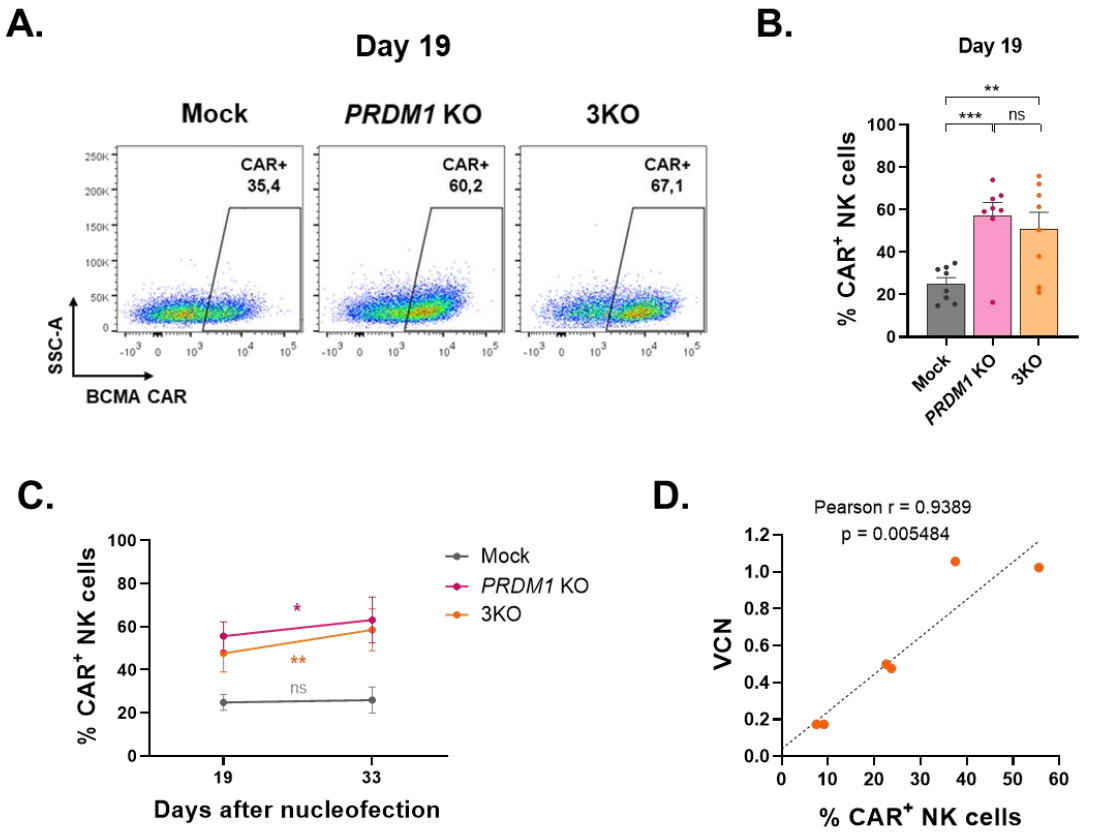

Figure 76. CAR expression in triple KO CAR NK cells increases over time. A. Representative flow cytometry dot plots of CAR expression in mock, single *PRDM1* KO, and 3KO CAR NK cells analyzed on day 19 after nucleofection. Numbers indicate percentage of cells in CAR$^+$ gate. **B.** Percentage of CAR$^+$ cells in mock, single *PRDM1* KO, and 3KO CAR NK cell cultures analyzed by flow cytometry 19 days after nucleofection (n=8). **C.** Percentage of CAR$^+$ NK cells in mock, single *PRDM1* KO, and 3KO CAR NK cell cultures analyzed by flow cytometry on days 19 and 33 after first nucleofection (n=7). Statistical analysis shows differences between day 19 and 33. **D.** Correlation between vector copy number (VCN) quantification by q-PCR and CAR detection by flow cytometry (n=6). Spearman r coefficient and correlation p value are indicated on graph. Means ± SEM are shown. *p<0.05; **p<0.01; ***p<0.001; ns: no significance.

3.6. Triple gene editing maintains cytotoxic NK cell profile but induces immunophenotypic changes

Similar to experiments performed in 2KO and *PRDM1* KO CAR NK cells, immunophenotypic variations in 3KO CAR NK cells were analyzed by flow cytometry.

Despite the observation that *PRDM1* KO temporarily decreased the expression of CD16, triple gene editing did not affect either the percentage of cytotoxic NK cells (87.9 ± 2.8% $CD56^+$ $CD16^+$ in mock NK cells vs 89.9 ± 2.4% $CD56^+$ $CD16^+$ in 3KO NK cells) or the relative CD16 surface expression 19 days after nucleofection. Importantly, cytotoxic population is maintained over time in culture (**Figure 77**).

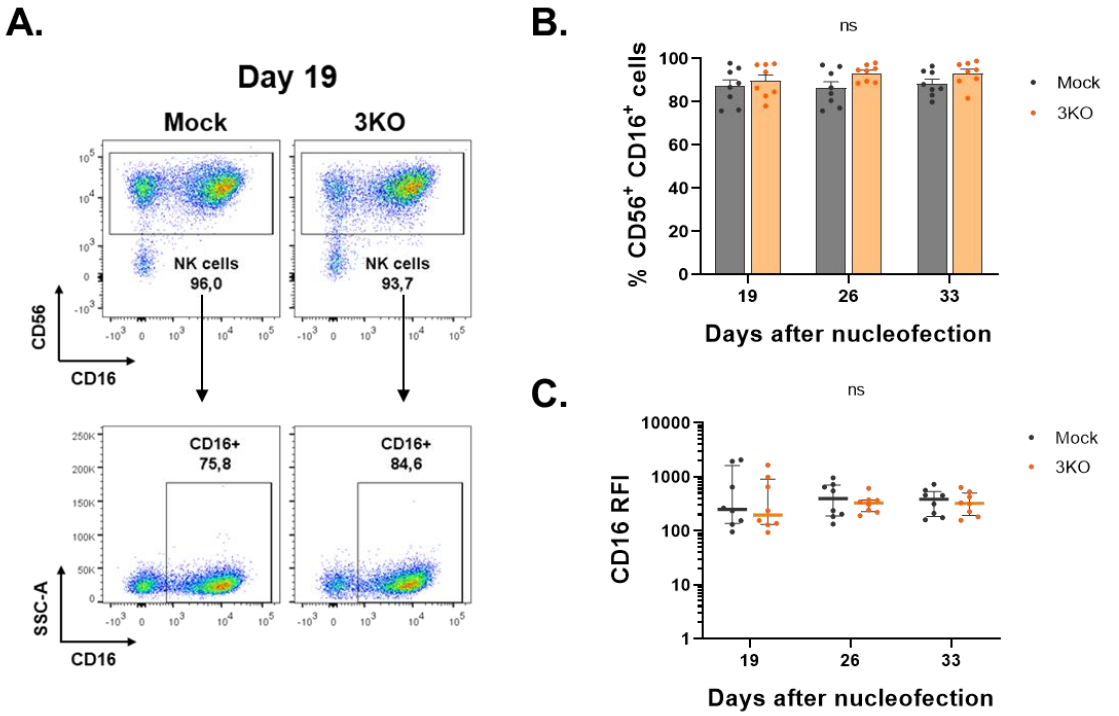

Figure 77. Triple KO CAR NK cells show same CD16 expression as non-edited CAR NK cells. A. Representative flow cytometry dot plots of CD16 expression in mock and 3KO CAR NK cells analyzed on day 19 after nucleofection. Numbers indicate percentage of cells in each gate. **B.** Percentage of cytotoxic $CD16^+$ NK cells in mock and 3KO NK cell cultures analyzed by flow cytometry at different times after nucleofection. Means ± SEM are shown (n=8). **C.** Relative fluorescence intensity (RFI) of CD16 in mock and 3KO CAR NK cells analyzed by flow cytometry at different times after nucleofection. Medians and IQR are shown (n=8). Data in C is presented in logarithmic scale. Statistical analysis shows differences with respect to mock CAR NK cells. ns: no significance.

Apart from CD16, other surface NK receptors were analyzed by flow cytometry. As a result of triple gene editing, NKp30, NKp44, and NKG2C activating receptors were downregulated. In contrast, DNAM-1 was upregulated in 3KO CAR NK cells. Regarding inhibitory receptors, TIGIT

was also upregulated. Moreover, consistent with immunophenotypic analysis of single *PRDM1* KO cells (**Figure 61**), 3KO CAR NK cells showed increased CD25 surface expression (**Figure 78**).

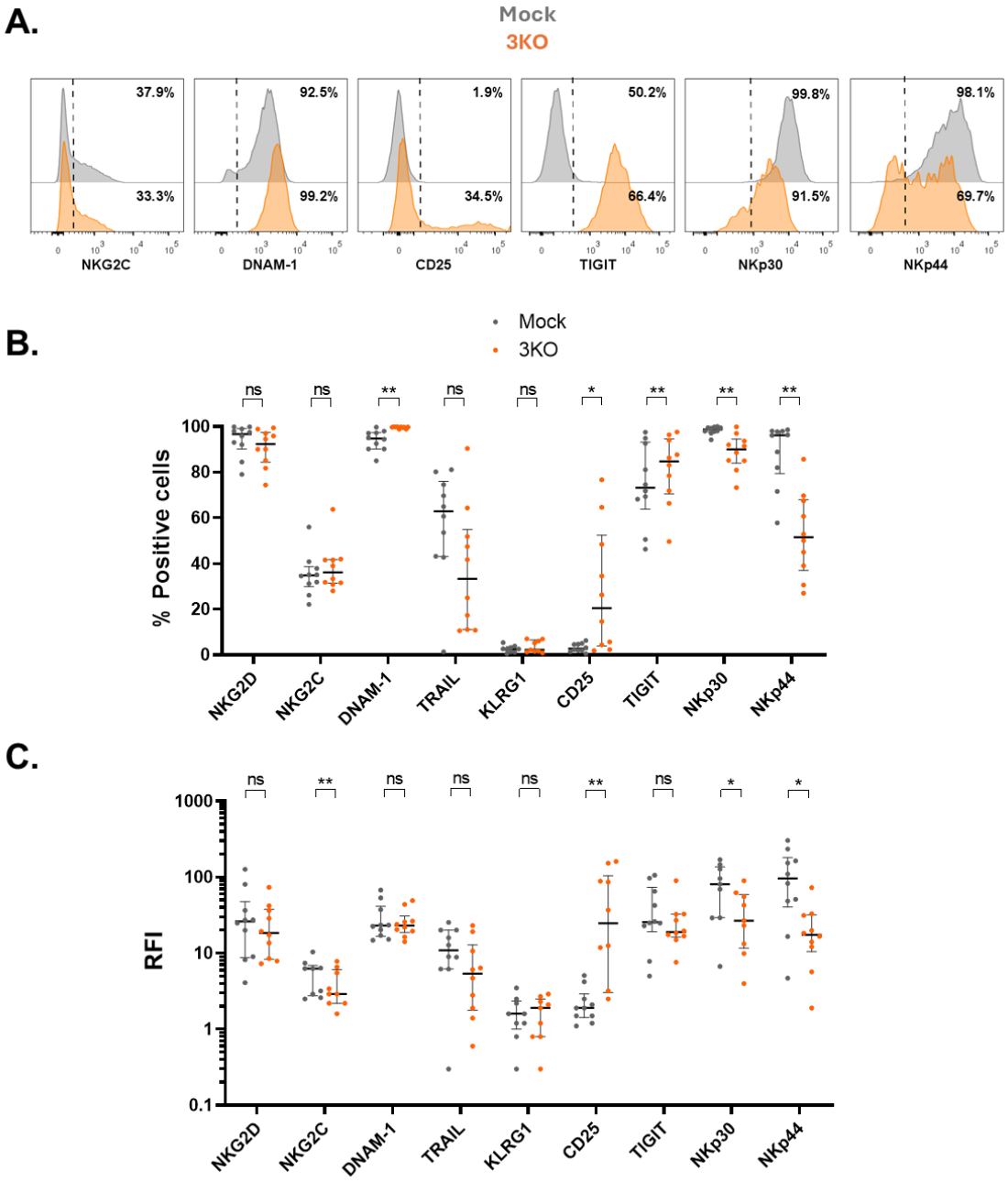

Figure 78. Triple gene editing triggers immunophenotypic changes in CAR NK cells. A. Representative flow cytometry histograms of the expression of different NK receptors in mock and 3KO CAR NK cells on day 19 after first nucleofection. Percentages indicate the proportion of cells expressing each receptor. **B.** Percentage of positive cells for each receptor in mock and 3KO CAR NK cells analyzed by flow cytometry 19 days after first nucleofection. **C.** Relative fluorescence intensity (RFI) of each receptor in mock and 3KO CAR NK cells analyzed by flow cytometry 19 days after first nucleofection. Data in C is presented in logarithmic scale. Medians and IQR are shown (n=10). *p<0.05; **p<0.01; ns: no significance.

3.7. Triple gene disruption of *KLRC1*, *TGFBR2,* and *PRDM1* modifies gene expression of CAR NK cells at the transcriptomic level

To better characterize 3KO CAR NK cell effectors, gene expression changes were analyzed by RNA-seq in CAR NK cells from 3 independent donors. In the same way as described for 2KO and *PRDM1* KO CAR NK cell transcriptomic analysis, cell sorting of CAR NK cells was performed before RNA-seq.

Differential gene expression analysis revealed a total of 182 downregulated genes and 380 upregulated genes in 3KO CAR NK cells compared to mock CAR NK cells (**Figure 79A**). Among them, some differentially expressed genes (DEG) with special relevance are listed in **Table 17**. Most of the observed transcriptomic variations were the same as for single *PRDM1* KO cell, including upregulation of genes associated with proliferation and cell survival, IFN-γ and TNF-α signaling, cytokine secretion, and NK cell migration towards lymphoid organs. 3KO CAR NK cells showed downregulation of activating receptors such as *NCR1-3, KLRF1, KLRF2, CD8A,* and *LILRA2* but upregulation of others like *TLR4, LTK* and *CD86*. We also observed downmodulation of many inhibitory NK cell receptors including *CEACAM1, CD300C, CD300A, KLRG1*, *KIR3DL3,* and *CD244*. *CD27* and *IKZF3* genes, which are associated with a mature phenotype, were also downregulated. *CISH*, encoding for the suppressor protein CIS, was upregulated. Similar to the results in *PRDM1* KO CAR NK cells, *PRDM1* expression was upregulated in 3KO CAR NK cells despite no functional protein was expressed. On the contrary, *KLRC1* expression was downregulated.

Additionally, to understand the biological significance of these 562 DEG in NK cells, gene set enrichment analysis (GSEA) was performed using KEGG database. Throughout all the pathways that were analyzed, the only pathway that was significantly enriched in 3KO CAR NK cells compared to mock CAR NK peers was expression of cell adhesion molecules (**Figure 79B**).

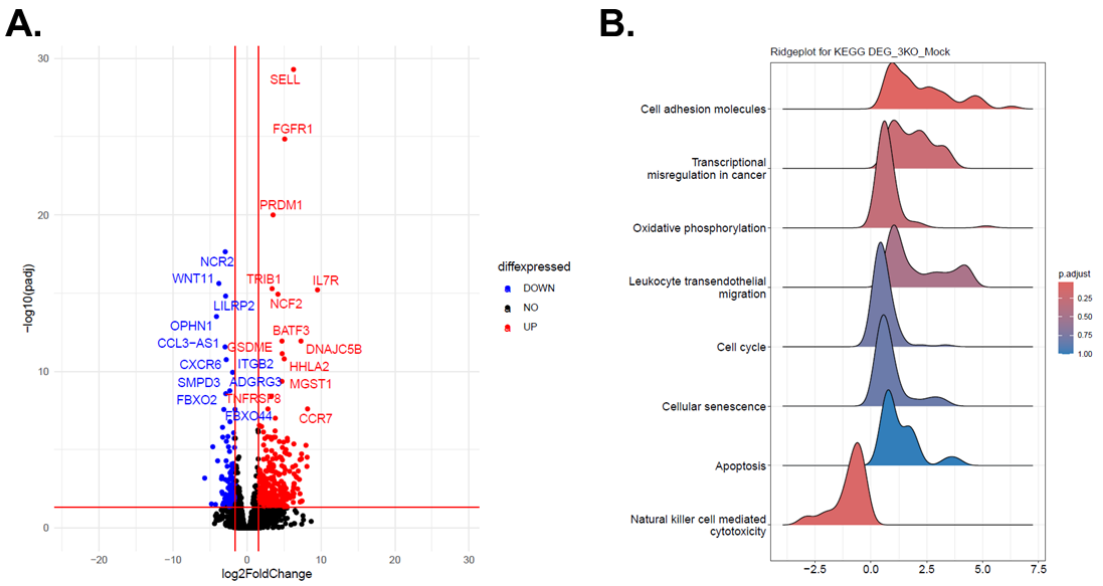

Figure 79. Combined disruption of *KLRC1*, *TGFBR2,* and *PRDM1* induces transcriptomic changes in CAR NK cells. A. Volcano plot of RNA-seq transcriptomic analysis showing upregulated (red) and downregulated (blue) genes in 3KO CAR NK cells compared to mock CAR NK cells. **B.** Ridgeplots of gene set enrichment analysis in 3KO CAR NK cells compared to mock CAR NK cells. Integrated RNA-seq data obtained from 3 independent NK donors.

	ENS entry	Gene name	Log2 Fold Change	Adjusted p
Downregulated	ENSG00000139193	*CD27*	-3.403	5.27E-04
	ENSG00000096264	*NCR2*	-2.938	2.28E-18
	ENSG00000172215	*CXCR6*	-2.799	1.78E-11
	ENSG00000161405	*IKZF3*	-2.666	1.16E-04
	ENSG00000079385	*CEACAM1*	-2.590	1.05E-03
	ENSG00000239998	*LILRA2*	-2.579	1.45E-06
	ENSG00000184371	*CSF1*	-2.501	6.59E-06
	ENSG00000135472	*FAIM2*	-2.456	1.40E-02
	ENSG00000256797	*KLRF2*	-2.391	8.03E-04
	ENSG00000150045	*KLRF1*	-2.289	3.04E-04
	ENSG00000242019	*KIR3DL3*	-2.279	2.36E-02
	ENSG00000134256	*CD101*	-2.176	1.20E-02
	ENSG00000167851	*CD300A*	-2.125	2.17E-03
	ENSG00000113088	*GZMK*	-2.018	7.81E-03
	ENSG00000134545	*KLRC1*	-1.782	9.12E-05
	ENSG00000163823	*CCR1*	-1.614	1.46E-03
	ENSG00000246985	*SOCS2-AS1*	-1.599	1.45E-02
	ENSG00000139187	*KLRG1*	-1.406	8.90E-03
	ENSG00000010810	*FYN*	-1.377	1.95E-02
	ENSG00000167850	*CD300C*	-1.308	5.62E-03
	ENSG00000204475	*NCR3*	-1.299	2.00E-02
	ENSG00000122223	*CD244*	-1.293	2.41E-02
	ENSG00000189430	*NCR1*	-1.207	3.88E-05
	ENSG00000153563	*CD8A*	-1.129	2.42E-02
	ENSG00000000938	*FGR*	-1.031	3.54E-02
	ENSG00000104998	*IL27RA*	-0.993	4.52E-03
	ENSG00000164136	*IL15*	-0.970	3.02E-02

	ENSG00000180644	*PRF1*	-0.751	1.19E-02
Upregulated	ENSG00000121966	*CXCR4*	0.906	3.17E-02
	ENSG00000128604	*IRF5*	0.936	2.36E-02
	ENSG00000166949	*SMAD3*	1.002	2.14E-02
	ENSG00000114013	*CD86*	1.020	6.23E-03
	ENSG00000114737	*CISH*	1.081	2.21E-03
	ENSG00000115415	*STAT1*	1.423	3.82E-02
	ENSG00000144118	*RALB*	1.476	5.69E-07
	ENSG00000125726	*CD70*	1.565	3.00E-03
	ENSG00000163453	*IGFBP7*	1.739	1.99E-04
	ENSG00000144354	*CDCA7*	1.819	6.09E-04
	ENSG00000162594	*IL23R*	1.962	2.42E-02
	ENSG00000103522	*IL21R*	1.965	8.52E-03
	ENSG00000177606	*JUN*	2.004	2.09E-03
	ENSG00000185989	*RASA3*	2.150	1.65E-02
	ENSG00000134460	*IL2RA*	2.193	1.94E-03
	ENSG00000128342	*LIF*	2.199	4.46E-04
	ENSG00000149212	*SESN3*	2.207	1.33E-03
	ENSG00000117586	*TNFSF4*	2.376	1.23E-02
	ENSG00000188130	*MAPK12*	2.459	3.68E-02
	ENSG00000060982	*BCAT1*	2.538	2.24E-04
	ENSG00000167964	*RAB26*	2.807	9.31E-03
	ENSG00000134508	*CABLES1*	2.889	8.78E-03
	ENSG00000106366	*SERPINE1*	2.910	1.85E-04
	ENSG00000120949	*TNFRSF8*	3.302	3.86E-09
	ENSG00000133101	*CCNA1*	3.335	1.16E-05
	ENSG00000010610	*CD4*	3.408	2.20E-04
	ENSG00000141655	*TNFRSF11A*	3.506	1.71E-06
	ENSG00000057657	*PRDM1*	3.524	1.01E-20
	ENSG00000171105	*INSR*	3.626	1.04E-02
	ENSG00000163734	*CXCL3*	3.658	7.21E-03
	ENSG00000137265	*IRF4*	3.794	6.40E-07
	ENSG00000118513	*MYB*	3.852	2.96E-04
	ENSG00000154654	*NCAM2*	4.417	3.73E-04
	ENSG00000123685	*BATF3*	4.726	1.16E-12
	ENSG00000136573	*BLK*	4.935	1.46E-03
	ENSG00000169194	*IL13*	4.944	3.33E-06
	ENSG00000062524	*LTK*	5.072	3.96E-03
	ENSG00000077782	*FGFR1*	5.096	1.43E-25
	ENSG00000136869	*TLR4*	5.505	1.12E-02
	ENSG00000188404	*SELL*	6.288	5.12E-30
	ENSG00000145506	*NKD2*	6.849	3.25E-03
	ENSG00000227145	*IL21-AS1*	7.076	8.02E-04
	ENSG00000183813	*CCR4*	7.437	1.89E-02
	ENSG00000126353	*CCR7*	8.182	2.51E-08
	ENSG00000168685	*IL7R*	9.522	6.22E-16

Table 17. List of the most relevant genes differentially expressed in triple KO CAR NK cells compared to mock CAR NK cells. Fold change and adjusted p values are indicated for each gene. Ensembl (ENS) entry codes are referred to GRCh38.p14 genome assembly.

3.8. Triple KO CAR NK cells preserve antitumor efficacy against MM cell lines

As a next step, 3KO CAR NK cell cytotoxic capacity against MM cell lines U-266 and RPMI-8226 was further analyzed in both the absence or presence of soluble TGF-β by calcein-release cytotoxicity assays. 3KO CAR NK cells presented similar killing efficacy as 2KO CAR NK cells. Importantly, antitumor capacity was not decreased after treatment with soluble TGF-β, with 3KO CAR NK cells outperforming non-edited cells (81.5 ± 7.2% vs 64.2 ± 10.8% specific lysis against U-266 at 1:1 E:T ratio; 65.9 ± 12.1% vs 44.1 ± 12.6% specific lysis against RPMI-8226 at 2:1 E:T ratio) (**Figure 80**).

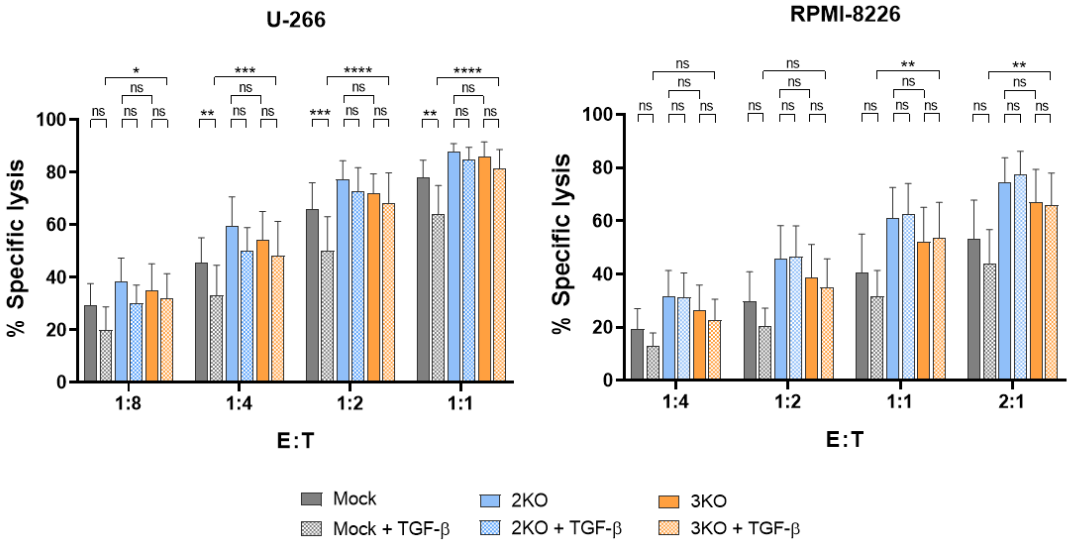

Figure 80. Triple KO CAR NK cells exhibit similar antitumor efficacy as double KO CAR NK cells. Specific lysis of mock, 2KO, and 3KO CAR NK cells against U-266 and RPMI-8226 MM cell lines at different E:T ratios, analyzed by 3h-Calcein release assay, after treatment or not with 10ng/ml TGF-β1 for 24 hours. Means ± SEM are shown (n=4). *p<0.05; **p<0.01; ***p<0.001; ****p<0.0001; ns: no significance.

3.9. Triple gene knock-out upregulates activating intracellular NK cell signaling pathways after tumor stimulation

Besides the cytotoxic capacity of edited CAR NK effectors against MM cell lines, we also measured by western blot the impact of *KLRC1, TGFBR2,* and *PRDM1* ablation on intracellular NK cell signaling pathways. With that aim, mock or different edited CAR NK populations were stimulated with U-266 cell line for 30 minutes. To corroborate that detected protein changes corresponded to CAR NK cells and not to U-266 cell line, a negative control without effector cells was included. Additionally, FLC λ expression by U-266 cells was also detected as a tumor marker. After 30-minutes co-culture, FLC λ expression decreased, confirming efficient U-266 killing (**Figure 81**).

Upon tumor stimulation, *KLRC1* KO, 2KO, and 3KO CAR NK cells showed increased expression of granzyme B compared to mock CAR NK cells, correlating with the previously observed tumor killing in the cytotoxicity assays. Importantly, granzyme B upregulation was higher in both 2KO and 3KO compared to *KLRC1* KO cells.

On the other hand, activation of SHP1 phosphatase was decreased in 2KO and 3KO CAR NK cells compared to mock cells which inversely correlated with the activation state of the SHP1 downstream target ZAP70/SYK. Moreover, phosphorylation of STAT5, another target of SHP1 phosphatase and one of the main IL-2/15 signal transducers[537,538], was increased in 3KO CAR NK cells after stimulation, compared to mock cells.

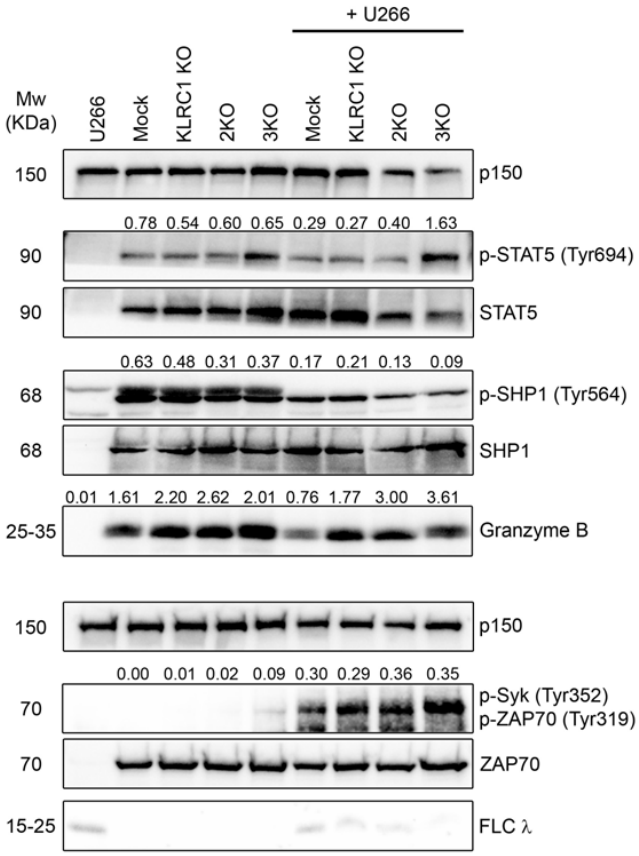

Figure 81. Triple KO CAR NK cells show different activating and inhibitory signaling in response to tumor stimulation. Western blot analysis of STAT-5 (Tyr694), SHP1 (Tyr564), and ZAP70 (Tyr319)/SYK (Tyr352) phosphorylation and granzyme B expression in mock, *KLRC1* KO, 2KO, and 3KO CAR NK cells after 30-minutes co-culture with U-266 MM cells at a ratio 4:1 E:T. Constitutive expression of p150 was analyzed as protein loading control. Numbers indicate expression of each phosphorylated protein relative to their respective total protein as well as expression of granzyme B relative to p150. Molecular weights (Mw) for each protein are indicated (n=1).

3.10. Triple KO CAR NK cells show enhanced efficacy against MM primary cells without compromising CD34$^+$ cells

Since 2KO and 3KO CAR NK cells exhibit increased antitumor efficacy against MM cell lines compared to non-edited cells, we sought to investigate their killing activity over primary plasma cells from MM patient samples. For this purpose, BMMCs from newly diagnosed and progressed MM patients were cocultured with CAR NK cells at a 5:1 E:T ratio for 24 hours, in the absence or presence of TGF-β. Patient characteristics as well as HLA-E and BCMA expression in plasma cells after sample processing measured by flow cytometry are detailed in **Table 18.** NK specific lysis against plasma cells and CD34$^+$ hematopoietic stem and progenitor cells was quantified by flow cytometry analysis.

Edited CAR NK cells had increased antitumor activity when compared to mock control cells (54.3 ± 9.1% and 72.7 ± 8.6% specific lysis for 2KO and 3KO CAR NK cells, respectively, vs 23.4% ± 5.9% for mock CAR NK cells) (**Figure 82A, 82C**). Remarkably, despite heightened antitumor potential, there was no significant killing activity over CD34$^+$ progenitor cells between edited and mock CAR NK cell cultures (4.5 ± 10.9%, 12.5 ± 12.4%, and 25.1 ± 13.6% specific lysis for mock, 2KO, and 3KO effectors, respectively) (**Figure 82B**).

To confirm low off-tumor killing activity of 2KO and 3KO CAR NK cells, we performed an additional toxicity assay against mature blood cells from HD. None of the CAR NK cells induced high toxicity against HD PBMCs at different E:T ratios. The maximum percentage of cell lysis was 5.1 ± 3.7%, obtained with 3KO CAR NK cells at 2:1 E:T ratio (**Figure 82D**).

To summarize, disruption of *KLRC1* and *TGFBR2* in combination with *PRDM1* enhanced antitumor potential of CAR NK effectors against MM without increasing off-tumor hematotoxicity.

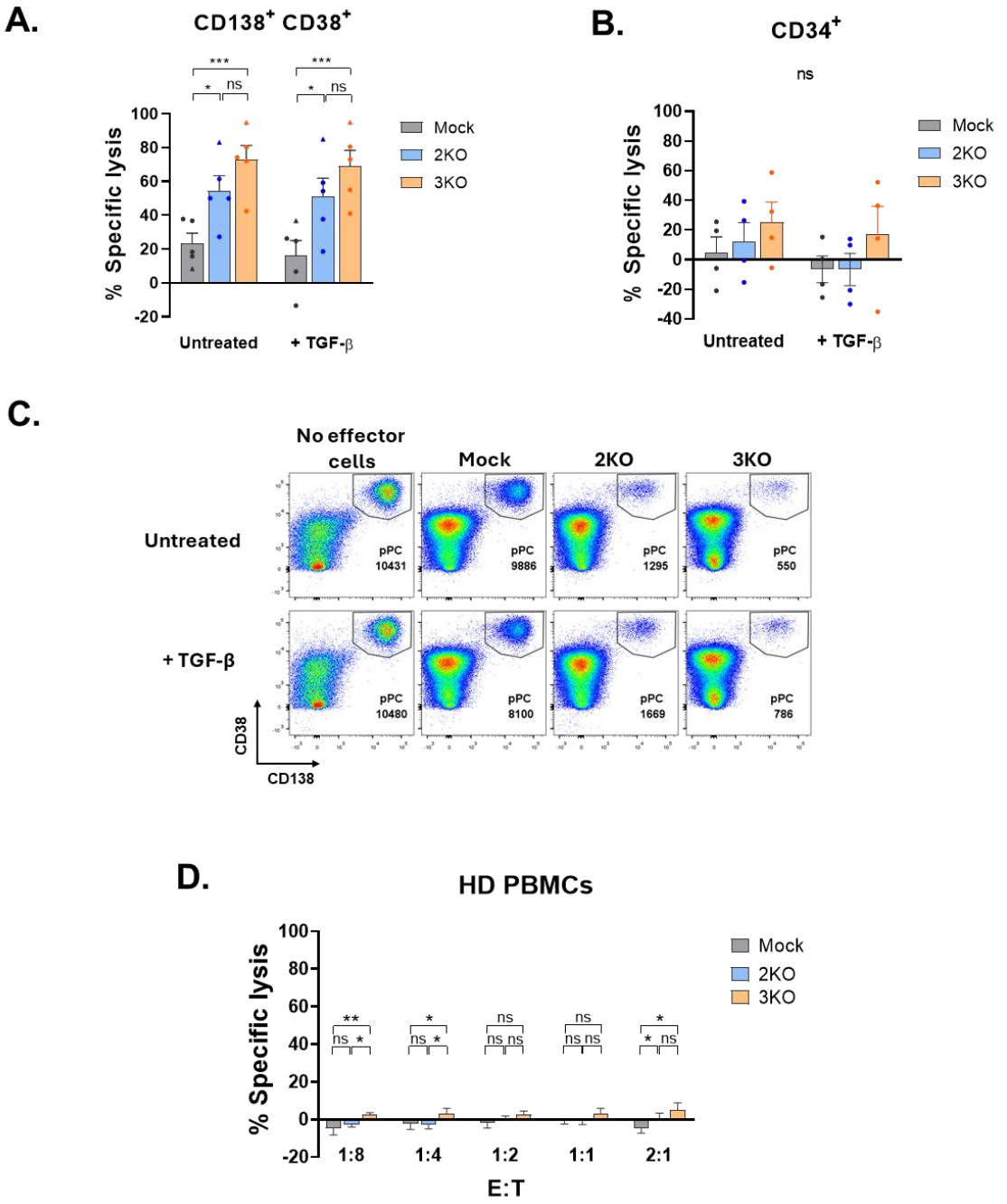

Figure 82. Double and triple KO CAR NK cells have higher cytotoxic activity against plasma cells from MM patients, with low off-tumor toxicity. A and B. Specific lysis of mock, 2KO, and 3KO CAR NK cells against pathologic plasma cells (pPC) (n=5) (**A**) and CD34^{+} cells (n=4) (**B**) from MM patients analyzed by flow cytometry after 24 hours in the absence or presence of 10 ng/ml TGF-β1. Triangle represents cytotoxicity against cells from relapsed/refractory (RR) patient #5 while circles represent newly diagnosed patients. **C.** Flow cytometry dot plots of pPC gating in CAR NK cell and BMMC from RR patient #5 24h-co-cultures in the absence or presence of 10 ng/ml of TGF-β1. **D.** Specific lysis of mock, 2KO, and 3KO CAR NK cells against PBMCs from healthy donors at different E:T ratios, analyzed by 3h-Calcein release assay (n=6). Means ± SEM are shown. *p<0.05; **p<0.01; ***p<0.001; ns: no significance.

	Clinical characteristics						MFC BMMC analysis			
	Age	Status	ISS	Treatment	Isotype	PC* (%)	PC (%)	BCMA (RFI)	HLA-E (RFI)	CD34$^+$ (%)
#1	63	ND	R-ISS I	-	IgA λ	22	4.0	7.9	3.3	1.3
#2	60	ND	R-ISS I	-	IgA κ	30	14.3	25.0	7.0	1.1
#3	65	ND	R-ISS II	-	IgG λ	60	8.1	104.6	2.1	1.0
#4	52	ND	R-ISS I	-	IgG κ	25	7.6	36.5	3.1	0.7
#5	40	RR	R-ISS III	→ 1st: VRd → 2nd: Isa-Kd → 3th: PACE → 4th: BCMA CAR T (ARI0002h) → 5th: Talquetamab	IgA λ	28	33.0	46.9	6.9	0.15

Table 18. Clinical characteristics of MM patients used in *ex vivo* experiments and flow cytometry analysis of BMMCs. MFC: multiparametric flow cytometry; BMMCs: bone marrow mononuclear cells; ISS: International Staging System; PC: plasma cell; RFI: relative fluorescence intensity; ND: newly diagnosed; RR: relapsed/refractory; VRd: bortezomib + lenalidomide + dexamethasone; Isa-Kd: isatuximab + carfilzomib + dexamethasone; PACE: cisplatin + doxorubicin + cyclophosphamide + etoposide; Ig: immunoglobulin. *Percentage of PC value from clinical cytologic tests.

3.11. Multiplex CRISPR/Cas9 genome editing does not generate off-targets in *in silico* predicted loci

To confirm the absence of off-target Cas9 HiFi nuclease activity, *in silico* predicted off-targets for *KLRC1* and *TGFBR2* sgRNAs were analyzed by NGS in 2KO and 3KO CAR NK cells. *PRDM1* sgRNA predicted sites were also analyzed in 3KO CAR NK cells. Using hg38 genome reference sequences, the percentage of indels as well as single nucleotide substitutions within 5 bp upstream and downstream of the Cas9 cutting site were determined. The same regions were also analyzed in mock CAR NK cells to detect donor-dependent variants.

Results from one donor revealed low off-target Cas9 activity. Regarding the 16 *KLRC1* sgRNA off-target sites, we only detected a minor off-target editing over OT3 site in 3KO CAR NK cells which was not present in mock and 2KO samples (**Figure 83**). This off-target locus is located in an intergenic region. As for *TGFBR2* sgRNA off-targets, we found low editing rates (around 1% of sequence reads) in 3 out of 12 predicted sites in 2KO and 3KO samples. Of note, these editing events appeared also in mock controls, discarding the association with the gene editing protocol. Similarly, we detected off-target indels in one predicted site for *PRDM1* sgRNA in 3KO cells although it represented around 1% of the sequence reads and was also present in the same proportion in mock control. On-target Cas9 activity was also confirmed by Sanger sequencing in this donor (87% and 77% indels for *KLRC1* and *TGFBR2*, respectively, in 2KO CAR NK cells and 73%, 33% and 55% indels for *KLRC1*, *TGFBR2* and *PRDM1* in 3KO CAR NK cells).

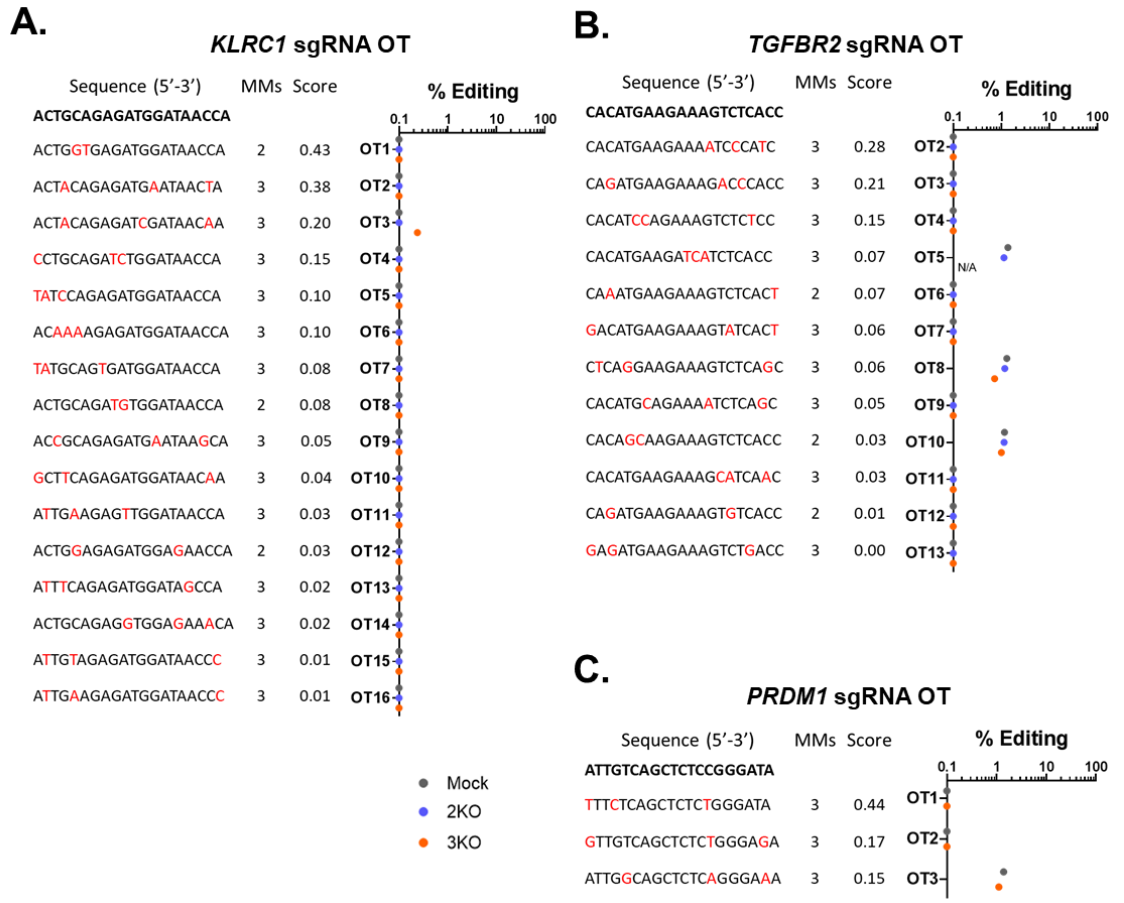

Figure 83. Low off-target Cas9 activity in multi-edited CAR NK cells. NGS analysis of *in silico* predicted off-target (OT) loci for *KLRC1* (**A**), *TGFBR2* (**B**), and *PRDM1* (**C**) sgRNAs in mock, 2KO, and 3KO CAR NK cell samples collected on day 19 after first nucleofection (n=1). Off-target activity was quantified within +/- 5 bp from the Cas9 cutting site. As mock sample harbored a SNP in the *TGFBR2* OT4 locus, mock sequence was used as reference sequence for editing analysis. On-target (bold) and off-target sequences, mismatch (MM) numbers with on-target site and off-target score based on MIT algorithm are indicated for each OT. N/A: non-available sample due to sequencing fail.

3.12. Multiplex CRISPR/Cas9 genome editing does not generate high-grade chromosomal structural alterations

When simultaneously targeting two or more genes, multiple Cas9-induced DSBs in DNA can derive in translocations or even complete chromosomal loss[496,497,539]. Therefore, to further ensure that our multiplexed gene editing protocol does not generate chromosomal aberrations, we performed a whole genome screening in non-edited and edited CAR NK cells derived from 3 different donors using Bionano's Optical Genome Mapping Saphyr™ System. Genomic DNA from NK92-MI cell line was used as a positive control for the technique (**Figure 84A**).

Circos plot from CAR NK cells only showed a few variants compared to Bionano's reference genomes (**Figure 84B**). Among these, only small insertions, deletions, and duplications were

spotted. Importantly, no translocations, intra-fusion, loss/absence of heterozygosity or aneuploidy gain/loss were detected in any of the analyzed samples. Notably, most of the chromosomal alterations observed in 2KO and 3KO CAR NK cell samples were also present in non-edited counterparts, strongly suggesting that they are not associated with Cas9 activity.

We focused on the variants that specifically arose in 2KO and 3KO samples but not in mock control peers (detailed information is shown in **Table 19**). Strikingly, none of the variants co-localized within on-target editing sites (chromosomes 3, 6, and 12). Only one small CVN gain in 3KO CAR NK cells from donor #2 appeared in chromosome 3 but at 165Mb from *TGFBR2* sgRNA cutting site. Additionally, these variants did not emerge in any of the predicted sgRNA off-target sites. Although these genomic alterations were not apparently associated with gene editing process, they were scrutinized in genomic databases to guarantee the safety of edited CAR NK products.

Taking all the information together, we concluded that multiplex CRISPR/Cas9 genome editing of CAR NK cells does not generate Cas9-assocaited translocations, inversions or aneuploidy gain/loss.

In summary, the addition of *PRDM1* ablation to *KLRC1* and *TGFBR2* double KO CAR NK cells by sequential gene editing protocol fosters proliferation capacity and reduces senescence state and DNA damage induction. Moreover, 3KO CAR NK cells maintain cytotoxic potency against MM cells without raising hematotoxicity or relevant off-target editing-associated events or chromosomal structural alterations such as translocations or aneuplodies.

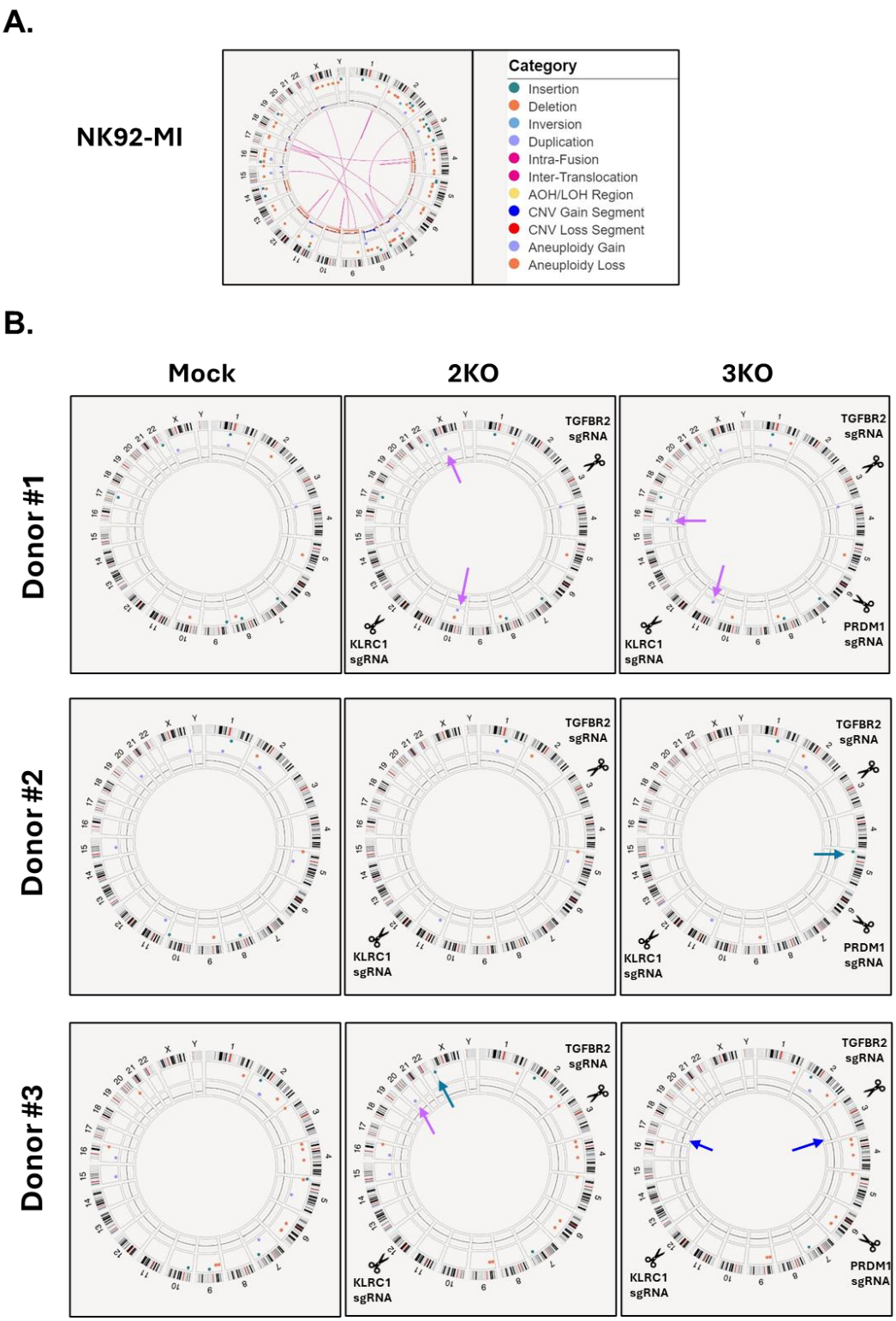

Figure 84. Multiplex CRISPR/Cas9 gene editing in CAR NK cells does not trigger large chromosomal aberrations. A and B. Optical genome mapping Circos plots from NK-92-MI cell line (**A**) and mock, 2KO, and 3KO CAR NK cells (**B**) from three different experiments. Circos plot are composed of the following layers: the outer circle displays cytoband locations, the middle circle displays color-coded (**A**) structural variations (SV) in those particular locations and the inner circle displays copy number changes (CNV) for each chromosome or region. In the center of the circle, pink lines represent translocations and intra-fusions between different parts of the genome. Arrows (color-coded) indicate SV and CNV that appear in 2KO and 3KO CAR NK cells but not in mock control cells. *KLRC1*, *TGFBR2,* and *PRDM1* sgRNA on-target sites are represented on Circos plots.

Sample	SV type	Chr	Start position	End position	VAF	Size (bp)	Affected genes
Donor #1 2KO	duplication	10	47539721	48060267	0.51	520546	*PTPN20, FRMPD2B, AGAP13P, BMS1P1, GLUD1P2, FAM25C, AGAP12P*
	duplication_inverted	23	52175043	52186934	0.95	20226	*MAGED4, SNORA11D*
Donor #1 3KO	duplication_inverted	11	500339042	50372392	0.51	33350	-
	duplication_inverted	16	28645339	28678543	0.78	33204	*NPIPB8*
Donor #2 3KO	insertion	5	254437	269655	0.34	25784	*SDHA, PDCD6-DT*
Donor #3 2KO	duplication_inverted	20	25681766	25839658	0.39	157893	*ZNF337, LOC105372582, FAM182B*
	insertion	23	911000	931532	0.47	2982	-
Donor #3 3KO	gain	3	195890779	198230596	0.14	2339818	*TNK2, TNK2-AS1, SDHAP1, LINC00885, TFRC, ZDHHC19, SLC51A, PCYT1A, DYNLT2B, TM4SF19, TM4SF19-DYNLT2B, TM4SF19-AS1, UBXN7, UBXN7-AS1, RNF168, SMCO1, WDR53, FBXO45, LINC01063, NRROS, CEP19, PIGX, PAK2, SENP5, NCBP2-AS1, -AS2, PIGZ, MELTF, MELTF-AS1, DLG1, MIR4797, DLG1-AS1, LINC02012, BDH1, SDHAP4, RUBCN, MIR922, FYTTD1, LRCH3, IQCG, RPL35A, LMLN, LMLN-AS1, ANKRD18DP, FAM157A, TBC1D3G, NPEPPSP1, LOC101929950, MRPL45, GPR179*
	gain	17	37946882	39345247	0.20	1195005	*SOCS7, ARHGAP23, SRCIN1, EPOP, LOC105371763, MIR4734, MLLT6, MIR4726, CISD3, PCGF2, LOC100287808, PSMB3, PIP4K2B, CWC25, MIR4727, C17orf98, RPL23, SNORA21B, SNORA21, LASP1, MIR6779, LINC00672, FBXO47, LINC02079, LRRC37A11P, RDM1P5, PLXDC1, ARL5C, CACNB1, RPL19, STAC2, LOC101929578, FBXL20, MIR548BC*

Table 19. Structural and copy number variants detected specifically in 2KO and 3KO CAR NK cells in comparison to mock control cells. Start and end positions are referred to GRCh38.p14 genome assembly. Chr: chromosome; VAF: Variant Allele Frequency.

4. Triple KO α-BCMA CAR NK cells have increased persistence and antitumor efficacy *in vivo*

After demonstrating *in vitro* antitumor activity, 3KO CAR NK cell *in vivo* persistence and efficacy were evaluated in comparison with mock and 2KO CAR NK effectors in a disseminated MM xenograft mouse model.

With this aim, sub-lethally irradiated NSG-Tg (Hu-IL15) were intravenously injected with 0.5 x 10^6 U-266 ffLucGFP cells. Three days later, 9 x 10^6 mock, 2KO, or 3KO fresh CAR NK cells, harvested on day 20 after the first nucleofection, were i.v. administered. Mice received serial i.p. administration of human IL-2 during the first two weeks to enhance human CAR NK cell persistence. Additionally, human TGF-β 1 was intraperitoneally injected to study the functional effect of *TGFBR2* knock-out (**Figure 85A**). Besides a control group without NK treatment (Group 2), another mice group without receiving hIL-2 and hTGF-β1 was included in the experiment (Group 1) to demonstrate that administration of these cytokines did not interfere with tumor development (**Figure 85B**).

Flow cytometry PB analysis was carried out at 4, 14, and 30 days after therapy infusion to evaluate CAR NK cell persistence. On day 4 after NK cell intravenous infusion, the average infiltration of human NK cells was 0.16 ± 0.02% in mock CAR NK group, 0.32 ± 0.04% in 2KO CAR NK group and 0.34 ± 0.05% in 3KO CAR NK group (**Figure 85C, 85D**). At this point, infiltrating 3KO NK cells showed higher CAR and CD16 expression (46.0 ± 3.9% CAR^+ cells, 80.8 ± 1.7% $CD16^+$ cells) compared to mock (8.6 ± 1.7% CAR^+ cells, 74.7 ± 1.0% $CD16^+$ cells) and 2KO (8.2 ± 0.6 CAR^+ cells, 59.2 ± 1.9% $CD16^+$ cells) NK cells. As expected, NK cells from 2KO and 3KO groups had decreased expression of NKG2A and TGFBR2 compared to mock cells (**Figure 85E**). On day 14, average infiltration of human NK cells was significantly higher in mice treated with 3KO CAR NK cells (0.15 ± 0.04% NK cells) compared to animals treated with mock and 2KO CAR NK cells (0.02 ± 0.00% and 0.02 ± 0.00% NK cells, respectively), suggesting an increased persistence of 3KO CAR NK cells. Importantly, on day 30 after NK cell infusion, no CAR NK cells were detected in PB.

A.

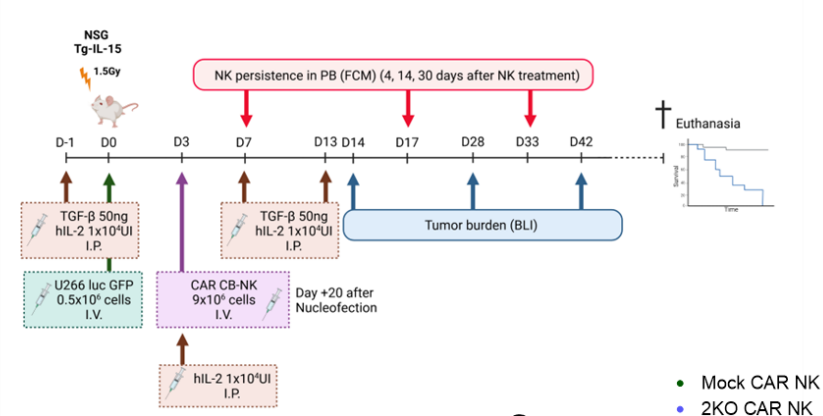

B.

	U-266 ffLuc-GFP I.V.	hTGF-β1 I.P.	hIL-2 I.P.	NK treatment
Group 1	+	-	-	Vehicle
Group 2	+	+	+	Vehicle
Group 3	+	+	+	Mock CAR NK
Group 4	+	+	+	2KO CAR NK
Group 5	+	+	+	3KO CAR NK

C.

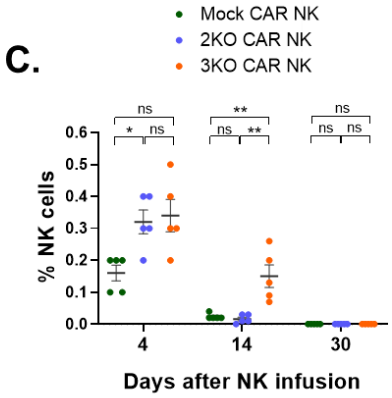

D.

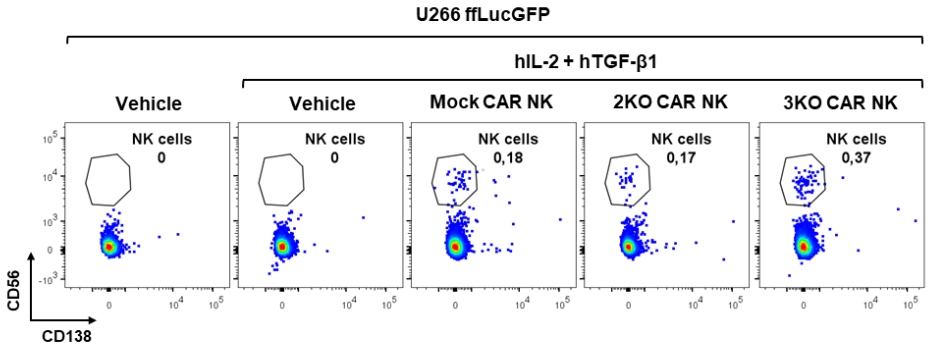

E.

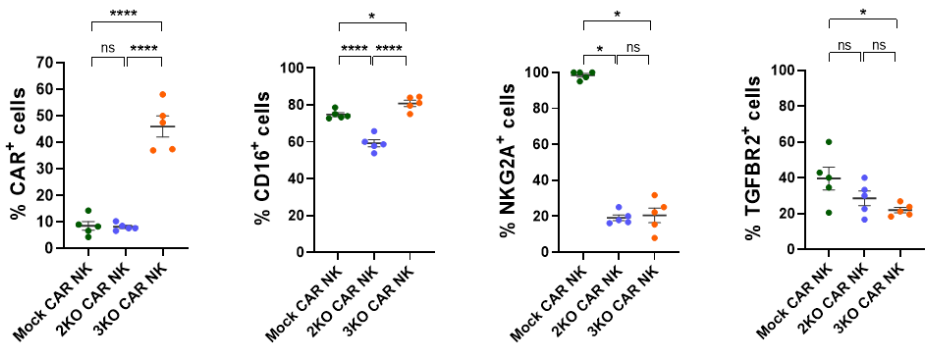

Figure 85. Triple KO CAR NK cells persist for 14 days in NSG-Tg (Hu-IL15) mice bearing U-266 ffLucGFP MM cells. A. Experimental design of the disseminated MM NSG-Tg (Hu-IL15) mouse model generated through the intravenous (I.V.) infusion of 5 x 10^5 U-266 ffLucGFP cells followed by an i.v. infusion of 9 x 10^6 mock, 2KO, or 3KO CAR NK cells. Mice received intraperitoneal (I.P.) injections of hIL-2 and hTGF-β1 as indicated. PB was analyzed on days 4, 14, and 30 after CAR NK therapy infusion. Tumor burden was monitored fortnightly by bioluminescence imaging (BLI). **B**. Experimental groups included in *in vivo* experiment. **C.** Percentage of human NK cells detected in PB from mice treated with mock, 2KO, and 3KO CAR NK cells analyzed by flow cytometry at different times after NK cell infusion. **D.** Representative flow

cytometry dot plots for NK cell detection in PB samples from one mouse of each treatment group. **E.** Percentage of CAR^+, $CD16^+$, $NKG2A^+$ and $TGFBR2^+$ cells within NK cell population in PB samples from mice treated with mock, 2KO, and 3KO CAR NK cells analyzed by flow cytometry on day 4 after NK cell infusion. Means ± SEM are shown (n=5 for each group). *p<0.05, **p<0.01; ****p<0.0001; ns: no significance.

Tumor burden was monitored fortnightly by BLI until the end of the experiment (day 152 after U-266 ffLuc-GFP infusion) (**Figure 86A**). Quantification of the luminescence photon flux signal was measured until day 56 (**Figure 86B**). From that point, mice started to succumb due to MM progression and differences in mice numbers in each group impede statistical analysis. We did not find any differences between both vehicle groups, confirming that hTGF-β and hIL-2 administration do not interfere with tumor development. In contrast, treatment with any of the three CAR NK cell effectors delayed tumor progression compared to vehicle group with both 2KO and 3KO CAR NK cells considerably outperforming mock CAR NK effectors. In line with tumor development, mice treated with the three effectors showed increased survival compared to vehicle groups (68 and 70 days, treated or not with hTGF-β and hIL-2, respectively) and both 2KO and 3KO CAR NK cells had higher efficacy (103 and 132 days, respectively) compared to mock CAR NK cells (80 days) (**Figure 86C**). Of note, although no statistical differences were found between 3KO and 2KO CAR NK effectors regarding survival, it is worth noting that 3KO CAR NK cells totally eradicated tumor cells in 2 out of 5 mice (#3 and #5) while none of the animals treated with 2KO CAR NK cells survived. Mice #3 and #5 did not show any clinical signs of disease or BLI signal at day 152, time in which we decided to discontinue the experiment.

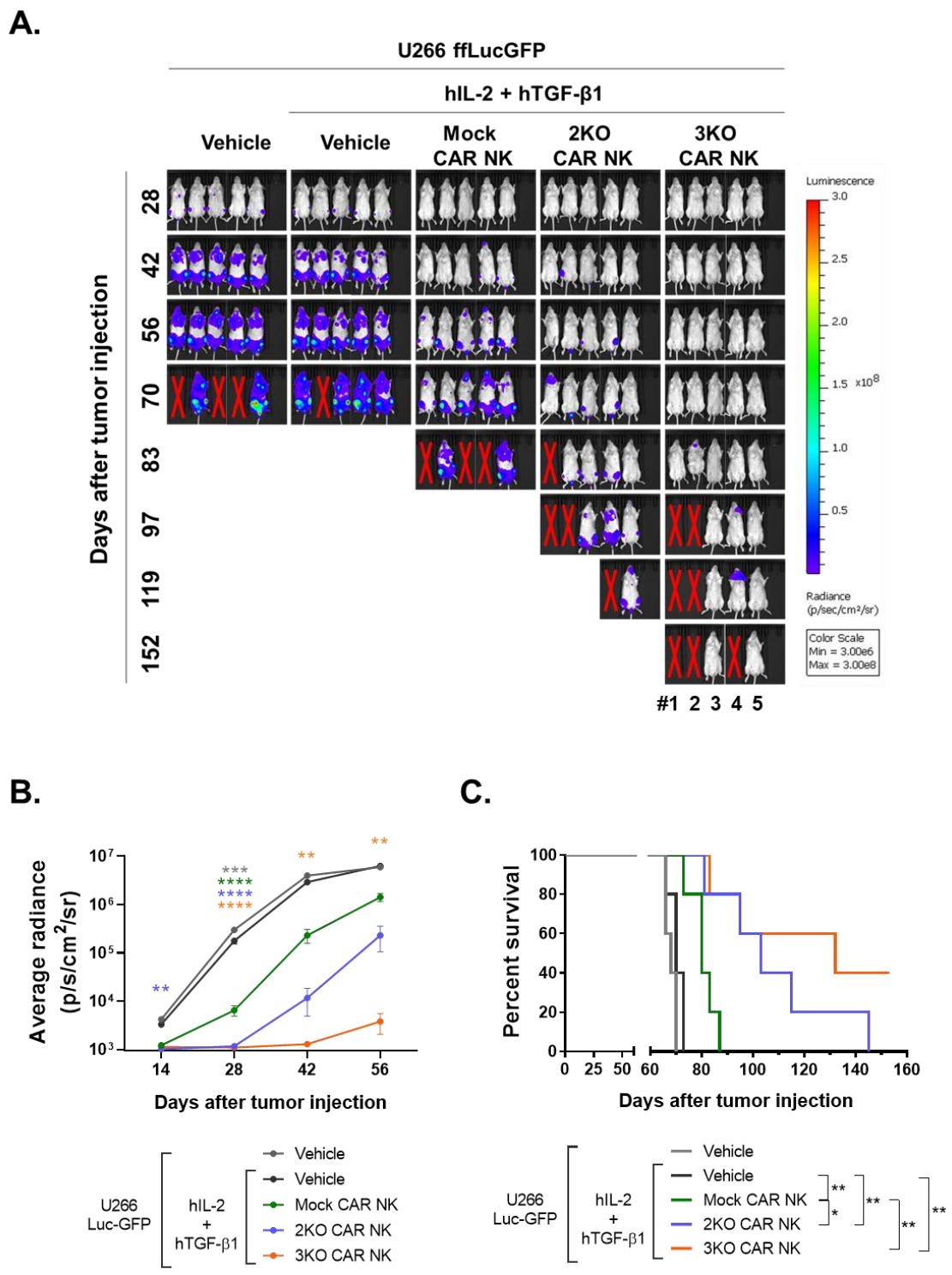

Figure 86. Double and triple KO CAR NK cells have increased antitumor efficacy *in vivo* and prolong mice survival in NSG-Tg (Hu-IL15) mice bearing U-266 ffLucGFP MM cells. A. Imaging of tumor burden monitored by bioluminescence at the indicated time points from NSG-Tg (Hu-IL15) mice bearing U-266 ffLucGFP treated with or without hIL-2 and hTGF-β1 and vehicle or mock, 2KO, or 3KO CAR NK cells. **B.** Quantification of luminescence for each group described in (**A**) at different time points. Means ± SEM are shown (n=5). Statistical analysis shows differences with respect to mice treated with hIL-2 and hTGF-β1 and vehicle. **C.** Kaplan-Meier survival curve of mice described in (**A**). *p<0.05, **p<0.01; ***p<0.001 ****p<0.0001.

At necropsy, NK and tumor cells in different tissues were analyzed by flow cytometry. We did not find any NK cells in PB or spleen in any of the animals. However, although no NK cells were observed in the BM from mock and 2KO CAR NK groups, we were able to detect a clear population of human NK cells ($CD56^+$ $CD138^-$ $CD45^+$ GFP^-) in one animal treated with 3KO CAR NK cells (mouse #1) (**Figure 87A**). Additionally, we also detected some disperse events corresponding to NK cells gate in the BM from another animal from this group (mouse #3) although a PCR should be performed to confirm this result. These results suggest that 3KO CAR NK cells slightly persist more *in vivo* compared to mock and 2KO CAR NK cells.

Regarding tumor infiltration at necropsy, the presence of MM pPC ($CD138^+$ GFP^+) was also analyzed in the BM and PB from all groups. Additionally, as some CAR NK treated animals developed a high BLI signal in the head, we decided to analyze tumor infiltration in the cranial dome (CD) of these animals. MM pPC were detected in femur and tibia BM from almost all mice from vehicle (20.9 ± 3.6% and 24.2 ± 6.0%, treated or not with hTGF-β and hIL-2, respectively), mock (15.2 ± 4.4%) and 2KO (11.5 ± 3.7%) groups which was in correlation with BLI imaging and development of clinical signs of paraplegia (**Figure 87B, 87C**). However, the three mice treated with 3KO CAR NK cells that succumbed to the disease were sacrificed not because of paraplegia but because of weight loss and lethargy. These animals showed tumor BLI signal in head and tumor cells were detected mainly in the CD. Only a low proportion of tumor cells were detected in BM (0.1 ± 0.0%). Because U-266 cell line mouse model mimics MM disease, we hardly detected pPC in PB from any experimental group. Noteworthy, non-detectable disease was found by flow cytometry in mice #3 and #5 in BM, PB nor CD, confirming efficient MM eradication in these animals.

Overall, although additional *in vivo* experiments are needed to determine whether there is a difference in antitumor activity between 2KO and 3KO CAR NK cells, these results demonstrate that both populations improved cytotoxic potency against MM in comparison with non-edited cells and the addition of *PRDM1* disruption promotes persistence of CAR NK cells.

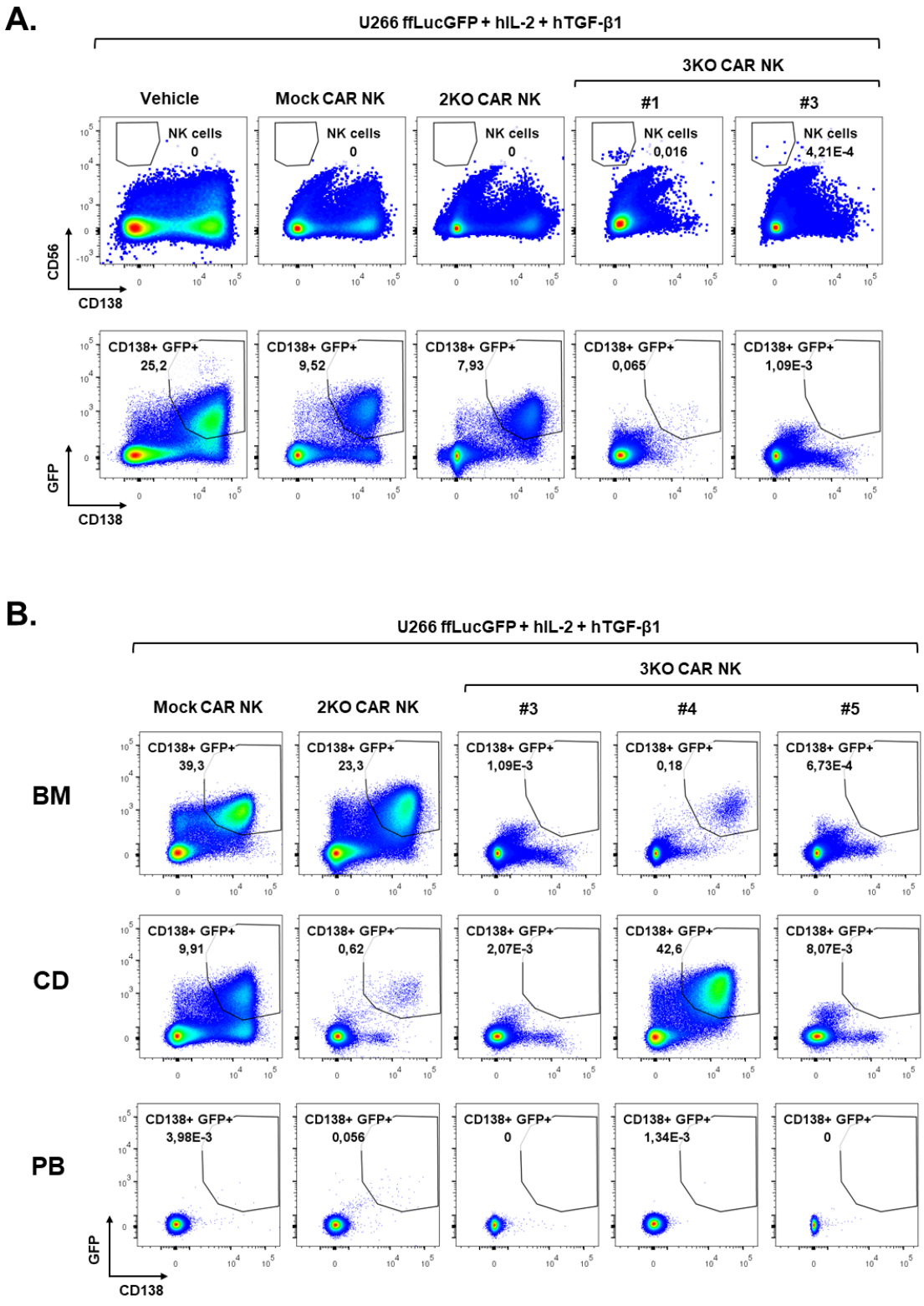
A.
U266 ffLucGFP + hIL-2 + hTGF-β1
3KO CAR NK
Vehicle
Mock CAR NK
2KO CAR NK
#1
#3
NK cells 0
NK cells 0
NK cells 0
NK cells 0,016
NK cells 4,21E-4
CD56
CD138
CD138+ GFP+ 25,2
CD138+ GFP+ 9,52
CD138+ GFP+ 7,93
CD138+ GFP+ 0,065
CD138+ GFP+ 1,09E-3
GFP
CD138
B.
U266 ffLucGFP + hIL-2 + hTGF-β1
3KO CAR NK
Mock CAR NK
2KO CAR NK
#3
#4
#5
BM
CD138+ GFP+ 39,3
CD138+ GFP+ 23,3
CD138+ GFP+ 1,09E-3
CD138+ GFP+ 0,18
CD138+ GFP+ 6,73E-4
CD
CD138+ GFP+ 9,91
CD138+ GFP+ 0,62
CD138+ GFP+ 2,07E-3
CD138+ GFP+ 42,6
CD138+ GFP+ 8,07E-3
PB
CD138+ GFP+ 3,98E-3
CD138+ GFP+ 0,056
CD138+ GFP+ 0
CD138+ GFP+ 1,34E-3
CD138+ GFP+ 0
GFP
CD138

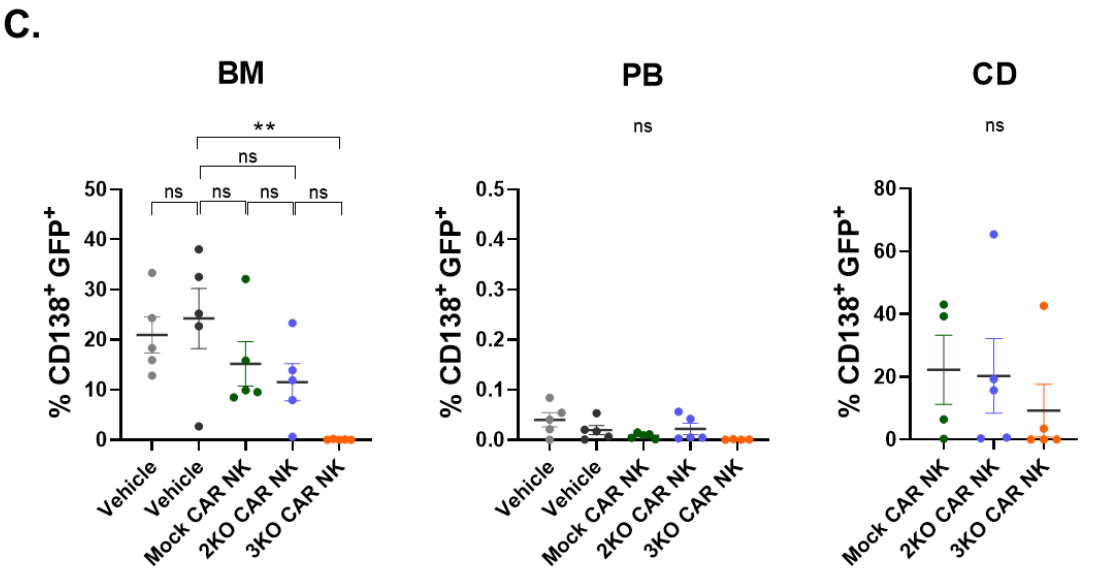

Figure 87. Tumor infiltration at necropsy in NSG-Tg (Hu-IL15) mice bearing U-266 ffLucGFP MM cells. A. Representative flow cytometry dot plots for NK ($CD56^+$ $CD138^-$) and tumor (GFP^+ $CD138^+$) cells in the femur and tibia bone marrow (BM) from NSG-Tg (Hu-IL15) mice bearing U-266 ffLucGFP MM cells and treated with vehicle, mock, 2KO, or 3KO CAR NK cells. **B.** Representative flow cytometry dot plots for tumor cell detection in BM, peripheral blood (PB) and cranium dome (CD) in mice treated with mock, 2KO, and 3KO CAR NK cells. **C.** Flow cytometry analysis of GFP^+ $CD138^+$ tumor cells in BM, PB and CD for the indicated experimental groups. Means ± SEM are shown (n=5 except for n=4 in PB from 3KO group and CD from mock group due to sample loss).

DISCUSSION

Despite the impressive advances in therapeutic approaches which have increased overall survival rates of MM patients during the last decades, MM is still an incurable disease. Immunotherapeutic strategies such as mAbs or BiAbs have been proposed to directly target MM cells but their efficacy as monotherapy relies on the activity of patient's immune system which is usually repressed in an immunosuppressive TME that surrounds MM, especially at progression. In this context, adoptive CAR T cell therapy has emerged as a revolutionary treatment for MM, with two products already available for the treatment of RRMM patients. However, despite good efficacy results in MM patients, many of them eventually relapse due to CAR T therapy resistances. This reduced long-term efficacy as well as the treatment-related high-grade toxicities, arises the need of finding new CAR effectors with a more efficacy and safety profile than T cells. CAR NK cells have shown preliminary promising results in clinical trials representing a safer alternative to CAR T therapy. However, the improvable efficacy outcomes highlight the urgency for combinatorial approaches to improve CAR NK antitumor activity. In this setting, the main objective of this thesis is the generation of allogeneic CAR NK cell therapies for RRMM patients with enhanced activity and persistence within the immunosuppressive MM TME.

On the one hand, NK immune checkpoints and immunosuppressive soluble factors secreted by MM cells, BMSCs and suppressor immune cells present in the TME, contribute to NK and T cell dysfunction, thus promoting tumor escape. Specifically, both NKG2A-HLA-E and TGF-β axes represent two dominant signaling pathways that inhibit NK activity in MM. Different strategies such as blocking mAbs or small molecule inhibitors have been independently proposed to directly target these pathways with the aim of boosting NK cell activity. In this thesis, we propose a combinatorial strategy through simultaneously targeting both axis in CAR NK effectors to obtain a synergistic improvement of the NK antitumor potential and persistence within the TME.

The use of inhibitors and mAbs seem to potentiate NK cell activity but show only partial and transient target inhibition due to their short half-lives[540-542]. Furthermore, multiple systemic administration to obtain long-term responses can lead to severe toxicities in cancer patients. The emergence of CRISPR/Cas9 technology has been a milestone in biomedicine research, including immunotherapy, representing a precise tool for stable targeting of one or more signaling pathways with high efficiency, overcoming some of the drug-related shortcomings. Previous studies have already demonstrated the higher efficacy of CRISPR/Cas9 genome editing over α-NKG2A mAbs and TGFBR2 inhibitors to enhance NK cell potency both *in vitro* and *in vivo*[365,416,417]. Therefore, in this study we proposed the application of this technology to target NKG2A-HLA-E and TGF-β pathways in CAR NK effectors.

On the other hand, *in vivo* persistence after adoptive transfer has been previously reported to correlate with clinical responses. NK cell short lifespan and limited proliferative capacity, caused by intrinsic properties of NK, immune rejection or the host immunosuppressive TME, may be responsible for the low persistence of CAR NK therapies. As an alternative approach to improve CAR NK effectors, we have analyzed the *in vivo* efficacy and persistence of a new CRISPR/Cas9 edited CAR NK product for the treatment of MM. Moreover, due to the encouraging results that we obtained, we proposed a combinatorial strategy of the two approaches to obtain a next-generation optimized CAR NK therapy against MM.

1. CRISPR/Cas9 technology allows efficient generation of multi-edited CAR NK cells from cord blood samples.

One of the principal advantages of CAR NK effectors over CAR T cells is the possibility to be applied in an allogeneic setting without inducing GvHD, representing a universal and "*off-the-shelf*" treatment option that allows to overcome TME- and treatment-derived impaired activity of endogenous immune effectors and reduces manufacturing costs and times. Although allogeneic CAR T cells have been successfully generated by the elimination of endogenous TCR, pilot clinical trials have revealed lower efficacy compared to autologous CAR T cells, probably due to immunogenicity and gene editing-derived toxicity[543].

NK cells for adoptive therapy can be obtained from multiple sources from healthy donors. Although the first CAR NK strategies against MM were based on NK-92 cell line due to their easy genetic manipulation and expansion, the need of irradiation prior to cell infusion diminishes their persistence and cytotoxic activity *in vivo*[544]. As an alternative, primary NK cells derived from PB and CB have been used to generate CAR NK effectors against different tumors. Regarding MM, while some preclinical studies have reported efficacy of CAR NK effectors derived from PB[164,287-289,291], to our knowledge, the use of CB-NK cells for CAR immunotherapy against MM has not been reported yet.

Based on previous studies describing CB-NK cell expansion methods[277,530,531,545,546], in our laboratory we have optimized a protocol to efficiently generate CAR NK effectors from fresh CB samples using aAPC and IL-2/15 stimulation and lentiviral transduction. The use of irradiated engineered K562 aAPCs to expand NK cells has been demonstrated to be a safe and risk-free approach[297,547-550]. Importantly, our final CAR NK products show minimal T cell contamination (<0.3%), which guarantees the low risk of GvHD when used in an allogeneic context.

NKG2A is highly expressed in CB-NK cells compared to PB-NK cells[275]. Moreover, some studies have demonstrated that after *ex vivo* expansion of these effectors, NKG2A high expression is maintained or even increased[530,531]. In agreement with this, we observed NKG2A expression in 95.2% of NK cells after expansion (**Figure 38**). On the other hand, it has been reported decreased NK cell activity in HD *ex vivo* expanded CB-NK cells in response to TGF-β due to the expression of TGFBR2[418,423]. Similarly, we found 63.5% TGFBR2$^+$ NK cells in our CAR NK cultures (**Figure 38**). Therefore, our α-BCMA CAR CB-NK cells may be susceptible to be inhibited by the high HLA-E expression in MM cells as well as by TGF-β, a factor that has been reported to be increased in the serum of MM patients[551].

To directly target these two major inhibitory pathways, we used CRISPR/Cas9 technology to abrogate the expression of NKG2A and TGFBR2 in our CAR NK cells. Twelve days after nucleofection, without any cell sorting procedure in between, we observed efficient protein reduction and gene editing (**Figures 44 and 45**). Gene editing analysis was also analyzed earlier, on day 5 after nucleofection. While flow cytometry data was similar to day 12, we found lower percentage of indels on day 5 (**Figure 43**). Because CAR NK cells were rechallenged again with aAPCs after nucleofection, following the same strategy as other groups[291,306,370,458], aAPC leftover were still present in the DNA samples analyzed on day 5 post-nucleofection, resulting in non-edited sequencing reads that reduced the overall percentage of indels. Flow cytometry analysis was not affected by aAPC presence because NKG2A and TGFBR2 expression was measured within alive CD56$^+$ cells and irradiated cells were excluded during gating strategy. Hence, analysis of gene editing efficiency, especially at molecular level, was more precise 12 days after nucleofection.

Other groups have used CRISPR/Cas9 technology to disrupt *KLRC1* and *TGFBR2* in NK cells. Reported gene editing efficiencies for *KLRC1* in PB-NK cells using electroporation and targeting exons 1 or 2 range from 36-80% and 75-85% analyzed by flow cytometry and sequencing, respectively[347,364,365,367,552]. Recently, Bexte *et al.* disrupted *KLRC1* in CAR PB-NK effectors, obtaining approximately 90% gene disruption and 55% protein expression reduction[370]. With our gene editing protocol, we achieved *KLRC1* KO efficiencies of 86.9% that correlate at the protein level (76.8% reduction), comparable with the best reported ones. Although Bexte *et al.* used the same sgRNA as the one used in our studies, they reported low editing efficiency in primary T cells[347]. However, our results are consistent with the recent knock-out efficiencies reported by Kaulfuss *et al.* in PB-NK cells[552]. Regarding *TGFBR2*, the only reported CRISPR/Cas9 gene editing efficiencies in PB-NK cells were from Naeimi *et al.* who demonstrated 60% mRNA reduction using

two sgRNAs to target *TGFBR2* exon 3[426]. Of note, our KO efficiency for this target reached the same levels in CAR CB-NK cells (61.0%) using one new sgRNA.

Notably, the simultaneous disruption of both genes was as efficient as the single knock-outs (**Figure 44**), demonstrating the great potential of CRISPR/Cas9 system to target several genes simultaneously. Regarding viability of cell cultures, we observed a reduction in the percentage of alive cells in 2KO cultures compared to control counterparts (**Figure 42**). This viability reduction could be derived from electroporating double amount of total Cas9-sgRNA RNP complex, as it was not observed in single *KLRC1* KO and *TGFBR2* KO cultures. However, cell viability was recovered one week later (**Figure 46**). Currently, there are only a few groups who have demonstrated simultaneous gene knock-outs in NK cells. Ureña-Bailen *et al.* generated triple KO CAR NK-92 cells. However, as they were using NK-92 cell line, they knocked-out each gene in a sequential approach sorting and expanding edited cells between nucleofection steps[491]. Regarding primary CAR NK cells, Bi *et al.* and Huang *et al.* are the only groups who have applied multiplex gene editing in PB-NK cells[452,497], although the first ones do not provide data on gene editing efficiencies or viability. In contrast, the latter demonstrated efficient dual and triple targeting of *TIGIT* in combination with *CD226* and/or *CD96*, reaching similar gene editing rates compared to single KO. However, cell culture viability dramatically decreased from approximately 95% to 50-60% after double and triple nucleofection. Moreover, they do not show data supporting a further recovery of the cells. In this sense, we have outperformed their results demonstrating the feasibility of generating multi-edited cells without compromising long-term viability of the cell cultures.

To introduce CAR transgene into NK cells, we used integrative competent LVs pseudotyped with VSV-G envelope. Stable NK cell transduction can be particularly arduous due to the intrinsic antiviral mechanisms in NK cells, thus different strategies have been proposed to favor the interaction between NK cells and lentivectors such as the use of cationic polymers (polybrene or protamine sulfate) or crosslinking agents such as retronectin or vectofusin-1[494]. To favor cell-vector interaction and enhance lentiviral transduction we used retronectin as well as spinoculation in our transduction protocol. Twelve days after transduction, we obtained a mean of 25% CAR^+ NK cells in both mock and 2KO CAR NK effectors with prominent variability among donors (**Figure 46**). CAR expression correlated with integrated vector copies (**Figure 47**). Theoretically, a VCN value of 0.45 would correspond to a 45% CAR expressing cells in culture. However, we observed a mean CAR transduction of 25%. As the CAR construct expression is driven by the well-studied robust EF1α promotor[553], there is low probability that CAR expression

is silenced in half of the transduced cells. Therefore, the most likely explanation is that transduced cells harbor around 2 copies of the vector per cell.

Other groups have reported slightly higher transduction efficiencies for CB-NK cells. For example, Herrera *et al.* showed 46.8% CAR transduction efficiency in CB-NK cells 7 days post transduction using LVs at the same MOI as ours, in combination with polybrene and centrifugation. Donor variability was also noticeable, ranging from 18.1 to 79.7%. However, when they studied CAR expression over time, transduction efficiency decreased to approximately 20%[277], which may indicate episomal CAR expression at early times after transduction. Unpublished results from our lab showed different transduction efficiencies in CB-NK cells for different CAR molecules targeting NKG2D-L, CD44v6 and CD72 ranging from 15 to 60%. Using γ-retroviral vectors (γ-RVs) pseudotyped with RD114 envelope, Rezvani's group has demonstrated efficient and stable CAR transductions of 60-90% in CB-NK cells. Furthermore, transduction efficiencies can also vary between donors, ranging from 23 to 90%[297,308,443,458]. Similarly, Chaudhry *et al.*[554] and Tachi *et al.*[555] reported mean CAR transductions of 93.5% and 80% using GaLV- (Gibbon ape leukemia virus) and VSG-G- pseudotyped γ-RVs, respectively. Contrary to LVs, γ-RVs are preferentially integrated near transcriptional start sites which results in a higher insertional oncogenesis risk compared to LVs[556]. Therefore, despite the good transduction outcomes using RVs, they may represent a higher risky option for translation into the clinic. A possible way to enhance NK LV transduction is to select different pseudotyping envelopes. Although VSV-G is commonly used to generate LV because of its wide tropism, NK cells express low levels of LDL-R which is the receptor that recognizes VSV-G[557]. Colamartino *et al.* showed that pseudotyping LV with Measles virus (MV) or RD144 envelopes resulted in similar low transduction efficiencies in PB-NK cells[558] although no reported results have been published in CB-NK cells yet. On the contrary, the use of envelopes derived from Baboon (BaEV) retrovirus, which recognize ASCT-1 and ASCT2 receptors, highly expressed on NK cells, has been shown to improve both transduction and integration in PB-NK cells[558-561]. In our experience, the production of BaEV-LVs with our α-BCMA CAR construct resulted in 100-fold lower titers and did not improve transduction efficiency in NK cells compared to VSV-G LV vectors. Recently, some groups have reported better vector titers up to $1x10^8$ UI/mL by optimizing BaEV-LV production protocol[562,563]. Nonetheless, these titers are still lower compared to VSV-G LVs, thereby making it difficult to generate large-scale GMP CAR NK products for clinical use. Moreover, Spanish regulatory agencies have not approved yet the use of this envelope for the generation of immune effectors in the clinical context. Another possibility could be the use of inhibitors to block intrinsic signaling pathways involved in antiviral mechanisms that may hamper NK cell transduction, such as BX-795[273].

The design of CRISPR/Cas9 knock-in strategies has emerged as an alternative approach to lentiviral or γ-retroviral vectors, allowing both CAR integration and gene knock-out in one single editing step. However, these strategies require the delivery of DNA donor templates that can be particularly challenging in the case of primary PB- and CB-NK cells, due to the high resistance of these cells to dsDNA molecules[494,495]. For example, Huang *et al.* reported really low knock-in efficiencies by introducing a HA tag or a GFP transgene in different loci by electroporation using dsDNA templates. Moreover, both single- and double-strand DNA templates were toxic to NK cells. FACS sorting after gene editing impaired NK cell proliferation[497], contrary to what they had previously observed for NK-92 cell line[496]. Nguyen *et al.* tried to improve KI efficiencies in primary cells by the design of polymer-stabilized Cas9 nanoparticles and modified DNA repair templates, reaching maximum levels of 15% efficiency[564]. Better KI outcomes (74.7%) were reported by Pomeroy *et al.* who combined CRISPR/Cas9 electroporation with AAVs to introduce a non-cleavable CD16 molecule in the *AAVS1* safe harbor locus in PB-NK cells[323]. Using the same strategy, Naeimi *et al.* reached 60% CAR knock-in efficiencies in PB-NK cells[498]. Clara *et al.* advanced the approach by designing a two-in-one KO/KI strategy using CRISPR/Cas9 and AAVs to disrupt *CD38* expression by the introduction of the non-cleavable CD16 version, achieving approximately a 50% efficiency[499]. It has been described that gene editing using AAVs is often toxic for HSPCs and may impair cell differentiation and engraftment due to prolonged persistence of AAV genomes and their fragments in the cell[565,566]. Although the combination of AAV with electroporation methods seems to be a promising approach in NK cells, none of these studies have shown data regarding cell viability, which should be assessed in detail.

Our study also showed that the disruption of *KLRC1* and *TGFBR2* did not affect CAR expression or reduced the percentage of cytotoxic cells in culture (**Figure 46**), consistent with other studies disrupting genes with CRISPR/Cas9 in CAR NK effectors[306,328,370,458].

2. Double *KLRC1* and *TGFBR2* KO CAR NK cells showed improved cytotoxic capacity against MM and are resistant to TGF-β mediated inhibition.

Once we confirmed the efficiency of gene disruption, we analyzed the cytotoxic potential of 2KO CAR NK cells against MM cell lines. Here we show, for the first time, that *KLRC1* disruption in CAR CB-NK enhanced antitumor potential against MM cell lines with different levels of HLA-E and BCMA surface expression. After combined gene editing and without the selection of edited cells, we reached almost a 20% increase in cytotoxicity against U-266 and MM.1S cells at 1:1 and 2:1 E:T ratio, respectively, and around 30% increase against RPMI-8226 and XG-1 cells at a 1:1 and

2:1 ratio. This enhanced killing capacity was mainly due to *KLRC1* ablation, as we did not observe any difference between 2KO and single *KLRC1* KO effectors (**Figure 50**). In line with this, we found higher granzyme B expression in 2KO CAR NK cells upon U-266 stimulation (**Figure 81**). The most similar approaches in a MM context, used PB-NK cells without CAR targeting. In these studies, Bexte *et al.*[347] reported a 20% increase in cytotoxicity against MM.1S and U-266 cells at a 1:1 ratio after cell sorting *KLRC1* KO NK effectors and Gong *et al.*[365] a 25% and 15% increase against RPMI-8226 and U-266, respectively, at 2:1 E:T ratio. Other studies have reported improvements in cytotoxicity ranging from 20 to 40% against other hematologic and solid tumor cell lines after eliminating NKG2A expression in PB-NK cells. In a CAR context, although not against MM, Bexte *et al.*[370] observed a 20% cytotoxicity heightening after purifying *KLRC1* KO NK cells. Other strategies such as the use of blocking mAbs have demonstrated to enhance PB-NK cell cytotoxicity against MM in a 15-20%[346] but, as we described before, could have some disadvantages. Moreover, Kamiya *et al.*[350] showed that eliminating NKG2A cell surface expression with PEBLs was able to augment NK cytotoxic potential in 40%. Our results, similarly to those of previous studies in PB-NK cells, demonstrate that NKG2A elimination in primary NK cells improves their antitumor capacity. In contrast, the finding of Mohammadian *et al.*[366] and Mahaweni *et al.*[362] suggest that targeting NKG2A through CRISPR/Cas9 editing or blocking mAbs do not confer a beneficial effect on cytotoxicity of PB-NK cells. We suspect that a potential low activation state of CAR NK effectors in these studies could be the reason of the lack of efficacy. Other studies in NK-92 cell line reported that *KLRC1* knock-out does not increase CAR NK-92 antitumor activity[368]. However, NK-92 biology differs from primary NK cells, and it can be possible that NKG2A-HLA-E signaling does not represent a dominant inhibitory signal, especially in the presence of an activating CAR molecule[368]. Furthermore, preliminary results from Kanaya *et al.* in CAR iNK cells also demonstrated that complete elimination of NKG2A through gene editing was counterproductive as it impaired NK cell licensing and, consequently, hindered NK cell maturation[369]. The lack of NK education has not been reported when knocking-out *KLRC1* in mature PB-NK cells and we have not observed it in our CAR CB-NK effectors, either.

NKG2A triggers an inhibitory signal through the activation of SHP1/2 phosphatases that inactivate downstream targets such as SYK, ERK, VAV1, FYN or STAT5. Gong *et al.* demonstrated that *KLRC1* KO NK cells showed decreased phosphorylation of SHP1 as well as higher activation of SYK, ERK, VAV1 and STAT5 upon tumor stimulation[365]. Our preliminary results suggest a similar profile in 2KO CAR NK cells with a reduction of SHP1 phosphorylation and slightly higher activation of SYK and STAT5 (**Figure 81**) although further complete phosphoproteomic studies, including more donors, are needed to unveil the complete signaling pattern. With the aim to

determine whether other immunomodulatory NK receptors may be responsible of the increased killing capacity of 2KO CAR NK cells, we characterized immunophenotypic and transcriptional changes after gene disruption (**Figures 48 and 49**). In agreement with other studies[347,367,370], we only observed minor changes in the expression of the main NK cell receptors. Among them, we found an increase in NKG2C$^+$ NK cells in both single *KLRC1* KO and 2KO CAR NK cells as Mac Donald *et al.* reported for *KLRC1* KO PB-NK cells[367]. Moreover, 2KO CAR NK cells but no single KO counterparts showed a slight decrease in the percentage of cells expressing NKG2D and TIGIT. At the transcriptomic level, we did not find great changes, as Bexte *et al.* have recently observed for CAR PB-NK cells[370]. Therefore, NKG2A elimination, *per se*, is enough to boost NK cell antitumor capacity.

On the other hand, *TGFBR2* disruption did not directly increase CAR NK potency against MM cells (**Figure 50**) or altered NK cell immunophenotype (**Figure 48**). However, it conferred resistance against TGF-β-mediated inhibition. TGF-β exerts an inhibitory function in NK cells through the downmodulation of activating receptors such as CD16, NKG2D, DNAM-1 and NKp30[406-409]. Accordingly, after treatment of CAR NK cells with TGF-β for 48 hours, we observed lower expression of these receptors in non-edited and *KLRC1* KO CAR NK cells. However, this effect was reduced in CAR NK cells in which *TGFBR2* had been knocked-out (**Figure 51**). As a consequence, 2KO CAR NK cells maintained their tumor killing capacity even under the presence of TGF-β (**Figure 50**). Although not in a MM setting, other groups have observed similar results after disrupting *TGFBR2* in PB-NK[416,417,426,427] and CAR iNK[425] cells as well as using other approaches such as the expression of TGFBR2 DNRs in CB-NK[422,423], CAR PB-NK[554] and CAR iNK[425] cells. Surprisingly, we also found that treatment of CAR NK cells with TGF-β downregulates the inhibitory receptor TIGIT, which could be associated to the natural balance of activation and inhibition signals in NK cells.

Remarkably, CAR NK cytotoxicity against primary cell lines from MM patients was also analyzed (**Figure 82**). In these experiments, CAR NK cells were co-cultured with BMMCs containing not only MM PC but also other immunosuppressive cells as well as CD34$^+$ progenitor cells. Plasma from BM samples, potentially containing soluble factors such as ADO, IDO or TGF-β as well as platelets, was also added to the culture to sustain PC and test the efficacy of the CAR NK effectors in a challenging scenario. To enhance TGF-β pressure on CAR NK cells, exogenous TGF-β was also added. Regardless of this extra TGF-β supplement, we observed approximately 30% increase (50.9% vs 16.2%) in CAR NK cytotoxicity against primary MM cells after simultaneously disrupting *KLRC1* and *TGFBR2*, corroborating that 2KO CAR NK cells have higher antitumor potential against MM and outperforming the results from Bexte *et al.*[347] who only obtained a 10% increase using

purified *KLRC1* KO PB-NK cells. Although not comparable to our study, *KLRC1* knock-out or NKG2A PEBL expression in PB-NK cells also demonstrated a 20% higher NK antitumor capacity against primary AML cells[350,370].

Another key aspect in designing more efficient CAR therapy should also be focused on minimizing off-target activity in healthy tissues. CAR T on-target off-tumor toxicities have been observed in the clinic. For example, B cell aplasia has been reported in B-ALL patients treated with α-CD19 CAR T effectors[567] and α-GPRC5D CAR T therapy has been associated with onychomadesis or mucosal toxicities[568]. Besides these target-dependent toxicities, another relevant off-target toxicities that have been associated to CAR T effectors are long and severe cytopenia[240]. However, clinical trials have shown that patients treated with α-CD19 CAR NK cells only had transient and reversible hematotoxic events (neutropenia and lymphopenia) although this was mainly associated with the lymphodepleting chemotherapy rather than with CAR NK infusion (NCT03056339[297,298] and NCT05020678[300]). Similarly, α-NKG2D-L CAR NK therapy caused grade 3 or higher cytopenia, probably related to the lymphodepletion treatment (NCT04623944)[569]. Most preclinical studies testing CAR NK cells do not study CAR NK cell toxicity against healthy cells. Leivas et *al.* demonstrated low toxicity of α-NKG2D-L CAR NK against healthy PBMCs and a lung cell line (around 20% specific lysis)[164]. They also reported a considerably toxicity against a colon cell line. However, the use of cell lines is not representative of a healthy tissue, as NKG2D-L are usually increased in these cells as a consequence of immortalization. In this study, we checked the toxic profile of both mock and multi-edited CAR NK cells against healthy PBMCs and $CD34^+$ cells from MM patients present in BM samples. We did not observe specific lysis against PBMCs and the toxicity against $CD34^+$ progenitor cells was very low (around 10%), although it varied among NK donors and patients (**Figure 82**). Importantly, despite increasing on-tumor cytotoxicity, combined elimination of *KLRC1* and *TGFBR2* in CAR NK cells did not induce significant hematologic toxicity, demonstrating the safety of this approach as a promising strategy to avoid severe long-term cytopenia.

The efficacy of 2KO CAR NK effectors was tested *in vivo* using a U-266 ffLucGFP disseminated xenograft immunodeficient NSG-Tg (Hu-IL15) mouse model. We used this strain that constitutively expresses physiological concentrations of human IL-15 (7.1 ± 0.3 pg/ml)[529] to sustain CAR NK cells in conditions that can partially ressemble patient microenvironment. We also potentiated NK support by injecting hIL-2. Additionally, inspired by the MM model designed by Alabanza *et al.*[420] we administered several intraperitoneal doses of TGF-β to test the efficacy of our CAR NK effectors in an suppressive *in vivo* environment. Using an 18:1 NK:tumor dose, we demonstrated that non edited α-BCMA CAR NK effectors reduced tumor burden and increased

mean survival from 68-70 days to 80 days. Importantly, 2KO CAR NK cells showed better tumor control and augmented mice survival up to 103 days (**Figure 86**). Other groups have demonstrated higher *in vivo* efficacy of *KLRC1* KO[367] NK cells and *TGFBR2* KO NK cells[416,417], separately, compared to non-edited cells, using a 100:1[417,437] and 4:1[416] NK:tumor dose. However, these studies focused on other hematological malignancies and solid tumors and used serial NK cell infusions. In MM, Gong *et al.* also studied the *in vivo* efficacy of *KLRC1* disruption in a U-266-bearing NSG mouse model, although they administered tumor cells subcutaneously, generating isolated tumors rather than a disseminated MM disease, therefore not being comparable with our model[365]. Hence, our results demonstrate for the first time that combined gene editing of *KLRC1* and *TGFBR2* enhances CAR NK efficacy against MM *in vivo*.

Taking altogether, we confirmed the efficacy improvement of directly targeting these two inhibitory pathways in CAR CB-NK effectors without increasing the toxicity against healthy hematological populations. However, as a result of the double gene elimination, we observed diminished *in vitro* expansion capacity, as will be discussed later, which represents the main limitation of this approach when thinking about its clinical application.

3. Disruption of *PRDM1* represents a promising approach to enhance expansion and persistence of CAR NK cells.

Another objective of this thesis was to explore *PRDM1* knock-out as a possible strategy to increase CAR NK persistence, addressing other of the main limitations of CAR NK immunotherapy. Moreover, the limited *in vitro* expansion capacity after disrupting *KLRC1* and *TGFBR2* in the effector cells, supported the consecution of this objective. To this end, we deeply characterized *PRDM1* KO α-BCMA CAR CB-NK cells by flow cytometry and RNA-seq analysis and investigated the functional consequences of disrupting this gene in terms of proliferation and NK cytotoxicity. The selection of this target was based on previous studies in which *PRDM1* gene disruption or silencing in primary NK cells resulted in an increased *in vitro* proliferation and reduced apoptotic state of the cells[469,472]. Moreover, two independent studies have demonstrated that *PRDM1* knock-out in CAR T cells conferred prolonged persistence of these effectors, and therefore augmented efficacy, and reduced T cell exhaustion[474,475]. Remarkably, despite the important role of BLIMP1 in cell cycle control, no oncogenic transformation or uncontrolled lymphoproliferation has been described after disrupting *PRDM1* in CAR T effectors. Regarding adoptive CAR NK cell therapy, to our knowledge, this is the first study that proposes a combinatorial approach targeting *PRDM1.*

To eliminate expression of BLIMP1, we designed two different sgRNAs targeting exons 4 and 5 of *PRDM1* gene thus disrupting expression of both α and β BLIMP1 isoforms. We tested both sgRNAs independently obtaining, in most cases, similar functional results. Gene editing efficiencies were high, both analyzed by Sanger sequencing (around 80-90% indels depending on the sgRNA) as well as by western blot (70-80% protein reduction). Similarly to knock down experiments of Küçük *et al.*[469] in primary PB-NK cells we found a positive selection of *PRDM1* KO CAR NK cells in culture and, as a result, the percentage of indels increased up to almost 100% without the need of cell sorting purification of edited cells (**Figure 54**), representing a great advantage for clinical applications. Interestingly, despite the low BLIMP1 protein levels, we detected *PRDM1* mRNA overexpression in *PRDM1* KO CAR NK cells compared to non-edited cells. This observation was also reported by Dong *et al.,* who attributed this effect to the loss of negative autoregulation of *PRDM1*[472].

Confirming our hypothesis, *PRDM1* KO CAR NK cells showed 16.2-fold (with sgRNA-1) and 10-fold (with sgRNA-2) increase in proliferation compared to non-edited cells one month after nucleofection which was accompanied by a higher percentage of cycling NK cells in culture (**Figure 55**). Interestingly, we additionally observed preferential selection of CAR expressing cells in culture (**Figure 59**). This is the first time that *PRDM1* expression is abrogated in CAR CB-NK effectors. Hence, there is no available data to directly compare gene editing efficiencies and *in vitro* proliferation. While Dong *et al.* used PB-NK cells for their experiments, they isolated *PRDM1* KO clones and studied cell proliferation in response to feeder stimulation but at a different time point for each clone. Other groups have reported 2-fold increased expansion of NK cells after one week culture as a result of using other strategies such as IL-15 armored CARs[445] or CRISPR/Cas9 editing of *CISH*[451] although no long-term *in vitro* monitorization was performed. In accordance with the higher proliferation capacity after *PRDM1* disruption, transcriptomic analysis revealed upregulation of several genes implicated in proliferation, survival and growth (**Table 16**). Among them, expression of *MYB*, *BCAT1* and *FGFR1* was upregulated in *PRDM1* KO CAR NK effectors coinciding with transcriptomic analysis of Dong *et al*[472]. These authors also remark on an upregulation of *MYC* and *MYC* signature in *PRDM1* KO clones, although we have not found statistically significant changes in the expression of this well-known protooncogene, which is very relevant to reduce risks of oncogenesis transformation. The differences in RNA-seq analysis outcomes are expected between studies, mainly due to the experimental setting, impeding detailed comparations. For example, these authors, as has been previously described, isolated *PRDM1* KO clones. On the contrary, in this study, although we enriched specific cell populations by cell sorting before RNA-seq analysis, our results are still representative of a

heterogeneous cell group, thus showing a more realistic overview of the final CAR NK cell product which will be administered as a pool to the cancer patients.

Importantly, *PRDM1* has been described as a tumor suppressor gene usually inactivated in NK cell lymphoma[469-471]. The reconstitution of *PRDM1* expression in *PRDM1* null cell lines induces cell-cycle arrest, demonstrating that this gene is an important inhibitor of malignant transformation[469,470]. In this setting, safety concerns may arise regarding disrupting *PRDM1* in NK cells that will be later infused into patients due to the risk of oncogenesis. Of note, it is worth noting that we observed a reduction in both Ki67 expression and percentage of cells in S-G2-M phase in *PRDM1* KO CAR NK cells as time progressed which suggests that the enhanced proliferative capacity is limited in time. The same observation was reported by Dong *et al.* for *PRDM1* KO NK clones[472]. Besides, to our knowledge, there are no studies that demonstrate that *PRDM1* is a tumor-driver gene in NK cell malignancies. Moreover, 3KO CAR NK cells, in which *PRDM1* was knocked-out, did not show uncontrolled proliferation *in vivo* as will be later described. Therefore, although more detailed studies should be performed to totally discard any risk of oncogenic transformation, for the moment, *PRDM1* knock-out using CRISPR/Cas9 seems to be a safe approach to enhance CAR NK proliferation and can be considered as monotherapy or in combinatorial regimen for treatment with CAR NK effectors.

Apart from restricting cell cycle progression, some studies have reported that *PRDM1* induces apoptosis in primary NK and NK cell lines[469,472]. We therefore analyzed the percentage of apoptotic cells in our edited CAR NK cultures at different expansion times. Viability of both non-edited and *PRDM1* KO cell cultures was maintained at 80% over time and, accordingly, the percentage of apoptotic cells was low (**Figure 57**). Hence, in our experimental setting, there is no apoptosis induction in CAR NK cells and, consequently, *PRDM1* knock-out does not confer any beneficial effect in this context.

BLIMP1 transcription factor is a master regulator of development and differentiation of different immune cells, regulating expression networks differently in a cell type-specific manner. Besides regulating cell cycle, BLIMP1 modulates maturation and differentiation of NK cells[466,468].

For example, BLIMP1 has been reported as a master regulator of T cell terminal differentiation being upregulated in KLRG1^{+} senescent CD8^{+} T cells[534,535]. In our experience, unmodified CAR NK cells expanded with our stablished protocol exhibited a proliferative profile during the first four weeks of cultivation. From that point, the expansion fold started to decrease over time until NK cells acquired a replicative senescence-like state (unpublished results) in a similar way as it was previously reported for *in vitro* expanded NK cells[459]. In this context, in this study we have

analyzed a possible regulating role of BLIMP1 in NK replicative senescence, which would contribute to the enhanced expansion observed in *PRDM1* KO CAR effectors. As expected, while time progressed, we observed an augment in the percentage of cells showing SA-β-gal activity in non-edited CAR NK cultures. However, we found a transitory reduction in the proportion of senescent cells in *PRDM1* KO cell cultures (**Figure 58**). Moreover, although KLRG1 expression changes were not statistically significant by flow cytometry analysis, we observed a slight downregulation of this exhaustion/senescent marker in *PRDM1* KO NK cells which was confirmed at the transcriptomic level (**Table 16**). These results suggest that *PRDM1* may contribute to senescence regulation in NK cells. Further telomere length and senescence-associated secretory profile (SASP) analyses would be required to completely confirm this hypothesis.

Another direct target gene repressed by BLIMP1 is *CD25,* also known as *IL2RA,* which codifies for the IL-2 receptor unit α (IL-2Rα). Indeed, BLIMP1 expression is upregulated in NK cells upon IL-2 stimulation, thus acting as a modulator and controller of IL-2 signaling. Specifically, it has been described that reconstitution of *PRDM1* in null NK cell lines strongly decreases CD25 mRNA levels and reduces sensitivity of NK cells to IL-2 stimulation[473]. Accordingly, we observed a higher expression of CD25 in *PRDM1* KO CAR NK cells by flow cytometry (**Figure 61**) suggesting increased sensitivity to cytokine stimulation and supporting an additional explanation of the enhanced *in vitro* proliferation of these edited effectors.

On the other hand, BLIMP1 plays a key role in negatively regulating IFN-γ and TNF-α secretion in NK cells, as it directly binds to *INFG* and *TNF* regulatory sequences[466]. However, when we analyzed CAR NK secretory profile in response to MM tumor cell stimulation, we did not observe increased secretion of these immunomodulatory cytokines after *PRDM1* disruption (**Figure 64**). Moreover, *INFG* and *TNF* gene expression was not upregulated at the transcriptomic level (**Table 16**). Nevertheless, other genes related to these pathways such as *TNFRSF8*, *TNFRSF11A* and *IRF4* were overexpressed in *PRDM1* KO CAR NK cells in line with the observations of other groups in PB-NK cells[472]. Besides, we found changes in mRNA expression of cytokines such as LIF, CABLES1, IL-13 and CSF-1, although were not confirmed at the protein level.

A recent study in α-BCMA CAR T cells showed that *PRDM1* disruption slightly diminished efficacy of CAR T effectors against MM cell lines and modulated cytokine production of some cytokines and cytolytic proteins[570]. On the contrary, knock down experiments in PB-NK from Smith *et al.* suggested that BLIMP1 was not associated with perforin-mediated NK cytotoxicity[466]. In this study, we detected notorious expression changes regarding activating receptors in NK cells (**Figures 60 and 61, Table 16**). For example, there was a slight downregulation of CD16 expression after *PRDM1* elimination. Moreover, expression of activating receptors such as NKp30 and NKp44

was downregulated while DNAM-1 expression, on the contrary, was enhanced in *PRDM1* KO CAR NK cells. Additionally, expression of inhibitory receptors such as NKG2A was also decreased. A similar tendency was observed for TIGIT and, as mentioned before, for KLRG1. Some of these changes were confirmed at the transcriptomic level. Additionally, we found differential gene expression of other activating receptors not included in the flow cytometry panel. For example, *LILRA2* or *KLRF2* were downmodulated while *CD86* and *TLR4* had increased expression. However, despite all these immunophenotypic changes and the increased proportion of CAR^+ NK cells, *PRDM1* KO CAR NK cultures maintained the same killing and degranulation capacity against MM cell lines (**Figures 63 and 64**) confirming that *PRDM1* ablation can increase CAR NK proliferation *in vitro* without compromising their killing capacity or affecting their cytokine secretion, thus representing a promising tool to facilitate clinical dose achievement as well as to increase CAR NK persistence.

4. Limited proliferation of double KO CAR NK cells can be overcome by additional *PRDM1* disruption

Although we demonstrated higher antitumor efficacy of CAR NK cells after simultaneous disruption of *KLRC1* and *TGFBR2*, we observed a limited expansion capacity of these cells *in vitro*, compared to non-edited counterparts (**Figure 53**). Electroporation, *per se*, was not the responsible of a diminished proliferation as there were no differences between mock and non-nucleofected controls in terms of expansion. However, this is not the case of RNP delivery, that clearly impacts on edited CAR NK expansion. We observed lower proliferation in single KO CAR NK cells, especially in *KLRC1* KO cultures, but the effect was more noticeable after targeting both genes at the same time. As previously described, although 2KO CAR NK cells showed reduced viability after nucleofection, it was later restored, suggesting that this is not the cause of the reduced expansion of the cells.

With the aim to elucidate the mechanisms responsible for this effect, we analyzed the apoptosis and senescence state of the CAR NK effectors on day 19 after nucleofection, time in which growth differences between edited and control cells were prominent. Regarding other studies in PB-NK cells, Gong *et al.* reported similar expansion of mock and *KLRC1* KO NK cells[365], but proliferation was only monitored until 6 days after nucleofection. On the contrary, two other groups have observed reduced expansion capacity in *KLRC1* KO CAR NK cells since nucleofection up to 3 to 6 weeks later[367,370] suggesting that *KLRC1* deletion, in some way, may impair NK cell expansion. Accordingly, a recent study from Kaulfuss *et al.* demonstrates that NKG2A checkpoint plays a

direct role in maintaining expansion capacity of human NK cells by dampening both proliferative activity and excessive activation-induced cell death[552]. However, contrary to these authors, when we analyzed apoptosis in our CAR NK cell cultures, we did not observe an increase in apoptotic cells in *KLRC1* KO or 2KO effectors (**Figure 53**). On the other hand, as far as we know, there are no studies analyzing the proliferation capacity of *TGFBR2* KO NK cells or multi-edited effectors which could explain the lower proliferation in 2KO CAR NK effectors compared to single KO counterparts. Unfortunately, we did not observe any increase in the number of senescent cells in edited cultures or found any relevant gene differentially expressed between mock and 2KO CAR NK cells that could explain the limited expansion capacity. Importantly, although no differences were observed at the transcriptomic level, a preliminary WB analysis, which should be confirmed in more donors and with other techniques, reveals higher accumulation of p-H2AX and p53 in both single and 2KO CAR NK cells compared to non-edited cells suggesting that these cells accumulate high DNA damage. Moreover, p16 expression was increased in 2KO CAR NK cells (**Figure 70**). The higher p53 and p16 expression induced by gene disruption could be associated with cell cycle arrest of multi-edited CAR NK cells explaining the limited expansion capacity. Furthermore, time point of analysis may result crucial in these experiments. Although we chose day 19 post-nucleofection as the time to perform the analyses because of the growth differences, the mechanisms hampering expansion may be induced earlier explaining why we did not observe any differences in apoptosis, senescence or even at the transcriptomic level. For example, experiments from Kaulfuss *et al*. were performed 6 days after nucleofection[552]. Hence, once the results have been seen, earlier analysis could be more informative.

Although we observed higher *in vivo* efficacy of 2KO CAR NK cells compared to non-edited cells, the limited expansion capacity may reduce cell persistence and consequently, would limit long-term efficacy. Moreover, a lessened *in vitro* expansion capacity could become a barrier to achieving sufficient clinical doses of NK effectors. Due to the impressive proliferation improvement after knocking-out *PRDM1* in our CAR NK effectors, we proposed to include this target gene in our multiplex CRISPR/Cas9 system to increase the expansion capacity of 2KO CAR NK cells.

A first approach was tested by electroporating the three RNP targeting each gene in the same nucleofection step (*one-shot*). In terms of efficacy, we achieved good editing rates similarly to the ones obtained for single KO and 2KO cells (**Figure 65**). Nevertheless, similarly to Huang *et al.*[497], we observed a decreased viability in 3KO CAR NK cultures. Regarding *in vitro* cell expansion, although we did not directly compare 2KO and one-shot 3KO conditions, we observed the similar fold expansion in 3KO cells compared to non-edited controls suggesting a moderate

improvement compared to 2KO effectors. However, *one-shot* 3KO CAR NK cells did not expand as strongly as single *PRDM1* KO cells (**Figure 66**). Suspecting that simultaneous triple DSBs and high amounts of total sgRNA-Cas9 RNP may be counterproductive, we designed an alternative strategy using two sequential nucleofection steps, conferring NK cells the *PRDM1* KO-mediated proliferative advantage before targeting the other genes and dividing RNP dose in two steps. Using this approach, gene editing efficiencies were also maintained with respect to single KO and 2KO (**Figures 67 and 68**). Cell viability was reduced, as expected following two electroporation procedures, but, importantly, it did not affect *in vitro* expansion of CAR NK effectors, which was significantly higher compared to the *one-shot* 3KO counterparts (**Figure 69**). The higher DNA damage accumulation in *one-shot* 3KO cells compared to *sequential* 3KO cells, observed in a preliminary WB analysis, may explain these growth differences (**Figure 70**).

We observed that the viability of *sequential* 3KO CAR NK cell cultures was lower and the percentage of apoptotic cells was increased compared to non-edited cells and *PRDM1* KO parental cultures, on day 19 after the first electroporation (which corresponds to 11 days after the second nucleofection round). This could be expected after two electroporation shots. However, as time progressed, viability was restored (**Figure 72**). Indeed, 3KO CAR NK cells showed similar *in vitro* expansion and proliferative potential as single *PRDM1* KO CAR NK cells (**Figure 71**). After 30 days of expansion after genetic modifications, the mean fold expansion of the 3KO CAR NK cells was 400, being compatible with the achievement of the needed clinical doses (1×10^6 - 1×10^7 cells/kg[297]).

Similar to what we had observed in *PRDM1* KO CAR NK cells, elimination of *PRDM1* reduced the percentage of senescent cells in 3KO CAR NK cell culture, contributing to the cumulative cell expansion (**Figure 74**). Importantly, as we described before, the growth advantage derived from *PRDM1* ablation was limited, as proliferative potential of 3KO CAR NK cells decreased over time. Besides, we observed that there was no clonal selection of specific edited populations as the percentage of NKG2A$^-$ TGFBR2$^-$ NK cells and the percentage of indels in the three target genes were maintained (**Figure 75**).

Overall, the combination of *PRDM1* ablation with sequential nucleofection steps, has emerged as a novel strategy to generate high numbers of multi-edited CAR NK cells without impairing their proliferative potential.

5. Multiplexed CRISPR/Cas9 technology represents a safe approach to genetically modify CAR NK cells

While the new generation of Cas9 nucleases, such as HiFi variants, have demonstrated highly precise gene editing capacity with reduced off target activity[93], sgRNA design is an important factor to take into account to avoid undesired gene editing events. In this thesis, besides predicted efficiency scores, the possible off-target recognition of specific loci constituted an important characteristic to choose the best sgRNAs. Hence, sgRNAs with either high probability of off-target recognition or possibly targeting off-target exonic regions were discarded during the selection of optimal sgRNAs. However, none of the designed sgRNAs was exempt from a minimal possible mismatched recognition. Therefore, to guarantee the safety of our CAR NK effectors and confirm the high editing precision of the selected sgRNAs, we decided to analyze the presence of indels in all the predicted off-target loci which could be recognized by our sgRNAs with up to 3 mismatches. To ensure the detection of the potential off-target activity, NGS was performed to analyze the top *in silico* predicted loci, as previously performed in other studies[323,347]. Our preliminary results in one donor indicated practically null sgRNA off-target activity (**Figure 83**). A small proportion of NGS reads with different sequences were found in 3 out of 12 *TGFBR2* sgRNA off-targets sites in both 2KO and 3KO CAR NK samples and in 1 out of 3 *PRDM1* sgRNA off-target sites in 3KO CAR NK cells. However, these altered reads were also present in mock samples in the same proportion, suggesting that they could be donor-dependent variants or, most probably due to their low proportion, sequencing artefacts. We only found a minimal off-target activity in *KLRC1* off-target site 3 in 3KO CAR NK cells. However, it is likely to be a sequencing artefact rather than being derived from *KLRC1* sgRNA as it was not detected in the 2KO CAR NK sample. Additionally, this off-target site is located in an intergenic region. Therefore, we conclude that the selection of sgRNAs was optimal, not only in terms of on-target efficacy, but also ensuring lack of off-target activity.

On the other hand, it has been reported that inducing multiple DSBs at the same time can lead to chromosomal translocations within the on-target sites in both triple edited NK-92 and PB-NK cells[496,497] as well as in CAR T cells[571,572]. These groups designed strategies to specifically detect translocations generated by on-target Cas9 activity. However, in this study, we opted for a whole genome screening system to further confirm the lack of off-target DSB-induced translocations. Contrary to the reports from Huang *et al.* in PB-NK cells[497], we did not observe any detectable translocations in 2KO or 3KO CAR NK cells derived from 3 independent donors 19 days after gene editing (**Figure 84**). The limit of detection of optical genome mapping (OGM) techniques range

between 1-5% for this type of chromosomal structural variations. Huang *et al.* used PCR to detect predicted translocations resulting in higher sensitivity but lacking frequency quantification. Moreover, these authors did not specify the time in which they detected translocations with respect to nucleofection. The studies performed in multi-edited CAR T cells used quantitative techniques and detected translocations frequencies ranging from 0.01 to 6% in early times after nucleofection (3 or 5 days)[571,572]. Importantly, a long-term analysis showed that the frequency decreased over time both in culture and *in vivo* and reached the limit of detection in most cases, suggesting that these structural variations did not confer a positive selection advantage to T cells[571]. Although we cannot discard the generation of DSB-induced translocations just after gene editing, our results guarantee that our 2KO or 3KO CAR NK effectors do not harbor oncogenic-risk translocations at the time as they would be infused into patients.

In relation to the appearance of translocations, other CRISPR/Cas9-related genotoxicities such entire chromosome loss have been reported in edited T cells, especially when there is poor expression of *TP53*[539]. Cas9-produced DSBs induce the activation of the p53 pathway as a control barrier which needs to be overcome by the edited cell to avoid cell cycle arrest or senescence or apoptosis induction[573]. It has been described for cell lines and HSPCs, that CRISPR/Cas9-induced *TP53* upregulation may favor the expansion of mutant or inactive *TP53* clones in culture[574,575]. Moreover, this would allow the proliferation of more DNA-damage tolerant[575] or, even, aneuploid clones. A clonal selection of cells with altered *TP53* expression as well as containing aneuploids could enhance the risk of oncogenic transformation of the CAR effectors. On the contrary, CRISPR/Cas9-derived TP53 inactivation has not been observed in clinical trials using CRISPR/Cas9-edited HSPCs[576,577]. Our bulk RNA-seq analysis did not reveal repression of *TP53* in 2KO or 3KO CAR NK cells. Additionally, we observed expression of p53 protein by WB analysis in our multi-edited CAR NK effectors. Further single-cell transcriptomic analysis and even deep sequencing of this important gene would be necessary to discard the presence of mutant or inactive *TP53* clones.

Furthermore, we could confirm the lack of entire chromosomal loss in multi-edited CAR NK effectors with our OGM analysis. The whole genome screening allowed us to detect other types of large structural variations such as insertions, deletions and duplications with a minimal size of 5000 bp as well as CNV gains and loss. Most of the chromosomal alterations were present in mock counterparts, suggesting that they were not associated with Cas9 activity. Instead, we hypothesize they are donor-dependent variants or acquired during the *ex vivo* expansion process. Only a few alterations emerged in 2KO and 3KO (**Table 19**) although they seem not to be a consequence of CRISPR/Cas9 activity as they do not co-localized with on-target or predicted

off-target sgRNA sites and are different in each donor and condition (2KO and 3KO). Even so, we analyzed the potential effects that could generate in the final CAR NK product using gene and disease databases. For example, 2KO CAR NK cells from donor #1 had two duplications located in chromosome 10 and chromosome X. Duplication in chromosome 10 englobed 7 different genes (*PTPN20, FRMPD2B, AGAP13P, BMC1P1, GLUD1P2, FAM25C* and *AGAP12P*). As far as we found in bibliography and genomic databases, none of these genes played an important role in NK cell biology nor are related to oncogenesis. Duplication in chromosome X comprised *SNORA11D* and *MAGED4*. High expression of *MAGED4* has been reported as a poor prognosis marker in melanoma, glioma, esophageal and oral squamous cell carcinoma, squamous cell lung cancer and colorectal cancer[578-582]. *In vitro* studies have demonstrated that this protein promotes cell proliferation and migration[578,579]. However, it has been reported that cancer-related *MAGED4* overexpression is mainly regulated by DNA methylation[580]. Moreover, ClinVar database did not contain a duplication with similar to the one we found in this sample. Additionally, as far as we know, no important role has been described for *MAGED4* in NK cells. Therefore, considering that these cells did not show any striking behavior *in vitro*, our data suggest that 2KO CAR NK functionality is not affected by this spontaneous duplication. Within the same donor, 3KO CAR NK cells had two different duplications. Duplication in chromosome 11 did not affect any gene sequence. Duplication in chromosome 16 only affected *NPIPB8* which codifies for a nuclear-pore complex protein. However, we neither found any reported evidence that this protein could lead to an oncogenesis process or alter NK cell biology. Regarding donor #2, we only found an insertion in chromosome 5 of 3KO CAR NK cells. This insertion co-localized with *SDHA* and *PDCD6-DT* loci. *SDHA* mutations have been associated with mitochondrial respiratory chain deficiencies and neurodevelopment processes[583] but not with special relevance in NK cell biology. As for *PDCD6-DT*, it has been described as a lncRNA with unknown function.

Finally, concerning donor #3, 2KO CAR NK cells showed a duplication in chromosome 20 and an insertion in chromosome X. Duplication englobed *ZNF337, LOC105372582* and *FAM182B* genes. *ZNF337* has been described as a prognostic biomarker in different cancers. *In vitro* experiments suggested that its function is directly associated with proliferation and migration[584]. *FAM182B* has been reported to be overexpressed in hepatic tumor samples[585] but not direct relation with oncogenesis process has been yet demonstrated. Although these two genes are cancer-related genes, specific duplication of this small region was not registered in ClinVar database and special roles have not been reported in NK cells. As for insertion in chromosome X, its size was under Bionano's OGM detection threshold (5000 bp) and it was not located in any gene locus. Within the same donor 3KO CAR NK cells showed two CNV gains in chromosomes 3 and 17. Although

ClinVar database contains CNV gains similar in size, no clear phenotype is provided for them. Within all the genes englobed in CNV gain in chromosome 3, *UBXN7, RNF168, CEP19, HNRNPU-AS1* and *IQCG* are cancer-related genes according to Network of Cancer Genes and Healthy Drivers and The Cancer Genome Atlas database. Among these, only overexpression of *RNF168* has been closely related to enhanced proliferation, migration and drug resistance in different tumors[586]. Regarding genes englobed in CNV gain in chromosome 17, only *PLXDC1* was associated with cancer. Overexpression of this gene is a biomarker for poor prognosis in gastric cancer and hepatocellular carcinoma[587,588] and it has been reported that promotes cancer cell migration[589]. To our knowledge, none of these genes are directly related to NK cell function. Although some of the affected genes seem to be implicated in tumor development, allelic frequencies for these CNV were low (0.13 and 0.20) which suggests that they do not confer a proliferative advantage to the cells. Moreover, these frequencies are near to the CNV detection limit of OGM (15-20%) so should be confirmed by more directed techniques with higher sensitivity.

In summary, in this thesis we have demonstrated that multiplex CRISPR/Cas9 using HiFi Cas9 variant and highly precise sgRNAs is a safe approach to genetically modify CAR NK effectors without inducing detectable off-target activity or chromosomal translocations. Some random structural variations could appear in the expansion process but are not related to gene editing and should be individually studied for each NK donor.

6. Highly proliferative triple KO CAR NK cells preserve the antitumor efficacy of 2KO CAR NK effectors *in vitro*

As expected, 3KO CAR NK cells harbor other features described for single *PRDM1* KO CAR NK cells besides the higher proliferation capacity, as a consequence of abrogating BLIMP1 expression. Among them, we observed a higher CAR expression compared to non-edited cells together with a positive selection of CAR^+ cells in culture over time (**Figure 77**). Phenotypic changes such as the increase of DNAM-1, CD25 and TIGIT expression or the downregulation of NKp30 and NKp44 were also observed in 3KO CAR NK effectors (**Figure 78**). However, contrary to *PRDM1* KO cells, 3KO CAR NK cells showed the same CD16 expression as non-edited cells. Paradigmatically, although 2KO CAR NK cells showed higher expression of NKG2C by flow cytometry, the expression of this receptor in 3KO CAR NK cells was lower than in non-edited cells probably due to internal compensatory mechanisms of NK cells.

At the transcriptomic level, most of the observed changes in *PRDM1* KO CAR NK effectors were detected in 3KO CAR NK cells, although new hits with special relevance that were not statistically significant in single KO cells appeared in 3KO CAR NK cells. Based on the fact that *KLRC1* and *TGFBR2* knock-out did not induce transcriptomic changes, these differences could arise from the low number of samples (n=3) with high inter-donor variability. Moreover, when we compared RNA-seq results from *PRDM1* KO and 3KO CAR NK cells, no genes appeared to be differentially expressed (data not shown). Independently of this, the general transcriptomic profile of 3KO CAR NK cells in comparison to non-edited cells was similar to the one obtained for PRDM1 KO CAR NK effectors (**Figure 79, Table 17**). In general, we observed enrichment in genes associated with proliferation and cell survival as well as with TNF-α and IFN-γ signaling. Interestingly, we found that the suppressor of cytokine signaling *CISH* was upregulated in 3KO CAR NK cells. This could be a compensatory mechanism to the upregulation of *CD25* to control NK cell response to cytokine stimulation. On the other hand, some activating and inhibitory receptors were also downregulated. Other genes such as *CD27*, *KLRG1* and *IKZF3* which are associated with a late maturation phenotype of NK cells and genes encoding for cytotoxic molecules such as *PRF1* and *GZMB* were repressed in 3KO CAR NK cells. Together, these results indicate that 3KO CAR NK cells closely resembled a more immature $CD56^{bright}$ phenotype rather the $CD56^{dim}$ terminally differentiated one and confirm the possible role of BLIMP1 in human NK cell maturation, as has been recently shown by Liu *et al*[590]. Finally, GSEA analysis showed enrichment of cell adhesion molecules in 3KO CAR NK cells. Moreover, *SELL* (encoding for L-selectin) and the chemokine receptor *CCR7* stood out among the most upregulated genes, suggesting that 3KO CAR NK effectors may show enhanced migration capacity towards secondary lymphoid tissues.

A more immature NK phenotype could be associated with a lower cytotoxic capacity of the cells. However, the additional disruption of *PRDM1* did not interfere with the enhanced cytotoxic capacity and the TGF-β resistance which had been obtained by *KLRC1* and *TGFBR2* knock-out. Our 3KO CAR NK effectors demonstrated to be as cytotoxic as 2KO CAR NK cells both against MM cell lines and primary patient cells outperforming non-edited cells (**Figures 80 and 82**). At the phosphoproteomic level, our preliminary results suggest that 3KO CAR NK cells have reduced activation of SHP-1 phosphatase as a consequence of *KLRC1* knock-out and therefore, SYK/ZAP70 activation was higher (**Figure 81**). Interestingly, 3KO CAR NK cells showed increased phosphorylation of STAT5, a signaling transducer of IL-2 pathway, being in accordance with the enhanced expression of CD25 in 3KO CAR NK cells. Importantly, our cytotoxicity assays against healthy PBMCs and MM $CD34^{+}$ progenitor cells demonstrated the same low hematotoxicity as 2KO CAR NK cells (**Figure 82**).

Altogether these results suggest that the increased activating signals derived from CAR expression and IL-2 stimulation together with the elimination of the inhibitory NKG2A checkpoint could counteract the less mature phenotype shown by 3KO CAR NK cells resulting in a final product with the same *in vitro* antitumor capacity as 2KO CAR NK effectors but with higher expansion potential.

7. Triple KO CAR NK cells show higher persistence and efficacy against MM *in vivo*

In this study, the *in vivo* persistence and efficacy of 3KO CAR NK effectors was also evaluated and compared to non-edited and 2KO CAR NK cells. The enhancement of the cell proliferative capacity aims not only to achieve clinical doses *ex vivo,* which has been already demonstrated in this thesis, but also to increase the *in vivo* persistence of the CAR NK therapy, thus obtaining better outcomes. In this sense, we observed that 3KO CAR NK cells persisted longer in PB after infusion than non-edited and 2KO CAR NK cells (**Figure 85**). Moreover, at necropsy, we could find NK cells in the BM of some of the animals treated with 3KO CAR NK cells but not in the mice treated with 2KO or mock CAR NK cells. Importantly, this higher persistence of 3KO CAR NK did not result to be oncogenic, at least up for the 150-day follow-up. On the one hand, PB analysis on day 30 after NK infusion and at necropsy demonstrated that 3KO CAR NK cells had completely disappeared from circulation, confirming absence of uncontrolled systemic expansion and suggesting the safety of multiplex edited CAR NK cells. On the other hand, the proportion of NK cells found in BM at necropsy was low, even when minimal detectable disease is present in the mouse, or in one free-detectable disease animal, which was maintained alive for 150 days after therapy infusion. These results, together with the proliferation kinetics observed *in vitro*, support the safety of 3KO CAR NK effectors in terms of oncogenesis.

Despite persistence differences, in general, PB NK infiltration was low for all the NK-treated groups. *In vivo* experiments from Rezvani's group showed 50% and 20% infiltration of non-edited CAR CB-NK on day 7 and 14 after infusion, using similar doses of cells (10×10^6 cells)[458]. However, their CB-NK cells contained an IL-15 armored CAR. Indeed, in a previous study, CAR CB-NK cells without IL-15 armoring were not detectable on day 21 after the infusion[443]. Moreover, contrary to those studies, our model represents a more challenging environment generated by multiple TGF-β infusions which may influence CAR NK *in vivo* persistence. Importantly, we observed NK BM infiltration at necropsy in two 3KO NK-treated mice as well as an almost complete tumor clearance in the BM of all animals from this group. These observations together with the BM-

migration transcriptomic profile of 3KO CAR NK cells, suggest that these effectors efficiently infiltrate BM thus explaining the lack of detection in PB. Further studies with different NK donors should be performed including BM analysis at different time points to confirm the higher BM infiltration of 3KO CAR NK cells.

Regarding antitumor efficacy, 3KO CAR NK cells showed better tumor control than 2KO CAR NK cells (**Figure 86**). Untreated as well as both mock and 2KO CAR NK-treated animals developed clinical symptoms of a late-stage BM resident MM (high MM infiltration causing paraplegia, ataxia and bloodstream egression in some cases). On the contrary, a really low proportion of MM cells were found in the BM of mice treated with 3KO CAR NK cells demonstrating the higher efficacy of these effectors. However, three mice treated with 3KO CAR NK cells succumbed to the disease because of tumor scape of PC to the cranial vault. Cranial plasmacytomas have been described in MM patients and sometimes derive in MM intracranial involvement, a rare MM complication with poor prognosis that has been associated with unfavorable cytogenetic abnormalities in malignant PCs and therapy-induced TME changes[591]. The migration of U-266 cells towards the cranium due to an efficient immunosurveillance of 3KO CAR NK cells in BM seems to resemble that clinical complication observed in MM patients. This aggressive complication led to premature death of the animals probably justifying the lack of statistical differences between 2KO and 3KO CAR NK effectors in terms of overall survival. Nevertheless, it is worth mentioning that, while none of the animals treated with 2KO CAR NK survived, 40% of mice from the 3KO group did not develop MM and 152 days after tumor injection, no malignant plasma cells were detected in BM, CD or PB. These results demonstrate the higher *in vivo* antitumor efficacy of 3KO CAR NK cells compared to 2KO CAR NK cells.

8. Study limitations

This study has certain limitations. For example, we have demonstrated that both 2KO and 3KO CAR NK cells show great antitumor efficacy *in vitro* against primary malignant PC from MM patients. However, only one MM sample was from a RRMM patient, due to the difficulty to obtain BM samples from these patients with a minimal volume and PC infiltration to perform the *in vitro* assays. As CAR NK therapies would be applied in a RRMM context and malignant PC from these patients show higher therapy resistance than those from NDMM, it would be necessary to test the efficacy of our CAR NK effectors against more RRMM patients, to support the clinical application of this therapy.

Regarding efficacy, we also tested *in vivo* activity of multi-edited CAR NK cells in NSG mice that constitutively express human IL-15. Although we administrated exogenous hIL-2 to support NK cell grow as well as hTGF-β to mimic an inhibitory MM environment to test functionality of *TGFBR2* KO, this does not completely resemble MM TME. A humanized mouse model engrafting not only primary MM cells, but also a complete immune system from the same patient, to study the efficacy of these combinations in the human context would have reported more accurate results. However, the difficulty of engrafting primary MM cells as well as a complete TME[592] reflect the lack of PDX-His MM mouse models to properly evaluate treatment efficacy and adverse effects such as therapy derived off-tumor toxicities, CRS or cytopenia. Regarding our *in vivo* studies, we have also found other limitations. U-266 migration to the head in response to the efficient BM immunosurveillance of 3KO CAR NK effectors, caused premature death of some of the animals. Therefore, despite two 3KO NK-treated animals were completely cured after 5 months from tumor injection, no statistical significances were found between 2KO and 3KO NK-treated groups in terms of survival. To obtain more robust evidence of the efficiency of 3KO CAR NK cells, replicate *in vivo* experiments should be performed to increase sample number. On the other hand, as intravenous 3KO CAR NK therapy was not enough to fight aggressive cranial MM complications in mice, further strategies should be considered in this cases, such as the localized intracranial injection of CAR NK therapy[416,555,593] which could be simultaneously administered to the intravenous dose.

9. Future perspectives

We propose future experiments to continue with this line of work. For example, despite the objectives of this thesis are mainly focused on the clinical translation of enhanced α-BCMA CAR CB-NK effectors, we have slightly investigated the changes in molecular signaling mechanisms after disrupting *KLRC1*, *TGFBR2* and *PRDM1* through CRISPR/Cas9 genome editing. A deepest phosphoproteome study in more CAR NK samples as well as including other proteins downstream NKG2A (VAV-1, SHP-2 and FYN), TGFBR2 (SMAD2/3) or cytokine signaling (JAK/STAT, PI3K/AKT and RAS/MAPK/ERK), or proteins that participate in CAR NK cell synapsis, would provide a deeper knowledge about the balanced intracellular signals that trigger effector functions in multi-edited CAR NK cells.

Moreover, we hypothesized that higher CD25 expression after *PRDM1* ablation may contribute to the enhanced *in vitro* expansion of CAR NK effectors. However, we have not analyzed growth kinetics *in vitro* and *in vivo* in the absence of cytokine stimulation. Daher *et al.* observed that

CISH knock-out only conferred growth advantage in an IL-15 stimulation context[458]. As *PRDM1* plays other functions in directly modulating cell cycle, it is less probable that the growth advantage totally disappeared in cytokine-restricted conditions. Nevertheless, these experiments would be interesting to discard that *PRDM1* KO-induced proliferation is not completely cytokine-dependent.

Finally, although we have demonstrated that multiplex CRISPR/Cas9 is an efficient and safe tool to disrupt the expression of genes and potentiate the efficacy of CAR NK immunotherapies, new generation CRISPR approaches are currently breaking through such as base editing and prime editing. These technologies allow DSB-free and precise genetic modification. Prime editing efficiency needs to be yet improved before being applicated in a multiplexed context. However, in continuation with this line of work, the use of base editors to disrupt expression of *KLRC1*, *TGFBR2* and *PRDM1* could be an interesting approach to minimize DSB generation in edited CAR-NK cells, and consequently, the induction of DDR pathways which, in turn, may favor NK cell expansion.

In summary, we propose two CRISPR/Cas9 approaches to enhance CAR CB-NK therapies for the treatment of RRMM. First preclinical data combining *KLRC1* and *TGFBR2* disruption in α-BCMA CAR NK cells demonstrate an enhanced efficacy against MM cells and resistance to MM TME-immunosuppression although impair NK proliferative potential. Furthermore, we have knocked-out *PRDM1*, for the first time, in α-BCMA CAR NK effectors, demonstrating improved *in vitro* expansion capacity. Finally, we combined these two independent strategies to obtain a first-in-class triple KO α-BCMA CAR CB-derived NK product with improve *in vivo* persistence and efficacy against MM (**Figure 88**).

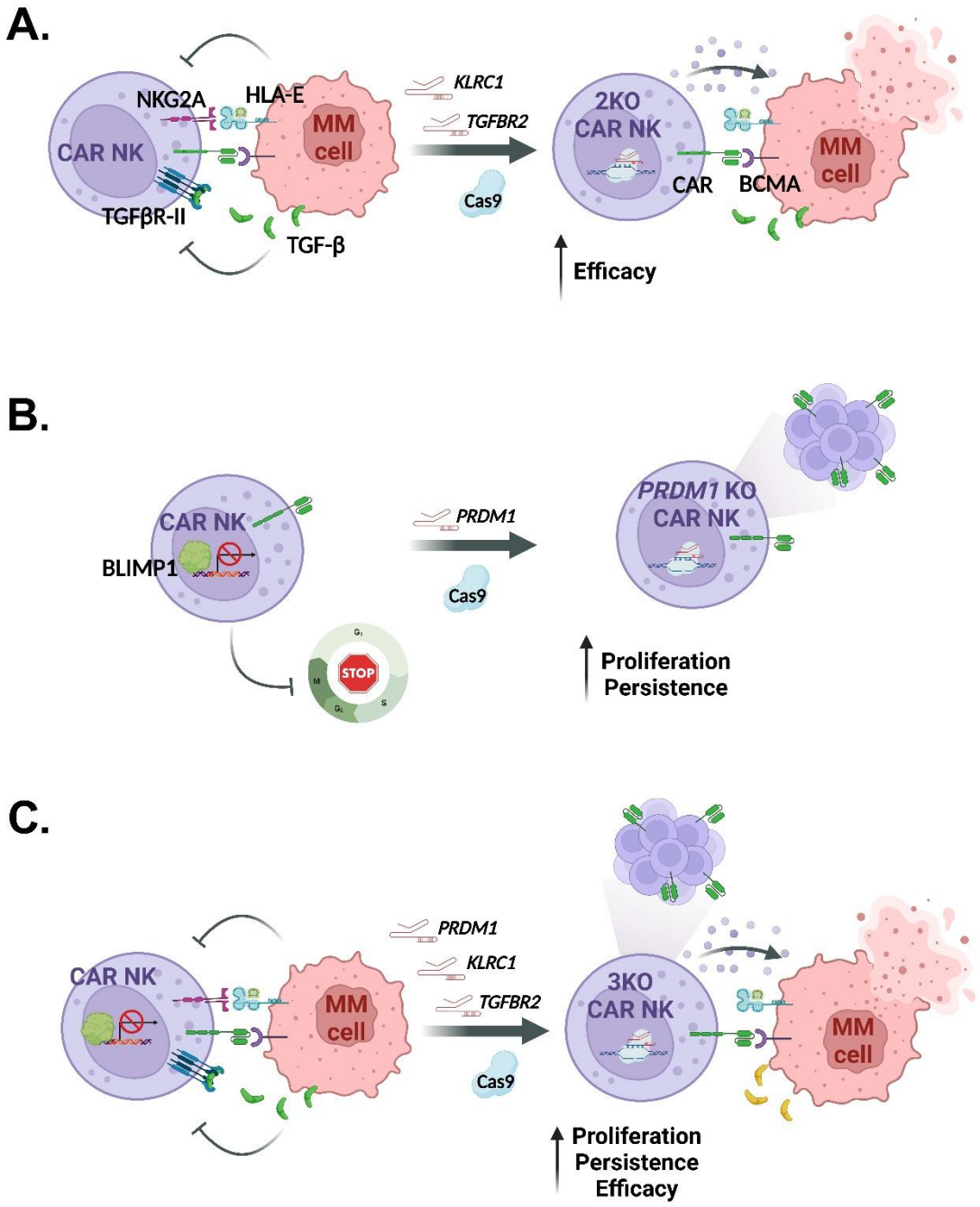

Figure 88. Multiplexed gene disruption using CRISPR/Cas9 genome editing enhances CAR NK immunotherapy. A. CAR signaling, together with native activating receptors, augment NK cell cytotoxicity against tumor cells. However, inhibitory signals triggered by the immune checkpoint NKG2A as well as by TGF-β signaling impair efficient NK killing. CRISPR/Cas9-mediated gene disruption of *KLRC1* and *TGFBR2* improves CAR NK antitumor killing. **B.** Expression of BLIMP1 in *ex vivo* expanded CAR NK cells controls cell proliferation limiting NK expansion capacity. *PRDM1* knock-out in CAR NK cells using CRISPR/Cas9 increase NK proliferative potential *in vitro*, without compromising CAR NK cytotoxic activity. **C.** Multiplex CRISPR/Cas9 genome editing allows the generation of a CAR NK product with enhanced expansion capacity and higher *in vivo* persistence and antitumor efficacy against MM. CAR: chimeric antigen receptor; NKG2A: natural killer group 2 member A; HLA: human leukocyte antigen; TGF-β: transforming growth factor β; TGF-βRII: TGF-β receptor II; BCMA: B-cell maturation antigen; 2KO: double knock-out; BLIMP1: B lymphocyte-induced maturation protein-1; 3KO: triple KO. Created with BioRender.com.

CONCLUSIONES

Las principales conclusiones obtenidas en esta tesis doctoral se enumeran a continuación:

Objetivo 1

1. La edición genómica multiplexada mediante CRISPR/Cas9 de *KLRC1* y *TGFBR2* en células α-BCMA CAR NK derivadas de sangre de cordón umbilical es factible y no compromete la viabilidad celular ni la expresión del CAR.
2. La interrupción combinada de *KLRC1* and *TGFBR2* en células α-BCMA CAR NK incrementa su eficacia antitumoral *in vitro* e *in vivo* comparado con los efectores sin editar, les confiere resistencia a la inhibición mediada por TGF-β pero disminuye su potencial proliferativo.

Objetivo 2

3. El aumento de la eficacia *in vitro* de las células α-BCMA CAR NK doble editadas se asocia a una mayor actividad de la célula NK mediada por un aumento de la señalización integrada de quinasas y por la producción de granzima B, sin alteraciones relevantes en el inmunofenotipo y en el transcriptoma.

Objetivo 3

4. La eliminación de la expresión de *PRDM1* potencia la expansión *in vitro* de las células α-BCMA CAR NK mediante el aumento de su capacidad proliferativa y el retraso de la inducción de senescencia, sin comprometer la eficacia de los efectores CAR NK frente a células de MM.

Objetivo 4

5. La eliminación de *PRDM1* en combinación con *KLRC1* y *TGFBR2* en los efectores α-BCMA CAR NK mejora su capacidad de expansión preservando la potencia citotóxica *in vitro* frente a células de MM *in vitro* de la población doble editada.
6. Las células α-BCMA CAR NK triple editadas no generan hematotoxicidad relevante sobre células maduras de sangre periférica de donantes sanos ni sobre progenitores $CD34^+$ de pacientes de MM.
7. La eliminación simultánea de *KLRC1*, *TGFBR2* y *PRDM1* mediante CRISPR/Cas9 utilizando la nucleasa Cas9 HiFi y sgRNAs altamente precisas es una estrategia segura que no produce actividad detectable fuera de la diana en las regiones esperadas ni genera grandes alteraciones cromosómicas como translocaciones, inversiones y aneuploidías.
8. Los efectores α-BCMA CAR NK triple editados tienen una mayor persistencia *in vivo* en sangre periférica y médula ósea en comparación con los efectores doble editados.

9. El tratamiento con células α-BCMA CAR NK triple editadas demuestra una mayor eficacia frente a MM *in vivo* y resulta curativo en 40% de los animales tratados.

CONCLUSIONS

The main conclusions obtained in this doctoral thesis are the following:

Objective 1

1. Multiplex CRISPR/Cas9 genome editing of *KLRC1* and *TGFBR2* in α-BCMA CAR NK cells from cord blood samples is feasible and does not compromise cell viability and CAR expression.
2. Combined disruption of *KLRC1* and *TGFBR2* in α-BCMA CAR NK cells potentiates their antitumor efficacy both *in vitro* and *in vivo* compared to non-edited effectors and provides them with resistance to TGF-β-mediated inhibition without cell selection, but lessens their proliferative potential.

Objective 2

3. The enhanced *in vitro* efficacy of double KO α-BCMA CAR NK cells is associated with a higher NK function mediated by an increase in kinase integrated signaling and granzyme B production, without major immunophenotypic and transcriptomic alterations.

Objective 3

4. *PRDM1* knock-out potentiates α-BCMA CAR NK cell *in vitro* expansion by increasing their proliferative capacity and delaying senescence induction without compromising CAR NK efficacy against MM cells.

Objective 4

5. Additional disruption of *PRDM1* in combination with *KLRC1* and *TGFBR2* in α-BCMA CAR NK effectors improves their expansion capacity preserving the *in vitro* cytotoxic potential against MM cells compared to double KO population.
6. Triple KO α-BCMA CAR NK effectors do not produce relevant hematotoxicity against either healthy mature PB cells or $CD34^+$ progenitor cells from MM patients.
7. Simultaneous CRISPR/Cas9 disruption of *KLRC1*, *TGFBR2,* and *PRDM1* using HiFi Cas9 nuclease and highly precise sgRNAs is a safe approach that does not produce detectable off-target activity in *in silico* predicted loci or large chromosomal aberrations, including translocations, inversions or aneuploidies.
8. Triple KO α-BCMA CAR NK effectors show prolonged *in vivo* persistence in mouse PB and BM compared to double KO CAR NK cells.
9. Triple KO α-BCMA CAR NK treatment demonstrates superior efficiency against MM *in vivo* and manages to completely cure 40% of the treated animals.

ABREVIATIONS

2KO: double knock-out

3KO: triple knock-out

4-1BBL: 4-1BB ligand

A

aAPC: artificial antigen presenting cell

AAV: adeno-associated viral vector

Ab: antibody

ADAM10/17: A disintegrin and metallopeptidase 10/17

ADC: antibody-drug conjugate

ADCC: antibody-dependent cellular cytotoxicity

ADO: adenosine

AKT: Ak strain transforming

AML: acute myeloid leukemia

ANOVA: analysis of variance

APC: allophycocyanin

APC/Cy7: allophycocyanin-cyanine7

APRIL: a proliferation-inducing ligand

ASCT: autologous stem cell transplant

ASCT-1/2: alanine/serine/cysteine transporter 1/2

B

B2M: β-2 microglobulin

BaEV: Baboon endogenous virus

B-ALL: B-cell acute lymphocytic leukemia

BCL-2: B-cell lymphoma 2

BCMA: B-cell maturation antigen

BCR: B-cell receptor

BiAb: bispecific antibodies

BiTE: bispecific T-cell engager

BLI: bioluminescent imaging

BLIMP1: B-lymphocyte-induced maturation protein 1

BM: bone marrow

BMMC: bone marrow mononuclear cell

bp: base pair

BRCA1/2: breast cancer gene 1/2

Bregs: regulatory B cells

BSA: bovine serum albumin

BTZ: bortezomib

C

Calcein-AM: calcein-acetoxymethylester

CAR: chimeric antigen receptor

Cas9: CRISPR-associated protein 9

CB: cord blood

CB-NK: cord blood-derived natural killer cell

CCL: CC chemokine ligand

CCR: CC chemokine receptor

CD: cranial dome

CD44v6: CD44 variant domain 6

CDK: cyclin-dependent kinase

CIITA: class II major histocompatibility complex transactivator

Cilta-cel: ciltacabtagene autoleucel

CIML NK: cytokine-induced memory-like natural killer cells

CIS: cytokine-inducible SH2-contianing protein; encoded by *CISH* gene

CLL: chronic lymphocytic leukemia

CNV: copy number variation

CR: complete response

CRAB: hypercalcemia, renal failure, anemia and bone lesions

CRISPR: clustered regularly interspaced short palindromic repeats

crRNA: CRIPSR RNA

CRS: cytokine release syndrome

CTLA-4: cytotoxic T-lymphocyte antigen 4

CXCL: CXC chemokine ligand

CXCR: CXC chemokine receptor

D

DAP10/12: DNAX-activating protein 10/12

DAPI: 4',6-diamidino-2-phenylindole

DC: dendritic cell

DDAO: 7-hydroxy-9H(I,3-dichloro-9,9-dimethylacridin-2-one)

DDAOG: 9H-(1,3-Dichloro-9,9-Dimethylacridin-2-One-7-yl) β-d-Galactopyranoside

DEG: differentially expressed genes

DNA: deoxyribonucleic acid

DNR: dominant negative receptor

DNAM-1: DNAX accessory molecule-1

DSB: double-strand DNA break

dsDNA: double-strand DNA

E

E:T: effector:target

ECL: enhanced chemiluminescence

EDTA: ethylenediaminetetraacetic acid

EMA: European Medicines Agency

EMD: extramedullary disease

ER: endoplasmic reticulum

ERK: extracellular signal-regulated kinase

F

FasL: Fas ligand

FBS: fetal bovine serum

FcεRIγ: γ-chain high-affinity IgE receptor

FcRγ: Fc receptor γ-chain

FcRH5: Fc receptor-homolog 5

FDA: Food and Drug Administration

FGFR3: fibroblast growth factor receptor 3

FITC: fluorescein isothiocyanate

FLC: free light chain

FMO: fluorescence minus one

FSC: forward side channel

Fw: forward

G

GaLV: Gibbon ape leukemia virus

GFP: green fluorescent protein

GM-CSF: granulocyte macrophage colony-stimulating factor

γ-RV: γ-retroviral vector

GO: gene ontology

GPRC5D: G protein-coupled receptor class C group 5 member D

Grb2: growth factor receptor-bound protein 2

GvHD: graft versus host disease

H

HBV: hepatitis B virus

HCV: hepatitis C virus

HD: healthy donor

HDAC: histone deacetylase

HDR: homology-directed repair

HER2: human epidermal growth factor receptor 2

hESC: human embryonic stem cell

HIV: human immunodeficiency virus

HLA: human leukocyte antigen

HNSCC: head and neck squamous cell carcinoma

HRP: horseradish peroxidase

HSPC: hematopoietic stem/progenitor cell

hTERT: human telomerase reverse transcriptase

I

i.p.: intraperitoneal

i.v.: intravenously

ICAM: intracellular adhesion molecule

ICANS: immune effector cell-associated neurotoxicity syndrome

Ide-cel: idecabtagene vicleucel

IDO: indoleamine-pyrrole 2,3-dioxygenase

IFN-γ: interferon-γ

Ig: immunoglobulin

IGF-1: insulin like growth factor 1

IgH: immunoglobulin heavy chain

IgL: immunoglobulin light chain

IKZF1/3: Ikaros family zinc finger 1/3

IL: interleukin

IMDM: Iscove´s Modified Dulbecco´s Medium

IMiD: immunomodulatory drug

iNK: iPSC-derived natural killer cell

iPSC: induced pluripotent stem cell

IQR: interquartile range

ISS: international staging system

ITAM: immunoreceptor tyrosine-based activation motif

ITIM: immunoreceptor tyrosine-based inhibitory motif

J

JAK/STAT: Janus kinase/signal transducers and activators of transcription

K

KI: knock-in

KIR: killer-cell immunoglobulin-like receptor

κLC: kappa light chain

KLRC1: killer cell lectin-like receptor C1

KLRG1: killer cell lectin-like receptor G1

KO: knock-out

L

LAG-3: lymphocyte activation gene 3

LAP: latency-associated peptide

LCK: lymphocyte-specific protein tyrosine kinase

LC: light chain

LDH: lactate dehydrogenase

LDL-R: low density lipoprotein receptor

LTC: latent complex

M

mAb: monoclonal antibody

MAPK: mitogen-activated protein kinase

MDE: myeloma-defining event

MDS: myelodysplastic syndrome

MDSC: myeloid-derived suppressor cell

MFI: median fluorescence intensity

MGUS: monoclonal gammopathy of undetermined significance

MH: microhomology

MHC: major histocompatibility complex

MICA/B: major histocompatibility complex class I chain-related protein A/B

MIP: macrophage inflammatory protein

MM: multiple myeloma

MMP: matrix metalloproteinase

MNC: mononuclear cell

MOI: multiplicity of infection

MRD: minimal residual disease

MRI: magnetic resonance imaging

mRNA: messenger RNA

MSC: mesenchymal stromal cell

MUC-1: mucin 1

N

nCas9: Cas9 nickase

NCR: natural cytotoxicity receptors

NCT: national clinical trial

NDMM: newly diagnosed multiple myeloma

NF-κB: nuclear factor κ B

NGS: next generation sequencing

NHEJ: non-homologous end joining

NK: natural killer

NKG2A/B/C/D/E: natural killer group 2 member A/B/C/D/E

NKG2D-L: natural killer group 2 member D ligand

NN: non-nucleofected

NSCLC: non-small cell lung cancer

NSG-Tg (Hu IL-15): Non-obese diabetic (NOD) Cg-Prkdc^{scid} Il2rg^{tm1Wjl} Tg(IL15)1Sz/SzJ

O

OGM: optical genome mapping

OPG: osteoprotegerin

OR: overall response

OS: overall survival

P

P/S: penicillin streptomycin

PAM: protospacer adjacent motif

PB: peripheral blood

PBMCs: peripheral blood mononuclear cells

PB-NK: peripheral blood-derived natural killer cell

PBS: phosphate-buffered saline

PC: plasma cell

PCA: principal component analysis

PCL: plasma cell leukemia

PCR: polymerase chain reaction

PD-1: programmed cell death 1

PD-L1/2: programmed cell death ligand 1/2

PE: phycoerythrin

PE/Cy7: phycoerythrin-cyanine7

PEBL: protein expression blocker

PerCP/Cy5.5: peridinin chlorophyll protein-Cyanine5.5

PET-CT: positron emission and computed tomography

PFS: progression-free survival

PI: propidium iodide

PI3K: phosphoinositide 3-kinase

pPC: pathologic plasma cell

PVR: poliovirus receptor

Q

q-PCR: quantitative polymerase chain reaction

R

R-ISS: revised international staging system

RANK: receptor activator for nuclear factor κ B

RANKL: receptor activator for nuclear factor κ B ligand

RAS: rat sarcoma

RFI: relative fluorescence intensity

rhBCMA: recombinant human B-cell maturation antigen

RNA: ribonucleic acid

RNA-seq: ribonucleic acid sequencing

RNP: ribonucleoprotein complex

RPMI: Roswell Park Memorial Institute

RRMM: relapsed/refractory multiple myeloma

RT: room temperature

Rv: reverse

S

SA-β-gal: senescence-associated β-galactosidase

sBCMA: soluble B-cell maturation antigen

scFv: single-chain variable fragment

SCGM: stem cell growth medium

SDS: sodium dodecyl sulfate

SDS-PAGE: sodium dodecyl sulfate polyacrylamide gel electrophoresis

SEM: standard error of the mean

sgRNA: single-guide RNA

SHP-1: Src homology region 2 domain-containing phosphatase-1

SLAMF7: signaling lymphocyte activation molecule family member 7

sMICA: soluble MICA

SMM: smoldering multiple myeloma

SOCS: suppressor of cytokine signaling

SSC: side scatter channel

ssDNA: single strand DNA

STAT: signal transducer and activator of transcription

Strep: streptavidin

SYK: spleen tyrosine kinase

T

TAM: tumor-associated macrophage

TBS: tris-buffered saline

TBS-T: tris-buffered saline with 0.1% Tween 20

TCR: T cell receptor

TGF-β: transforming growth factor β

TGF-βR: transforming growth factor β receptor

TGFBR2: transforming growth factor β receptor II

TIGIT: T cell immunoreceptor with Ig and ITIM domains

TIM-3: T cell immunoglobulin domain and mucin domain-3

TME: tumor microenvironment

TNF-α: tumor necrosis factor α

TP53: tumor protein p53

TRAIL: tumor necrosis factor related apoptosis-inducing ligand

TRAIL-R: tumor necrosis factor related apoptosis-inducing ligand receptor

tracrRNA: transactivating CRISPR RNA

Tregs: regulatory T cells

U

ULBP: unique long 16 binding protein

V

VCAM-1: vascular cell adhesion protein 1

VCN: vector copy number

VEGF: vascular endothelial growth factor

VLA-4: very late antigen-4

VRd: Bortezomib, lenalidomide, and dexamethasone

VSV-G: vesicular stomatitis virus glycoprotein

VTd: Bortezomib, thalidomide, and dexamethasone

W

WB: western blot

Z

ZAP70: zeta-chain-associated protein kinase 70

BIBLIOGRAPHY

1 Rajkumar, S. V. Multiple myeloma: 2024 update on diagnosis, risk-stratification, and management. *Am J Hematol* **99**, 1802-1824, doi:10.1002/ajh.27422 (2024).

2 Kumar, S. K. *et al.* Multiple myeloma. *Nat Rev Dis Primers* **3**, 17046, doi:10.1038/nrdp.2017.46 (2017).

3 Kyle, R. A. *et al.* Clinical course of light-chain smouldering multiple myeloma (idiopathic Bence Jones proteinuria): a retrospective cohort study. *Lancet Haematol* **1**, e28-e36, doi:10.1016/S2352-3026(14)70001-8 (2014).

4 Ribatti, D. A historical perspective on milestones in multiple myeloma research. *Eur J Haematol* **100**, 221-228, doi:10.1111/ejh.13003 (2018).

5 Migkou, M. *et al.* Clinical characteristics and outcomes of oligosecretory and non-secretory multiple myeloma. *Ann Hematol* **99**, 1251-1255, doi:10.1007/s00277-020-03984-w (2020).

6 Mullikin, T. C. *et al.* Clinical characteristics and outcomes in biclonal gammopathies. *Am J Hematol* **91**, 473-475, doi:10.1002/ajh.24319 (2016).

7 Kyle, R. A. Multiple myeloma: an odyssey of discovery. *Br J Haematol* **111**, 1035-1044, doi:10.1046/j.1365-2141.2000.02318.x (2000).

8 Hevroni, G. *et al.* From MGUS to multiple myeloma: Unraveling the unknown of precursor states. *Blood Rev*, 101242, doi:10.1016/j.blre.2024.101242 (2024).

9 Fernandez de Larrea, C. *et al.* Primary plasma cell leukemia: consensus definition by the International Myeloma Working Group according to peripheral blood plasma cell percentage. *Blood Cancer J* **11**, 192, doi:10.1038/s41408-021-00587-0 (2021).

10 Malard, F. *et al.* Multiple myeloma. *Nat Rev Dis Primers* **10**, 45, doi:10.1038/s41572-024-00529-7 (2024).

11 Siegel, R. L., Giaquinto, A. N. & Jemal, A. Cancer statistics, 2024. *CA Cancer J Clin* **74**, 12-49, doi:10.3322/caac.21820 (2024).

12 (SEER). *Cancer Stat Facts: Myeloma*, <https://seer.cancer.gov/statfacts> (2023).

13 (GCO). *Globocan Cancer Observatory*, <https://gco.iarc.who.int/media/globocan/factsheets/> (2022).

14 (AECC). Mieloma Múltiple. (2023).

15 Landgren, O. & Weiss, B. M. Patterns of monoclonal gammopathy of undetermined significance and multiple myeloma in various ethnic/racial groups: support for genetic factors in pathogenesis. *Leukemia* **23**, 1691-1697, doi:10.1038/leu.2009.134 (2009).

16 Brigle, K. & Rogers, B. Pathobiology and Diagnosis of Multiple Myeloma. *Semin Oncol Nurs* **33**, 225-236, doi:10.1016/j.soncn.2017.05.012 (2017).

17 Perrotta, C., Staines, A. & Cocco, P. Multiple myeloma and farming. A systematic review of 30 years of research. Where next? *J Occup Med Toxicol* **3**, 27, doi:10.1186/1745-6673-3-27 (2008).

18 Jephcote, C., Brown, D., Verbeek, T. & Mah, A. A systematic review and meta-analysis of haematological malignancies in residents living near petrochemical facilities. *Environ Health* **19**, 53, doi:10.1186/s12940-020-00582-1 (2020).

19 Altekruse, S. F., Henley, S. J. & Thun, M. J. Deaths from hematopoietic and other cancers in relation to permanent hair dye use in a large prospective study (United States). *Cancer Causes Control* **10**, 617-625, doi:10.1023/a:1008926027805 (1999).

20 De Roos, A. J. *et al.* Pooled study of occupational exposure to aromatic hydrocarbon solvents and risk of multiple myeloma. *Occup Environ Med* **75**, 798-806, doi:10.1136/oemed-2018-105154 (2018).

21 Boffetta, P. *et al.* Exposure to ultraviolet radiation and risk of malignant lymphoma and multiple myeloma--a multicentre European case-control study. *Int J Epidemiol* **37**, 1080-1094, doi:10.1093/ije/dyn092 (2008).

22 Ichimaru, M., Ishimaru, T., Mikami, M. & Matsunaga, M. Multiple myeloma among atomic bomb survivors in Hiroshima and Nagasaki, 1950-76: relationship to radiation dose absorbed by marrow. *J Natl Cancer Inst* **69**, 323-328 (1982).

23 Preston, D. L. *et al.* Cancer incidence in atomic bomb survivors. Part III. Leukemia, lymphoma and multiple myeloma, 1950-1987. *Radiat Res* **137**, S68-97 (1994).

24 Wright, J. D. *et al.* Pelvic radiotherapy and the risk of secondary leukemia and multiple myeloma. *Cancer* **116**, 2486-2492, doi:10.1002/cncr.25067 (2010).

25 Tentolouris, A., Ntanasis-Stathopoulos, I. & Terpos, E. Obesity and multiple myeloma: Emerging mechanisms and perspectives. *Semin Cancer Biol* **92**, 45-60, doi:10.1016/j.semcancer.2023.04.003 (2023).

26 Renehan, A. G., Tyson, M., Egger, M., Heller, R. F. & Zwahlen, M. Body-mass index and incidence of cancer: a systematic review and meta-analysis of prospective observational studies. *Lancet* **371**, 569-578, doi:10.1016/S0140-6736(08)60269-X (2008).

27 Marques-Mourlet, C., Di Iorio, R., Fairfield, H. & Reagan, M. R. Obesity and myeloma: Clinical and mechanistic contributions to disease progression. *Front Endocrinol (Lausanne)* **14**, 1118691, doi:10.3389/fendo.2023.1118691 (2023).

28 Marinac, C. R. *et al.* Body mass index throughout adulthood, physical activity, and risk of multiple myeloma: a prospective analysis in three large cohorts. *Br J Cancer* **118**, 1013-1019, doi:10.1038/s41416-018-0010-4 (2018).

29 Birmann, B. M. *et al.* Young Adult and Usual Adult Body Mass Index and Multiple Myeloma Risk: A Pooled Analysis in the International Multiple Myeloma Consortium (IMMC). *Cancer Epidemiol Biomarkers Prev* **26**, 876-885, doi:10.1158/1055-9965.EPI-16-0762-T (2017).

30 Wang, B. *et al.* Body Mass Index and Overall Survival of Patients with Newly Diagnosed Multiple Myeloma. *Cancers (Basel)* **14**, doi:10.3390/cancers14215331 (2022).

31 Vogl, D. T. *et al.* Effect of obesity on outcomes after autologous hematopoietic stem cell transplantation for multiple myeloma. *Biol Blood Marrow Transplant* **17**, 1765-1774, doi:10.1016/j.bbmt.2011.05.005 (2011).

32 McShane, C. M. *et al.* Prior autoimmune disease and risk of monoclonal gammopathy of undetermined significance and multiple myeloma: a systematic review. *Cancer Epidemiol Biomarkers Prev* **23**, 332-342, doi:10.1158/1055-9965.EPI-13-0695 (2014).

33 Brown, L. M., Gridley, G., Check, D. & Landgren, O. Risk of multiple myeloma and monoclonal gammopathy of undetermined significance among white and black male United States veterans with prior autoimmune, infectious, inflammatory, and allergic disorders. *Blood* **111**, 3388-3394, doi:10.1182/blood-2007-10-121285 (2008).

34 Su, T. H. *et al.* Chronic hepatitis B is associated with an increased risk of B-cell non-Hodgkin's lymphoma and multiple myeloma. *Aliment Pharmacol Ther* **49**, 589-598, doi:10.1111/apt.15132 (2019).

35 Grulich, A. E., Wan, X., Law, M. G., Coates, M. & Kaldor, J. M. Risk of cancer in people with AIDS. *AIDS* **13**, 839-843, doi:10.1097/00002030-199905070-00014 (1999).

36 Rodriguez-Garcia, A. *et al.* Efficacy of Antiviral Treatment in Hepatitis C Virus (HCV)-Driven Monoclonal Gammopathies Including Myeloma. *Front Immunol* **12**, 797209, doi:10.3389/fimmu.2021.797209 (2021).

37 Nair, S. *et al.* Antigen-mediated regulation in monoclonal gammopathies and myeloma. *JCI Insight* **3**, doi:10.1172/jci.insight.98259 (2018).

38 Nair, S. *et al.* Clonal Immunoglobulin against Lysolipids in the Origin of Myeloma. *N Engl J Med* **374**, 555-561, doi:10.1056/NEJMoa1508808 (2016).

39 Vachon, C. M. *et al.* Increased risk of monoclonal gammopathy in first-degree relatives of patients with multiple myeloma or monoclonal gammopathy of undetermined significance. *Blood* **114**, 785-790, doi:10.1182/blood-2008-12-192575 (2009).

40 Pertesi, M. *et al.* Genetic predisposition for multiple myeloma. *Leukemia* **34**, 697-708, doi:10.1038/s41375-019-0703-6 (2020).

41 Maldonado, J. E. & Kyle, R. A. Familial myeloma. Report of eight families and a study of serum proteins in their relatives. *Am J Med* **57**, 875-884, doi:10.1016/0002-9343(74)90164-8 (1974).

42 Brown, L. M. *et al.* Multiple myeloma and family history of cancer among blacks and whites in the U.S. *Cancer* **85**, 2385-2390 (1999).

43 Altieri, A., Chen, B., Bermejo, J. L., Castro, F. & Hemminki, K. Familial risks and temporal incidence trends of multiple myeloma. *Eur J Cancer* **42**, 1661-1670, doi:10.1016/j.ejca.2005.11.033 (2006).

44 Morgan, G. J., Walker, B. A. & Davies, F. E. The genetic architecture of multiple myeloma. *Nat Rev Cancer* **12**, 335-348, doi:10.1038/nrc3257 (2012).

45 Barwick, B. G., Gupta, V. A., Vertino, P. M. & Boise, L. H. Cell of Origin and Genetic Alterations in the Pathogenesis of Multiple Myeloma. *Front Immunol* **10**, 1121, doi:10.3389/fimmu.2019.01121 (2019).

46 Barwick, B. G. *et al.* Multiple myeloma immunoglobulin lambda translocations portend poor prognosis. *Nat Commun* **10**, 1911, doi:10.1038/s41467-019-09555-6 (2019).

47 Walker, B. A. *et al.* Mutational Spectrum, Copy Number Changes, and Outcome: Results of a Sequencing Study of Patients With Newly Diagnosed Myeloma. *J Clin Oncol* **33**, 3911-3920, doi:10.1200/JCO.2014.59.1503 (2015).

48 Yuregir, O. O. *et al.* Detecting methylation patterns of p16, MGMT, DAPK and E-cadherin genes in multiple myeloma patients. *Int J Lab Hematol* **32**, 142-149, doi:10.1111/j.1751-553X.2009.01146.x (2010).

49 Amodio, N., D'Aquila, P., Passarino, G., Tassone, P. & Bellizzi, D. Epigenetic modifications in multiple myeloma: recent advances on the role of DNA and histone methylation. *Expert Opin Ther Targets* **21**, 91-101, doi:10.1080/14728222.2016.1266339 (2017).

50 Maiso, P., Mogollon, P., Ocio, E. M. & Garayoa, M. Bone Marrow Mesenchymal Stromal Cells in Multiple Myeloma: Their Role as Active Contributors to Myeloma Progression. *Cancers (Basel)* **13**, doi:10.3390/cancers13112542 (2021).

51 Hideshima, T., Mitsiades, C., Tonon, G., Richardson, P. G. & Anderson, K. C. Understanding multiple myeloma pathogenesis in the bone marrow to identify new therapeutic targets. *Nat Rev Cancer* **7**, 585-598, doi:10.1038/nrc2189 (2007).

52 Palumbo, A. & Anderson, K. Multiple myeloma. *N Engl J Med* **364**, 1046-1060, doi:10.1056/NEJMra1011442 (2011).

53 Yang, Y., Liu, Z., Wang, H. & Zhang, G. HLA-E Binding Peptide as a Potential Therapeutic Candidate for High-Risk Multiple Myeloma. *Front Oncol* **11**, 670673, doi:10.3389/fonc.2021.670673 (2021).

54 Carbone, E. *et al.* HLA class I, NKG2D, and natural cytotoxicity receptors regulate multiple myeloma cell recognition by natural killer cells. *Blood* **105**, 251-258, doi:10.1182/blood-2004-04-1422 (2005).

55 Racanelli, V. *et al.* Alterations in the antigen processing-presenting machinery of transformed plasma cells are associated with reduced recognition by CD8+ T cells and characterize the progression of MGUS to multiple myeloma. *Blood* **115**, 1185-1193, doi:10.1182/blood-2009-06-228676 (2010).

56 Rosenblatt, J. *et al.* PD-1 blockade by CT-011, anti-PD-1 antibody, enhances ex vivo T-cell responses to autologous dendritic cell/myeloma fusion vaccine. *J Immunother* **34**, 409-418, doi:10.1097/CJI.0b013e31821ca6ce (2011).

57 Liu, J. *et al.* Plasma cells from multiple myeloma patients express B7-H1 (PD-L1) and increase expression after stimulation with IFN-gamma and TLR ligands via a MyD88-, TRAF6-, and MEK-dependent pathway. *Blood* **110**, 296-304, doi:10.1182/blood-2006-10-051482 (2007).

58 Visram, A., Dasari, S., Anderson, E., Kumar, S. & Kourelis, T. V. Relapsed multiple myeloma demonstrates distinct patterns of immune microenvironment and malignant cell-mediated immunosuppression. *Blood Cancer J* **11**, 45, doi:10.1038/s41408-021-00440-4 (2021).

59 Garcia-Ortiz, A. *et al.* The Role of Tumor Microenvironment in Multiple Myeloma Development and Progression. *Cancers (Basel)* **13**, doi:10.3390/cancers13020217 (2021).

60 Panaroni, C., Yee, A. J. & Raje, N. S. Myeloma and Bone Disease. *Curr Osteoporos Rep* **15**, 483-498, doi:10.1007/s11914-017-0397-5 (2017).

61 Kyle, R. A. *et al.* Review of 1027 patients with newly diagnosed multiple myeloma. *Mayo Clin Proc* **78**, 21-33, doi:10.4065/78.1.21 (2003).

62 Courant, M. *et al.* Incidence, prognostic impact and clinical outcomes of renal impairment in patients with multiple myeloma: a population-based registry. *Nephrol Dial Transplant* **36**, 482-490, doi:10.1093/ndt/gfz211 (2021).

63 Dimopoulos, M. A., Kastritis, E., Rosinol, L., Blade, J. & Ludwig, H. Pathogenesis and treatment of renal failure in multiple myeloma. *Leukemia* **22**, 1485-1493, doi:10.1038/leu.2008.131 (2008).

64 Ludwig, H., Pohl, G. & Osterborg, A. Anemia in multiple myeloma. *Clin Adv Hematol Oncol* **2**, 233-241 (2004).

65 Liu, L. *et al.* Multiple myeloma hinders erythropoiesis and causes anaemia owing to high levels of CCL3 in the bone marrow microenvironment. *Sci Rep* **10**, 20508, doi:10.1038/s41598-020-77450-y (2020).

66 Sorrig, R. *et al.* Immunoparesis in newly diagnosed Multiple Myeloma patients: Effects on overall survival and progression free survival in the Danish population. *PLoS One* **12**, e0188988, doi:10.1371/journal.pone.0188988 (2017).

67 Schutt, P. *et al.* Immune parameters in multiple myeloma patients: influence of treatment and correlation with opportunistic infections. *Leuk Lymphoma* **47**, 1570-1582, doi:10.1080/10428190500472503 (2006).

68 Nucci, M. & Anaissie, E. Infections in patients with multiple myeloma in the era of high-dose therapy and novel agents. *Clin Infect Dis* **49**, 1211-1225, doi:10.1086/605664 (2009).

69 Garcia-Sanz, R., Mateos, M. V. & San Miguel, J. F. [Multiple myeloma]. *Med Clin (Barc)* **129**, 104-115, doi:10.1157/13107365 (2007).

70 Blade, J. *et al.* Extramedullary disease in multiple myeloma: a systematic literature review. *Blood Cancer J* **12**, 45, doi:10.1038/s41408-022-00643-3 (2022).

71 Bhutani, M., Foureau, D. M., Atrash, S., Voorhees, P. M. & Usmani, S. Z. Extramedullary multiple myeloma. *Leukemia* **34**, 1-20, doi:10.1038/s41375-019-0660-0 (2020).

72 Hillengass, J. *et al.* International myeloma working group consensus recommendations on imaging in monoclonal plasma cell disorders. *Lancet Oncol* **20**, e302-e312, doi:10.1016/S1470-2045(19)30309-2 (2019).

73 Rajkumar, S. V. *et al.* International Myeloma Working Group updated criteria for the diagnosis of multiple myeloma. *Lancet Oncol* **15**, e538-548, doi:10.1016/S1470-2045(14)70442-5 (2014).

74 Cowan, A. J. *et al.* Diagnosis and Management of Multiple Myeloma: A Review. *JAMA* **327**, 464-477, doi:10.1001/jama.2022.0003 (2022).

75 Rajkumar, S. V. & Kyle, R. A. Multiple myeloma: diagnosis and treatment. *Mayo Clin Proc* **80**, 1371-1382, doi:10.4065/80.10.1371 (2005).

76 Johnsen, H. E. *et al.* Multiparametric flow cytometry profiling of neoplastic plasma cells in multiple myeloma. *Cytometry B Clin Cytom* **78**, 338-347, doi:10.1002/cyto.b.20523 (2010).

77 Robillard, N., Wuilleme, S., Moreau, P. & Bene, M. C. Immunophenotype of normal and myelomatous plasma-cell subsets. *Front Immunol* **5**, 137, doi:10.3389/fimmu.2014.00137 (2014).

78 Bataille, R. *et al.* CD117 (c-kit) is aberrantly expressed in a subset of MGUS and multiple myeloma with unexpectedly good prognosis. *Leuk Res* **32**, 379-382, doi:10.1016/j.leukres.2007.07.016 (2008).

79 Paiva, B. *et al.* Clinical significance of CD81 expression by clonal plasma cells in high-risk smoldering and symptomatic multiple myeloma patients. *Leukemia* **26**, 1862-1869, doi:10.1038/leu.2012.42 (2012).

80 Kyle, R. A. *et al.* Clinical course and prognosis of smoldering (asymptomatic) multiple myeloma. *N Engl J Med* **356**, 2582-2590, doi:10.1056/NEJMoa070389 (2007).

81 Kyle, R. A. & Rajkumar, S. V. Monoclonal gammopathy of undetermined significance and smoldering multiple myeloma. *Hematol Oncol Clin North Am* **21**, 1093-1113, ix, doi:10.1016/j.hoc.2007.08.005 (2007).

82 Palumbo, A. *et al.* Revised International Staging System for Multiple Myeloma: A Report From International Myeloma Working Group. *J Clin Oncol* **33**, 2863-2869, doi:10.1200/JCO.2015.61.2267 (2015).

83 Tan, J. L. C. *et al.* The second revision of the International Staging System (R2-ISS) stratifies progression-free and overall survival in multiple myeloma: Real world data results in an Australian and New Zealand Population. *Br J Haematol* **200**, e17-e21, doi:10.1111/bjh.18536 (2023).

84 D'Agostino, M. *et al.* Second Revision of the International Staging System (R2-ISS) for Overall Survival in Multiple Myeloma: A European Myeloma Network (EMN) Report Within the HARMONY Project. *J Clin Oncol* **40**, 3406-3418, doi:10.1200/JCO.21.02614 (2022).

85 Richardson, P. G. *et al.* Mezigdomide plus Dexamethasone in Relapsed and Refractory Multiple Myeloma. *N Engl J Med* **389**, 1009-1022, doi:10.1056/NEJMoa2303194 (2023).

86 Lagrue, K., Carisey, A., Morgan, D. J., Chopra, R. & Davis, D. M. Lenalidomide augments actin remodeling and lowers NK-cell activation thresholds. *Blood* **126**, 50-60, doi:10.1182/blood-2015-01-625004 (2015).

87 Kotla, V. *et al.* Mechanism of action of lenalidomide in hematological malignancies. *J Hematol Oncol* **2**, 36, doi:10.1186/1756-8722-2-36 (2009).

88 Jungkunz-Stier, I., Zekl, M., Stuhmer, T., Einsele, H. & Seggewiss-Bernhardt, R. Modulation of natural killer cell effector functions through lenalidomide/dasatinib and their combined effects against multiple myeloma cells. *Leuk Lymphoma* **55**, 168-176, doi:10.3109/10428194.2013.794270 (2014).

89 Heim, C. & Hartmann, M. D. High-resolution structures of the bound effectors avadomide (CC-122) and iberdomide (CC-220) highlight advantages and limitations of the MsCl4 soaking system. *Acta Crystallogr D Struct Biol* **78**, 290-298, doi:10.1107/S2059798322000092 (2022).

90 Fionda, C. *et al.* The IMiDs targets IKZF-1/3 and IRF4 as novel negative regulators of NK cell-activating ligands expression in multiple myeloma. *Oncotarget* **6**, 23609-23630, doi:10.18632/oncotarget.4603 (2015).

91 Davies, F. E. *et al.* Thalidomide and immunomodulatory derivatives augment natural killer cell cytotoxicity in multiple myeloma. *Blood* **98**, 210-216, doi:10.1182/blood.v98.1.210 (2001).

92 Corral, L. G. *et al.* Differential cytokine modulation and T cell activation by two distinct classes of thalidomide analogues that are potent inhibitors of TNF-alpha. *J Immunol* **163**, 380-386 (1999).

93 Quach, H. *et al.* Mechanism of action of immunomodulatory drugs (IMiDS) in multiple myeloma. *Leukemia* **24**, 22-32, doi:10.1038/leu.2009.236 (2010).

94 Delforge, M. & Ludwig, H. How I manage the toxicities of myeloma drugs. *Blood* **129**, 2359-2367, doi:10.1182/blood-2017-01-725705 (2017).

95 Manasanch, E. E. & Orlowski, R. Z. Proteasome inhibitors in cancer therapy. *Nat Rev Clin Oncol* **14**, 417-433, doi:10.1038/nrclinonc.2016.206 (2017).

96 Carlsten, M. *et al.* Bortezomib sensitizes multiple myeloma to NK cells via ER-stress-induced suppression of HLA-E and upregulation of DR5. *Oncoimmunology* **8**, e1534664, doi:10.1080/2162402X.2018.1534664 (2019).

97 Besse, A. *et al.* Proteasome Inhibition in Multiple Myeloma: Head-to-Head Comparison of Currently Available Proteasome Inhibitors. *Cell Chem Biol* **26**, 340-351 e343, doi:10.1016/j.chembiol.2018.11.007 (2019).

98 Shi, J. *et al.* Bortezomib down-regulates the cell-surface expression of HLA class I and enhances natural killer cell-mediated lysis of myeloma. *Blood* **111**, 1309-1317, doi:10.1182/blood-2007-03-078535 (2008).

99 Niu, C. *et al.* Low-dose bortezomib increases the expression of NKG2D and DNAM-1 ligands and enhances induced NK and gammadelta T cell-mediated lysis in multiple myeloma. *Oncotarget* **8**, 5954-5964, doi:10.18632/oncotarget.13979 (2017).

100 Wieten, L., Mahaweni, N. M., Voorter, C. E., Bos, G. M. & Tilanus, M. G. Clinical and immunological significance of HLA-E in stem cell transplantation and cancer. *Tissue Antigens* **84**, 523-535, doi:10.1111/tan.12478 (2014).

101 Hallett, W. H. *et al.* Sensitization of tumor cells to NK cell-mediated killing by proteasome inhibition. *J Immunol* **180**, 163-170, doi:10.4049/jimmunol.180.1.163 (2008).

102 Nencioni, A., Grunebach, F., Patrone, F., Ballestrero, A. & Brossart, P. Proteasome inhibitors: antitumor effects and beyond. *Leukemia* **21**, 30-36, doi:10.1038/sj.leu.2404444 (2007).

103 Mattingly, L. H., Gault, R. A. & Murphy, W. J. Use of systemic proteasome inhibition as an immune-modulating agent in disease. *Endocr Metab Immune Disord Drug Targets* **7**, 29-34, doi:10.2174/187153007780059397 (2007).

104 Zheng, Y. *et al.* Cardiovascular Toxicity of Proteasome Inhibitors in Multiple Myeloma Therapy. *Curr Probl Cardiol* **48**, 101536, doi:10.1016/j.cpcardiol.2022.101536 (2023).

105 Kaplan, G. S., Torcun, C. C., Grune, T., Ozer, N. K. & Karademir, B. Proteasome inhibitors in cancer therapy: Treatment regimen and peripheral neuropathy as a side effect. *Free Radic Biol Med* **103**, 1-13, doi:10.1016/j.freeradbiomed.2016.12.007 (2017).

106 Schjesvold, F. & Oriol, A. Current and Novel Alkylators in Multiple Myeloma. *Cancers (Basel)* **13**, doi:10.3390/cancers13102465 (2021).

107 Costa, B. A., Mouhieddine, T. H., Ortiz, R. J. & Richter, J. Revisiting the role of alkylating agents in multiple myeloma: Up-to-date evidence and future perspectives. *Crit Rev Oncol Hematol* **187**, 104040, doi:10.1016/j.critrevonc.2023.104040 (2023).

108 Pour, L. *et al.* Efficacy and safety of melflufen plus daratumumab and dexamethasone in relapsed/refractory multiple myeloma: results from the randomized, open-label, phase III LIGHTHOUSE study. *Haematologica* **109**, 895-905, doi:10.3324/haematol.2023.283509 (2024).

109 Friedenberg, W. R. *et al.* High-dose dexamethasone for refractory or relapsing multiple myeloma. *Am J Hematol* **36**, 171-175, doi:10.1002/ajh.2830360303 (1991).

110 Burwick, N. & Sharma, S. Glucocorticoids in multiple myeloma: past, present, and future. *Ann Hematol* **98**, 19-28, doi:10.1007/s00277-018-3465-8 (2019).

111 Oray, M., Abu Samra, K., Ebrahimiadib, N., Meese, H. & Foster, C. S. Long-term side effects of glucocorticoids. *Expert Opin Drug Saf* **15**, 457-465, doi:10.1517/14740338.2016.1140743 (2016).

112 Rajkumar, S. V. *et al.* Consensus recommendations for the uniform reporting of clinical trials: report of the International Myeloma Workshop Consensus Panel 1. *Blood* **117**, 4691-4695, doi:10.1182/blood-2010-10-299487 (2011).

113 Moreau, P. *et al.* Treatment of relapsed and refractory multiple myeloma: recommendations from the International Myeloma Working Group. *Lancet Oncol* **22**, e105-e118, doi:10.1016/S1470-2045(20)30756-7 (2021).

114 Foundation, I. M. <https://www.myeloma.org/multiple-myeloma-drugs> (2024).

115 Podar, K., Shah, J., Chari, A., Richardson, P. G. & Jagannath, S. Selinexor for the treatment of multiple myeloma. *Expert Opin Pharmacother* **21**, 399-408, doi:10.1080/14656566.2019.1707184 (2020).

116 Fisher, J. G. *et al.* Selinexor Enhances NK Cell Activation Against Malignant B Cells via Downregulation of HLA-E. *Front Oncol* **11**, 785635, doi:10.3389/fonc.2021.785635 (2021).
117 Huang, Q., Zhao, R., Xu, L., Hao, X. & Tao, S. Treatment of multiple myeloma with selinexor: a review. *Ther Adv Hematol* **15**, 20406207231219442, doi:10.1177/20406207231219442 (2024).
118 Sidiqi, M. H. *et al.* Venetoclax for the treatment of multiple myeloma: Outcomes outside of clinical trials. *Am J Hematol* **96**, 1131-1136, doi:10.1002/ajh.26269 (2021).
119 Kumar, S. K. *et al.* Venetoclax or placebo in combination with bortezomib and dexamethasone in patients with relapsed or refractory multiple myeloma (BELLINI): a randomised, double-blind, multicentre, phase 3 trial. *Lancet Oncol* **21**, 1630-1642, doi:10.1016/S1470-2045(20)30525-8 (2020).
120 Kumar, S. *et al.* Efficacy of venetoclax as targeted therapy for relapsed/refractory t(11;14) multiple myeloma. *Blood* **130**, 2401-2409, doi:10.1182/blood-2017-06-788786 (2017).
121 Richardson, P. G. *et al.* Patient-reported outcomes of multiple myeloma patients treated with panobinostat after >/=2 lines of therapy based on the international phase 3, randomized, double-blind, placebo-controlled PANORAMA-1 trial. *Br J Haematol* **181**, 628-636, doi:10.1111/bjh.15248 (2018).
122 Pan, D. *et al.* Outcomes with panobinostat in heavily pretreated multiple myeloma patients. *Semin Oncol* **50**, 40-48, doi:10.1053/j.seminoncol.2023.03.006 (2023).
123 Moreau, P. *et al.* Maintenance with daratumumab or observation following treatment with bortezomib, thalidomide, and dexamethasone with or without daratumumab and autologous stem-cell transplant in patients with newly diagnosed multiple myeloma (CASSIOPEIA): an open-label, randomised, phase 3 trial. *Lancet Oncol* **22**, 1378-1390, doi:10.1016/S1470-2045(21)00428-9 (2021).
124 Mateos, M. V. *et al.* Daratumumab plus Bortezomib, Melphalan, and Prednisone for Untreated Myeloma. *N Engl J Med* **378**, 518-528, doi:10.1056/NEJMoa1714678 (2018).
125 Gandhi, U. H. *et al.* Outcomes of patients with multiple myeloma refractory to CD38-targeted monoclonal antibody therapy. *Leukemia* **33**, 2266-2275, doi:10.1038/s41375-019-0435-7 (2019).
126 Shah, N., Chari, A., Scott, E., Mezzi, K. & Usmani, S. Z. B-cell maturation antigen (BCMA) in multiple myeloma: rationale for targeting and current therapeutic approaches. *Leukemia* **34**, 985-1005, doi:10.1038/s41375-020-0734-z (2020).
127 Tai, Y. T. *et al.* APRIL and BCMA promote human multiple myeloma growth and immunosuppression in the bone marrow microenvironment. *Blood* **127**, 3225-3236, doi:10.1182/blood-2016-01-691162 (2016).
128 Ndacayisaba, L. J. *et al.* Characterization of BCMA Expression in Circulating Rare Single Cells of Patients with Plasma Cell Neoplasms. *Int J Mol Sci* **23**, doi:10.3390/ijms232113427 (2022).
129 Moreaux, J. *et al.* BAFF and APRIL protect myeloma cells from apoptosis induced by interleukin 6 deprivation and dexamethasone. *Blood* **103**, 3148-3157, doi:10.1182/blood-2003-06-1984 (2004).
130 Hahne, M. *et al.* APRIL, a new ligand of the tumor necrosis factor family, stimulates tumor cell growth. *J Exp Med* **188**, 1185-1190, doi:10.1084/jem.188.6.1185 (1998).
131 Giordano, D. *et al.* B cell-activating factor (BAFF) from dendritic cells, monocytes and neutrophils is required for B cell maturation and autoantibody production in SLE-like autoimmune disease. *Front Immunol* **14**, 1050528, doi:10.3389/fimmu.2023.1050528 (2023).
132 Cho, S. F., Xing, L., Anderson, K. C. & Tai, Y. T. Promising Antigens for the New Frontier of Targeted Immunotherapy in Multiple Myeloma. *Cancers (Basel)* **13**, doi:10.3390/cancers13236136 (2021).
133 Van Oekelen, O. *et al.* Neurocognitive and hypokinetic movement disorder with features of parkinsonism after BCMA-targeting CAR-T cell therapy. *Nat Med* **27**, 2099-2103, doi:10.1038/s41591-021-01564-7 (2021).
134 Wiedemann, A. *et al.* Soluble B-cell maturation antigen as a monitoring marker for multiple myeloma. *Pathol Oncol Res* **29**, 1611171, doi:10.3389/pore.2023.1611171 (2023).
135 Pont, M. J. *et al.* gamma-Secretase inhibition increases efficacy of BCMA-specific chimeric antigen receptor T cells in multiple myeloma. *Blood* **134**, 1585-1597, doi:10.1182/blood.2019000050 (2019).
136 Pillarisetti, K. *et al.* A T-cell-redirecting bispecific G-protein-coupled receptor class 5 member D x CD3 antibody to treat multiple myeloma. *Blood* **135**, 1232-1243, doi:10.1182/blood.2019003342 (2020).
137 Atamaniuk, J. *et al.* Overexpression of G protein-coupled receptor 5D in the bone marrow is associated with poor prognosis in patients with multiple myeloma. *Eur J Clin Invest* **42**, 953-960, doi:10.1111/j.1365-2362.2012.02679.x (2012).
138 Chari, A. *et al.* Talquetamab, a T-Cell-Redirecting GPRC5D Bispecific Antibody for Multiple Myeloma. *N Engl J Med* **387**, 2232-2244, doi:10.1056/NEJMoa2204591 (2022).

139 Carlo-Stella, C. *et al.* RG6234, a GPRC5DxCD3 T-Cell Engaging Bispecific Antibody, Is Highly Active in Patients (pts) with Relapsed/Refractory Multiple Myeloma (RRMM): Updated Intravenous (IV) and First Subcutaneous (SC) Results from a Phase I Dose-Escalation Study. *Blood* **140**, 397-399, doi:10.1182/blood-2022-157988 %J Blood (2022).

140 Smith, E. L. *et al.* GPRC5D is a target for the immunotherapy of multiple myeloma with rationally designed CAR T cells. *Sci Transl Med* **11**, doi:10.1126/scitranslmed.aau7746 (2019).

141 Saltarella, I. *et al.* Mechanisms of Resistance to Anti-CD38 Daratumumab in Multiple Myeloma. *Cells* **9**, doi:10.3390/cells9010167 (2020).

142 Piedra-Quintero, Z. L., Wilson, Z., Nava, P. & Guerau-de-Arellano, M. CD38: An Immunomodulatory Molecule in Inflammation and Autoimmunity. *Front Immunol* **11**, 597959, doi:10.3389/fimmu.2020.597959 (2020).

143 van de Donk, N. & Usmani, S. Z. CD38 Antibodies in Multiple Myeloma: Mechanisms of Action and Modes of Resistance. *Front Immunol* **9**, 2134, doi:10.3389/fimmu.2018.02134 (2018).

144 Zambello, R., Barila, G., Manni, S., Piazza, F. & Semenzato, G. NK cells and CD38: Implication for (Immuno)Therapy in Plasma Cell Dyscrasias. *Cells* **9**, doi:10.3390/cells9030768 (2020).

145 Wang, Y. *et al.* Fratricide of NK Cells in Daratumumab Therapy for Multiple Myeloma Overcome by Ex Vivo-Expanded Autologous NK Cells. *Clin Cancer Res* **24**, 4006-4017, doi:10.1158/1078-0432.CCR-17-3117 (2018).

146 Ogiya, D. *et al.* The JAK-STAT pathway regulates CD38 on myeloma cells in the bone marrow microenvironment: therapeutic implications. *Blood* **136**, 2334-2345, doi:10.1182/blood.2019004332 (2020).

147 Malaer, J. D. & Mathew, P. A. CS1 (SLAMF7, CD319) is an effective immunotherapeutic target for multiple myeloma. *Am J Cancer Res* **7**, 1637-1641 (2017).

148 Kumaresan, P. R., Lai, W. C., Chuang, S. S., Bennett, M. & Mathew, P. A. CS1, a novel member of the CD2 family, is homophilic and regulates NK cell function. *Mol Immunol* **39**, 1-8, doi:10.1016/s0161-5890(02)00094-9 (2002).

149 Chan, W. K. *et al.* A CS1-NKG2D Bispecific Antibody Collectively Activates Cytolytic Immune Cells against Multiple Myeloma. *Cancer Immunol Res* **6**, 776-787, doi:10.1158/2326-6066.CIR-17-0649 (2018).

150 O'Neal, J. *et al.* CS1 CAR-T targeting the distal domain of CS1 (SLAMF7) shows efficacy in high tumor burden myeloma model despite fratricide of CD8+CS1 expressing CAR-T cells. *Leukemia* **36**, 1625-1634, doi:10.1038/s41375-022-01559-4 (2022).

151 Chu, J. *et al.* CS1-specific chimeric antigen receptor (CAR)-engineered natural killer cells enhance in vitro and in vivo antitumor activity against human multiple myeloma. *Leukemia* **28**, 917-927, doi:10.1038/leu.2013.279 (2014).

152 Akhmetzyanova, I. *et al.* Dynamic CD138 surface expression regulates switch between myeloma growth and dissemination. *Leukemia* **34**, 245-256, doi:10.1038/s41375-019-0519-4 (2020).

153 Rapraeger, A. C. Syndecan-regulated receptor signaling. *J Cell Biol* **149**, 995-998, doi:10.1083/jcb.149.5.995 (2000).

154 Moreaux, J. *et al.* APRIL and TACI interact with syndecan-1 on the surface of multiple myeloma cells to form an essential survival loop. *Eur J Haematol* **83**, 119-129, doi:10.1111/j.1600-0609.2009.01262.x (2009).

155 Kind, S. *et al.* Prevalence of Syndecan-1 (CD138) Expression in Different Kinds of Human Tumors and Normal Tissues. *Dis Markers* **2019**, 4928315, doi:10.1155/2019/4928315 (2019).

156 Kawano, Y. *et al.* Multiple myeloma cells expressing low levels of CD138 have an immature phenotype and reduced sensitivity to lenalidomide. *Int J Oncol* **41**, 876-884, doi:10.3892/ijo.2012.1545 (2012).

157 Beauvais, D. M., Jung, O., Yang, Y., Sanderson, R. D. & Rapraeger, A. C. Syndecan-1 (CD138) Suppresses Apoptosis in Multiple Myeloma by Activating IGF1 Receptor: Prevention by SynstatinIGF1R Inhibits Tumor Growth. *Cancer Res* **76**, 4981-4993, doi:10.1158/0008-5472.CAN-16-0232 (2016).

158 Ward, J. *et al.* HIV modulates the expression of ligands important in triggering natural killer cell cytotoxic responses on infected primary T-cell blasts. *Blood* **110**, 1207-1214, doi:10.1182/blood-2006-06-028175 (2007).

159 Sallman, D. A. *et al.* CYAD-01, an autologous NKG2D-based CAR T-cell therapy, in relapsed or refractory acute myeloid leukaemia and myelodysplastic syndromes or multiple myeloma (THINK): haematological cohorts of the dose escalation segment of a phase 1 trial. *Lancet Haematol* **10**, e191-e202, doi:10.1016/S2352-3026(22)00378-7 (2023).

160 Gasser, S., Orsulic, S., Brown, E. J. & Raulet, D. H. The DNA damage pathway regulates innate immune system ligands of the NKG2D receptor. *Nature* **436**, 1186-1190, doi:10.1038/nature03884 (2005).
161 Raulet, D. H., Gasser, S., Gowen, B. G., Deng, W. & Jung, H. Regulation of ligands for the NKG2D activating receptor. *Annu Rev Immunol* **31**, 413-441, doi:10.1146/annurev-immunol-032712-095951 (2013).
162 Fionda, C., Soriani, A., Zingoni, A., Santoni, A. & Cippitelli, M. NKG2D and DNAM-1 Ligands: Molecular Targets for NK Cell-Mediated Immunotherapeutic Intervention in Multiple Myeloma. *Biomed Res Int* **2015**, 178698, doi:10.1155/2015/178698 (2015).
163 Pende, D. *et al.* Major histocompatibility complex class I-related chain A and UL16-binding protein expression on tumor cell lines of different histotypes: analysis of tumor susceptibility to NKG2D-dependent natural killer cell cytotoxicity. *Cancer Res* **62**, 6178-6186 (2002).
164 Leivas, A. *et al.* NKG2D-CAR-transduced natural killer cells efficiently target multiple myeloma. *Blood Cancer J* **11**, 146, doi:10.1038/s41408-021-00537-w (2021).
165 Upshaw, J. L. *et al.* NKG2D-mediated signaling requires a DAP10-bound Grb2-Vav1 intermediate and phosphatidylinositol-3-kinase in human natural killer cells. *Nat Immunol* **7**, 524-532, doi:10.1038/ni1325 (2006).
166 Roda-Navarro, P. & Reyburn, H. T. The traffic of the NKG2D/Dap10 receptor complex during natural killer (NK) cell activation. *J Biol Chem* **284**, 16463-16472, doi:10.1074/jbc.M808561200 (2009).
167 Groh, V. *et al.* Cell stress-regulated human major histocompatibility complex class I gene expressed in gastrointestinal epithelium. *Proc Natl Acad Sci U S A* **93**, 12445-12450, doi:10.1073/pnas.93.22.12445 (1996).
168 Zhang, T., Barber, A. & Sentman, C. L. Generation of antitumor responses by genetic modification of primary human T cells with a chimeric NKG2D receptor. *Cancer Res* **66**, 5927-5933, doi:10.1158/0008-5472.CAN-06-0130 (2006).
169 Jiang, D. *et al.* Chimeric antigen receptor T cells targeting FcRH5 provide robust tumour-specific responses in murine xenograft models of multiple myeloma. *Nat Commun* **14**, 3642, doi:10.1038/s41467-023-39395-4 (2023).
170 Stewart, A. K. *et al.* Phase I study of the anti-FcRH5 antibody-drug conjugate DFRF4539A in relapsed or refractory multiple myeloma. *Blood Cancer J* **9**, 17, doi:10.1038/s41408-019-0178-8 (2019).
171 Elkins, K. *et al.* FcRL5 as a target of antibody-drug conjugates for the treatment of multiple myeloma. *Mol Cancer Ther* **11**, 2222-2232, doi:10.1158/1535-7163.MCT-12-0087 (2012).
172 Wang, Y. *et al.* Long-Term Follow-Up of Combination of B-Cell Maturation Antigen and CD19 Chimeric Antigen Receptor T Cells in Multiple Myeloma. *J Clin Oncol* **40**, 2246-2256, doi:10.1200/JCO.21.01676 (2022).
173 Li, X. *et al.* CD19, from bench to bedside. *Immunol Lett* **183**, 86-95, doi:10.1016/j.imlet.2017.01.010 (2017).
174 Wang, Y. *et al.* BCMA-targeting Bispecific Antibody That Simultaneously Stimulates NKG2D-enhanced Efficacy Against Multiple Myeloma. *J Immunother* **43**, 175-188, doi:10.1097/CJI.0000000000000320 (2020).
175 Shi, X. *et al.* Anti-CD19 and anti-BCMA CAR T cell therapy followed by lenalidomide maintenance after autologous stem-cell transplantation for high-risk newly diagnosed multiple myeloma. *Am J Hematol* **97**, 537-547, doi:10.1002/ajh.26486 (2022).
176 Garfall, A. L. *et al.* Anti-CD19 CAR T cells with high-dose melphalan and autologous stem cell transplantation for refractory multiple myeloma. *JCI Insight* **3**, doi:10.1172/jci.insight.120505 (2018).
177 Wang, Z., Zhao, K., Hackert, T. & Zoller, M. CD44/CD44v6 a Reliable Companion in Cancer-Initiating Cell Maintenance and Tumor Progression. *Front Cell Dev Biol* **6**, 97, doi:10.3389/fcell.2018.00097 (2018).
178 Ponta, H., Sherman, L. & Herrlich, P. A. CD44: from adhesion molecules to signalling regulators. *Nat Rev Mol Cell Biol* **4**, 33-45, doi:10.1038/nrm1004 (2003).
179 Jung, T., Gross, W. & Zoller, M. CD44v6 coordinates tumor matrix-triggered motility and apoptosis resistance. *J Biol Chem* **286**, 15862-15874, doi:10.1074/jbc.M110.208421 (2011).
180 Heider, K. H., Kuthan, H., Stehle, G. & Munzert, G. CD44v6: a target for antibody-based cancer therapy. *Cancer Immunol Immunother* **53**, 567-579, doi:10.1007/s00262-003-0494-4 (2004).
181 Casucci, M. *et al.* CD44v6-targeted T cells mediate potent antitumor effects against acute myeloid leukemia and multiple myeloma. *Blood* **122**, 3461-3472, doi:10.1182/blood-2013-04-493361 (2013).

182 Riechelmann, H. *et al.* Phase I trial with the CD44v6-targeting immunoconjugate bivatuzumab mertansine in head and neck squamous cell carcinoma. *Oral Oncol* **44**, 823-829, doi:10.1016/j.oraloncology.2007.10.009 (2008).
183 Awuah, D. *et al.* Developing a Safer Anti-CD44v6 Chimeric Antigen Receptor T Cell Against Hematological Cancers By Mitigating on-Target Off-Tumor Toxicity. *Blood* **138**, 2796-2796, doi:10.1182/blood-2021-153927 %J Blood (2021).
184 Bruno, B. *et al.* European Myeloma Network perspective on CAR T-Cell therapies for multiple myeloma. *Haematologica* **106**, 2054-2065, doi:10.3324/haematol.2020.276402 (2021).
185 Braumuller, H., Gansauge, S., Ramadani, M. & Gansauge, F. CD44v6 cell surface expression is a common feature of macrophages and macrophage-like cells - implication for a natural macrophage extravasation mechanism mimicked by tumor cells. *FEBS Lett* **476**, 240-247, doi:10.1016/s0014-5793(00)01737-3 (2000).
186 Soekojo, C. Y., Ooi, M., de Mel, S. & Chng, W. J. Immunotherapy in Multiple Myeloma. *Cells* **9**, doi:10.3390/cells9030601 (2020).
187 Hiemstra, I. H. *et al.* Preclinical anti-tumour activity of HexaBody-CD38, a next-generation CD38 antibody with superior complement-dependent cytotoxic activity. *EBioMedicine* **93**, 104663, doi:10.1016/j.ebiom.2023.104663 (2023).
188 Sonneveld, P. *et al.* Overall Survival With Daratumumab, Bortezomib, and Dexamethasone in Previously Treated Multiple Myeloma (CASTOR): A Randomized, Open-Label, Phase III Trial. *J Clin Oncol* **41**, 1600-1609, doi:10.1200/JCO.21.02734 (2023).
189 Dimopoulos, M. A. *et al.* Overall Survival With Daratumumab, Lenalidomide, and Dexamethasone in Previously Treated Multiple Myeloma (POLLUX): A Randomized, Open-Label, Phase III Trial. *J Clin Oncol* **41**, 1590-1599, doi:10.1200/JCO.22.00940 (2023).
190 Krejcik, J. *et al.* Daratumumab depletes CD38+ immune regulatory cells, promotes T-cell expansion, and skews T-cell repertoire in multiple myeloma. *Blood* **128**, 384-394, doi:10.1182/blood-2015-12-687749 (2016).
191 Nijhof, I. S. *et al.* CD38 expression and complement inhibitors affect response and resistance to daratumumab therapy in myeloma. *Blood* **128**, 959-970, doi:10.1182/blood-2016-03-703439 (2016).
192 Verkleij, C. P. M. *et al.* NK Cell Phenotype Is Associated With Response and Resistance to Daratumumab in Relapsed/Refractory Multiple Myeloma. *Hemasphere* **7**, e881, doi:10.1097/HS9.0000000000000881 (2023).
193 Naeimi Kararoudi, M. *et al.* CD38 deletion of human primary NK cells eliminates daratumumab-induced fratricide and boosts their effector activity. *Blood* **136**, 2416-2427, doi:10.1182/blood.2020006200 (2020).
194 Moreau, P. *et al.* Isatuximab, carfilzomib, and dexamethasone in relapsed multiple myeloma (IKEMA): a multicentre, open-label, randomised phase 3 trial. *Lancet* **397**, 2361-2371, doi:10.1016/S0140-6736(21)00592-4 (2021).
195 Martin, T. *et al.* Isatuximab, carfilzomib, and dexamethasone in patients with relapsed multiple myeloma: updated results from IKEMA, a randomized Phase 3 study. *Blood Cancer J* **13**, 72, doi:10.1038/s41408-023-00797-8 (2023).
196 Dhillon, S. Isatuximab: First Approval. *Drugs* **80**, 905-912, doi:10.1007/s40265-020-01311-1 (2020).
197 Moore, D. C., Elmes, J. B., Arnall, J. R., Strassels, S. A. & Patel, J. N. Hepatitis B reactivation in patients with multiple myeloma treated with anti-CD38 monoclonal antibody-based therapies: a pharmacovigilance analysis. *Int J Clin Pharm* **45**, 1492-1495, doi:10.1007/s11096-023-01608-7 (2023).
198 Magen, H. & Muchtar, E. Elotuzumab: the first approved monoclonal antibody for multiple myeloma treatment. *Ther Adv Hematol* **7**, 187-195, doi:10.1177/2040620716652862 (2016).
199 De Luca, F. *et al.* Monoclonal Antibodies: The Greatest Resource to Treat Multiple Myeloma. *Int J Mol Sci* **24**, doi:10.3390/ijms24043136 (2023).
200 Dimopoulos, M. A. *et al.* Elotuzumab Plus Pomalidomide and Dexamethasone for Relapsed/Refractory Multiple Myeloma: Final Overall Survival Analysis From the Randomized Phase II ELOQUENT-3 Trial. *J Clin Oncol* **41**, 568-578, doi:10.1200/JCO.21.02815 (2023).
201 Tai, Y. T. *et al.* Anti-CS1 humanized monoclonal antibody HuLuc63 inhibits myeloma cell adhesion and induces antibody-dependent cellular cytotoxicity in the bone marrow milieu. *Blood* **112**, 1329-1337, doi:10.1182/blood-2007-08-107292 (2008).
202 Ritchie, D. & Colonna, M. Mechanisms of Action and Clinical Development of Elotuzumab. *Clin Transl Sci* **11**, 261-266, doi:10.1111/cts.12532 (2018).

203 Liu, Y. C., Szmania, S. & van Rhee, F. Profile of elotuzumab and its potential in the treatment of multiple myeloma. *Blood Lymphat Cancer* **2014**, 15-27, doi:10.2147/BLCTT.S49780 (2014).

204 Lonial, S. *et al.* Belantamab mafodotin for relapsed or refractory multiple myeloma (DREAMM-2): a two-arm, randomised, open-label, phase 2 study. *Lancet Oncol* **21**, 207-221, doi:10.1016/S1470-2045(19)30788-0 (2020).

205 Abramson, H. N. Immunotherapy of Multiple Myeloma: Current Status as Prologue to the Future. *Int J Mol Sci* **24**, doi:10.3390/ijms242115674 (2023).

206 Markham, A. Belantamab Mafodotin: First Approval. *Drugs* **80**, 1607-1613, doi:10.1007/s40265-020-01404-x (2020).

207 Weisel, K. *et al.* A phase 3, open-label, randomized study to evaluate the efficacy and safety of single-agent belantamab mafodotin (belamaf) compared to pomalidomide plus low-dose dexamethasone (Pd) in patients (pts) with relapsed/refractory multiple myeloma (RRMM): DREAMM-3. **41**, 8007-8007, doi:10.1200/JCO.2023.41.16_suppl.8007 (2023).

208 de la Rubia, J. *et al.* Belantamab Mafodotin in Patients with Relapsed/Refractory Multiple Myeloma: Results of the Compassionate Use or the Expanded Access Program in Spain. *Cancers (Basel)* **15**, doi:10.3390/cancers15112964 (2023).

209 Cho, S. F., Yeh, T. J., Anderson, K. C. & Tai, Y. T. Bispecific antibodies in multiple myeloma treatment: A journey in progress. *Front Oncol* **12**, 1032775, doi:10.3389/fonc.2022.1032775 (2022).

210 Rampotas, A., Sangha, G. & Collins, G. P. Integration of cell therapies and bispecific antibodies into the treatment pathway of relapsed diffuse large B-cell lymphoma. *Ther Adv Hematol* **12**, 20406207211053120, doi:10.1177/20406207211053120 (2021).

211 Li, J. *et al.* Membrane-Proximal Epitope Facilitates Efficient T Cell Synapse Formation by Anti-FcRH5/CD3 and Is a Requirement for Myeloma Cell Killing. *Cancer Cell* **31**, 383-395, doi:10.1016/j.ccell.2017.02.001 (2017).

212 Kumar, S. *et al.* CAMMA 2: A phase I/II trial evaluating the efficacy and safety of cevostamab in patients with relapsed/refractory multiple myeloma (RRMM) who have triple-class refractory disease and have received a prior anti-B-cell maturation antigen (BCMA) agent. **41**, TPS8064-TPS8064, doi:10.1200/JCO.2023.41.16_suppl.TPS8064 (2023).

213 Pillarisetti, K. *et al.* Teclistamab is an active T cell-redirecting bispecific antibody against B-cell maturation antigen for multiple myeloma. *Blood Adv* **4**, 4538-4549, doi:10.1182/bloodadvances.2020002393 (2020).

214 Moreau, P. *et al.* Teclistamab in Relapsed or Refractory Multiple Myeloma. *N Engl J Med* **387**, 495-505, doi:10.1056/NEJMoa2203478 (2022).

215 Lesokhin, A. M. *et al.* Elranatamab in relapsed or refractory multiple myeloma: phase 2 MagnetisMM-3 trial results. *Nat Med* **29**, 2259-2267, doi:10.1038/s41591-023-02528-9 (2023).

216 Verkleij, C. P. M. *et al.* Preclinical activity and determinants of response of the GPRC5DxCD3 bispecific antibody talquetamab in multiple myeloma. *Blood Adv* **5**, 2196-2215, doi:10.1182/bloodadvances.2020003805 (2021).

217 Zhao, J., Ren, Q., Liu, X., Guo, X. & Song, Y. Bispecific antibodies targeting BCMA, GPRC5D, and FcRH5 for multiple myeloma therapy: latest updates from ASCO 2023 Annual Meeting. *J Hematol Oncol* **16**, 92, doi:10.1186/s13045-023-01489-3 (2023).

218 Tokarew, N., Ogonek, J., Endres, S., von Bergwelt-Baildon, M. & Kobold, S. Teaching an old dog new tricks: next-generation CAR T cells. *Br J Cancer* **120**, 26-37, doi:10.1038/s41416-018-0325-1 (2019).

219 Boussi, L. S., Avigan, Z. M. & Rosenblatt, J. Immunotherapy for the treatment of multiple myeloma. *Front Immunol* **13**, 1027385, doi:10.3389/fimmu.2022.1027385 (2022).

220 Yeo, D., Giardina, C., Saxena, P. & Rasko, J. E. J. The next wave of cellular immunotherapies in pancreatic cancer. *Mol Ther Oncolytics* **24**, 561-576, doi:10.1016/j.omto.2022.01.010 (2022).

221 Daher, M. & Rezvani, K. Outlook for New CAR-Based Therapies with a Focus on CAR NK Cells: What Lies Beyond CAR-Engineered T Cells in the Race against Cancer. *Cancer Discov* **11**, 45-58, doi:10.1158/2159-8290.CD-20-0556 (2021).

222 Mullard, A. FDA approves first CAR T therapy. *Nat Rev Drug Discov* **16**, 669, doi:10.1038/nrd.2017.196 (2017).

223 Maude, S. L. *et al.* Tisagenlecleucel in Children and Young Adults with B-Cell Lymphoblastic Leukemia. *N Engl J Med* **378**, 439-448, doi:10.1056/NEJMoa1709866 (2018).

224 Chen, Y. J., Abila, B. & Mostafa Kamel, Y. CAR-T: What Is Next? *Cancers (Basel)* **15**, doi:10.3390/cancers15030663 (2023).

225 Choi, B. D. *et al.* Intraventricular CARv3-TEAM-E T Cells in Recurrent Glioblastoma. *N Engl J Med* **390**, 1290-1298, doi:10.1056/NEJMoa2314390 (2024).

226 Bagley, S. J. *et al.* Intrathecal bivalent CAR T cells targeting EGFR and IL13Ralpha2 in recurrent glioblastoma: phase 1 trial interim results. *Nat Med* **30**, 1320-1329, doi:10.1038/s41591-024-02893-z (2024).

227 Clinicaltrials.gov. (2024).

228 Rodriguez-Otero, P. *et al.* Ide-cel or Standard Regimens in Relapsed and Refractory Multiple Myeloma. *N Engl J Med* **388**, 1002-1014, doi:10.1056/NEJMoa2213614 (2023).

229 Berdeja, J. G. *et al.* Ciltacabtagene autoleucel, a B-cell maturation antigen-directed chimeric antigen receptor T-cell therapy in patients with relapsed or refractory multiple myeloma (CARTITUDE-1): a phase 1b/2 open-label study. *Lancet* **398**, 314-324, doi:10.1016/S0140-6736(21)00933-8 (2021).

230 San-Miguel, J. *et al.* Cilta-cel or Standard Care in Lenalidomide-Refractory Multiple Myeloma. *N Engl J Med* **389**, 335-347, doi:10.1056/NEJMoa2303379 (2023).

231 Rodriguez-Otero, P. & San-Miguel, J. F. Cellular therapy for multiple myeloma: what's now and what's next. *Hematology Am Soc Hematol Educ Program* **2022**, 180-189, doi:10.1182/hematology.2022000396 (2022).

232 Khan, A. N. *et al.* Immunogenicity of CAR-T Cell Therapeutics: Evidence, Mechanism and Mitigation. *Front Immunol* **13**, 886546, doi:10.3389/fimmu.2022.886546 (2022).

233 Jayaraman, J. *et al.* CAR-T design: Elements and their synergistic function. *EBioMedicine* **58**, 102931, doi:10.1016/j.ebiom.2020.102931 (2020).

234 Zhu, X., Li, Q. & Zhu, X. Mechanisms of CAR T cell exhaustion and current counteraction strategies. *Front Cell Dev Biol* **10**, 1034257, doi:10.3389/fcell.2022.1034257 (2022).

235 Gumber, D. & Wang, L. D. Improving CAR-T immunotherapy: Overcoming the challenges of T cell exhaustion. *EBioMedicine* **77**, 103941, doi:10.1016/j.ebiom.2022.103941 (2022).

236 Ruffo, E. *et al.* Post-translational covalent assembly of CAR and synNotch receptors for programmable antigen targeting. *Nat Commun* **14**, 2463, doi:10.1038/s41467-023-37863-5 (2023).

237 Fernandez de Larrea, C. *et al.* Defining an Optimal Dual-Targeted CAR T-cell Therapy Approach Simultaneously Targeting BCMA and GPRC5D to Prevent BCMA Escape-Driven Relapse in Multiple Myeloma. *Blood Cancer Discov* **1**, 146-154, doi:10.1158/2643-3230.BCD-20-0020 (2020).

238 Roeven, M. W., Hobo, W., Schaap, N. & Dolstra, H. Immunotherapeutic approaches to treat multiple myeloma. *Hum Vaccin Immunother* **10**, 896-910, doi:10.4161/hv.27380 (2014).

239 Morris, E. C., Neelapu, S. S., Giavridis, T. & Sadelain, M. Cytokine release syndrome and associated neurotoxicity in cancer immunotherapy. *Nat Rev Immunol* **22**, 85-96, doi:10.1038/s41577-021-00547-6 (2022).

240 Jain, T., Olson, T. S. & Locke, F. L. How I treat cytopenias after CAR T-cell therapy. *Blood* **141**, 2460-2469, doi:10.1182/blood.2022017415 (2023).

241 Hines, M. R. *et al.* Hemophagocytic lymphohistiocytosis-like toxicity (carHLH) after CD19-specific CAR T-cell therapy. *Br J Haematol* **194**, 701-707, doi:10.1111/bjh.17662 (2021).

242 Valeri, A. *et al.* Overcoming tumor resistance mechanisms in CAR-NK cell therapy. *Front Immunol* **13**, 953849, doi:10.3389/fimmu.2022.953849 (2022).

243 Chen, S. & van den Brink, M. R. M. Allogeneic "Off-the-Shelf" CAR T cells: Challenges and advances. *Best Pract Res Clin Haematol* **37**, 101566, doi:10.1016/j.beha.2024.101566 (2024).

244 Cichocki, F., Miller, J. S., Anderson, S. K. & Bryceson, Y. T. Epigenetic regulation of NK cell differentiation and effector functions. *Front Immunol* **4**, 55, doi:10.3389/fimmu.2013.00055 (2013).

245 Berrien-Elliott, M. M., Jacobs, M. T. & Fehniger, T. A. Allogeneic natural killer cell therapy. *Blood* **141**, 856-868, doi:10.1182/blood.2022016200 (2023).

246 Del Zotto, G. *et al.* Comprehensive Phenotyping of Human PB NK Cells by Flow Cytometry. *Cytometry A* **97**, 891-899, doi:10.1002/cyto.a.24001 (2020).

247 Pereira, B. I. *et al.* Senescent cells evade immune clearance via HLA-E-mediated NK and CD8(+) T cell inhibition. *Nat Commun* **10**, 2387, doi:10.1038/s41467-019-10335-5 (2019).

248 Shimasaki, N., Jain, A. & Campana, D. NK cells for cancer immunotherapy. *Nat Rev Drug Discov* **19**, 200-218, doi:10.1038/s41573-019-0052-1 (2020).

249 Guillerey, C., Huntington, N. D. & Smyth, M. J. Targeting natural killer cells in cancer immunotherapy. *Nat Immunol* **17**, 1025-1036, doi:10.1038/ni.3518 (2016).

250 Sivori, S. *et al.* NK Cell-Based Immunotherapy for Hematological Malignancies. *J Clin Med* **8**, doi:10.3390/jcm8101702 (2019).

251 Debska-Zielkowska, J. *et al.* KIR Receptors as Key Regulators of NK Cells Activity in Health and Disease. *Cells* **10**, doi:10.3390/cells10071777 (2021).

252 Marofi, F. *et al.* Renaissance of armored immune effector cells, CAR-NK cells, brings the higher hope for successful cancer therapy. *Stem Cell Res Ther* **12**, 200, doi:10.1186/s13287-021-02251-7 (2021).

253 Borrego, F., Masilamani, M., Marusina, A. I., Tang, X. & Coligan, J. E. The CD94/NKG2 family of receptors: from molecules and cells to clinical relevance. *Immunol Res* **35**, 263-278, doi:10.1385/IR:35:3:263 (2006).

254 Barrow, A. D., Martin, C. J. & Colonna, M. The Natural Cytotoxicity Receptors in Health and Disease. *Front Immunol* **10**, 909, doi:10.3389/fimmu.2019.00909 (2019).

255 Romee, R. *et al.* NK cell CD16 surface expression and function is regulated by a disintegrin and metalloprotease-17 (ADAM17). *Blood* **121**, 3599-3608, doi:10.1182/blood-2012-04-425397 (2013).

256 Zhang, Z. *et al.* DNAM-1 controls NK cell activation via an ITT-like motif. *J Exp Med* **212**, 2165-2182, doi:10.1084/jem.20150792 (2015).

257 Harjunpaa, H. & Guillerey, C. TIGIT as an emerging immune checkpoint. *Clin Exp Immunol* **200**, 108-119, doi:10.1111/cei.13407 (2020).

258 Cozar, B. *et al.* Tumor-Infiltrating Natural Killer Cells. *Cancer Discov* **11**, 34-44, doi:10.1158/2159-8290.CD-20-0655 (2021).

259 Wolf, Y., Anderson, A. C. & Kuchroo, V. K. TIM3 comes of age as an inhibitory receptor. *Nat Rev Immunol* **20**, 173-185, doi:10.1038/s41577-019-0224-6 (2020).

260 Borys, S. M., Bag, A. K., Brossay, L. & Adeegbe, D. O. The Yin and Yang of Targeting KLRG1(+) Tregs and Effector Cells. *Front Immunol* **13**, 894508, doi:10.3389/fimmu.2022.894508 (2022).

261 Ghosh, C., Luong, G. & Sun, Y. A snapshot of the PD-1/PD-L1 pathway. *J Cancer* **12**, 2735-2746, doi:10.7150/jca.57334 (2021).

262 Poznanski, S. M. *et al.* Expanded human NK cells from lung cancer patients sensitize patients' PDL1-negative tumors to PD1-blockade therapy. *J Immunother Cancer* **9**, doi:10.1136/jitc-2020-001933 (2021).

263 Hasim, M. S. *et al.* When killers become thieves: Trogocytosed PD-1 inhibits NK cells in cancer. *Sci Adv* **8**, eabj3286, doi:10.1126/sciadv.abj3286 (2022).

264 Caruso, S. *et al.* Safe and effective off-the-shelf immunotherapy based on CAR.CD123-NK cells for the treatment of acute myeloid leukaemia. *J Hematol Oncol* **15**, 163, doi:10.1186/s13045-022-01376-3 (2022).

265 Glienke, W. *et al.* Advantages and applications of CAR-expressing natural killer cells. *Front Pharmacol* **6**, 21, doi:10.3389/fphar.2015.00021 (2015).

266 Biederstadt, A. & Rezvani, K. Engineering the next generation of CAR-NK immunotherapies. *Int J Hematol* **114**, 554-571, doi:10.1007/s12185-021-03209-4 (2021).

267 Chiossone, L. & Vivier, E. Bringing natural killer cells to the clinic. *J Exp Med* **219**, doi:10.1084/jem.20220830 (2022).

268 Kang, L. *et al.* Characterization and ex vivo Expansion of Human Placenta-Derived Natural Killer Cells for Cancer Immunotherapy. *Front Immunol* **4**, 101, doi:10.3389/fimmu.2013.00101 (2013).

269 Shah, N. N. & Fry, T. J. Mechanisms of resistance to CAR T cell therapy. *Nat Rev Clin Oncol* **16**, 372-385, doi:10.1038/s41571-019-0184-6 (2019).

270 Schmidt, D. *et al.* Engineering CAR-NK cells: how to tune innate killer cells for cancer immunotherapy. *Immunother Adv* **2**, ltac003, doi:10.1093/immadv/ltac003 (2022).

271 Zhang, L. *et al.* Natural killer cells: of-the-shelf cytotherapy for cancer immunosurveillance. *Am J Cancer Res* **11**, 1770-1791 (2021).

272 Gong, Y., Klein Wolterink, R. G. J., Wang, J., Bos, G. M. J. & Germeraad, W. T. V. Chimeric antigen receptor natural killer (CAR-NK) cell design and engineering for cancer therapy. *J Hematol Oncol* **14**, 73, doi:10.1186/s13045-021-01083-5 (2021).

273 Sutlu, T. *et al.* Inhibition of intracellular antiviral defense mechanisms augments lentiviral transduction of human natural killer cells: implications for gene therapy. *Hum Gene Ther* **23**, 1090-1100, doi:10.1089/hum.2012.080 (2012).

274 Sarvaria, A., Jawdat, D., Madrigal, J. A. & Saudemont, A. Umbilical Cord Blood Natural Killer Cells, Their Characteristics, and Potential Clinical Applications. *Front Immunol* **8**, 329, doi:10.3389/fimmu.2017.00329 (2017).

275 Luevano, M. *et al.* The unique profile of cord blood natural killer cells balances incomplete maturation and effective killing function upon activation. *Hum Immunol* **73**, 248-257, doi:10.1016/j.humimm.2011.12.015 (2012).

276 Myers, J. A. & Miller, J. S. Exploring the NK cell platform for cancer immunotherapy. *Nat Rev Clin Oncol* **18**, 85-100, doi:10.1038/s41571-020-0426-7 (2021).

277 Herrera, L. *et al.* Adult peripheral blood and umbilical cord blood NK cells are good sources for effective CAR therapy against CD19 positive leukemic cells. *Sci Rep* **9**, 18729, doi:10.1038/s41598-019-55239-y (2019).

278 Zhang, L., Meng, Y., Feng, X. & Han, Z. CAR-NK cells for cancer immunotherapy: from bench to bedside. *Biomark Res* **10**, 12, doi:10.1186/s40364-022-00364-6 (2022).

279 Dhakal, B. *et al.* Interim Phase I Clinical Data of FT576 As Monotherapy and in Combination with Daratumumab in Subjects with Relapsed/Refractory Multiple Myeloma. *Blood* **140**, 4586-4587, doi:10.1182/blood-2022-166994 %J Blood (2022).

280 Jiang, H. *et al.* Transfection of chimeric anti-CD138 gene enhances natural killer cell activation and killing of multiple myeloma cells. *Mol Oncol* **8**, 297-310, doi:10.1016/j.molonc.2013.12.001 (2014).

281 Hambach, J. *et al.* Targeting CD38-Expressing Multiple Myeloma and Burkitt Lymphoma Cells In Vitro with Nanobody-Based Chimeric Antigen Receptors (Nb-CARs). *Cells* **9**, doi:10.3390/cells9020321 (2020).

282 Park, E. *et al.* CAR NK92 Cells Targeting BCMA Can Effectively Kill Multiple Myeloma Cells Both In Vitro and In Vivo. *Biomedicines* **12**, doi:10.3390/biomedicines12010248 (2024).

283 Motais, B., Charvátová, S., Hrdinka, M., Hájek, R. & Bago, J. R. Anti-BCMA-CAR NK Cells Expressing Soluble TRAIL: Promising Therapeutic Approach for Multiple Myeloma in Combination with Bortezomib and γ-Secretase Inhibitors. *Blood* **140**, 12683-12684, doi:10.1182/blood-2022-166167 %J Blood (2022).

284 Roex, G. *et al.* Two for one: targeting BCMA and CD19 in B-cell malignancies with off-the-shelf dual-CAR NK-92 cells. *J Transl Med* **20**, 124, doi:10.1186/s12967-022-03326-6 (2022).

285 Luanpitpong, S., Poohadsuan, J., Klaihmon, P. & Issaragrisil, S. Selective Cytotoxicity of Single and Dual Anti-CD19 and Anti-CD138 Chimeric Antigen Receptor-Natural Killer Cells against Hematologic Malignancies. *J Immunol Res* **2021**, 5562630, doi:10.1155/2021/5562630 (2021).

286 Martín, E. M. *et al.* P-007: Exploring a safety switch in NKG2D and BCMA CAR NK-92MI immunotherapy. *Clinical Lymphoma, Myeloma and Leukemia* **21**, S42-S43, doi:10.1016/S2152-2650(21)02141-8 (2021).

287 Golubovskaya, V. *et al.* CAR-NK Cells Generated with mRNA-LNPs Kill Tumor Target Cells In Vitro and In Vivo. *Int J Mol Sci* **24**, doi:10.3390/ijms241713364 (2023).

288 Ng, Y. Y., Du, Z., Zhang, X., Chng, W. J. & Wang, S. CXCR4 and anti-BCMA CAR co-modified natural killer cells suppress multiple myeloma progression in a xenograft mouse model. *Cancer Gene Ther* **29**, 475-483, doi:10.1038/s41417-021-00365-x (2022).

289 Wang, X. *et al.* Inducible MyD88/CD40 synergizes with IL-15 to enhance antitumor efficacy of CAR-NK cells. *Blood Adv* **4**, 1950-1964, doi:10.1182/bloodadvances.2020001510 (2020).

290 Maroto-Martin, E. *Desarrollo preclinico de la inmunoterapia adoptiva con células NK-CAR alogénicas para el tratamiento de mieloma múltiple refractario y en recaída* Doctorado en Investigación Biomédica thesis, Universidad Complutense de Madrid. Facultad de Medicina., (2023).

291 Edri, A. *et al.* Nicotinamide-Expanded Allogeneic Natural Killer Cells with CD38 Deletion, Expressing an Enhanced CD38 Chimeric Antigen Receptor, Target Multiple Myeloma Cells. **24**, 17231 (2023).

292 Brophy, S., et al.,. CB derived, optimized affinity CD38 CAR-NK cells with CD38 KO show promising in-vivo activity in a Multiple Myeloma model. *IMS 2022* (2022).

293 Duggal, R. *et al.* Promising Preliminary Activity of Optimized Affinity, CD38 CAR NK Cells Generated Using a Non-Viral Engineering Approach in Gene Edited Cord Blood Derived NK Cells for the Treatment of Multiple Myeloma. *Blood* **138**, 4793-4793, doi:10.1182/blood-2021-151379 %J Blood (2021).

294 O'Neal, J. *et al.* Anti-myeloma efficacy of CAR-iNKT is enhanced with a long-acting IL-7, rhIL-7-hyFc. *Blood Advances* **7**, 6009-6022, doi:10.1182/bloodadvances.2023010032 %J Blood Advances (2023).

295 Reiser, J. *et al.* FT555: Off-the-Shelf CAR-NK Cell Therapy Co-Targeting GPRC5D and CD38 for the Treatment of Multiple Myeloma. *Blood* **140**, 4560-4561, doi:10.1182/blood-2022-170501 %J Blood (2022).

296 Cichocki, F. *et al.* Quadruple gene-engineered natural killer cells enable multi-antigen targeting for durable antitumor activity against multiple myeloma. *Nat Commun* **13**, 7341, doi:10.1038/s41467-022-35127-2 (2022).

297 Liu, E. *et al.* Use of CAR-Transduced Natural Killer Cells in CD19-Positive Lymphoid Tumors. *N Engl J Med* **382**, 545-553, doi:10.1056/NEJMoa1910607 (2020).

298 Marin, D. *et al.* Safety, efficacy and determinants of response of allogeneic CD19-specific CAR-NK cells in CD19(+) B cell tumors: a phase 1/2 trial. *Nat Med* **30**, 772-784, doi:10.1038/s41591-023-02785-8 (2024).
299 Bachanova, V. *et al.* Safety and Efficacy of FT596, a First-in-Class, Multi-Antigen Targeted, Off-the-Shelf, iPSC-Derived CD19 CAR NK Cell Therapy in Relapsed/Refractory B-Cell Lymphoma. *Blood* **138**, 823-823, doi:10.1182/blood-2021-151185 %J Blood (2021).
300 Dickinson, M. *et al.* First in human data of NKX019, an allogeneic CAR NK for the treatment of relapsed/refractory (R/R) B-cell malignancies. **41**, 526-527, doi:https://doi.org/10.1002/hon.3164_389 (2023).
301 Cichocki, F. *et al.* GSK3 Inhibition Drives Maturation of NK Cells and Enhances Their Antitumor Activity. *Cancer Res* **77**, 5664-5675, doi:10.1158/0008-5472.CAN-17-0799 (2017).
302 Afolabi, L. O. *et al.* Synergistic Tumor Cytolysis by NK Cells in Combination With a Pan-HDAC Inhibitor, Panobinostat. *Front Immunol* **12**, 701671, doi:10.3389/fimmu.2021.701671 (2021).
303 Xiao, X. *et al.* Bispecific NK-cell engager targeting BCMA elicits stronger antitumor effects and produces less proinflammatory cytokines than T-cell engager. *Front Immunol* **14**, 1113303, doi:10.3389/fimmu.2023.1113303 (2023).
304 Zhang, C. *et al.* Bispecific antibody-mediated redirection of NKG2D-CAR natural killer cells facilitates dual targeting and enhances antitumor activity. *J Immunother Cancer* **9**, doi:10.1136/jitc-2021-002980 (2021).
305 Pawlowski, K. D., Duffy, J. T., Tiwari, A., Zannikou, M. & Balyasnikova, I. V. Bi-Specific Killer Cell Engager Enhances NK Cell Activity against Interleukin-13 Receptor Alpha-2 Positive Gliomas. *Cells* **12**, doi:10.3390/cells12131716 (2023).
306 Gurney, M. *et al.* CD38 knockout natural killer cells expressing an affinity optimized CD38 chimeric antigen receptor successfully target acute myeloid leukemia with reduced effector cell fratricide. *Haematologica* **107**, 437-445, doi:10.3324/haematol.2020.271908 (2022).
307 Choi, E. *et al.* Engineering CD70-Directed CAR-NK Cells for the Treatment of Hematological and Solid Malignancies. *Blood* **138**, 1691-1691, doi:10.1182/blood-2021-148649 %J Blood (2021).
308 Li, Y. *et al.* KIR-based inhibitory CARs overcome CAR-NK cell trogocytosis-mediated fratricide and tumor escape. *Nat Med* **28**, 2133-2144, doi:10.1038/s41591-022-02003-x (2022).
309 Konjevic, G. *et al.* Decreased CD161 activating and increased CD158a inhibitory receptor expression on NK cells underlies impaired NK cell cytotoxicity in patients with multiple myeloma. *J Clin Pathol*, doi:10.1136/jclinpath-2016-203614 (2016).
310 Nijhof, I. S. *et al.* Daratumumab-mediated lysis of primary multiple myeloma cells is enhanced in combination with the human anti-KIR antibody IPH2102 and lenalidomide. *Haematologica* **100**, 263-268, doi:10.3324/haematol.2014.117531 (2015).
311 Benson, D. M., Jr. *et al.* IPH2101, a novel anti-inhibitory KIR antibody, and lenalidomide combine to enhance the natural killer cell versus multiple myeloma effect. *Blood* **118**, 6387-6391, doi:10.1182/blood-2011-06-360255 (2011).
312 Vey, N. *et al.* A phase 1 study of lirilumab (antibody against killer immunoglobulin-like receptor antibody KIR2D; IPH2102) in patients with solid tumors and hematologic malignancies. *Oncotarget* **9**, 17675-17688, doi:10.18632/oncotarget.24832 (2018).
313 Benson, D. M., Jr. *et al.* A phase 1 trial of the anti-KIR antibody IPH2101 in patients with relapsed/refractory multiple myeloma. *Blood* **120**, 4324-4333, doi:10.1182/blood-2012-06-438028 (2012).
314 Benson, D. M., Jr. *et al.* A Phase I Trial of the Anti-KIR Antibody IPH2101 and Lenalidomide in Patients with Relapsed/Refractory Multiple Myeloma. *Clin Cancer Res* **21**, 4055-4061, doi:10.1158/1078-0432.CCR-15-0304 (2015).
315 Laskowski, T. J., Biederstadt, A. & Rezvani, K. Natural killer cells in antitumour adoptive cell immunotherapy. *Nat Rev Cancer* **22**, 557-575, doi:10.1038/s41568-022-00491-0 (2022).
316 Carlsten, M. *et al.* Checkpoint Inhibition of KIR2D with the Monoclonal Antibody IPH2101 Induces Contraction and Hyporesponsiveness of NK Cells in Patients with Myeloma. *Clin Cancer Res* **22**, 5211-5222, doi:10.1158/1078-0432.CCR-16-1108 (2016).
317 Benson, D. M., Jr. *et al.* The PD-1/PD-L1 axis modulates the natural killer cell versus multiple myeloma effect: a therapeutic target for CT-011, a novel monoclonal anti-PD-1 antibody. *Blood* **116**, 2286-2294, doi:10.1182/blood-2010-02-271874 (2010).

318 Mateos, M. V. *et al.* Pembrolizumab plus pomalidomide and dexamethasone for patients with relapsed or refractory multiple myeloma (KEYNOTE-183): a randomised, open-label, phase 3 trial. *Lancet Haematol* **6**, e459-e469, doi:10.1016/S2352-3026(19)30110-3 (2019).
319 D'Souza, A. *et al.* A Phase 2 Study of Pembrolizumab during Lymphodepletion after Autologous Hematopoietic Cell Transplantation for Multiple Myeloma. *Biol Blood Marrow Transplant* **25**, 1492-1497, doi:10.1016/j.bbmt.2019.04.005 (2019).
320 Badros, A. Z., Ma, N., Rapoport, A. P., Lederer, E. & Lesokhin, A. M. Long-term remissions after stopping pembrolizumab for relapsed or refractory multiple myeloma. *Blood Adv* **3**, 1658-1660, doi:10.1182/bloodadvances.2019000191 (2019).
321 Judge, S. J. *et al.* Minimal PD-1 expression in mouse and human NK cells under diverse conditions. *J Clin Invest* **130**, 3051-3068, doi:10.1172/JCI133353 (2020).
322 Yang, C. *et al.* Abstract 4077: Dual-targeted CAR-NK cell therapy: optimized CAR design to prevent antigen escape and elicit a deep and durable response in multiple myeloma. *Cancer Research* **83**, 4077-4077, doi:10.1158/1538-7445.AM2023-4077 %J Cancer Research (2023).
323 Pomeroy, E. J. *et al.* A Genetically Engineered Primary Human Natural Killer Cell Platform for Cancer Immunotherapy. *Mol Ther* **28**, 52-63, doi:10.1016/j.ymthe.2019.10.009 (2020).
324 Liu, Z. Y. *et al.* CD155/TIGIT signalling plays a vital role in the regulation of bone marrow mesenchymal stem cell-induced natural killer-cell exhaustion in multiple myeloma. *Clin Transl Med* **12**, e861, doi:10.1002/ctm2.861 (2022).
325 Zhang, Q. *et al.* Blockade of the checkpoint receptor TIGIT prevents NK cell exhaustion and elicits potent anti-tumor immunity. *Nat Immunol* **19**, 723-732, doi:10.1038/s41590-018-0132-0 (2018).
326 Maas, R. J. *et al.* TIGIT blockade enhances functionality of peritoneal NK cells with altered expression of DNAM-1/TIGIT/CD96 checkpoint molecules in ovarian cancer. *Oncoimmunology* **9**, 1843247, doi:10.1080/2162402X.2020.1843247 (2020).
327 Brauneck, F. *et al.* Combined Blockade of TIGIT and CD39 or A2AR Enhances NK-92 Cell-Mediated Cytotoxicity in AML. *Int J Mol Sci* **22**, doi:10.3390/ijms222312919 (2021).
328 Jo, D. H. *et al.* Simultaneous engineering of natural killer cells for CAR transgenesis and CRISPR-Cas9 knockout using retroviral particles. *Mol Ther Methods Clin Dev* **29**, 173-184, doi:10.1016/j.omtm.2023.03.006 (2023).
329 Hasan, M. F. *et al.* Knockout of the inhibitory receptor TIGIT enhances the antitumor response of ex vivo expanded NK cells and prevents fratricide with therapeutic Fc-active TIGIT antibodies. *J Immunother Cancer* **11**, doi:10.1136/jitc-2023-007502 (2023).
330 Wang, M. *et al.* Precision Enhancement of CAR-NK Cells through Non-Viral Engineering and Highly Multiplexed Base Editing. *bioRxiv*, doi:10.1101/2024.03.05.582637 (2024).
331 Jiang, W. *et al.* Tim-3 Blockade Elicits Potent Anti-Multiple Myeloma Immunity of Natural Killer Cells. *Front Oncol* **12**, 739976, doi:10.3389/fonc.2022.739976 (2022).
332 Morimoto, T. *et al.* CRISPR-Cas9-Mediated TIM3 Knockout in Human Natural Killer Cells Enhances Growth Inhibitory Effects on Human Glioma Cells. *Int J Mol Sci* **22**, doi:10.3390/ijms22073489 (2021).
333 Ulbrecht, M. *et al.* Cell surface expression of HLA-E: interaction with human beta2-microglobulin and allelic differences. *Eur J Immunol* **29**, 537-547, doi:10.1002/(SICI)1521-4141(199902)29:02<537::AID-IMMU537>3.0.CO;2-6 (1999).
334 Paech, C. *et al.* HLA-E diversity unfolded: Identification and characterization of 170 novel HLA-E alleles. *HLA* **97**, 389-398, doi:10.1111/tan.14195 (2021).
335 Braud, V. M. *et al.* HLA-E binds to natural killer cell receptors CD94/NKG2A, B and C. *Nature* **391**, 795-799, doi:10.1038/35869 (1998).
336 Ulbrecht, M., Modrow, S., Srivastava, R., Peterson, P. A. & Weiss, E. H. Interaction of HLA-E with peptides and the peptide transporter in vitro: implications for its function in antigen presentation. *J Immunol* **160**, 4375-4385 (1998).
337 Kanevskiy, L. *et al.* Dimorphism of HLA-E and its Disease Association. *Int J Mol Sci* **20**, doi:10.3390/ijms20215496 (2019).
338 Borst, L., van der Burg, S. H. & van Hall, T. The NKG2A-HLA-E Axis as a Novel Checkpoint in the Tumor Microenvironment. *Clin Cancer Res* **26**, 5549-5556, doi:10.1158/1078-0432.CCR-19-2095 (2020).
339 Lagana, A. *et al.* Increased HLA-E Expression Correlates with Early Relapse in Multiple Myeloma. *Blood* **132**, 59-59, doi:10.1182/blood-2018-99-116828 %J Blood (2018).
340 Ismael, A. *et al.* CREB1 promotes expression of immune checkpoint HLA-E leading to immune escape in multiple myeloma. *Leukemia* **38**, 1777-1786, doi:10.1038/s41375-024-02303-w (2024).
341 Encinas Mayoral, J. *ESTRATEGIAS PARA LA MEJORA DE LA PERSISTENCIA Y LA EFICACIA DE LAS*

REFRACTARIO Y EN RECAÍDA Doctorado en Investigación Biomédica thesis, Universidad Complutense de Madrid. Facultad de Medicina. , (2024).

342 Le Roy, A. *et al.* Immunomodulatory Drugs Exert Anti-Leukemia Effects in Acute Myeloid Leukemia by Direct and Immunostimulatory Activities. *Front Immunol* **9**, 977, doi:10.3389/fimmu.2018.00977 (2018).

343 Enqvist, M. *et al.* Selenite induces posttranscriptional blockade of HLA-E expression and sensitizes tumor cells to CD94/NKG2A-positive NK cells. *J Immunol* **187**, 3546-3554, doi:10.4049/jimmunol.1100610 (2011).

344 Yun, H. D., Schirm, D. K., Felices, M., Miller, J. S. & Eckfeldt, C. E. Dinaciclib enhances natural killer cell cytotoxicity against acute myelogenous leukemia. *Blood Adv* **3**, 2448-2452, doi:10.1182/bloodadvances.2019000064 (2019).

345 Perez-Andres, M. *et al.* Characterization of bone marrow T cells in monoclonal gammopathy of undetermined significance, multiple myeloma, and plasma cell leukemia demonstrates increased infiltration by cytotoxic/Th1 T cells demonstrating a squed TCR-Vbeta repertoire. *Cancer* **106**, 1296-1305, doi:10.1002/cncr.21746 (2006).

346 Tognarelli, S. *et al.* Enhancing the Activation and Releasing the Brakes: A Double Hit Strategy to Improve NK Cell Cytotoxicity Against Multiple Myeloma. *Front Immunol* **9**, 2743, doi:10.3389/fimmu.2018.02743 (2018).

347 Bexte, T. *et al.* CRISPR-Cas9 based gene editing of the immune checkpoint NKG2A enhances NK cell mediated cytotoxicity against multiple myeloma. *Oncoimmunology* **11**, 2081415, doi:10.1080/2162402X.2022.2081415 (2022).

348 McWilliams, E. M. *et al.* Therapeutic CD94/NKG2A blockade improves natural killer cell dysfunction in chronic lymphocytic leukemia. *Oncoimmunology* **5**, e1226720, doi:10.1080/2162402X.2016.1226720 (2016).

349 Lee, J. *et al.* Monalizumab efficacy correlates with HLA-E surface expression and NK cell activity in head and neck squamous carcinoma cell lines. *J Cancer Res Clin Oncol* **149**, 5705-5715, doi:10.1007/s00432-022-04532-x (2023).

350 Kamiya, T., Seow, S. V., Wong, D., Robinson, M. & Campana, D. Blocking expression of inhibitory receptor NKG2A overcomes tumor resistance to NK cells. *J Clin Invest* **129**, 2094-2106, doi:10.1172/JCI123955 (2019).

351 Ismael, A. *et al.* CREB1 Promotes Immune Escape of Multiple Myeloma Cells By Inducing HLA-E. *Blood* **142**, 1930-1930, doi:10.1182/blood-2023-186134 %J Blood (2023).

352 Wang, X., Xiong, H. & Ning, Z. Implications of NKG2A in immunity and immune-mediated diseases. *Front Immunol* **13**, 960852, doi:10.3389/fimmu.2022.960852 (2022).

353 Fisher, J. G., Doyle, A. D. P., Graham, L. V., Khakoo, S. I. & Blunt, M. D. Disruption of the NKG2A:HLA-E Immune Checkpoint Axis to Enhance NK Cell Activation against Cancer. *Vaccines (Basel)* **10**, doi:10.3390/vaccines10121993 (2022).

354 Paul, S. & Lal, G. The Molecular Mechanism of Natural Killer Cells Function and Its Importance in Cancer Immunotherapy. *Front Immunol* **8**, 1124, doi:10.3389/fimmu.2017.01124 (2017).

355 Masilamani, M., Nguyen, C., Kabat, J., Borrego, F. & Coligan, J. E. CD94/NKG2A inhibits NK cell activation by disrupting the actin network at the immunological synapse. *J Immunol* **177**, 3590-3596, doi:10.4049/jimmunol.177.6.3590 (2006).

356 Zhang, X., Feng, J., Chen, S., Yang, H. & Dong, Z. Synergized regulation of NK cell education by NKG2A and specific Ly49 family members. *Nat Commun* **10**, 5010, doi:10.1038/s41467-019-13032-5 (2019).

357 Battin, C. *et al.* NKG2A-checkpoint inhibition and its blockade critically depends on peptides presented by its ligand HLA-E. *Immunology* **166**, 507-521, doi:10.1111/imm.13515 (2022).

358 Ruggeri, L. *et al.* Effects of anti-NKG2A antibody administration on leukemia and normal hematopoietic cells. *Haematologica* **101**, 626-633, doi:10.3324/haematol.2015.135301 (2016).

359 Andre, P. *et al.* Anti-NKG2A mAb Is a Checkpoint Inhibitor that Promotes Anti-tumor Immunity by Unleashing Both T and NK Cells. *Cell* **175**, 1731-1743 e1713, doi:10.1016/j.cell.2018.10.014 (2018).

360 Melero, I. *et al.* Intratumoral co-injection of NK cells and NKG2A-neutralizing monoclonal antibodies. *EMBO Mol Med* **15**, e17804, doi:10.15252/emmm.202317804 (2023).

361 Liu, X. *et al.* Immune checkpoint HLA-E:CD94-NKG2A mediates evasion of circulating tumor cells from NK cell surveillance. *Cancer Cell* **41**, 272-287 e279, doi:10.1016/j.ccell.2023.01.001 (2023).

362 Mahaweni, N. M. *et al.* NKG2A Expression Is Not per se Detrimental for the Anti-Multiple Myeloma Activity of Activated Natural Killer Cells in an In Vitro System Mimicking the Tumor Microenvironment. *Front Immunol* **9**, 1415, doi:10.3389/fimmu.2018.01415 (2018).

363 Figueiredo, C., Seltsam, A. & Blasczyk, R. Permanent silencing of NKG2A expression for cell-based therapeutics. *J Mol Med (Berl)* **87**, 199-210, doi:10.1007/s00109-008-0417-0 (2009).

364 Berrien-Elliott, M. M. *et al.* Multidimensional Analyses of Donor Memory-Like NK Cells Reveal New Associations with Response after Adoptive Immunotherapy for Leukemia. *Cancer Discov* **10**, 1854-1871, doi:10.1158/2159-8290.CD-20-0312 (2020).

365 Gong, Y. *et al.* NKG2A genetic deletion promotes human primary NK cell anti-tumor responses better than an anti-NKG2A monoclonal antibody. *Mol Ther* **32**, 2711-2727, doi:10.1016/j.ymthe.2024.06.034 (2024).

366 Mohammadian Gol, T. *et al.* CRISPR-Cas9-Based Gene Knockout of Immune Checkpoints in Expanded NK Cells. *Int J Mol Sci* **24**, doi:10.3390/ijms242216065 (2023).

367 Mac Donald, A. *et al.* KLRC1 knockout overcomes HLA-E-mediated inhibition and improves NK cell antitumor activity against solid tumors. *Front Immunol* **14**, 1231916, doi:10.3389/fimmu.2023.1231916 (2023).

368 Grote, S. *et al.* In Vitro Evaluation of CD276-CAR NK-92 Functionality, Migration and Invasion Potential in the Presence of Immune Inhibitory Factors of the Tumor Microenvironment. *Cells* **10**, doi:10.3390/cells10051020 (2021).

369 Kanaya, M. *et al.* CAR19 iPSC-Derived NK Cells Utilize the Innate Functional Potential Mediated through NKG2A-Driven Education and Override the HLA-E Check Point to Effectively Target B Cell Lymphoma. *Blood* **136**, 34-35, doi:10.1182/blood-2020-138527 %J Blood (2020).

370 Bexte, T. *et al.* CRISPR/Cas9 editing of NKG2A improves the efficacy of primary CD33-directed chimeric antigen receptor natural killer cells. *Nat Commun* **15**, 8439, doi:10.1038/s41467-024-52388-1 (2024).

371 Tinker, A. V. *et al.* Dose-Ranging and Cohort-Expansion Study of Monalizumab (IPH2201) in Patients with Advanced Gynecologic Malignancies: A Trial of the Canadian Cancer Trials Group (CCTG): IND221. *Clin Cancer Res* **25**, 6052-6060, doi:10.1158/1078-0432.CCR-19-0298 (2019).

372 Galot, R. *et al.* A phase II study of monalizumab in patients with recurrent/metastatic squamous cell carcinoma of the head and neck: The I1 cohort of the EORTC-HNCG-1559 UPSTREAM trial. *Eur J Cancer* **158**, 17-26, doi:10.1016/j.ejca.2021.09.003 (2021).

373 Colevas, D. A. *et al.* 123MO Monalizumab, cetuximab and durvalumab in first-line treatment of recurrent or metastatic squamous cell carcinoma of the head and neck (R/M SCCHN): A phase II trial. *Annals of Oncology* **32**, S1432, doi:10.1016/j.annonc.2021.10.142 (2021).

374 Cohen, R. B. *et al.* Combination of monalizumab and cetuximab in recurrent or metastatic head and neck cancer patients previously treated with platinum-based chemotherapy and PD-(L)1 inhibitors. **38**, 6516-6516, doi:10.1200/JCO.2020.38.15_suppl.6516 (2020).

375 Herbst, R. S. *et al.* COAST: An Open-Label, Phase II, Multidrug Platform Study of Durvalumab Alone or in Combination With Oleclumab or Monalizumab in Patients With Unresectable, Stage III Non-Small-Cell Lung Cancer. *J Clin Oncol* **40**, 3383-3393, doi:10.1200/JCO.22.00227 (2022).

376 Geurts, V. C. M. *et al.* Unleashing NK- and CD8 T cells by combining monalizumab and trastuzumab for metastatic HER2-positive breast cancer: Results of the MIMOSA trial. *Breast* **70**, 76-81, doi:10.1016/j.breast.2023.06.007 (2023).

377 Devillier, R. *et al.* Safety of Anti-NKG2A Blocking Antibody Monalizumab As Maintenance Therapy after Allogeneic Hematopoietic Stem Cell Transplantation: A Phase I Study. *Blood* **138**, 1817-1817, doi:10.1182/blood-2021-150730 %J Blood (2021).

378 Jinushi, M. *et al.* MHC class I chain-related protein A antibodies and shedding are associated with the progression of multiple myeloma. *Proc Natl Acad Sci U S A* **105**, 1285-1290, doi:10.1073/pnas.0711293105 (2008).

379 Diaz-Tejedor, A. *et al.* Immune System Alterations in Multiple Myeloma: Molecular Mechanisms and Therapeutic Strategies to Reverse Immunosuppression. *Cancers (Basel)* **13**, doi:10.3390/cancers13061353 (2021).

380 Uhl, C., Nyirenda, T., Siegel, D. S., Lee, W. Y. & Zilberberg, J. Natural killer cells activity against multiple myeloma cells is modulated by osteoblast-induced IL-6 and IL-10 production. *Heliyon* **8**, e09167, doi:10.1016/j.heliyon.2022.e09167 (2022).

381 Ratta, M. *et al.* Dendritic cells are functionally defective in multiple myeloma: the role of interleukin-6. *Blood* **100**, 230-237, doi:10.1182/blood.v100.1.230 (2002).

382 D'Andrea, A. *et al.* Interleukin 10 (IL-10) inhibits human lymphocyte interferon gamma-production by suppressing natural killer cell stimulatory factor/IL-12 synthesis in accessory cells. *J Exp Med* **178**, 1041-1048, doi:10.1084/jem.178.3.1041 (1993).
383 Iwasa, M. *et al.* PD-L1 upregulation in myeloma cells by panobinostat in combination with interferon-gamma. *Oncotarget* **10**, 1903-1917, doi:10.18632/oncotarget.26726 (2019).
384 Li, W., Liang, L., Liao, Q., Li, Y. & Zhou, Y. CD38: An important regulator of T cell function. *Biomed Pharmacother* **153**, 113395, doi:10.1016/j.biopha.2022.113395 (2022).
385 Zhou, L., Liu, X., Guan, T., Xu, H. & Wei, F. CD73 Dysregulates Monocyte Anti-Tumor Activity in Multiple Myeloma. *Cancer Manag Res* **15**, 729-738, doi:10.2147/CMAR.S411547 (2023).
386 Ray, A. *et al.* Targeting tryptophan catabolic kynurenine pathway enhances antitumor immunity and cytotoxicity in multiple myeloma. *Leukemia* **34**, 567-577, doi:10.1038/s41375-019-0558-x (2020).
387 Katz, J. B., Muller, A. J. & Prendergast, G. C. Indoleamine 2,3-dioxygenase in T-cell tolerance and tumoral immune escape. *Immunol Rev* **222**, 206-221, doi:10.1111/j.1600-065X.2008.00610.x (2008).
388 Della Chiesa, M. *et al.* The tryptophan catabolite L-kynurenine inhibits the surface expression of NKp46- and NKG2D-activating receptors and regulates NK-cell function. *Blood* **108**, 4118-4125, doi:10.1182/blood-2006-03-006700 (2006).
389 Rebmann, V. *et al.* Soluble MICA as an independent prognostic factor for the overall survival and progression-free survival of multiple myeloma patients. *Clin Immunol* **123**, 114-120, doi:10.1016/j.clim.2006.11.007 (2007).
390 Beyar-Katz, O. *et al.* Bortezomib-induced pro-inflammatory macrophages as a potential factor limiting anti-tumour efficacy. *J Pathol* **239**, 262-273, doi:10.1002/path.4723 (2016).
391 Wang, H. *et al.* High numbers of CD163+ tumor-associated macrophages correlate with poor prognosis in multiple myeloma patients receiving bortezomib-based regimens. *J Cancer* **10**, 3239-3245, doi:10.7150/jca.30102 (2019).
392 Panchabhai, S. *et al.* Tumor-associated macrophages and extracellular matrix metalloproteinase inducer in prognosis of multiple myeloma. *Leukemia* **30**, 951-954, doi:10.1038/leu.2015.191 (2016).
393 Chen, X. *et al.* Prognostic value of diametrically polarized tumor-associated macrophages in multiple myeloma. *Oncotarget* **8**, 112685-112696, doi:10.18632/oncotarget.22340 (2017).
394 Alrasheed, N. *et al.* Marrow-Infiltrating Regulatory T Cells Correlate with the Presence of Dysfunctional CD4(+)PD-1(+) Cells and Inferior Survival in Patients with Newly Diagnosed Multiple Myeloma. *Clin Cancer Res* **26**, 3443-3454, doi:10.1158/1078-0432.CCR-19-1714 (2020).
395 Wang, Q. *et al.* Therapeutic effects of CSF1R-blocking antibodies in multiple myeloma. *Leukemia* **32**, 176-183, doi:10.1038/leu.2017.193 (2018).
396 Chen, H. *et al.* JAK1/2 pathway inhibition suppresses M2 polarization and overcomes resistance of myeloma to lenalidomide by reducing TRIB1, MUC1, CD44, CXCL12, and CXCR4 expression. *Br J Haematol* **188**, 283-294, doi:10.1111/bjh.16158 (2020).
397 Holthof, L. C. *et al.* Bone Marrow Mesenchymal Stromal Cells Can Render Multiple Myeloma Cells Resistant to Cytotoxic Machinery of CAR T Cells through Inhibition of Apoptosis. *Clin Cancer Res* **27**, 3793-3803, doi:10.1158/1078-0432.CCR-20-2188 (2021).
398 Stikvoort, A. *et al.* CD38-specific Chimeric Antigen Receptor Expressing Natural Killer KHYG-1 Cells: A Proof of Concept for an "Off the Shelf" Therapy for Multiple Myeloma. *Hemasphere* **5**, e596, doi:10.1097/HS9.0000000000000596 (2021).
399 Dehbashi, M. *et al.* A Novel CAR Expressing NK Cell Targeting CD25 With the Prospect of Overcoming Immune Escape Mechanism in Cancers. *Front Oncol* **11**, 649710, doi:10.3389/fonc.2021.649710 (2021).
400 Ferrari de Andrade, L. *et al.* Inhibition of MICA and MICB Shedding Elicits NK-Cell-Mediated Immunity against Tumors Resistant to Cytotoxic T Cells. *Cancer Immunol Res* **8**, 769-780, doi:10.1158/2326-6066.CIR-19-0483 (2020).
401 Heldin, C. H. & Moustakas, A. Signaling Receptors for TGF-beta Family Members. *Cold Spring Harb Perspect Biol* **8**, doi:10.1101/cshperspect.a022053 (2016).
402 Huang, T., Schor, S. L. & Hinck, A. P. Biological activity differences between TGF-beta1 and TGF-beta3 correlate with differences in the rigidity and arrangement of their component monomers. *Biochemistry* **53**, 5737-5749, doi:10.1021/bi500647d (2014).
403 Deng, Z. *et al.* TGF-beta signaling in health, disease, and therapeutics. *Signal Transduct Target Ther* **9**, 61, doi:10.1038/s41392-024-01764-w (2024).

404 Rana, P. S., Soler, D. C., Kort, J. & Driscoll, J. J. Targeting TGF-beta signaling in the multiple myeloma microenvironment: Steering CARs and T cells in the right direction. *Front Cell Dev Biol* **10**, 1059715, doi:10.3389/fcell.2022.1059715 (2022).

405 Trotta, R. *et al.* TGF-beta utilizes SMAD3 to inhibit CD16-mediated IFN-gamma production and antibody-dependent cellular cytotoxicity in human NK cells. *J Immunol* **181**, 3784-3792, doi:10.4049/jimmunol.181.6.3784 (2008).

406 Fujii, R. *et al.* An IL-15 superagonist/IL-15Ralpha fusion complex protects and rescues NK cell-cytotoxic function from TGF-beta1-mediated immunosuppression. *Cancer Immunol Immunother* **67**, 675-689, doi:10.1007/s00262-018-2121-4 (2018).

407 Wilson, E. B. *et al.* Human tumour immune evasion via TGF-beta blocks NK cell activation but not survival allowing therapeutic restoration of anti-tumour activity. *PLoS One* **6**, e22842, doi:10.1371/journal.pone.0022842 (2011).

408 Castriconi, R. *et al.* Transforming growth factor beta 1 inhibits expression of NKp30 and NKG2D receptors: consequences for the NK-mediated killing of dendritic cells. *Proc Natl Acad Sci U S A* **100**, 4120-4125, doi:10.1073/pnas.0730640100 (2003).

409 Wong, J. K. M. *et al.* TGF-beta signalling limits effector function capacity of NK cell anti-tumour immunity in human bladder cancer. *EBioMedicine* **104**, 105176, doi:10.1016/j.ebiom.2024.105176 (2024).

410 Slattery, K. & Gardiner, C. M. NK Cell Metabolism and TGFbeta - Implications for Immunotherapy. *Front Immunol* **10**, 2915, doi:10.3389/fimmu.2019.02915 (2019).

411 Regis, S., Dondero, A., Caliendo, F., Bottino, C. & Castriconi, R. NK Cell Function Regulation by TGF-beta-Induced Epigenetic Mechanisms. *Front Immunol* **11**, 311, doi:10.3389/fimmu.2020.00311 (2020).

412 Kim, B. G., Malek, E., Choi, S. H., Ignatz-Hoover, J. J. & Driscoll, J. J. Novel therapies emerging in oncology to target the TGF-beta pathway. *J Hematol Oncol* **14**, 55, doi:10.1186/s13045-021-01053-x (2021).

413 Chen, X. *et al.* Secretion of bispecific protein of anti-PD-1 fused with TGF-beta trap enhances antitumor efficacy of CAR-T cell therapy. *Mol Ther Oncolytics* **21**, 144-157, doi:10.1016/j.omto.2021.03.014 (2021).

414 Malek, E. *et al.* The TGFbeta type I receptor kinase inhibitor vactosertib in combination with pomalidomide in relapsed/refractory multiple myeloma: a phase 1b trial. *Nat Commun* **15**, 7388, doi:10.1038/s41467-024-51442-2 (2024).

415 Takeuchi, K. *et al.* Tgf-Beta inhibition restores terminal osteoblast differentiation to suppress myeloma growth. *PLoS One* **5**, e9870, doi:10.1371/journal.pone.0009870 (2010).

416 Shaim, H. *et al.* Targeting the alphav integrin/TGF-beta axis improves natural killer cell function against glioblastoma stem cells. *J Clin Invest* **131**, doi:10.1172/JCI142116 (2021).

417 Kumar, B. *et al.* BATF is a major driver of NK cell epigenetic reprogramming and dysfunction in AML. *Sci Transl Med* **16**, eadp0004, doi:10.1126/scitranslmed.adp0004 (2024).

418 Chaudhry, K. *et al.* Comparable transforming growth factor beta-mediated immune suppression in ex vivo-expanded natural killer cells from cord blood and peripheral blood: implications for adoptive immunotherapy. *Cytotherapy* **24**, 802-817, doi:10.1016/j.jcyt.2022.04.001 (2022).

419 Otegbeye, F. *et al.* Inhibiting TGF-beta signaling preserves the function of highly activated, in vitro expanded natural killer cells in AML and colon cancer models. *PLoS One* **13**, e0191358, doi:10.1371/journal.pone.0191358 (2018).

420 Alabanza, L. M. *et al.* Armored BCMA CAR T Cells Eliminate Multiple Myeloma and Are Resistant to the Suppressive Effects of TGF-beta. *Front Immunol* **13**, 832645, doi:10.3389/fimmu.2022.832645 (2022).

421 Narayan, V. *et al.* PSMA-targeting TGFbeta-insensitive armored CAR T cells in metastatic castration-resistant prostate cancer: a phase 1 trial. *Nat Med* **28**, 724-734, doi:10.1038/s41591-022-01726-1 (2022).

422 Yvon, E. S. *et al.* Cord blood natural killer cells expressing a dominant negative TGF-beta receptor: Implications for adoptive immunotherapy for glioblastoma. *Cytotherapy* **19**, 408-418, doi:10.1016/j.jcyt.2016.12.005 (2017).

423 Powell, A. B. *et al.* Medulloblastoma rendered susceptible to NK-cell attack by TGFbeta neutralization. *J Transl Med* **17**, 321, doi:10.1186/s12967-019-2055-4 (2019).

424 Yang, B. *et al.* Blocking transforming growth factor-beta signaling pathway augments antitumor effect of adoptive NK-92 cell therapy. *Int Immunopharmacol* **17**, 198-204, doi:10.1016/j.intimp.2013.06.003 (2013).
425 Thangaraj, J. L., Coffey, M., Lopez, E. & Kaufman, D. S. Disruption of TGF-beta signaling pathway is required to mediate effective killing of hepatocellular carcinoma by human iPSC-derived NK cells. *Cell Stem Cell* **31**, 1327-1343 e1325, doi:10.1016/j.stem.2024.06.009 (2024).
426 Naeimi Kararoudi, M. *et al.* Generation of Knock-out Primary and Expanded Human NK Cells Using Cas9 Ribonucleoproteins. *J Vis Exp*, doi:10.3791/58237 (2018).
427 Zhang, L. *et al.* AsCas12a ultra nuclease facilitates the rapid generation of therapeutic cell medicines. *Nat Commun* **12**, 3908, doi:10.1038/s41467-021-24017-8 (2021).
428 Gerew, A. *et al.* Deletion of CISH and TGFβR2 in iPSC-Derived NK Cells Promotes High Cytotoxicity and Enhances In Vivo Tumor Killing. *Blood* **138**, 2780-2780, doi:10.1182/blood-2021-150731 %J Blood (2021).
429 Guo, C. *et al.* Abstract 891: CRISPR-Cas9-gRNA RNP mediated gene knockout of TGFBR2 and CISH enhances CD19-CAR NK cell function and provides resistance to TGFβ. *Cancer Research* **80**, 891-891, doi:10.1158/1538-7445.AM2020-891 %J Cancer Research (2020).
430 Grzywacz, B. *et al.* Natural Killer Cell Homing and Persistence in the Bone Marrow After Adoptive Immunotherapy Correlates With Better Leukemia Control. *J Immunother* **42**, 65-72, doi:10.1097/CJI.0000000000000250 (2019).
431 Curti, A. *et al.* Successful transfer of alloreactive haploidentical KIR ligand-mismatched natural killer cells after infusion in elderly high risk acute myeloid leukemia patients. *Blood* **118**, 3273-3279, doi:10.1182/blood-2011-01-329508 (2011).
432 Hoerster, K. *et al.* HLA Class I Knockout Converts Allogeneic Primary NK Cells Into Suitable Effectors for "Off-the-Shelf" Immunotherapy. *Front Immunol* **11**, 586168, doi:10.3389/fimmu.2020.586168 (2020).
433 Patel, K. *et al.* The ELiPSE-1 study: A phase 1, multicenter, open-label study of CNTY-101 in subjects with relapsed or refractory CD19-positive B-cell malignancies. **41**, TPS7580-TPS7580, doi:10.1200/JCO.2023.41.16_suppl.TPS7580 (2023).
434 Borges, L. *et al.* Development of Multi-Engineered iPSC-Derived CAR-NK Cells for the Treatment of B-Cell Malignancies. *Blood* **138**, 1729-1729, doi:10.1182/blood-2021-148438 %J Blood (2021).
435 Pfefferle, A. *et al.* Deciphering Natural Killer Cell Homeostasis. *Front Immunol* **11**, 812, doi:10.3389/fimmu.2020.00812 (2020).
436 Geller, M. A. *et al.* A phase II study of allogeneic natural killer cell therapy to treat patients with recurrent ovarian and breast cancer. *Cytotherapy* **13**, 98-107, doi:10.3109/14653249.2010.515582 (2011).
437 MacDonald, A., Wu, T. C. & Hung, C. F. Interleukin 2-Based Fusion Proteins for the Treatment of Cancer. *J Immunol Res* **2021**, 7855808, doi:10.1155/2021/7855808 (2021).
438 Assier, E. *et al.* NK cells and polymorphonuclear neutrophils are both critical for IL-2-induced pulmonary vascular leak syndrome. *J Immunol* **172**, 7661-7668, doi:10.4049/jimmunol.172.12.7661 (2004).
439 Rosario, M. *et al.* The IL-15-Based ALT-803 Complex Enhances FcgammaRIIIa-Triggered NK Cell Responses and In Vivo Clearance of B Cell Lymphomas. *Clin Cancer Res* **22**, 596-608, doi:10.1158/1078-0432.CCR-15-1419 (2016).
440 Fernandez, R. A. *et al.* Improving NK cell function in multiple myeloma with NKTR-255, a novel polymer-conjugated human IL-15. *Blood Adv* **7**, 9-19, doi:10.1182/bloodadvances.2022007985 (2023).
441 Cooley, S. *et al.* First-in-human trial of rhIL-15 and haploidentical natural killer cell therapy for advanced acute myeloid leukemia. *Blood Adv* **3**, 1970-1980, doi:10.1182/bloodadvances.2018028332 (2019).
442 Berger, C. *et al.* Safety and immunologic effects of IL-15 administration in nonhuman primates. *Blood* **114**, 2417-2426, doi:10.1182/blood-2008-12-189266 (2009).
443 Liu, E. *et al.* Cord blood NK cells engineered to express IL-15 and a CD19-targeted CAR show long-term persistence and potent antitumor activity. *Leukemia* **32**, 520-531, doi:10.1038/leu.2017.226 (2018).
444 Christodoulou, I. *et al.* Engineering CAR-NK cells to secrete IL-15 sustains their anti-AML functionality but is associated with systemic toxicities. *J Immunother Cancer* **9**, doi:10.1136/jitc-2021-003894 (2021).

445 Du, Z., Ng, Y. Y., Zha, S. & Wang, S. piggyBac system to co-express NKG2D CAR and IL-15 to augment the in vivo persistence and anti-AML activity of human peripheral blood NK cells. *Mol Ther Methods Clin Dev* **23**, 582-596, doi:10.1016/j.omtm.2021.10.014 (2021).

446 Soldierer, M. *et al.* Genetic Engineering and Enrichment of Human NK Cells for CAR-Enhanced Immunotherapy of Hematological Malignancies. *Front Immunol* **13**, 847008, doi:10.3389/fimmu.2022.847008 (2022).

447 Yoshimura, A., Nishinakamura, H., Matsumura, Y. & Hanada, T. Negative regulation of cytokine signaling and immune responses by SOCS proteins. *Arthritis Res Ther* **7**, 100-110, doi:10.1186/ar1741 (2005).

448 Inagaki-Ohara, K., Hanada, T. & Yoshimura, A. Negative regulation of cytokine signaling and inflammatory diseases. *Curr Opin Pharmacol* **3**, 435-442, doi:10.1016/s1471-4892(03)00070-5 (2003).

449 Naeimi Kararoudi, M. *et al.* Disruption of SOCS3 Promotes the Anti-Cancer Efficacy of Primary NK Cells. *Blood* **132**, 5687-5687, doi:10.1182/blood-2018-99-116621 %J Blood (2018).

450 Yusubalieva, G. M. *et al.* [Enhanced Natural Killers with CISH and B2M Gene Knockouts Reveal Increased Cytotoxicity in Glioblastoma Primary Cultures]. *Mol Biol (Mosk)* **56**, 848-859, doi:10.31857/S0026898422050159 (2022).

451 Nakazawa, T. *et al.* CIS deletion by CRISPR/Cas9 enhances human primary natural killer cell functions against allogeneic glioblastoma. *J Exp Clin Cancer Res* **42**, 205, doi:10.1186/s13046-023-02770-6 (2023).

452 Bi, J. *et al.* TIPE2 deletion improves the therapeutic potential of adoptively transferred NK cells. *J Immunother Cancer* **11**, doi:10.1136/jitc-2022-006002 (2023).

453 Bernard, P. L. *et al.* Targeting CISH enhances natural cytotoxicity receptor signaling and reduces NK cell exhaustion to improve solid tumor immunity. *J Immunother Cancer* **10**, doi:10.1136/jitc-2021-004244 (2022).

454 Zhu, H. *et al.* Metabolic Reprograming via Deletion of CISH in Human iPSC-Derived NK Cells Promotes In Vivo Persistence and Enhances Anti-tumor Activity. *Cell Stem Cell* **27**, 224-237 e226, doi:10.1016/j.stem.2020.05.008 (2020).

455 Rautela, J., Surgenor, E. & Huntington, N. D. Drug target validation in primary human natural killer cells using CRISPR RNP. *J Leukoc Biol* **108**, 1397-1408, doi:10.1002/JLB.2MA0620-074R (2020).

456 Gurney, M. *et al.* Concurrent transposon engineering and CRISPR/Cas9 genome editing of primary CLL-1 chimeric antigen receptor-natural killer cells. *Cytotherapy* **24**, 1087-1094, doi:10.1016/j.jcyt.2022.07.008 (2022).

457 Swanson, L. *et al.* Development of Next-Generation NK Cell Optimized Chimeric Antigen Receptors (CARs) for iPSC-Derived NK Cell Therapies Targeting Both Solid and Liquid Tumors. *Blood* **140**, 4540-4541, doi:10.1182/blood-2022-163884 %J Blood (2022).

458 Daher, M. *et al.* Targeting a cytokine checkpoint enhances the fitness of armored cord blood CAR-NK cells. *Blood* **137**, 624-636, doi:10.1182/blood.2020007748 (2021).

459 Fujisaki, H., Kakuda, H., Imai, C., Mullighan, C. G. & Campana, D. Replicative potential of human natural killer cells. *Br J Haematol* **145**, 606-613, doi:10.1111/j.1365-2141.2009.07667.x (2009).

460 Bai, Y. *et al.* Enhancement of the in vivo persistence and antitumor efficacy of CD19 chimeric antigen receptor T cells through the delivery of modified TERT mRNA. *Cell Discov* **1**, 15040, doi:10.1038/celldisc.2015.40 (2015).

461 Streltsova, M. A. *et al.* Telomerase Reverse Transcriptase Increases Proliferation and Lifespan of Human NK Cells without Immortalization. *Biomedicines* **9**, doi:10.3390/biomedicines9060662 (2021).

462 Tarannum, M. & Romee, R. Cytokine-induced memory-like natural killer cells for cancer immunotherapy. *Stem Cell Res Ther* **12**, 592, doi:10.1186/s13287-021-02655-5 (2021).

463 Rastelli, L. *et al.* A first-in-class ex vivo combination between cytokine-induced memory like (CIML) NK cells and a CD38 targeting antibody recruiting molecule (ARM) as a novel approach to target NK cells without cellular engineering for the treatment of multiple myeloma. **38**, 8523-8523, doi:10.1200/JCO.2020.38.15_suppl.8523 (2020).

464 Nadeau, S. & Martins, G. A. Conserved and Unique Functions of Blimp1 in Immune Cells. *Front Immunol* **12**, 805260, doi:10.3389/fimmu.2021.805260 (2021).

465 Gyory, I., Fejer, G., Ghosh, N., Seto, E. & Wright, K. L. Identification of a functionally impaired positive regulatory domain I binding factor 1 transcription repressor in myeloma cell lines. *J Immunol* **170**, 3125-3133, doi:10.4049/jimmunol.170.6.3125 (2003).

466 Smith, M. A. *et al.* PRDM1/Blimp-1 controls effector cytokine production in human NK cells. *J Immunol* **185**, 6058-6067, doi:10.4049/jimmunol.1001682 (2010).

467 Kallies, A. *et al.* A role for Blimp1 in the transcriptional network controlling natural killer cell maturation. *Blood* **117**, 1869-1879, doi:10.1182/blood-2010-08-303123 (2011).

468 Liu, X. *et al.* PRDM1 Binds an Extensive Network of Genes to Regulate Human Natural Killer Cell Homeostasis. *Blood* **134**, 2536-2536, doi:10.1182/blood-2019-129270 %J Blood (2019).

469 Kucuk, C. *et al.* PRDM1 is a tumor suppressor gene in natural killer cell malignancies. *Proc Natl Acad Sci U S A* **108**, 20119-20124, doi:10.1073/pnas.1115128108 (2011).

470 Karube, K. *et al.* Identification of FOXO3 and PRDM1 as tumor-suppressor gene candidates in NK-cell neoplasms by genomic and functional analyses. *Blood* **118**, 3195-3204, doi:10.1182/blood-2011-04-346890 (2011).

471 Iqbal, J. *et al.* Genomic analyses reveal global functional alterations that promote tumor growth and novel tumor suppressor genes in natural killer-cell malignancies. *Leukemia* **23**, 1139-1151, doi:10.1038/leu.2009.3 (2009).

472 Dong, G. *et al.* Genetic manipulation of primary human natural killer cells to investigate the functional and oncogenic roles of PRDM1. *Haematologica* **106**, 2427-2438, doi:10.3324/haematol.2020.254276 (2021).

473 Akman, B. *et al.* PRDM1 decreases sensitivity of human NK cells to IL2-induced cell expansion by directly repressing CD25 (IL2RA). *J Leukoc Biol* **109**, 901-914, doi:10.1002/JLB.2A0520-321RR (2021).

474 Yoshikawa, T. *et al.* Genetic ablation of PRDM1 in antitumor T cells enhances therapeutic efficacy of adoptive immunotherapy. *Blood* **139**, 2156-2172, doi:10.1182/blood.2021012714 (2022).

475 Jung, I. Y. *et al.* BLIMP1 and NR4A3 transcription factors reciprocally regulate antitumor CAR T cell stemness and exhaustion. *Sci Transl Med* **14**, eabn7336, doi:10.1126/scitranslmed.abn7336 (2022).

476 Barrangou, R. *et al.* CRISPR provides acquired resistance against viruses in prokaryotes. *Science* **315**, 1709-1712, doi:10.1126/science.1138140 (2007).

477 Mojica, F. J., Diez-Villasenor, C., Garcia-Martinez, J. & Soria, E. Intervening sequences of regularly spaced prokaryotic repeats derive from foreign genetic elements. *J Mol Evol* **60**, 174-182, doi:10.1007/s00239-004-0046-3 (2005).

478 Ghorbani, A. *et al.* A short overview of CRISPR-Cas technology and its application in viral disease control. *Transgenic Res* **30**, 221-238, doi:10.1007/s11248-021-00247-w (2021).

479 Garneau, J. E. *et al.* The CRISPR/Cas bacterial immune system cleaves bacteriophage and plasmid DNA. *Nature* **468**, 67-71, doi:10.1038/nature09523 (2010).

480 Mojica, F. J. M. & Montoliu, L. On the Origin of CRISPR-Cas Technology: From Prokaryotes to Mammals. *Trends Microbiol* **24**, 811-820, doi:10.1016/j.tim.2016.06.005 (2016).

481 Liu, Z., Dong, H., Cui, Y., Cong, L. & Zhang, D. Application of different types of CRISPR/Cas-based systems in bacteria. *Microb Cell Fact* **19**, 172, doi:10.1186/s12934-020-01431-z (2020).

482 Jinek, M. *et al.* A programmable dual-RNA-guided DNA endonuclease in adaptive bacterial immunity. *Science* **337**, 816-821, doi:10.1126/science.1225829 (2012).

483 Yang, H. *et al.* Methods Favoring Homology-Directed Repair Choice in Response to CRISPR/Cas9 Induced-Double Strand Breaks. *Int J Mol Sci* **21**, doi:10.3390/ijms21186461 (2020).

484 Liu, M. *et al.* Methodologies for Improving HDR Efficiency. *Front Genet* **9**, 691, doi:10.3389/fgene.2018.00691 (2018).

485 Sfeir, A. & Symington, L. S. Microhomology-Mediated End Joining: A Back-up Survival Mechanism or Dedicated Pathway? *Trends Biochem Sci* **40**, 701-714, doi:10.1016/j.tibs.2015.08.006 (2015).

486 Seol, J. H., Shim, E. Y. & Lee, S. E. Microhomology-mediated end joining: Good, bad and ugly. *Mutat Res* **809**, 81-87, doi:10.1016/j.mrfmmm.2017.07.002 (2018).

487 Sancar, A., Lindsey-Boltz, L. A., Unsal-Kacmaz, K. & Linn, S. Molecular mechanisms of mammalian DNA repair and the DNA damage checkpoints. *Annu Rev Biochem* **73**, 39-85, doi:10.1146/annurev.biochem.73.011303.073723 (2004).

488 Ouellette, M. M., Zhou, S. & Yan, Y. Cell Signaling Pathways That Promote Radioresistance of Cancer Cells. *Diagnostics (Basel)* **12**, doi:10.3390/diagnostics12030656 (2022).

489 Asmamaw, M. & Zawdie, B. Mechanism and Applications of CRISPR/Cas-9-Mediated Genome Editing. *Biologics* **15**, 353-361, doi:10.2147/BTT.S326422 (2021).

490 Fix, S. M., Jazaeri, A. A. & Hwu, P. Applications of CRISPR Genome Editing to Advance the Next Generation of Adoptive Cell Therapies for Cancer. *Cancer Discov* **11**, 560-574, doi:10.1158/2159-8290.CD-20-1083 (2021).

491 Urena-Bailen, G. *et al.* Preclinical Evaluation of CRISPR-Edited CAR-NK-92 Cells for Off-the-Shelf Treatment of AML and B-ALL. *Int J Mol Sci* **23**, doi:10.3390/ijms232112828 (2022).

492 Guo, C. *et al.* Abstract 890: ADAM17 knockout NK or CAR NK cells augment antibody dependent cellular cytotoxicity (ADCC) and anti-tumor activity. *Cancer Research* **83**, 890-890, doi:10.1158/1538-7445.AM2023-890 %J Cancer Research (2023).

493 Du, Y., Liu, Y., Hu, J., Peng, X. & Liu, Z. CRISPR/Cas9 systems: Delivery technologies and biomedical applications. *Asian J Pharm Sci* **18**, 100854, doi:10.1016/j.ajps.2023.100854 (2023).

494 Schmidt, P., Raftery, M. J. & Pecher, G. Engineering NK Cells for CAR Therapy-Recent Advances in Gene Transfer Methodology. *Front Immunol* **11**, 611163, doi:10.3389/fimmu.2020.611163 (2020).

495 Robbins, G. M., Wang, M., Pomeroy, E. J. & Moriarity, B. S. Nonviral genome engineering of natural killer cells. *Stem Cell Res Ther* **12**, 350, doi:10.1186/s13287-021-02406-6 (2021).

496 Huang, R. S., Shih, H. A., Lai, M. C., Chang, Y. J. & Lin, S. Enhanced NK-92 Cytotoxicity by CRISPR Genome Engineering Using Cas9 Ribonucleoproteins. *Front Immunol* **11**, 1008, doi:10.3389/fimmu.2020.01008 (2020).

497 Huang, R. S., Lai, M. C., Shih, H. A. & Lin, S. A robust platform for expansion and genome editing of primary human natural killer cells. *J Exp Med* **218**, doi:10.1084/jem.20201529 (2021).

498 Naeimi Kararoudi, M. *et al.* Optimization and validation of CAR transduction into human primary NK cells using CRISPR and AAV. *Cell Rep Methods* **2**, 100236, doi:10.1016/j.crmeth.2022.100236 (2022).

499 Clara, J. A. *et al.* High-affinity CD16 integration into a CRISPR/Cas9-edited CD38 locus augments CD38-directed antitumor activity of primary human natural killer cells. *J Immunother Cancer* **10**, doi:10.1136/jitc-2021-003804 (2022).

500 Naidoo, J. *et al.* Toxicities of the anti-PD-1 and anti-PD-L1 immune checkpoint antibodies. *Ann Oncol* **26**, 2375-2391, doi:10.1093/annonc/mdv383 (2015).

501 Kim, T. W. *et al.* Efficacy and safety of vactosertib and pembrolizumab combination in patients with previously treated microsatellite stable metastatic colorectal cancer. **39**, 3573-3573, doi:10.1200/JCO.2021.39.15_suppl.3573 (2021).

502 Wick, A. *et al.* Phase 1b/2a study of galunisertib, a small molecule inhibitor of transforming growth factor-beta receptor I, in combination with standard temozolomide-based radiochemotherapy in patients with newly diagnosed malignant glioma. *Invest New Drugs* **38**, 1570-1579, doi:10.1007/s10637-020-00910-9 (2020).

503 Zhang, X. H., Tee, L. Y., Wang, X. G., Huang, Q. S. & Yang, S. H. Off-target Effects in CRISPR/Cas9-mediated Genome Engineering. *Mol Ther Nucleic Acids* **4**, e264, doi:10.1038/mtna.2015.37 (2015).

504 Lin, Y. *et al.* CRISPR/Cas9 systems have off-target activity with insertions or deletions between target DNA and guide RNA sequences. *Nucleic Acids Res* **42**, 7473-7485, doi:10.1093/nar/gku402 (2014).

505 Pena-Gutierrez, I., Olalla-Sastre, B., Rio, P. & Rodriguez-Madoz, J. R. Beyond precision: evaluation of off-target clustered regularly interspaced short palindromic repeats/Cas9-mediated genome editing. *Cytotherapy*, doi:10.1016/j.jcyt.2024.10.010 (2024).

506 Wang, H. *et al.* Advances in Off-Target Detection for CRISPR-Based Genome Editing. *Hum Gene Ther* **34**, 112-128, doi:10.1089/hum.2022.198 (2023).

507 Tyumentseva, M., Tyumentsev, A. & Akimkin, V. CRISPR/Cas9 Landscape: Current State and Future Perspectives. *Int J Mol Sci* **24**, doi:10.3390/ijms242216077 (2023).

508 Vakulskas, C. A. *et al.* A high-fidelity Cas9 mutant delivered as a ribonucleoprotein complex enables efficient gene editing in human hematopoietic stem and progenitor cells. *Nat Med* **24**, 1216-1224, doi:10.1038/s41591-018-0137-0 (2018).

509 Komor, A. C., Kim, Y. B., Packer, M. S., Zuris, J. A. & Liu, D. R. Programmable editing of a target base in genomic DNA without double-stranded DNA cleavage. *Nature* **533**, 420-424, doi:10.1038/nature17946 (2016).

510 Gaudelli, N. M. *et al.* Programmable base editing of A*T to G*C in genomic DNA without DNA cleavage. *Nature* **551**, 464-471, doi:10.1038/nature24644 (2017).

511 Rees, H. A. & Liu, D. R. Base editing: precision chemistry on the genome and transcriptome of living cells. *Nat Rev Genet* **19**, 770-788, doi:10.1038/s41576-018-0059-1 (2018).

512 Rees, H. A., Wilson, C., Doman, J. L. & Liu, D. R. Analysis and minimization of cellular RNA editing by DNA adenine base editors. *Sci Adv* **5**, eaax5717, doi:10.1126/sciadv.aax5717 (2019).

513 Anzalone, A. V. *et al.* Search-and-replace genome editing without double-strand breaks or donor DNA. *Nature* **576**, 149-157, doi:10.1038/s41586-019-1711-4 (2019).

514 Anzalone, A. V., Koblan, L. W. & Liu, D. R. Genome editing with CRISPR-Cas nucleases, base editors, transposases and prime editors. *Nat Biotechnol* **38**, 824-844, doi:10.1038/s41587-020-0561-9 (2020).
515 Denman, C. J. *et al.* Membrane-bound IL-21 promotes sustained ex vivo proliferation of human natural killer cells. *PLoS One* **7**, e30264, doi:10.1371/journal.pone.0030264 (2012).
516 Pear, W. S., Nolan, G. P., Scott, M. L. & Baltimore, D. Production of high-titer helper-free retroviruses by transient transfection. *Proc Natl Acad Sci U S A* **90**, 8392-8396, doi:10.1073/pnas.90.18.8392 (1993).
517 Concordet, J. P. & Haeussler, M. CRISPOR: intuitive guide selection for CRISPR/Cas9 genome editing experiments and screens. *Nucleic Acids Res* **46**, W242-W245, doi:10.1093/nar/gky354 (2018).
518 Hsu, P. D. *et al.* DNA targeting specificity of RNA-guided Cas9 nucleases. *Nat Biotechnol* **31**, 827-832, doi:10.1038/nbt.2647 (2013).
519 Clement, K. *et al.* CRISPResso2 provides accurate and rapid genome editing sequence analysis. *Nat Biotechnol* **37**, 224-226, doi:10.1038/s41587-019-0032-3 (2019).
520 Koopman, G. *et al.* Annexin V for flow cytometric detection of phosphatidylserine expression on B cells undergoing apoptosis. *Blood* **84**, 1415-1420 (1994).
521 Gong, H. *et al.* beta-Galactosidase activity assay using far-red-shifted fluorescent substrate DDAOG. *Anal Biochem* **386**, 59-64, doi:10.1016/j.ab.2008.11.031 (2009).
522 Charrier, S. *et al.* Quantification of lentiviral vector copy numbers in individual hematopoietic colony-forming cells shows vector dose-dependent effects on the frequency and level of transduction. *Gene Ther* **18**, 479-487, doi:10.1038/gt.2010.163 (2011).
523 Scholzen, T. & Gerdes, J. The Ki-67 protein: from the known and the unknown. *J Cell Physiol* **182**, 311-322, doi:10.1002/(SICI)1097-4652(200003)182:3<311::AID-JCP1>3.0.CO;2-9 (2000).
524 Wingett, S. W. & Andrews, S. FastQ Screen: A tool for multi-genome mapping and quality control. *F1000Res* **7**, 1338, doi:10.12688/f1000research.15931.2 (2018).
525 Dobin, A. *et al.* STAR: ultrafast universal RNA-seq aligner. *Bioinformatics* **29**, 15-21, doi:10.1093/bioinformatics/bts635 (2013).
526 Zhang, Y., Parmigiani, G. & Johnson, W. E. ComBat-seq: batch effect adjustment for RNA-seq count data. *NAR Genom Bioinform* **2**, lqaa078, doi:10.1093/nargab/lqaa078 (2020).
527 Love, M. I., Huber, W. & Anders, S. Moderated estimation of fold change and dispersion for RNA-seq data with DESeq2. *Genome Biol* **15**, 550, doi:10.1186/s13059-014-0550-8 (2014).
528 Yu, G., Wang, L. G., Han, Y. & He, Q. Y. clusterProfiler: an R package for comparing biological themes among gene clusters. *OMICS* **16**, 284-287, doi:10.1089/omi.2011.0118 (2012).
529 Aryee, K. E. *et al.* Enhanced development of functional human NK cells in NOD-scid-IL2rg(null) mice expressing human IL15. *FASEB J* **36**, e22476, doi:10.1096/fj.202200045R (2022).
530 Shah, N. *et al.* Antigen presenting cell-mediated expansion of human umbilical cord blood yields log-scale expansion of natural killer cells with anti-myeloma activity. *PLoS One* **8**, e76781, doi:10.1371/journal.pone.0076781 (2013).
531 Granzin, M. *et al.* Fully automated expansion and activation of clinical-grade natural killer cells for adoptive immunotherapy. *Cytotherapy* **17**, 621-632, doi:10.1016/j.jcyt.2015.03.611 (2015).
532 Mingari, M. C. *et al.* Interleukin-15-induced maturation of human natural killer cells from early thymic precursors: selective expression of CD94/NKG2-A as the only HLA class I-specific inhibitory receptor. *Eur J Immunol* **27**, 1374-1380, doi:10.1002/eji.1830270612 (1997).
533 Brady, J., Hayakawa, Y., Smyth, M. J. & Nutt, S. L. IL-21 induces the functional maturation of murine NK cells. *J Immunol* **172**, 2048-2058, doi:10.4049/jimmunol.172.4.2048 (2004).
534 Rutishauser, R. L. *et al.* Transcriptional repressor Blimp-1 promotes CD8(+) T cell terminal differentiation and represses the acquisition of central memory T cell properties. *Immunity* **31**, 296-308, doi:10.1016/j.immuni.2009.05.014 (2009).
535 Thaventhiran, J. E. *et al.* Activation of the Hippo pathway by CTLA-4 regulates the expression of Blimp-1 in the CD8+ T cell. *Proc Natl Acad Sci U S A* **109**, E2223-2229, doi:10.1073/pnas.1209115109 (2012).
536 Mah, L. J., El-Osta, A. & Karagiannis, T. C. gammaH2AX: a sensitive molecular marker of DNA damage and repair. *Leukemia* **24**, 679-686, doi:10.1038/leu.2010.6 (2010).
537 Cooley, I. D., Read, K. A. & Oestreich, K. J. Trans-presentation of IL-15 modulates STAT5 activation and Bcl-6 expression in TH1 cells. *Sci Rep* **5**, 15722, doi:10.1038/srep15722 (2015).
538 Lin, J. X. & Leonard, W. J. The role of Stat5a and Stat5b in signaling by IL-2 family cytokines. *Oncogene* **19**, 2566-2576, doi:10.1038/sj.onc.1203523 (2000).

539 Tsuchida, C. A. *et al.* Mitigation of chromosome loss in clinical CRISPR-Cas9-engineered T cells. *Cell* **186**, 4567-4582 e4520, doi:10.1016/j.cell.2023.08.041 (2023).

540 Spinosa, P. *et al.* Quantitative modeling predicts competitive advantages of a next generation anti-NKG2A monoclonal antibody over monalizumab for the treatment of cancer. *CPT Pharmacometrics Syst Pharmacol* **10**, 220-229, doi:10.1002/psp4.12592 (2021).

541 Hwang, M. *et al.* Population Pharmacokinetics of Monalizumab in Patients With Advanced Solid Tumors. *J Clin Pharmacol* **63**, 817-829, doi:10.1002/jcph.2220 (2023).

542 Cassidy, K. C. *et al.* Disposition and metabolism of [(14)C]-galunisertib, a TGF-betaRI kinase/ALK5 inhibitor, following oral administration in healthy subjects and mechanistic prediction of the effect of itraconazole on galunisertib pharmacokinetics. *Xenobiotica* **48**, 382-399, doi:10.1080/00498254.2017.1323137 (2018).

543 Rasche, L., Hudecek, M. & Einsele, H. CAR T-cell therapy in multiple myeloma: mission accomplished? *Blood* **143**, 305-310, doi:10.1182/blood.2023021221 (2024).

544 Navarrete, M. S., Adrian, C. & Bachelet, V. C. Respondent-driven sampling: Advantages and disadvantages from a sampling method. *Medwave* **21**, e8513, doi:10.5867/medwave.2022.01.002528 (2022).

545 Satwani, P. *et al.* Interleukin (IL)-15 in combination with IL-2, fms-like tyrosine kinase-3 ligand and anti-CD3 significantly enhances umbilical cord blood natural killer (NK) cell and NK-cell subset expansion and NK function. *Cytotherapy* **13**, 730-738, doi:10.3109/14653249.2011.563292 (2011).

546 Alnabhan, R., Madrigal, A. & Saudemont, A. Differential activation of cord blood and peripheral blood natural killer cells by cytokines. *Cytotherapy* **17**, 73-85, doi:10.1016/j.jcyt.2014.08.003 (2015).

547 Vela, M. *et al.* Haploidentical IL-15/41BBL activated and expanded natural killer cell infusion therapy after salvage chemotherapy in children with relapsed and refractory leukemia. *Cancer Lett* **422**, 107-117, doi:10.1016/j.canlet.2018.02.033 (2018).

548 Leivas, A. *et al.* Novel treatment strategy with autologous activated and expanded natural killer cells plus anti-myeloma drugs for multiple myeloma. *Oncoimmunology* **5**, e1250051, doi:10.1080/2162402X.2016.1250051 (2016).

549 Ciurea, S. O. *et al.* Phase 1 clinical trial using mbIL21 ex vivo-expanded donor-derived NK cells after haploidentical transplantation. *Blood* **130**, 1857-1868, doi:10.1182/blood-2017-05-785659 (2017).

550 Shah, N. *et al.* Phase I study of cord blood-derived natural killer cells combined with autologous stem cell transplantation in multiple myeloma. *Br J Haematol* **177**, 457-466, doi:10.1111/bjh.14570 (2017).

551 Coskun, H. S. *et al.* Serum transforming growth factor beta 1 levels in multiple myeloma patients. *Turk J Haematol* **23**, 47-52 (2006).

552 Kaulfuss, M. *et al.* The NK cell checkpoint NKG2A maintains expansion capacity of human NK cells. *Sci Rep* **13**, 10555, doi:10.1038/s41598-023-37779-6 (2023).

553 Gopalkrishnan, R. V., Christiansen, K. A., Goldstein, N. I., DePinho, R. A. & Fisher, P. B. Use of the human EF-1alpha promoter for expression can significantly increase success in establishing stable cell lines with consistent expression: a study using the tetracycline-inducible system in human cancer cells. *Nucleic Acids Res* **27**, 4775-4782, doi:10.1093/nar/27.24.4775 (1999).

554 Chaudhry, K. *et al.* Co-transducing B7H3 CAR-NK cells with the DNR preserves their cytolytic function against GBM in the presence of exogenous TGF-beta. *Mol Ther Methods Clin Dev* **27**, 415-430, doi:10.1016/j.omtm.2022.10.010 (2022).

555 Tachi, T. *et al.* Antitumor effects of intracranial injection of B7-H3-targeted Car-T and Car-Nk cells in a patient-derived glioblastoma xenograft model. *Cancer Immunol Immunother* **73**, 256, doi:10.1007/s00262-024-03808-0 (2024).

556 Bulcha, J. T., Wang, Y., Ma, H., Tai, P. W. L. & Gao, G. Viral vector platforms within the gene therapy landscape. *Signal Transduct Target Ther* **6**, 53, doi:10.1038/s41392-021-00487-6 (2021).

557 Gong, Y. *et al.* Rosuvastatin Enhances VSV-G Lentiviral Transduction of NK Cells via Upregulation of the Low-Density Lipoprotein Receptor. *Mol Ther Methods Clin Dev* **17**, 634-646, doi:10.1016/j.omtm.2020.03.017 (2020).

558 Colamartino, A. B. L. *et al.* Efficient and Robust NK-Cell Transduction With Baboon Envelope Pseudotyped Lentivector. *Front Immunol* **10**, 2873, doi:10.3389/fimmu.2019.02873 (2019).

559 Ciulean, I. S. *et al.* CD44v6 specific CAR-NK cells for targeted immunotherapy of head and neck squamous cell carcinoma. *Front Immunol* **14**, 1290488, doi:10.3389/fimmu.2023.1290488 (2023).

560 Pfefferle, A. *et al.* Optimisation of a primary human CAR-NK cell manufacturing pipeline. *Clin Transl Immunology* **13**, e1507, doi:10.1002/cti2.1507 (2024).

561 Bari, R. *et al.* A Distinct Subset of Highly Proliferative and Lentiviral Vector (LV)-Transducible NK Cells Define a Readily Engineered Subset for Adoptive Cellular Therapy. *Front Immunol* **10**, 2001, doi:10.3389/fimmu.2019.02001 (2019).
562 Noguchi, K. *et al.* Protocol for a high titer of BaEV-Rless pseudotyped lentiviral vector: Focus on syncytium formation and detachment. *J Virol Methods* **314**, 114689, doi:10.1016/j.jviromet.2023.114689 (2023).
563 Li, J. *et al.* Improving the production of BaEV lentivirus by comprehensive optimization. *J Virol Methods* **333**, 115106, doi:10.1016/j.jviromet.2024.115106 (2024).
564 Nguyen, D. N. *et al.* Polymer-stabilized Cas9 nanoparticles and modified repair templates increase genome editing efficiency. *Nat Biotechnol* **38**, 44-49, doi:10.1038/s41587-019-0325-6 (2020).
565 Dudek, A. M. & Porteus, M. H. Answered and Unanswered Questions in Early-Stage Viral Vector Transduction Biology and Innate Primary Cell Toxicity for Ex-Vivo Gene Editing. *Front Immunol* **12**, 660302, doi:10.3389/fimmu.2021.660302 (2021).
566 Ferrari, S. *et al.* Choice of template delivery mitigates the genotoxic risk and adverse impact of editing in human hematopoietic stem cells. *Cell Stem Cell* **29**, 1428-1444 e1429, doi:10.1016/j.stem.2022.09.001 (2022).
567 Molinos-Quintana, A. *et al.* Impact of disease burden and late loss of B cell aplasia on the risk of relapse after CD19 chimeric antigen receptor T Cell (Tisagenlecleucel) infusion in pediatric and young adult patients with relapse/refractory acute lymphoblastic leukemia: role of B-cell monitoring. *Front Immunol* **14**, 1280580, doi:10.3389/fimmu.2023.1280580 (2023).
568 Rodriguez-Otero, P. *et al.* GPRC5D as a novel target for the treatment of multiple myeloma: a narrative review. *Blood Cancer J* **14**, 24, doi:10.1038/s41408-023-00966-9 (2024).
569 Sauter, C. S. *et al.* A Phase 1 Study of NKX101, a Chimeric Antigen Receptor Natural Killer (CAR-NK) Cell Therapy, with Fludarabine and Cytarabine in Patients with Acute Myeloid Leukemia. *Blood* **142**, 2097-2097, doi:10.1182/blood-2023-173582 %J Blood (2023).
570 Battram, A. M. *et al.* Genetic Disruption of Blimp-1 Drastically Augments the Antitumor Efficacy of BCMA-Targeting CAR-T Cells. *Blood Adv*, doi:10.1182/bloodadvances.2024013209 (2024).
571 Stadtmauer, E. A. *et al.* CRISPR-engineered T cells in patients with refractory cancer. *Science* **367**, doi:10.1126/science.aba7365 (2020).
572 Bothmer, A. *et al.* Detection and Modulation of DNA Translocations During Multi-Gene Genome Editing in T Cells. *CRISPR J* **3**, 177-187, doi:10.1089/crispr.2019.0074 (2020).
573 Schiroli, G. *et al.* Precise Gene Editing Preserves Hematopoietic Stem Cell Function following Transient p53-Mediated DNA Damage Response. *Cell Stem Cell* **24**, 551-565 e558, doi:10.1016/j.stem.2019.02.019 (2019).
574 Enache, O. M. *et al.* Cas9 activates the p53 pathway and selects for p53-inactivating mutations. *Nat Genet* **52**, 662-668, doi:10.1038/s41588-020-0623-4 (2020).
575 Alvarez, M. M., Biayna, J. & Supek, F. TP53-dependent toxicity of CRISPR/Cas9 cuts is differential across genomic loci and can confound genetic screening. *Nat Commun* **13**, 4520, doi:10.1038/s41467-022-32285-1 (2022).
576 Locatelli, F. *et al.* Exagamglogene Autotemcel for Transfusion-Dependent beta-Thalassemia. *N Engl J Med* **390**, 1663-1676, doi:10.1056/NEJMoa2309673 (2024).
577 Frangoul, H. *et al.* Exagamglogene Autotemcel for Severe Sickle Cell Disease. *N Engl J Med* **390**, 1649-1662, doi:10.1056/NEJMoa2309676 (2024).
578 Uno, Y. *et al.* Expression, Function, and Prognostic Value of MAGE-D4 Protein in Esophageal Squamous Cell Carcinoma. *Anticancer Res* **39**, 6015-6023, doi:10.21873/anticanres.13807 (2019).
579 Chong, C. E. *et al.* Over-expression of MAGED4B increases cell migration and growth in oral squamous cell carcinoma and is associated with poor disease outcome. *Cancer Lett* **321**, 18-26, doi:10.1016/j.canlet.2012.03.025 (2012).
580 Zhang, Q. M. *et al.* MAGED4 expression in glioma and upregulation in glioma cell lines with 5-aza-2'-deoxycytidine treatment. *Asian Pac J Cancer Prev* **15**, 3495-3501, doi:10.7314/apjcp.2014.15.8.3495 (2014).
581 Sutic, M. *et al.* Transcriptomic Profiling for Prognostic Biomarkers in Early-Stage Squamous Cell Lung Cancer (SqCLC). *Cancers (Basel)* **16**, doi:10.3390/cancers16040720 (2024).
582 Zhang, Q. M. *et al.* Overexpression of MAGE-D4 in colorectal cancer is a potentially prognostic biomarker and immunotherapy target. *Int J Clin Exp Pathol* **7**, 3918-3927 (2014).

583 Briere, J. J. *et al.* Mitochondrial succinate is instrumental for HIF1alpha nuclear translocation in SDHA-mutant fibroblasts under normoxic conditions. *Hum Mol Genet* **14**, 3263-3269, doi:10.1093/hmg/ddi359 (2005).
584 Zhang, D., Liang, P., Xia, B., Wu, J. & Hu, X. Comprehensive pan-cancer analysis of ZNF337 as a potential diagnostic, immunological, and prognostic biomarker. *BMC Cancer* **24**, 987, doi:10.1186/s12885-024-12703-x (2024).
585 Liu, J. *et al.* Identification of key genes and long non-coding RNA associated ceRNA networks in hepatocellular carcinoma. *PeerJ* **7**, e8021, doi:10.7717/peerj.8021 (2019).
586 Xie, T. *et al.* Emerging Roles of RNF168 in Tumor Progression. *Molecules* **28**, doi:10.3390/molecules28031417 (2023).
587 Tang, M. Y. *et al.* Plexin domain-containing 1 may be a biomarker of poor prognosis in hepatocellular carcinoma patients, may mediate immune evasion. *World J Gastrointest Oncol* **16**, 2091-2112, doi:10.4251/wjgo.v16.i5.2091 (2024).
588 Li, X. *et al.* PLXDC1 Can Be a Biomarker for Poor Prognosis and Immune Evasion in Gastric Cancer. *J Inflamm Res* **15**, 5439-5455, doi:10.2147/JIR.S383191 (2022).
589 Zhang, Z. Z. *et al.* TEM7 (PLXDC1), a key prognostic predictor for resectable gastric cancer, promotes cancer cell migration and invasion. *Am J Cancer Res* **5**, 772-781 (2015).
590 Liu, X. *et al.* PRDM1 Promotes Primary Human Circulating CD56 dim NK-Cell Differentiation. *Blood* **142**, 1177-1177, doi:10.1182/blood-2023-180323 %J Blood (2023).
591 Lasocki, A., Gangatharan, S., Gaillard, F. & Harrison, S. J. Intracranial involvement by multiple myeloma. *Clin Radiol* **70**, 890-897, doi:10.1016/j.crad.2015.03.014 (2015).
592 Mehdi, S. H. *et al.* Animal Models of Multiple Myeloma Bone Disease. *Front Genet* **12**, 640954, doi:10.3389/fgene.2021.640954 (2021).
593 Fares, J. *et al.* Advances in NK cell therapy for brain tumors. *NPJ Precis Oncol* **7**, 17, doi:10.1038/s41698-023-00356-1 (2023).